PhD degree in Molecular Medicine (curriculum in Molecular Oncology)

European School of Molecular Medicine (SEMM),

University of Milan and University of Naples "Federico II"

Settore disciplinare: Bio/10

The dual role of YAP in driving TGFβ-mediated EndMT

Cecilia Savorani

IFOM, Milan

Matricola n. R10785

Supervisor: Prof.ssa Elisabetta Dejana

IFOM, Milan

Added Supervisor: Dr.ssa Costanza Giampietro

ETH, Zurich

Anno Accademico 2017-2018

A mia madre e mio padre,

A Ciliegia,

E a tutte le persone d'oro che fanno parte della mia vita

TABLE OF CONTEXT

LIST OF ABBREVIATIONS

αSMA = α-Smooth Muscle Actin

Acta2 = gene encoding for αSMA

ACVR2A, ACVR2B = activin receptor 2A and 2B

ALK1 = activin receptor-like kinase

AMHRII = anti-Muellerian hormone type II receptor

AMOT = Angiomotin

ANG-2 = Angiopoietin-2

AV = atrioventricular

BBB = blood brain barrier

BMP = bone morphogenic protein

BMPRII = BMP type II receptor

BSA = bovine serum albumin

CAFs = cancer-associated fibroblasts

CCM = cerebral vascular malformation

CD31 = PECAM1

Cdh1 = E-cadherin

Cdh2 = N-cadherin

Cdh5 = VE-cadherin

CDKs = cyclin-dependent kinases

ChIP = chromatin immunoprecipitation

CTGF = connective tissue growth factor

CYR61 = Cysteine-rich angiogenic inducer 61

DC = destruction complex

dCVP = dorsal part of the caudal vein plexus

Dll4 = Delta-like protein 4

Dvl = Disheveled

E-cadherin = epithelial cadherin, or Cdh1

ECM = extracellular matrix

ECs = endothelial cells

EMT = epithelial-to-mesenchymal transition

EndMT = endothelial-to-mesenchymal transition

EPS8 = EGF-receptor kinase substrate 8

ESAM = Endothelial cell-selective adhesion molecule

FBS = fetal bovine serum

FDA = Food and Drug Administration

FGF2 = fibroblast growth factor 2

FKBP12 = FK506 binding-protein

Fn1 = fibronectin 1

FOP = Fibrodysplasia ossificans progressive

FSP1 = Fibroblast Specific Protein-1

Fz = Frizzled

GDFs = Growth Differentiation Factors

GPRC = G-protein coupled receptors

GSK = glycogen synthase kinase

h = hours

HO = heterotypic ossification

hESC = human embryonic stem cells

Id1 = Inhibitor of differentiation 1

INHBA = Inhibin beta A

IP = immunoprecipitation

JAMs = junctional adhesion molecules

KD = knockdown

KLF4 = Krüppel-like factor 4

KO = knock-out

LATS 1/2 = Large tumor suppressor 1 and 2

LECs = lymphatic ECs

LEF-1 = lymphoid enhancer binding factor-1

MAPKs = mitogen-activated protein kinases

Mats = Mob as tumor suppressor

MIFs = Mullerian Inhibitory Factors

MOB1/2 = Msp-one-binder 1 and 2

Mst1/2 = Mammalian STE-20 kinase 1 and 2

N/C = nuclear-cytoplasmic

N-cadherin = neuronal cadherin

Nrp-1 = neuropilin 1

O/N = overnight

OF = outflow

PAI-1 = plasminogen activator inhibitor 1, or Serpine1

Par = Partitioning defective protein

PECAM1 = platelet endothelial cell adhesion molecule 1

PFA = paraformaldehyde

pYAP S127 = YAP phosphorylated at Ser127

PROX1 = prospero homeobox protein 1

qPCR = quantitive real-time polymerase chain reaction

RA = retinoic acid

RT = room temperature

S = serine

S100a4 = FSP1

S1P = sphingosine-1-phosphate

SA = South American

SAV = Salvador

SB = sample buffer

SBE = Smad binding element

Sca1 = Stem-cells antigen 1

scr = scrambled

SDS = sodium dodecyl sulfate

Serpine1 = Serpin Family E Member 1, or PAI-1

SIP-1 = Smad-interacting protein-1

SM22α = transgelin

SMADs = small mothers against decapentaplegic

TAD = transactivation domain

TAZ = transcriptional activator with a PDZ-binding domain

TCF = T-cell factor/lymphoid enhancer-binding-factor-1

TGFβR2 = TGFβ type II receptor

TGFβ = transforming-growth factor β

TβRI = type I TGFβ receptor

TβRII = type II TGFβ receptor

TSS = transcription start site

TJs = tight junctions

UUO = unilateral ureteral obstruction

VE-Cadherin = vascular endothelial cadherin

VEGF = vascular endothelial growth factor

VP = Verteporfin

vSMCs = vascular smooth muscle cells

vWF = von Willebrand Factor

YAP = Yes-associated protein

$YAP^{f/f}$ = YAP floxed/floxed

Yki = Yorkie

W = tryptophan

WB = Western blot

Wnt = Wingless-Int1

WT = wild-type

Wts = Warts

ZEB-1 = zinc finger E-box–binding homeobox-1

ZO = Zonula Occludens

ZONAB = Zonula occludens associated nucleic-acid-binding protein

LIST OF FIGURES

Abstract

Endothelial-to-mesenchymal transition (EndMT) is a biological process that allows the transdifferentiation of endothelial cells into mesenchymal cells, thus originating cells capable of novel functions necessary for the surrounding environment. EndMT regulates endocardial cushion formation during embryo development, and it is stimulated by the TGFβ/BMP family of ligands. In adults, EndMT is activated upon an injury event or during pathological conditions like organ fibrosis, cerebral cavernous malformation, cancer-associated fibroblast generation, and others. Hence, it is necessary to better characterize the molecular regulators cooperating with TGFβ signaling in driving EndMT, to possibly provide novel therapeutic targets to treat these pathological conditions. Here we studied YAP, a co-transcriptional regulator involved in several cell biology processes, among which epithelial-to-mesenchymal transition (EMT). Since EndMT is considered a "specialized" form of EMT, and since YAP and TGFβ signaling were shown to cross-talk in other contexts, we hypothesized that YAP contributes to EndMT by modulating TGFβ signaling, and characterized the underlying molecular mechanism.

Results here presented demonstrate that YAP is required for a complete TGFβ-mediated EndMT response *in vitro*, and that YAP contributes specifically to SMAD3-, but not SMAD1-, driven EndMT gene transcription.

We provide novel evidence that YAP positively regulates EndMT playing the twofold role of acting as SMAD3 co-transcriptional factor on the promoter of EndMT target genes and, in parallel, preventing GSK3β-mediated SMAD3 linker phosphorylation, thus protecting SMAD3 from degradation. YAP is therefore emerging as a possible candidate target to inhibit pathological TGFβ-driven EndMT.

Chapter 1 - Introduction

1.1 Vascular Endothelium

The innermost layer of blood vessels is composed by an organized, continuous stratum of endothelial cells (ECs), and it is referred as vascular endothelium (Potente and Makinen, 2017). Initially, vascular ECs were considered a simple physical barrier that separate blood from the surrounding tissues, but, over the time, it became more and more clear that ECs are true determinants of vascular architecture and functions (Sena et al., 2013). Through well-defined steps, indeed, the vascular endothelium gives rise to an extremely organized vascular network – the blood vasculature – consisting of hierarchically-structured blood vessels, that nourish body tissues by transporting nutrients, gases and metabolites along with blood cells (Potente and Makinen, 2017). To regulate vascular function, ECs respond to biomolecular and mechanical stimuli by finely tuning molecular responses, and they engage with other cell types, such as perivascular cells (vascular smooth muscle cells (vSMCs), pericytes and mural cells), circulating cells and organ-specific constituents (Potente and Makinen, 2017). The vascular endothelium is therefore responsible for multiple vascular functions, such as vascular growth and remodeling, lumen formation, vessel homeostasis, permeability, vasoconstriction and vasodilation and control of immune responses (Sena et al., 2013). Hence, maintaining proper EC integrity is crucial to avoid vascular dysfunction.

1.1.1 Vascular development and remodeling

The vascular endothelium originates early during the embryo development through a process known as vasculogenesis, that is the formation of *de novo* blood

vessels (**Figure 1**, upper part) (Goldie et al., 2008; Potente and Makinen, 2017). This process initially occurs in the yolk-sac, when, at embryonic day 7.5 (E7.5), endothelial precursors confine hematopoietic cells in primitive structures known as blood islands (Choi, 2002). Afterwards, blood islands fuse together and give rise to a primitive vascular network, which undergoes extensive vascular remodeling to ultimately form the yolk sac vasculature.

Meanwhile, in the embryo proper, angioblasts differentiate from the mesoderm to become EC precursors (Potente and Makinen, 2017). Generation and differentiation of angioblasts is driven by signaling from multiple growth factors, like the bone morphogenic protein 4 (BMP4) and the fibroblast growth factor 2 (FGF2) (Marcelo et al., 2013; Winnier et al., 1995). While BMP4 and FGF2 signaling are fundamental for mesodermal development, vascular endothelial growth factor (VEGF) signaling is employed for subsequent EC proliferation and migration and it is also crucial for vasculature development (Carmeliet et al., 1996; Ferrara et al., 1996). VEGFR1 (Flt-1) and VEGFR2 (Flk-1) receptors are activated in response to VEGF-A stimulation, while VEGFR3 is bound by VEGF-C. The differential activation of these receptors not only guide EC proliferation but also determine EC specification in either tip or stalk cells. Tip cells function as leader cells that sprout from pre-existing blood vessels to pave the way for the formation of new ones, in a process termed angiogenesis (Potente and Makinen, 2017). Following tip cells there are proliferating stalk cells, which contribute to the actual vessel formation and lumenization. Interestingly, tip cells present potently activated VEGFR2 and VEGFR3-mediated signaling, together with high secretion of Delta-like protein 4 (Dll4). Dll4, then, binds to Notch receptors on neighboring ECs, leading to VEGFR2 and VEGFR3 reduced expression along with VEGFR1 up-regulation and consequent VEGF-A sequestration (Hellstrom et al., 2007; Jakobsson et al., 2010). In this way, tip ECs tightly control the fate of adjacent cells and determine their stalk

identity. Accordingly, endothelial-specific deletion of Notch-1 sustains tip cell formation (Hellstrom et al., 2007). Moreover, other reports have demonstrated that the VEGF co-receptor neuropilin 1 (Nrp-1) blocks transforming-growth factor β (TGFβ)-BMP signaling driving Notch down-stream target genes expression and, thus, promote a tip cell-fate determination (Aspalter et al., 2015; Larrivee et al., 2012; Moya et al., 2012).

Vascular network maturation not only requires adequate proliferation and migration of ECs to form tube vessels (angiogenesis), but also employs tightly coordinated vascular remodeling and mechanosensing. The proliferating activity of ECs is kept under control by retinoic acid (RA) and TGFβ -initiated signaling, which up-regulate the expression and the activity of cell-cycle progression inhibitors (like p21, p15 and p27) (Hannon and Beach, 1994; Lai et al., 2003; Reynisdottir et al., 1995). Additionally, TGFβ promotes fibronectin (Fn1) production and deposition in the extracellular matrix (ECM), which engages with either αVβ3 to promote ECs proliferation or α5β1 integrin to inhibit it (Bohnsack et al., 2004; Marcelo et al., 2013). Branching vessels can also originate through the remodeling of existing vasculature, in a process whereby interstitial tissue is formed within a vessel lumen and give rise to splitting vessels (intussusception). Vascular remodeling, moreover, can occur though removal of unnecessary sprouts, known as vascular regression. Finally, activation of transcriptional regulators in response to biochemical and mechanical stimuli determines the endothelial specification into arteries, venules, capillaries to form a structured and circular closed vascular network system (Potente and Makinen, 2017).

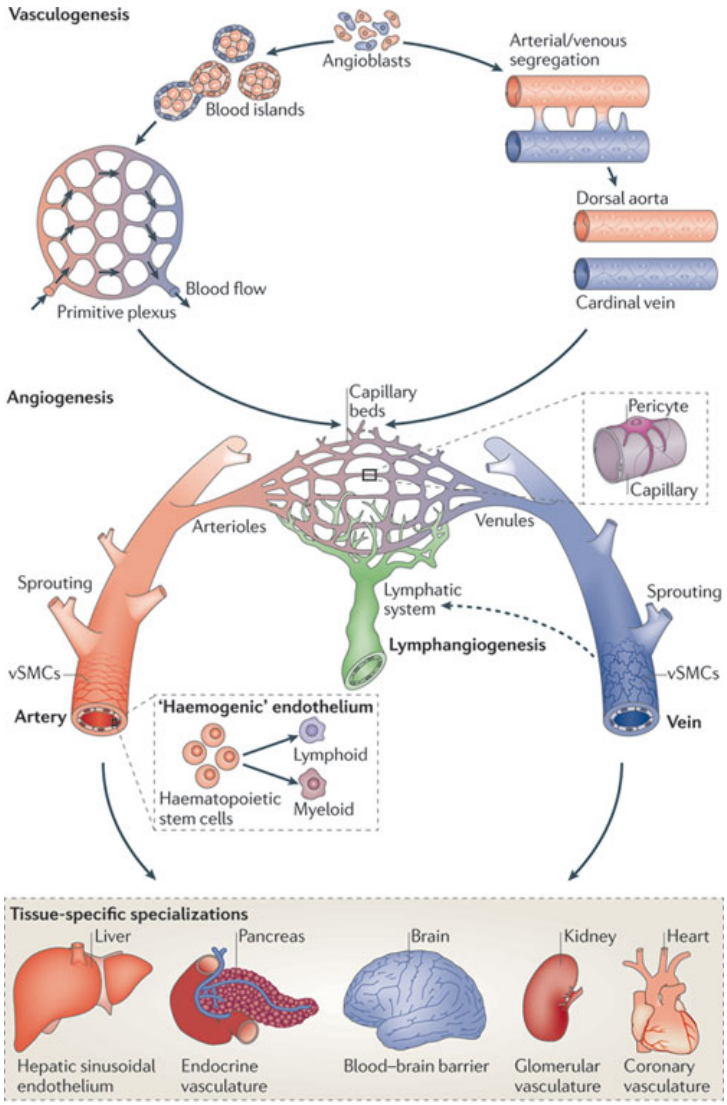

Figure 1. Vascular system development. The development of a vascular network begins with the differentiation of angioblasts (considered EC progenitors) from the mesoderm to form blood islands and acquire an arterial or venous identity, under the influence of different growth factors. Blood islands and primitive form of vessels eventually coalesce, originating a primitive vascular network. This then undergoes sprouting angiogenesis and vascular remodeling to form a hierarchical network consisting of arteries, veins and capillaries. Furthermore, myeloid and lymphoid cell lineages develop from hematopoietic stem cells originating from arterial hemogenic endothelium, and the lymphatic network system arise from the venuous endothelium. Finally, ECs attain organ-specific features thank to the recruitment of perivascular cells and to the contribution of tissue-specific biomolecular and mechanical factors. *Taken from: Herbert, SP "Molecular control of endothelial cell behaviour during blood vessel morphogenesis" 2011, Nat Rev Mol Cell Bio 12, 551-564*

1.1.2 Vascular differentiation

During vasculature development in the embryo, the primitive vessels not only undergo extensive remodeling but also acquire distinctive molecular tracts that allow them to differentiate first into arteries or veins, and later into lymphatic vessels (**Figure 1**, central part). Arteries and veins form a closed circular network, where blood is pumped by the heart into arteries, flows through arterioles, reaches the tissues through capillaries along with nutrients and gases, and finally returns to the heart by first passing through venules and then through veins. Initially, it was thought that the hemodynamic forces originated by the flowing blood were those responsible for the endothelium differentiation in either arteries or veins (le Noble et al., 2004). Indeed, arteries are continuously exposed to high-pressure blood flow, which they sustain in concert with layers of smooth muscle cells and connective tissue. Veins, instead, collect low-pressure blood flowing back to the heart. However, later studies have also pointed several molecular determinants that contribute to arterial-venous specification. Particularly, this specification seems to be genetically determined even before blood begins to flow in response to cardiac contraction (E 8.5).

Among the first arterial-venous determinants are the EphB receptors and their ligands; in particular, preceding the onset of circulation, EphB2 expressing ECs acquire arterial specifications, while vein ECs express EphB4 (Wang et al., 1998). The currently established model suggests that VEGF-A binds to VEGFR2 and Nrp-1 co-receptor to activate and then cooperate with Notch-mediated signaling, leading ultimately to EphB2 expression and EphB4 suppression (Gu et al., 2003; Lawson et al., 2002). Studies in zebrafish reported that vegf knockdown (KD) suppressed the expression of EphB2 and sustained that one of EphB4, causing defective arterial identification. Interestingly, this phenotype was rescued upon Notch signaling activation, strongly suggesting a marked inter-pathway cooperation to drive arterial

specification (Lawson et al., 2002). In the venous endothelium, instead, expression of chicken ovalbumin upstream promoter-transcription factor II (COUP-TFII) prevents Nrp-1 and Notch signaling activation, and thus promotes a venous identity (You et al., 2005).

The *Wingless*-Int1 (Wnt)/β-catenin signaling pathway is also a crucial determinant for arterial-venous differentiation. Corada and colleagues have indeed shown that β-catenin promotes the expression of the Notch-ligand Dll4 in the developing embryo vasculature, which then activates Notch1 and Notch4 receptors (Corada et al., 2010). By overexpressing β-catenin, the authors observed a prominent arterial specification of the endothelium in conjunction with a strongly reduced venous differentiation, resembling what described in a Dll4 *gain-of-function* situation (Trindade et al., 2008). Subsequently, Corada showed that the expression of the transcriptional factor Sox17 is crucial for arterial differentiation and, remarkably, it is triggered by β-catenin (Corada et al., 2013). Sox17, in turns, triggers the expression of Notch-related signaling molecules that promote Notch signaling activation. Hence, Wnt and Notch signaling are markedly inter-regulated and together they drive the endothelium towards an arterial specification.

Development of the lymphatic vasculature starts around E9, when the transcriptional factor Sox18 starts to be expressed by venous ECs and progressively induces prospero homeobox protein 1 (PROX1) expression and venous EC transdifferentiation into lymphatic ECs (LECs) (Francois et al., 2008). PROX1 is considered the key regulator of lymphatic EC specification, that together with COUP-TFII, drive the expression of VEGFR3, whose activation stimulates LEC angiogenesis from the cardinal vein. Additional sprouting from other veins concurs to establish a primitive lymphatic structural plexus.

1.1.3 Endothelial heterogeneity

The vascular tree can further specialize by adapting the EC features to meet the needs of different tissues and organs (**Figure 1**, bottom part) (Potente and Makinen, 2017). Such level of specialization confers a high degree of heterogeneity among different endothelia, in terms of both morphology and function. Structurally, the endothelium can be classified in continuous, fenestrated and discontinuous/sinusoidal (**Figure 2**) (Atkins et al., 2011).

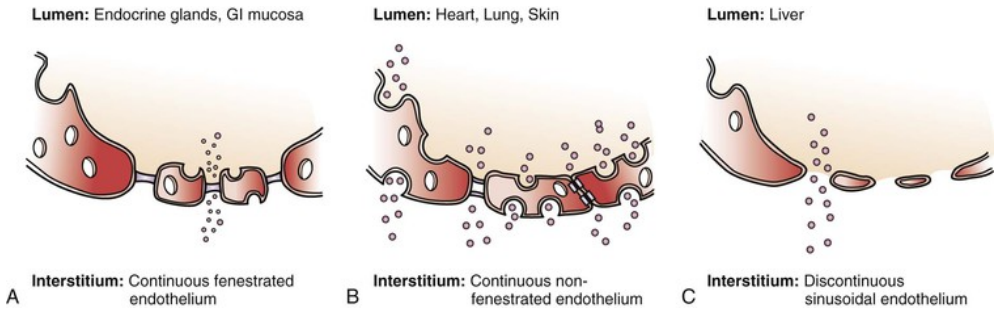

Figure 2. Heterogeneity among different endothelia lining organ-specific vascular beds. Endothelium can be: A) Continuous fenestrated, B) Continuous non-fenestrated, or C) Discontinuous/sinusoidal. For detailed description, please refer to the main text. *Taken from: Velazquez, O "Cells of the Vascular System" https://clinicalgate.com/cells-of-the-vascular-system/*

A continuous non-fenestrated endothelium is primarily observed in brain, heart, lung and skin vessels, where the need of controlled solute and cell passage is of primary importance (**Figure 2B**). ECs lining these vascular beds achieve such strict control by forming inter-endothelial junctions between adjacent cells. Their function is to impede diffusion of solutes larger than 3 nm in radius, preventing what is known as paracellular or diffusive pathway, and thus making the endothelium a physical "barrier" that separate circulating blood from the nearby tissues (Bazzoni and Dejana, 2001; Komarova and Malik, 2010). In this way, big solutes need to be actively transported through trans-cellular pathway to cross the endothelium, that is through caveolae or vesciculovacuolar organelles. Alternatively, solutes can be

uptaken thanks to specific transporters. In the brain, for example, a form of highly specialized endothelium, called “blood brain barrier” (BBB), expresses high levels of the glucose transporter GLUT1 to satisfy the high demand of glucose in the brain (Potente and Makinen, 2017). Inter-endothelial junctions are classified into two main groups, named tight and adherens junctions (from now on respectively abbreviated as TJs and AJs). Both TJs and AJs consist of transmembrane proteins that build homophilic interactions between contiguous cells and convey intracellular signaling by engaging with cytosolic partners (Dejana, 2004). Thus, junctions are not only a simple site of attachment between neighboring cells, but are true signaling modules that sense the extracellular environment and respond by modulating molecular pathways monitoring cell proliferation and apoptotic rate, EC polarity, lumen formation and, more generally, vascular homeostasis. Transmembrane components of the TJs include prevalently Claudins, Junctional adhesion molecules (JAMs), and Endothelial cell-selective adhesion molecule (ESAM), while their cytosolic counterparts are represented by Occludins, Zonula Occludens (ZO) 1 and 2, Cingulin, Zonula Occludens associated nucleic-acid-binding protein (ZONAB), and Partitioning defective protein (Par) 3 and 6 (for a more comprehensive explanation, see **Figure 3**) (Dejana et al., 2009). Endothelial AJs are formed by interacting Vascular Endothelial-cadherin (VE-cadherin or Cdh5) proteins, whose expression is specific for the endothelium and begins early during development (Breier et al., 1996; Lampugnani et al., 1992). In the cytosol, VE-cadherin binds to the catenins β-catenin, plakoglobing (or γ-catenin) and p120 and, indirectly, to α-catenin. Catenins, in turn, contribute to junctional stability, support AJs-actin cytoskeleton interaction, and form complexes with other signaling partners to convey a variety of intracellular messages (**Figure 3**) (Dejana et al., 2009). VE-cadherin clustering and junctional stabilization goes in parallel with increasing EC density, so that, when cells reach confluency, VE-cadherin limits cellular overgrowth, modulates the activity of

membrane receptors (like TGFβRII and VEGFR2), and induces TJs formation (Lampugnani et al., 2006; Rudini et al., 2008; Taddei et al., 2008). The expression of the endothelial-specific Claudin-5, indeed, is increased as a result of VE-cadherin expression and clustering (Taddei et al., 2008). By controlling various properties and aspects of ECs, thus, VE-cadherin functions as a master regulator of vascular homeostasis, whose genetic ablation results in collapse and regression of the vascular system (Carmeliet et al., 1999). Moreover, ECs express another member of the cadherin family, the neuronal cadherin (N-cadherin or Cdh2), which is not involved in endothelial cell-cell interaction, rather it seems to mediate connections between ECs and perivascular cells, like pericytes and vSMCs (Dejana et al., 2009). Intriguingly, Giampietro et al. reported that VE-cadherin limits N-cadherin expression by sequestering β-catenin at the cytoplasmic membrane and impeding its transcriptional activity, thus attenuating N-cadherin transcription (Giampietro et al., 2012). Accordingly, constitutively active β-catenin promotes N-cadherin expression while diminishing the one of VE-cadherin. Nowadays, this cadherin switch is considered a hallmark of endothelial-to-mesenchymal transition (EndMT), a biological process that will be further discussed in section 1.2.

Notably, in fenestrated and discontinuous vessels, the adhesive and permeability properties of the inter-endothelial junctions are more loose compared to the continuous endothelium. A fenestrated endothelium is characteristic of organs involved in either filtration or secretion, like kidney glomeruli, glands and intestinal mucosa (**Figure 2A**) (Atkins et al., 2011). In these organs, the presence of big transcellular pores (around 70 nm in diameter) allows a quick exchange of molecules between the circulating blood and the nearby tissues. Finally, a discontinuous endothelium is observed in liver and bone marrow vessels, where the presence of large fenestrae (around 100-200 nm in diameter) permits cellular trafficking (**Figure 2C**).

Considering what described so far, vessel can differentiate in organ-specific vasculature and contribute to fulfill the needs of surrounding tissues by acquiring different phenotypic characteristics. This differentiation is elicited by external and tissue-specific stimuli, such as through the interaction with locally-resident cell types, through the exposure to different growth factors, in response to variable ECM composition and stiffness, in response to different mechanical forces (Potente and Makinen, 2017). Moreover, once the vasculature reaches a mature and definitive state, ECs do not sprout or undergo angiogenesis any longer, unless challenged by injuries or pathological conditions like tumors. Thus, a mature endothelium enters in a reversible quiescence status, in which ECs stop migrating and proliferating and form a monolayer of fully functional cells (Potente and Makinen, 2017).

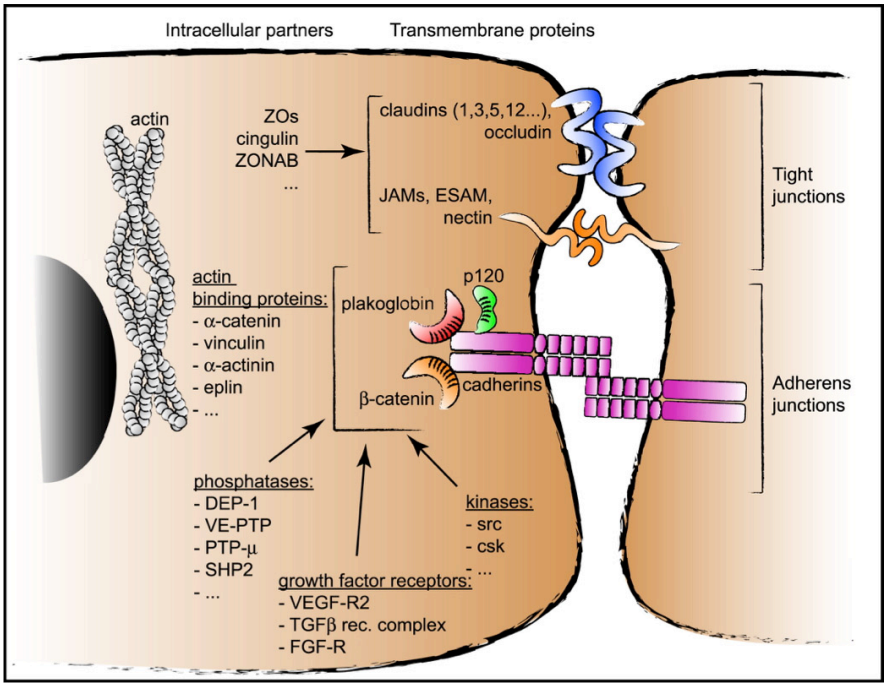

Figure 3. Endothelial tight and adherens junctions and their cytoplasmic partners. Junctions between ECs can be mainly grouped in two: Tight junctions (TJs), or Adherens junctions (AJs). 1) TJs comprise different families of proteins, like claudins, occludins, JAMs or ESAM. ECs express several claudins, like Claudin-1, -3, -5 and -12 but only Claudin-5 is specific for the endothelium. Claudin-5 is highly expressed in brain endothelium and, together with Claudin-3, contribute to control brain permeability. *(continues on the next page)*

(continues from the previous page) TJs are connected to the actin cytoskeleton through cingulin and ZO proteins 1, 2 and 3, while ZONAB is a transcriptional factor. Moreover, TJs can recruite polarity complex proteins Par3/Par6/aPKC and contribute to cell polarization. JAM are also involved in permeability control, but the exact mechanism is still not fully elucidated. 2) AJs are formed by homophilic interacting cadherins. In the endothelium, the prominent form of cadherin is VE-cadherin, whose cytoplasmic tail is bound to catenins and contributes to modulate intracellular signaling important for ECs homeostasis. Catenins include p120, involved in VE-cadherin stabilization and signaling, plakoglobin, contributing to junctional stability, and β-catenin, the Wnt canonical transcriptional factor. β-catenin can function both as cell junction scaffolding protein, interacting with multiple partners and promoting junctional stability, as well as a transcriptional regulator. For example, junctional β-catenin can associate to monomeric α-catenin and may negatively impact on actin polymerization (yet the exact molecular mechanism is still under investigation). Conversely, junctional destabilization induces β-catenin nuclear translocation and activation of its transcriptional program. In addition to catenins, VE-cadherin can associate to growth factor receptors, like VEGFR2 and TGFβR, and modulate their signaling activity. *Taken from: Dejana, E. "The control of vascular integrity by endothelial cell junctions: molecular basis and pathological implications." Dev Cell. 2009;16(2):209-21*.

1.2 Endothelial-to-mesenchymal transition (EndMT)

1.2.1 General characteristics of endothelial-to-mesenchymal transition

Endothelial-to-mesenchymal transition (EndMT) is a biological process that occurs when ECs differentiate to become mesenchymal-like cells, detach from an organized endothelium, migrate, and invade surrounding tissues (van Meeteren and ten Dijke, 2012). During mesenchymal differentiation, ECs lose some endothelial-specific characteristics, like quiescence, junctional stability, and the expression of the endothelial markers VE-cadherin, Claudin-5 and CD31 (or PECAM1, platelet endothelial cell adhesion molecule 1). In parallel, ECs acquire mesenchymal-like tracts, that is they become more invasive and migratory and they express transcription factors responsible for the EndMT switch like Snai1 (also known as Snail), Snai2 (or Slug) and Twist1 along with mesenchymal markers such as α-Smooth Muscle Actin (αSMA, encoded by Acta2), transgelin (SM22α), Fibronectin-1 (Fn1), Fibroblast Specific Protein-1 (FSP1, also known as S100a4), N-Cadherin, and Serpine1 (or PAI-1). The EndMT process confers high plasticity to ECs and physiologically occurs during embryo development (Markwald et al., 1975). In adults, instead, EndMT is generally switched off, although it can be re-activated upon an injury event or during pathological conditions, such as kidney and pulmonary fibrosis (van Meeteren and ten Dijke, 2012), cerebral cavernous malformation (CCM) (Maddaluno et al., 2013), and cancer-associated fibroblasts (CAFs) generation (Zeisberg et al., 2007a), as later discussed in section 1.2.6.

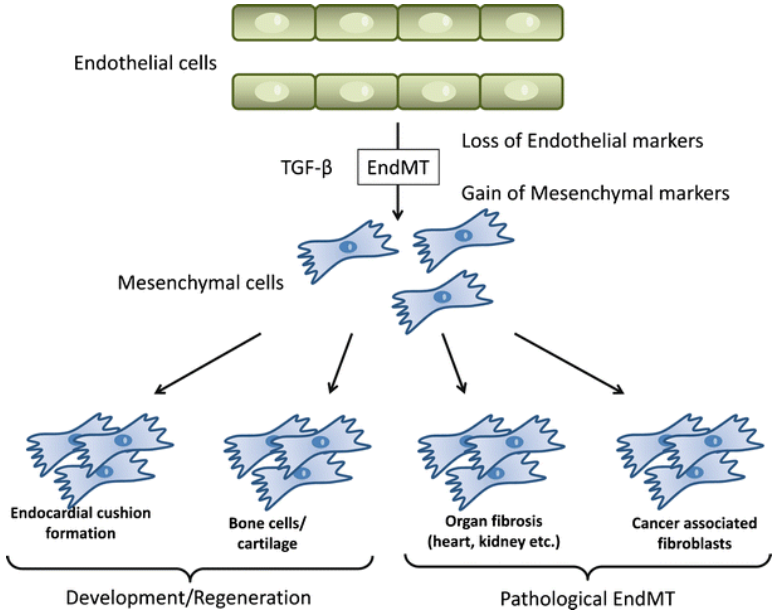

Figure 4. Schematic overview of endothelial-to-mesenchymal transition. ECs undergoing EndMT due to sustained TGFβ exposure progressively lose their specific characteristics and, instead, acquire more mesenchymal-like features. TGFβ-mediated EndMT occurs during development, in response to either temporary or chronic inflammation resulting in organ fibrosis, or during cancer progression. *Taken from: van Meeteren LA, ten Dijke P. Regulation of endothelial cell plasticity by TGF-beta. Cell Tissue Res. 2012;347(1):177-86*

EndMT resembles and shares common characteristics with the more-widely known epithelial-to-mesenchymal transition (EMT), which is a key epithelial cell mechanism involved in several embryogenesis steps (Type I EMT) (Kalluri and Weinberg, 2009). Similar to ECs undergoing EndMT, epithelial cells differentiating into mesenchymal cells during EMT progressively lose their epithelial molecular markers, like the expression of epithelial cadherin (E-cadherin, or Cdh1), ZO-1, Cytokeratin and Desmoplakin, while acquiring mesenchymal ones. Of note, during either EMT or EndMT, there is a progressive degradation of the basal lamina caused by increased MMP-2 and MMP-9 matrix metalloproteinase activity, paralleled with an increased deposition of Fn1 and type I and III collagen, that can in turn activate different integrin-mediated signaling and lead to cytoskeletal reorganization of neighboring cells. EMT does not occur only during embryonic development, but also

during wound healing, tissue regeneration and organ fibrosis (Type II EMT). According to Kalluri and Weinberg, this second type of EMT is triggered by an inflammatory response, and terminates once the source of inflammation is removed (Kalluri and Weinberg, 2009). Since in fibrotic conditions the inflammatory status is continuous, EMT can ultimately lead to severe organ alterations. Finally, a third type of EMT is observed during tumorigenesis and tumor progression, when cancer cells become highly invasive and migratory and contribute to tumor metastatization (Kalluri and Weinberg, 2009).

Both EMT and EndMT are triggered by similar signaling pathways, among which TGFβ and Wnt signaling are the predominant molecular inducers.

1.2.2 Canonical TGFβ signaling pathway

The canonical TGFβ signaling cascade is a central molecular pathway, known to regulate tumor-suppressive functions, like cell proliferation, apoptosis, and cell differentiation, but also tumor-promoting processes, like cell migration, ECM production, EMT and EndMT (Massague, 2012; van Meeteren and ten Dijke, 2012). These apparently opposite functions can be explained through the existence of numerous ligands, types of receptors, co-receptors, and intracellular modulators that are differently activated depending both on the type and on the amount of the stimulating ligand (Massague, 2012; Weiss and Attisano, 2013). The TGFβ superfamily of ligands, indeed, comprises three isoforms of TGFβ (TGFβ1, TGFβ2, TGFβ3), more than twenty BMPs, Activins, Inhibins, Growth Differentiation Factors (GDFs), and Mullerian Inhibitory Factors (MIFs), all having a dimeric structure with a cysteine structural motif. The signaling is propagated by ligand-activated receptors presenting serine/threonine kinase activity, which are broadly divided in type I (TβRI) and type II (TβRII) receptors. The human genome encodes seven different type I receptors, named activin receptor-like kinase (ALK1-7), and five type II receptors,

which are TGFβ type II receptor (TGFβR2), BMP type II receptor (BMPRII), activin receptor 2A and 2B (ACVR2A, ACVR2B) and anti-Muellerian hormone type II receptor (AMHRII). Receptors belonging to TβRI or TβRII family have a similar structure, composed of a cysteine-rich extracellular domain, a single transmembrane spanning region and a cytoplasmic tail bearing a kinase domain (Weiss and Attisano, 2013).

In a canonical context, a TGFβ or BMP ligand binds to a multimeric receptor complex formed by two TβRII and two TβRI, and cause TβRI phosphorylation and activation by TβRII (**Figure 5**) (Massague, 2012). Once phosphorylated, TβRI undergoes a conformational change, and releases FK506 binding-protein (FKBP12) masking its kinase domain. As a result, the affinity of the receptor complex towards the intracellular signaling modulators “small mothers against decapentaplegic” (SMADs) is increased and leads to SMAD phosphorylation in a conserved SSXS motif at their C-term. Once the receptor-activated SMADs (R-SMADs) have been phosphorylated, they bind to SMAD4, and together shuttle to the nucleus, where they regulate the expression of different genes depending on the co-transcriptional partner engaged.

Mammals express 8 different SMAD isoforms, classified in R-SMADs, common mediator SMAD (co-SMAD), and inhibitory SMADs (I-SMADs) (Massague et al., 2005). R-SMADs comprise SMAD1, SMAD2, SMAD3, SMAD5 and SMAD8, and are activated by the TGFβ receptor complex to modulate gene expression. In ECs, TGFβ preferentially activates SMAD2 and SMAD3 by binding to ALK5-TGFβR2 complex, while BMP triggers SMAD1, -5 and -8 phosphorylation and activation through ALK1- TGFβR2 (van Meeteren and ten Dijke, 2012). Thus, SMAD2 and SMAD3 are known as the canonical TGFβ-induced R-SMADs, while SMAD1, -5 and -8 are usually referred as BMP-induced R-SMADs. Interestingly, in ECs TGFβ can

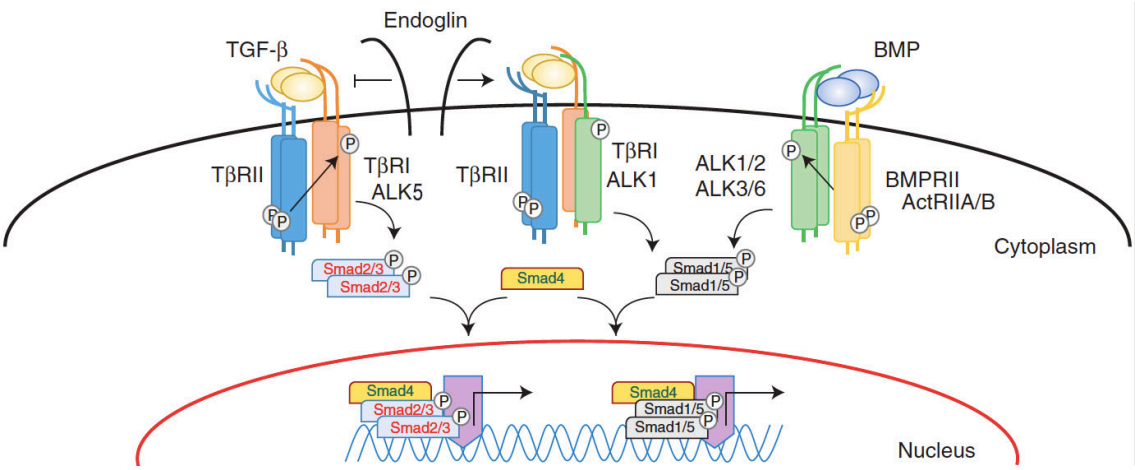

Figure 5. Canonical TGFβ/BMP signaling overview in ECs. Upon TGFβ or BMP ligand binding, TβRII phosphorylates and activates TβRI. TβRI, then, phosphorylates and activates down-stream target molecules, that are canonically represented by R-SMADs. ALK5 drives SMAD2 and SMAD3 C-term phosphorylation, while ALK1 phosphorylates SMAD1, -5 and -8. Subsequently, R-SMADs form a complex with SMAD4, translocate to the nucleus and, there, drive transcription of different sets of genes, like Serpine1 by SMAD2/3 and Id1 by SMAD1. *Adapted from: Goumans MJ, Ten Dijke P. TGF-beta Signaling in Control of Cardiovascular Function. Cold Spring Harb Perspect Biol. 2017.*

also bind to ALK1 and promote SMAD1 phosphorylation (Goumans et al., 2003a; Goumans et al., 2002). The activation of either one or the other response can be modulated by the amount of TGFβ and by presence of the co-receptor endoglin, which has stimulatory activity on the TGFβ/ALK1 signaling axis while blocking the TGFβ/ALK5 one (Lebrin et al., 2004; Velasco et al., 2008). Thus, TGFβ co-receptors provide another level of signaling differentiation. Once phosphorylated at their C-term, all R-SMADs interact with the co-SMAD SMAD4 and form an heteromeric complex that helps R-SMAD nuclear translocation and gene transcription (Massague, 2012). Finally, the activated mechanism is counteracted by the inhibitory activity of the I-SMAD, SMAD6 and SMAD7, whose mode of action differs between them. Indeed, SMAD7 blocks the TβRI activation, while SMAD6 prevents SMAD1 binding to SMAD4. Interestingly, TGFβ drives the expression of the I-

SMADs, providing a negative forward mechanism that helps terminating the elicited signaling (Goumans and Ten Dijke, 2017).

In basal conditions, R-SMADs continuously shuttle in and out of the nucleus, until a TGFβ stimulus induces their C-term phosphorylation and nuclear accumulation (Hill, 2009). From the structural point of view, R-SMAD are formed by two globular domains named Mad-homology 1 and 2 (MH1 and MH2). The MH1 domain lies at the N-term of all R-SMADs and of SMAD4 and mediates binding to DNA (Massague et al., 2005). Notably, SMAD2 does not have DNA binding capabilities, due to an additional short insert found in the binding region of its MH1 domain. MH2, instead, is found at the C-term and serves as a docking site for different R-SMAD binding partners, such as cytoplasmic interactors, TGFβ-activated receptor complex, and different co-transcriptional factors. Connecting MH1 with MH2, there is a linker region, which differs greatly among the different R-SMADs and contains phosphorylation sites for different classes of protein kinases, like mitogen-activated protein kinases (MAPKs), cyclin-dependent kinases (CDKs), and glycogen synthase kinase (GSK), to cite few (Massague, 2012). Indeed, the linker region provides important regulatory sites that, once phosphorylated, promote SMAD binding to co-transcriptional partners and/or SMADs turnover. Accordingly, recent studies have proposed that Erk2 MAPK phosphorylates SMAD1 at S186, S195, S206, S214 and SMAD3 at S204, priming these proteins for subsequent E3-ubiquitin ligases recruitment and proteosomal degradation (**Figure 6**) (Alarcon et al., 2009). The ubiquitin ligases responsible for terminating SMAD signaling are Smurf1 in case of SMAD1, and Nedd4L for SMAD3 (Gao et al., 2009; Zhu et al., 1999). Hence, MAPKs-induced linker phosphorylation prevents SMADs activation by targeting them to destruction and occur without ligand stimulation. Interestingly, SMAD3 linker region is of primary importance for its transcriptional activity, since mutants lacking this region are not capable of driving gene expression even after

TGFβ stimulation and C-term phosphorylation (Velden et al., 2011). Indeed, it has been shown that, in the nucleus, CDK8/9 phosphorylate SMAD1 at S206 and S214 in response to BMP, thus stimulating the recruitment of the co-transcriptional factor yes-associated protein (YAP) and target gene expression (**Figure 6**) (Alarcon et al., 2009). Similarly, upon TGFβ, CDK8/9 phosphorylate SMAD3 at T179 and S208 and favor the binding to Pin1 co-transcription factor (Alarcon et al., 2009). Recruitment of transcriptional partners, then, prevents the subsequent GSK3β-mediated phosphorylation of SMAD1 (at T202 and S210) (Alarcon et al., 2009) and of SMAD3 (at S204) (Wang et al., 2009a), thus impeding their subsequent interaction with E3 ubiquitin ligases and proteosomal degradation (Aragon et al., 2011). In conclusion, by phosphorylating different residues in the linker region of SMAD1 and SMAD3 upon BMP/TGFβ stimulation, CDK8/9 promote SMAD1 and -3 transcriptional activity and, at the same time, prevent their subsequent degradation by recruiting co-transcription factors that mask the sites targeted by GSK3β.

Once in the nucleus, R-SMADs bind to the consensus sequence 5'-CAGAC-3' on the DNA, known as "Smad binding element" (SBE) (Hill, 2016). SMAD1, instead, preferentially binds to CG-rich sequences that were found in the promoter regions of BMP-regulated genes, like *Smad6*, *Id1* (Inhibitor of differentiation 1) and others. R-SMADs have low DNA-binding affinity and, thus, they need to synergize with co-transcriptional modulators in order to control gene transcription, for example with members of the FoxO family, run-related transcription factor 2 (Runx2), ATF3 and several others (for a more detailed list, please refer to (Hill, 2016)). The final biological outcome of the signaling cascade can be therefore modulated not only by the amount and type of ligand, or by the receptors and the co-receptor activated, but also by the co-transcriptional regulator bound by the SMADs.

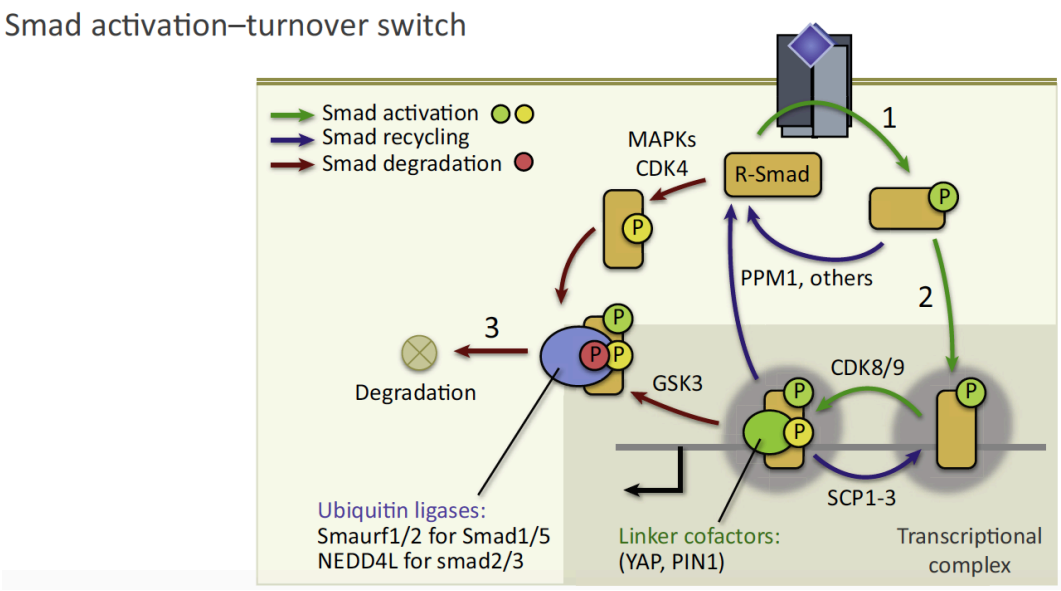

Figure 6. R-SMAD activation and turnover. 1) TGFβ or BMP stimulation results in SMAD3 and SMAD1 C-term phosphorylation, respectively. 2) Once in the nucleus SMAD1 is further phosphorylated in its linker region by CDK8/9 at S206 and S214. Similarly, SMAD3 is phosphorylated by CDK8/9 in T179 and S208. The phosphorylation at these residues co-adiuvates SMAD binding to transcriptional co-activators, like YAP for SMAD1 and Pin1 for SMAD3. 3) At the same time, phosphorylation at these residues primes R-SMADs for an additional linker phosphorylation mediated by GSK3β (S204 in SMAD3, and T202 and S210 in SMAD1), which are then recognized by ubiquitin ligases and target R-SMAD for degradation. However, R-SMAD can also undergo linker phosphorylation without ligand stimulation. In this case, MAPK-mediated phosphorylation contributes to maintain R-SMAD expression levels low, as it targets them to degradation. *Taken from: Macias MJ, Martin-Malpartida P, Massague J. Structural determinants of Smad function in TGF-beta signaling. Trends Biochem Sci. 2015;40(6):296-308*

1.2.3 TGFβ signaling in ECs

Genetic studies on TGFβ signaling members in mice and humans have shown the central importance of this molecular pathway in driving vascular development and vascular dysfunctions (Jakobsson and van Meeteren, 2013). Indeed, mouse models bearing genetic inactivation in one of the TGFβ/BMP signaling members (either ligands, or receptors, or SMADs) often die early during embryo development

and show cardiovascular alterations and impaired pericyte and vSMC recruitment (reviewed in (Goumans and Ten Dijke, 2017)).

TGFβ can exert multiple and divergent functions on ECs. For example, TGFβ was shown to promote but also to inhibit angiogenesis, and this apparently opposite role can be due to different causes, like the concentration of the ligand, the duration of the treatment, cellular density and the types of receptors expressed on the cellular membrane (Goumans and Ten Dijke, 2017). TGFβ can indeed bind to two different TβRI in ECs: ALK5 (known also as TGFβRI) or, with lower affinity, ALK1 (or Acvrl1), the last one being expressed strictly in ECs (**Figure 5**).

TGFβ signaling through ALK5-TGFβR2 complex stimulates the phosphorylation of SMAD2 and SMAD3 and, in turn, induces the expression of PAI-1, which negatively regulates EC migration (Dennler et al., 1998; Goumans et al., 2002). Moreover, TGFβ-ALK5 signaling axis arrests cell proliferation and cell migration by upregulating the expression of cell-cycle regulating genes, such as p21 and p15 (Zhang et al., 2016). On the reverse side, inhibiting ALK5 activity with the specific inhibitor SB-431542 stimulates EC proliferation and sheet formation of mouse embryonic cultured ECs (Watabe et al., 2003). SB-431542 treatment of ECs, moreover, up-regulates Claudin-5 expression, thus conferring a role for ALK5 in controlling vascular permeability. Interestingly, clustering of VE-cadherin is essential for proper TGFβ signaling in ECs, as cells lacking VE-cadherin expression display reduced R-SMADs phosphorylation and signaling (Rudini et al., 2008). Moreover, TGFβ signaling activation is impaired in VE-cadherin positive ECs upon junctional dismantling, thus suggesting that the clustering of VE-cadherin occurring in confluent EC monolayer is essential to trigger a proper TGFβ signaling activation. It has to be noted that VE-cadherin interacts with all the TGFβ-receptor complex components, that are ALK5, ALK1, TGFβR2 and endoglin. Thus, TGFβ signaling through ALK5 contributes to maintain ECs in quiescent state by inhibiting cell

proliferation, migration and angiogenesis, and plays a role in controlling ECs permeability.

Nevertheless, studies have shown that TGFβ can also activate ALK1-mediated signaling cascade and induce SMAD1/5 phosphorylation, leading to EC proliferation, migration and tube formation (Goumans et al., 2003b). Hence, TGFβ can also promote angiogenesis, and it does it by inducing ALK1 signaling cascade. Accordingly, EC migration and tube formation are partly driven by Id1 expression, which is stimulated by TGFβ-ALK1 signaling axis (Goumans et al., 2002). These indications support a pro-angiogenic role of TGFβ signaling through ALK1, and set the TGFβ-ALK1 signaling axis as a positive regulator of EC proliferation and migration.

Although TGFβ-ALK5 and TGFβ-ALK1 signaling cascade result in opposite biological outputs, they have been shown to interact and regulate each other. Accordingly, ECs lacking ALK5 expression display not only an impaired TGFβ-ALK5 signaling, but also an impaired TGFβ-ALK1 activity, as ALK5 is required for ALK1 recruitment into the TGFβ receptor complex (Goumans et al., 2003b). Nevertheless, ALK1 can negatively regulate ALK5-induced R-SMAD signaling. Thus, balancing of ALK1 and ALK5 signaling in ECs is required for finely modulating EC functions and homeostasis. Controlling this tight balance intervene the amount and duration of the signaling, but also the expression of the co-receptor endoglin. Endoglin is abundantly expressed in ECs, especially in highly proliferating ones (van Meeteren and ten Dijke, 2012). Studies have shown that endoglin can potentiate the TGFβ-ALK1 axis and also inhibit the TGFβ-ALK5 signaling cascade (Lebrin et al., 2004; Velasco et al., 2008). Accordingly, pancreatic tumor mouse models heterozygous for endoglin showed an increased expression of the ALK5-induced target genes *Fn1* and *Serpine1* (Anderberg et al., 2013).

Of note, members of the BMP family of ligands are also required for proper vascular development, as their genetic inactivation can result in defective cardiovascular development and impaired angiogenesis. Among the ligands, BMP2 and BMP4 were shown to positively regulate EC proliferation and migration, and induce angiogenesis (Medici et al., 2011). BMP9, instead, inhibits VEGF-stimulated angiogenesis and FGF2-induced EC proliferation and migration (Scharpfenecker et al., 2007).

In conclusion, both TGFβ and BMP signaling are crucial regulator of vascular development and homeostasis and, deregulation in their signaling activity might result in vascular pathologies, like arteriovenous malformation (AVMs), remodeling of retinal vasculature, cardiac fibrosis, improper heart valve formation, CCM and endothelial tumors (hemangiomas) (Goumans and Ten Dijke, 2017). Importantly, TGFβ and BMP signaling have been proposed as master drivers of EndMT, and further explanation will be provided in the following sections.

1.2.4 TGFβ-driven EndMT

EndMT is a biological process through which ECs, under the continuous exposure to TGFβ or BMP ligands (but also Wnt and Notch), transdifferentiate into mesenchymal-like cells (Gong et al., 2017). All the three TGFβ isoforms (TGFβ1, -2 and -3), indeed, have been reported to stimulate EndMT *in vitro* and *in vivo*, although TGFβ2 has been shown to be the prominent inducer of embryonic EndMT that occurs during heart-valve formation (Azhar et al., 2009; Medici et al., 2010). TGFβ1 or TGFβ3 null mice, instead, developed normal heart cushions, and similar results have been recapitulated in chick embryos (Azhar et al., 2009; Boyer et al., 1999; Camenisch et al., 2002). It seems then that TGFβ1 and TGFβ3 do not to play a role during the EndMT observed in the developing heart of mice and chicks. Yet, TGFβ3 has been reported to promote post-EndMT invasion and migration of cells

in the chick embryo (Boyer et al., 1999), while TGFβ1 is involved in the EndMT-driven cardiac fibrosis (Zeisberg et al., 2007b).

In vitro studies have shown that EC progenitors can undergo phenotypic transformation into smooth-muscle-like cells once stimulated with TGFβ1, and the resulting EndMT process is driven by ALK5-mediated signaling (Moonen et al., 2010). Moreover, TGFβ1 can promote EndMT of adult coronary ECs and of a mouse microvascular endothelial cell line (MMEC) (Li et al., 2009; Zeisberg et al., 2007b). Interestingly, EC-specific ALK5 null mice fail to undergo EndMT during cardiac development, and specific inhibition of ALK through SB-431542 resulted in defective EndMT response of cultured ECs (Sridurongrit et al., 2008; Watabe et al., 2003). Later evidence suggested that TGFβ2 promotes EndMT by activating both ALK2 and ALK5, which co-immunoprecipitate and activate both R-SMAD signaling pathways (Medici et al., 2010). One year later, by attempting to unravel the molecular mechanism through which TGFβ2 induces EndMT, the same group showed that ECs undergoing transdifferentiation displayed Snai1 enhanced expression. This, in turn, resulted in decreased VE-cadherin and CD31 expression, while FSP-1 and αSMA were found to be up-regulated (Medici et al., 2011). However, Snai1 alone overexpression was not capable of inducing an EndMT phenotype, and, other studies have indeed reported that many transcription factors are involved in the activation of an effective EndMT response, like Snai2, zinc finger E-box-binding homeobox-1 (ZEB-1), Smad-interacting protein-1 (SIP-1), lymphoid enhancer-binding factor-1 (LEF-1), and Twist1 (Medici et al., 2010).

Interestingly, several ligands belonging to the BMP family have also been shown to positively regulate the EndMT differentiation. For example, BMP2 and BMP4 signaling through ALK2 could induce an EndMT response during heart valve formation, while specific inhibition of ALK2 impaired the activation of this response (Medici et al., 2010). Moreover, genetic deletion of either BMP2, BMP4 or ALK2

prevented embryonic EndMT due to a failure in the heart valve formation (Liu et al., 2004; Ma et al., 2005). Conversely, BMP7 was shown to inhibit EndMT through the SMAD1/5/8 signaling pathway activated by ALK2 (Zeisberg et al., 2007b). Although these seem to be contradictory results, they strongly suggest that the EndMT response can be differentially modulated in response to distinctive TGFβ/BMP ligands, probably thanks to the enrolment of different SMAD co-transcriptional factors. Thus, further studies are required to better define the molecular mechanisms driven by different TGFβ/BMP ligands under context-specific conditions.

1.2.5 Physiological EndMT

The first reported case of EndMT was described in 1975, when Markwald and colleagues identified it as a crucial differentiation process necessary for the cardiac valve formation occurring in embryo development (Markwald et al., 1975). During heart development, two distinct types of cardiac cells are originated from cardiogenic mesodermal cells, named myocardial cells and endocardial cells (Yamagishi et al., 2009). Endocardial cells are actual ECs expressing EC-specific markers, like VE-cadherin, CD31, Tie1 and Tie2. They take part in the generation of cardiac valves in the atrioventricular (AV) canal, which divides the atria from the ventricles, and in the outflow tract (OFT), whose function is to connect the ventricles to the aortic sac and guarantee a correct blood flow (**Figure 7**).

At initial stages, cushions found in the AV and OFT are formed by an inner layer of myocardial cells and an outer layer of endocardial cells, separated by a stratum of ECM known as cardiac jelly (**Figure 7**). Myocardial cells release BMP2 as a triggering signal that elicits an autocrine endocardial TGFβ production (Ma et al., 2005; Rivera-Feliciano and Tabin, 2006; Sugi et al., 2004). TGFβ, in turns, stimulates endocardial/ECs to undergo EndMT, acquire mesenchymal phenotype,

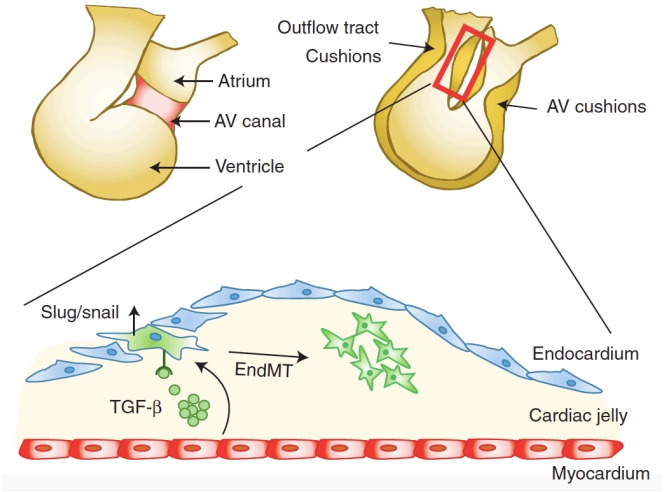

Figure 7. Endocardial cushion formation is driven by EndMT. During embryo development, the heart valves originate from endocardial cushions in the atrioventricular (AV) zone and in the outflow tract (OTF). These cushions are formed by a layer of myocardial cells and one of endocardial cells, divided by a cardiac jelly composed of ECM. Endocardial cells undergo EndMT to form the cushions under TGFβ-driven stimulation. *Taken from: Goumans MJ, Ten Dijke P. TGF-beta Signaling in Control of Cardiovascular Function. Cold Spring Harb Perspect Biol. 2017*

delaminate from the endocardium, migrate toward the cardiac jelly and contribute to form cushions in the AV region and in the OFT, finally originating cardiac valves (Yamagishi et al., 2009).

As previously discussed, all the three TGFβ isoforms have been implicated in the endocardial cushion formation at different levels. Indeed, as nicely reviewed by Yamagishi and colleagues, TGFβ1 expression is initially found in the endocardium at E8, and when the EndMT process begins, it is mainly retrieved in the ECs forming the cardiac cushion tissue (Yamagishi et al., 2009). TGFβ2, instead, is expressed both in the OFT and AV during cushion formation. Its importance in driving heart-valve EndMT has been repeatedly shown, both *in vitro* and *in vivo* experiments, and mice lacking TGFβ2 expression fail to form the AV cushion (Millan et al., 1991). After the EndMT takes place, TGFβ3 is expressed in the endocardium and in mesenchymal cells (Millan et al., 1991). *In vitro* studies have shown that TGFβ3 stimulates an EndMT phenotype only in “pre-activated AV ECs”. Thus, TGFβ3

seems to be required only after the onset of EndMT (Boyer et al., 1999; Camenisch et al., 2002). *In vivo* studies have revealed that both TGFβ1- and TGFβ3-null mice do not develop cardiac cushion formation defects (Azhar et al., 2009), although TGFβ1 knock-out (KO) embryos born from TGFβ1$^{-/-}$ mothers display disorganized AV valves along with other cardiac defects (Letterio et al., 1994). Instead, cardiac valve development strictly requires TGFβ2 expression, as shown by KO mice experiments (Azhar et al., 2009). Taken together, these results demonstrate that the three mammalian isoforms of TGFβ are involved in the heart-cushion EndMT, but probably are expressed by myocardial and/or endocardial cells during different developmental steps and their spatiotemporal expression needs to be better clarified.

Moreover, BMP ligands have also been described as regulators of heart-cushion EndMT. For example, heart-specific BMP2 KO mice are characterized by impaired AV cushion formation, but normal OFT (Ma et al., 2005). Also, specific BMP4 deletion in the heart resulted in defective OFT valve formation, while BMP5, -6, or -7 null mice display fairly normal heart development (Liu et al., 2004; Yamagishi et al., 2009).

1.2.6 Pathological EndMT

1.2.6.1 EndMT during fibrosis in the heart, kidneys and lungs

Fibrosis is a condition wherein continuous exposure to inflammatory cytokines stimulates fibroblasts differentiation into myofibroblasts, which, in turn, promote ECM production, tissue hardening, and ultimately lead to organ structural and functional changes and failure. (Myo)fibroblasts can originate from a pool of locally resident interstitial fibroblasts, but can also derive from epithelial cells undergoing transdifferentation. Interestingly, in the past years ECs have also been pointed as a

source of fibroblasts during tissue fibrosis in the heart, kidneys, liver and lungs (van Meeteren and ten Dijke, 2012).

A pioneer study in 2007 has demonstrated that EndMT contributes to cardiac fibrosis. By using lineage-tracing cell systems under the endothelial specific Tie1 promoter, Zeisberg and colleagues have shown that around 30% of cardiac fibroblasts have EC origin and they arise from an EndMT process driven by TGFβ1/SMAD3 signaling axis (Zeisberg et al., 2007b). In the same study, the authors have also proposed that BMP7 expression can revert the TGFβ1-induced EndMT both *in vitro* and *in vivo.* More recently, administration of an orally active ALK5 inhibitor, that prevent the receptor kinase activity, resulted in reduced cardiac fibrosis and ameliorated cardiac output, although cardiac dilation was also observed (Engebretsen et al., 2014). Moreover, the TGFβ co-receptor endoglin has been linked to cardiac fibrosis promotion, since endoglin-deficient mice showed a reduced cardiac fibrosis in a mouse model where heart failure is induced by pressure-overload (Kapur et al., 2012).

EndMT has been proven to drive kidney fibrosis too. By using three different animal mouse models of chronic kidney disease, Zeisberg and colleagues have indeed reported that around 30 to 50% of activated fibroblasts express the endothelial marker CD31 along with fibroblast-specific markers (Zeisberg et al., 2008). As EndMT is often triggered by TGFβ/BMP signaling pathways, researchers have then focused on their possible involvement in kidney fibrosis development. Interestingly, studies have documented that SMAD3 conditional KO (cKO) mice do not develop kidney fibrosis, and SMAD3 inhibitors are be able to delay the development of diabetic nephropathy by blocking EndMT (Sato et al., 2003; van Meeteren and ten Dijke, 2012). Moreover, Li and colleagues have reported that exposure of primary renal cultured ECs to TGFβ1 reduced VE-cadherin and CD31

expression while promoting αSMA increase, thus suggesting that TGFβ can promote EndMT in the kidney (Li et al., 2009).

Moreover, EndMT has been associated with lung fibrosis development. By inducing lung fibrosis in a lineage-tracing animal model system, Hashimoto and colleagues have indeed demonstrated that activated fibroblasts derive from ECs during a lung fibrotic response (Hashimoto et al., 2010). Interestingly, TGFβ and Ras signaling were reported as mediator of this EndMT.

All these indications, along with others, support the idea that TGFβ signaling is deeply involved in cardiac, renal and lung fibrosis, and understanding how it mechanistically regulates EndMT could be of primary importance for improving currently available treatments.

1.2.6.2 EndMT in cancer, FOP and CCM diseases

A tumor mass consists of cells having a malignant behavior, embedded in a stroma of ECM and cells of various origins (Wang et al., 2017). In order to grow and expand, tumor cells require a favorable environment that fosters their proliferation and help them invading nearby tissues.

Within the tumor stroma, contributing to generate an advantageous environment, there are fibroblasts, and, in particular, a sub-population of them named cancer-associated fibroblasts (CAFs). CAFs are considered key promoters of tumor growth and progression, and consist of activated fibroblasts, whose newly acquired phenotype contributes to the oncogenic transformation of epithelial cells within the tumor. The population of CAFs derives from cells of different origins, mainly from locally resident fibroblasts, but also cells composing the basal membrane or periadventitial cells. Interestingly, a 2008 work by Zeisberg and colleagues has revealed for the first time that CAFs can also have an endothelial origin (Zeisberg et al., 2007a). Indeed, by performing immunostaining of tumor

tissues coming from a melanoma mouse model, the authors found that tumor stroma fibroblasts were positive both for mesenchymal markers (FSP1 and αSMA) and for the endothelial marker CD31. In particular, around 40% of FSP1 and 10% αSMA positive fibroblasts were also co-expressing CD31, thus suggesting an endothelial origin. To prove this hypothesis, the authors employed a lineage-tracing cell system, where the expression of Cre recombinase enzyme is under the control of the endothelial specific promoter Tie2 (**Figure 8**). Tie2Cre mice were then crossed with Rosa26LacZ mice, so that, once the Cre recombinase expression was induced, ECs were permanently "labeled" and could be traced even after a presumed transdifferentiation. Thanks to this system, Zeisberg and colleagues observed that many CAFs were indeed of endothelial origin, and strongly suggested that ECs generated CAFs through an EndMT switch. The authors have also shown that sustained exposure to TGFβ1 of cultured ECs generated cells positive for FSP1,

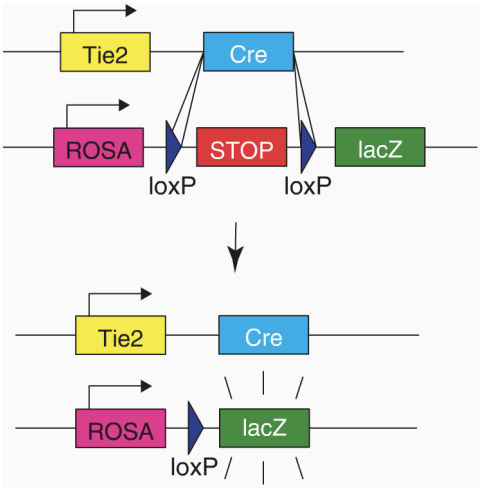

Figure 8. Lineage-tracing system strategy to label ECs undergoing EndMT. In order to specifically express Cre recombinase only in the endothelium, *Cre* gene is placed under the control of the endothelial-specific promoter Tie2. Thus, the Rosa26 reporter vector mediates lacZ expression once the loxP sites flanking a stop codon are genetically excised by Cre recombinase expressed in ECs. As a result, the irreversible expression of lacZ marker occurs only in ECs, and this allows to trace back activated fibroblasts to ECs that underwent EndMT. *Taken from: Potenta S, Zeisberg E, Kalluri R. The role of endothelial-to-mesenchymal transition in cancer progression. Br J Cancer. 2008;99(9):1375-9*

again suggesting that endothelial-derived CAFs could originate from ECs undergoing EndMT. Further evidence of ongoing EndMT in tumor context comes from a 2013 work from Pietras' group (Anderberg et al., 2013). In this very interesting paper, the authors generated pancreatic tumor mouse models heterozygous for the TGFβ co-receptor endoglin (RIP1-Tag2;*Eng*$^{+/-}$) and observed an increased tumor dissemination in mutant mice compared to control ones. The augmented metastatic spread was not due to an increased tumor vessel permeability or density, rather it could be accounted for an ongoing EndMT. Indeed, the authors found a markedly reduced expression of the endothelial specific marker CD31 paralleled by an increased number of αSMA positive ECs in RIP1-Tag2;*Eng*$^{+/-}$ mice. Moreover, they observed a significantly increased expression of Twist1 and of the ALK5-induced EndMT genes Fn1 and Serpine1 specifically in ECs isolated from RIP1-Tag2;*Eng*$^{+/-}$ mice. Very interestingly, the increased tumor cell transmigration observed upon endoglin KO in ECs was strongly reduced by using TGFβRI specific inhibitors. In conclusion, these data suggested that ALK5-mediated EndMT in RIP1-Tag2;*Eng*$^{+/-}$ contributes to metastatic spread and, thus, EndMT is emerging as a driving process that favors tumor progression.

Fibrodysplasia ossificans progressive (FOP) is a sever genetic disorder in which muscle and ligaments are progressively replaced by bone tissue, in a process known as heterotypic ossification (HO). One of the leading causes of FOP disease is represented by an autosomal dominant activating mutation of the BMP TβRI ALK2 (Shore et al., 2006). Therefore, ALK2 and downstream SMAD signaling are continuously activated. Interestingly, a transgenic mouse model for HO, wherein ALK2 is constitutively activated, showed that ectopic bone cells expressed also endothelial-specific markers, like VE-cadherin, Tie1, Tie2 and von Willebrand Factor (vWF) (Medici et al., 2010). Subsequent *in vivo* analyses, using lineage-tracing systems, have clearly demonstrated that mesenchymal cells responsible for HO at

early stage disease were of endothelial origin, thus proving that EndMT is a key molecular mechanism that drive ossification in FOP (Medici et al., 2010).

Moreover, in the past years, our group has discovered that EndMT is the driving mechanism that contributes to vascular lesion development in CCM pathology (Maddaluno et al., 2013). This devastating disease mainly affects the brain microcirculation, as it induces the formation of enlarged, irregular, leaky and multi-lumen blood vessels that are prone to rupture and can lead to brain hemorrhages. CCM can occur both in a sporadic or familial form, and etiological causes for familial CCM are *loss-of-function* mutations in any of the three CCM genes (CCM1, CCM2 or CCM3). We reported for the first time that brain lesions in CCM are formed by ECs undergoing EndMT, as shown by the acquisition of mesenchymal (FSP1, αSMA, N-cadherin, Snai2 and Krüppel-like factor 4 (KLF4)) and stem cell markers (CD44 and Id1), paralleled by a loss of Claudin-5 expression (Maddaluno et al., 2013). We further found that deletion of CCM1 led to the activation of the MEKK3-MEK5-ERK5-MEF2 signaling cascade, resulting in a strong upregulation of KLF4 in ECs *in vivo* (Cuttano et al., 2016). KLF4, in turn, causes BMP6 production and BMP/SMAD1 signaling activation. Interestingly, the EndMT switch observed in CCM1 deficient mice is promoted by both KLF4 transcriptional activity and KLF4-dependent BMP signaling activation, because their inhibition through genetic or pharmacological approaches markedly reduced CCM lesion development and progression. Remarkably, genetic ablation of KLF4 in CCM1 KO mice prevented their death, indicating that KLF4 could be a crucial therapeutic target for the treatment of CCM (Cuttano et al., 2016).

Taken together, these reports have shown a clear correlation between the EndMT switch occurring in numerous pathologies and the TGFβ/BMP signaling. Future studies will then investigate how to prevent pathological EndMT by modulating TGFβ/BMP signaling and, thus, provide novel therapeutic strategies.

1.3 Yes-Associated Protein (YAP)

1.3.1 The discovery of YAP as a target of the Hippo signaling pathway

The Hippo signaling pathway is a serine-kinase cascade and the first YAP regulatory pathway described. The different proteins composing the pathway core were discovered individually in *Drosophila melanogaster*, through genetic screening aiming at identifying novel tumor suppressors and genes regulating organ growth (**Figure 9**). The first one to be identified was the kinase *Warts* (Wts) in 1995, encoded by *lats* gene (Xu et al., 1995), and, few years later, a similar screening approach allowed the identification of *Salvador* (Sav) as a Wts adaptor protein (Tapon et al., 2002). Subsequently, in 2003, four different groups found Hippo as the kinase responsible for Wts phosphorylation and activation and described that Hippo *loss-of-function* approaches led to increased proliferation and apoptosis overcome (Harvey et al., 2003; Jia et al., 2003; Pantalacci et al., 2003; Wu et al., 2003). The last component discovered was the Wts cofactor *Mob as tumor suppressor* (Mats) (Lai et al., 2005). Notably, loss of any of the Hippo core components resulted in uncontrolled cell proliferation, reduced apoptosis and tissue overgrowth. In addition to this, the discovery of their physical and functional interaction led to the establishment of a novel pathway named after the commonly shared phenotype of overgrowth resembling a hippopotamus (Hippo), where the kinase Hippo phosphorylates and activates the downstream Wts kinase in concern with Sav and Mob co-adiuvators. By that time, however, the downstream target was not yet identified.

It was not until 2005 that the Hippo core components Wts, Sav and Hippo were linked to the downstream effector *Yorkie* (Yki) (Huang et al., 2005). In this milestone paper, Huang and colleagues showed that Wts kinase binds to and phosphorylates Yki, thereby inhibiting the transcription of down-stream target genes. Interestingly,

Yki overexpression resulted in increased cell proliferation and tissue overgrowth, phenocopying what previously observed in *loss-of-function* analysis of Wts, Sav and Hippo. In light of these results, the authors concluded that the Hippo signaling pathway is a negative regulator of Yki transcriptional activity and proposed Yki as a novel potential oncogene.

Intriguingly, the core components of the Hippo signaling cascade are conserved throughout metazoan, and this includes mammals as well. Parallel studies performed in human and mouse cell lines allowed the identification of the Hippo mammal orthologues, illustrated in **Figure 9**. Hippo orthologue are represented by Mammalian STE-20 kinase 1 and 2 (Mst1/2); Sav1, also known as hWW45, is the orthologue of Sav; Msp-one-binder 1/2 (Mob1/2) are the orthologue of Mats; Large tumor suppressor 1 and 2 (LATS 1/2) are the orthologue of Wts; and Yes-associated protein (YAP) together with transcriptional activator with a PDZ-binding domain (TAZ) are Yki mammal orthologues. Very interestingly, these proteins share a high degree of homology with their correspondent protein and, functionally, human LATS1, MATS1, MST2 and YAP can rescue *loss-of-function* mutations of their respective orthologues in *D. melanogaster* (Edgar, 2006). Moreover, subsequent studies showed that the Hippo signaling pathway functions in a similar way in mammals as in *Drosophila* (Camargo et al., 2007; Dong et al., 2007; Hao et al., 2008; Zhao et al., 2007), corroborating the importance of this pathway in controlling tissue growth and preventing cancer development.

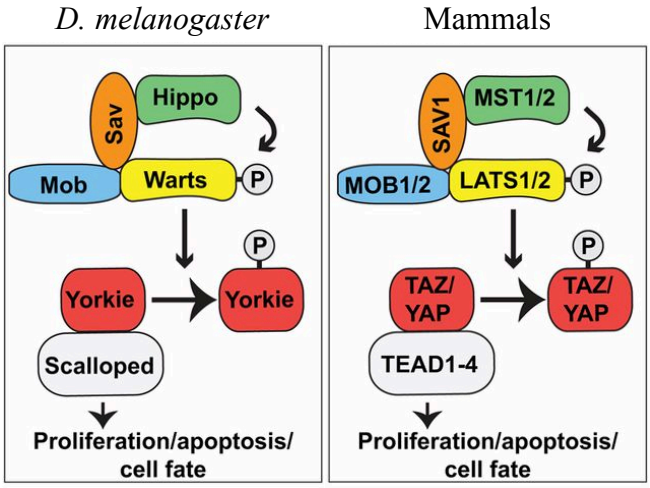

Figure 9. The core components of the Hippo signaling pathway in *D. melanogaster* and mammals. Once triggered, the Hippo kinase (MST1/2 in mammals) phosphorylates and activates the downstream effector kinase Wts (LATS 1/2) through the aid of the co-activators Sav (SAV1) and Mob (MOB1/2). Activated Wts, in turns, phosphorylates Yorkie (YAP or TAZ in mammals) in several serine residues, promotes its cytoplasmic retention and negatively regulates Yorkie co-transcriptional activity. To simplify the parallelism between *D. melanogaster* and mammal Hippo pathway, orthologs are illustrated with the same color. *Adapted from: Varelas, X. Development 2014;141:1614-1626*

1.3.2 YAP protein structure and main functions

YAP is a 65 kDa protein, initially identified by Marius Sudol in 1994 as an interactor of the tyrosine-kinase c-Yes (Sudol, 1994; Sudol et al., 1995a). YAP SH3-binding motif was shown to mediate YAP-c-Yes interaction, but little is known about the biological function of this interaction. Functionally, YAP is the orthologue of the *Drosophila* protein Yki together with TAZ and, like Yki, it is a downstream effector of the well-conserved signaling cascade Hippo pathway (Huang et al., 2005; Zhao et al., 2007).

Humans possess 8 different isoforms of YAP, broadly divided in two main classes containing either one (YAP1) or two WW domains (YAP2) (Gaffney et al., 2012; Komuro et al., 2003) (**Figure 10**). These domains are composed of around

30 to 35 amino acids comprising two conserved tryptophan (W) residues and mediate binding to partner proteins bearing a proline-rich motif PPxY (where P stands for proline, x for any amino acid and Y for tyrosine) (Sudol et al., 1995a; Sudol et al., 1995b). PPxY motif is found in many different proteins, like transcriptional factors and proteins mediating YAP localization and activity. Interestingly, many components of the Hippo signaling pathway (including YAP itself) bear this motif, and they employ it to interact with YAP and regulate its localization and activity. Furthermore, this motif is found in SMADs, like SMAD1 and -3, and studies have documented their importance in mediating the binding between YAP and SMADs (Aragon et al., 2011).

At YAP C-term lies a PDZ-binding motif, through which proteins carrying a PDZ domain interact with YAP. These proteins can be transmembrane or cytoskeleton proteins (Ye and Zhang, 2013).

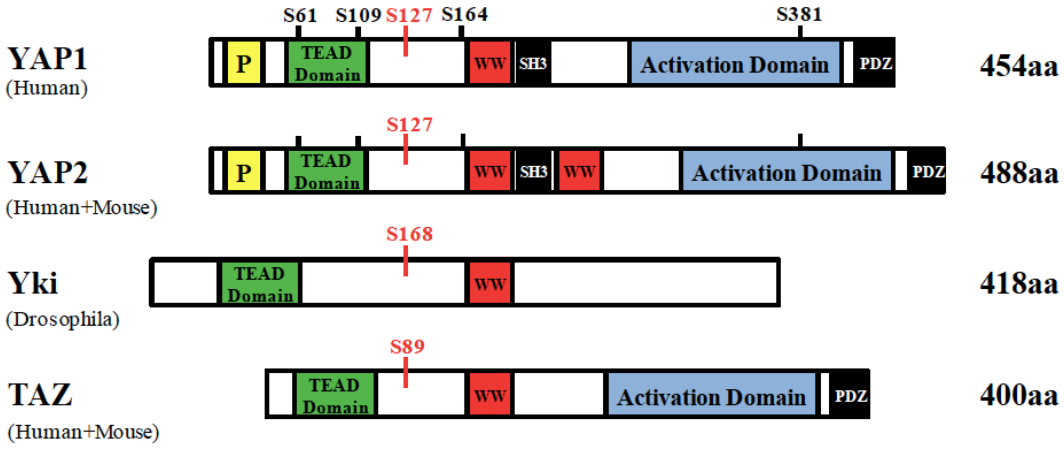

Figure 10. Regulatory domains of YAP1, YAP2, Yki and TAZ. Comparison between YAP1 and YAP2 isoforms with Yki and TAZ show that all of them contain WW domains and a TEAD binding domain. Other important domains are the transactivation at the C-term found on YAP1/2 and on TAZ, together with a PDZ-binding motif. YAP1 and YAP2 possess also a prolin-rich motif at their N-term. The residues important for YAP cytoplasmic retention are also illustrated. Details about the function of each domain are explained in the main text. *Taken from: Robert Neil Judson "The Role of Yes-Associated Protein (YAP) in Skeletal Muscle Satellite Cells and Myofibres"*

Activated LATS1/2 phosphorylates YAP in five different serine (S) residues: S61, S109, S127, S164, and S381 (Basu et al., 2003; Zhao et al., 2007). Among these residues, S127 is probably the most important to regulate YAP localization, since phosphorylated S127 increases YAP binding affinity to 14-3-3 protein and causes its cytoplasmic retention (Basu et al., 2003). Additionally, S127 can be phosphorylated by Akt kinase, resulting in cytoplasmic sequestration by 14-3-3 too (Basu et al., 2003). Phosphorylation at S381 by LATS1/2, instead, is involved in YAP turnover as it promotes further phosphorylation at S384 and S387 by CK1δ/ε kinase and ubiquitination by $SCF^{beta\text{-}TRCP}$ E3 ligase, leading ultimately to YAP proteosomal degradation. These residues lye within the transactivation domain (TAD) located at the C-term of both YAP and TAZ, but missing in Yki. Thus, YAP/TAZ and Yki share evolutionarily conserved domains, functions and regulatory pathway, although some differences have evolved to finely tune YAP/TAZ localization and turnover in mammals. By substituting the five serine residues S61, S109, S127, S164, and S381 with alanine (YAP 5SA), Zhao and colleagues demonstrated that YAP 5SA localizes predominantly in the cell nucleus, where it strongly promotes cell proliferation and loss of contact-inhibition growth. These indications support the idea that YAP is an oncogene and the Hippo pathway work to prevent oncogenic transformation by negatively regulating YAP (Zhao et al., 2009; Zhao et al., 2007).

One of the key molecular functions of YAP is to promote gene transcription by serving as a transcriptional co-activator (Yagi et al., 1999). Since YAP lacks a DNA binding-motif and cannot bind DNA on its own, joined effort from several groups has been made to identify transcriptional factors interacting with YAP. These factors include, among others, β-catenin, MYC, p53, p73, SMAD1/2/3/4 and RUNX 1/2/3 (reviewed in (Varelas, 2014)). Consequently, YAP can regulate an array of diverse biological functions depending on the transcriptional partner engaged, as further

discussed in section 1.3.5. The most characterized class of YAP transcriptional partners is however represented by TEAD protein family (*Scalloped* in Drosophila), which includes TEAD1-4. This protein family bind to YAP through the TEAD-binding domain lying at YAP N-term to promote the transcription of proliferation genes and restrain apoptosis and differentiation (Vassilev et al., 2001; Wu et al., 2008; Zhang et al., 2008; Zhao et al., 2008). Indeed, YAP-TEAD binding inhibition results in reduced proliferation of the epidermis and of cardiomyocytes in mice (Schlegelmilch et al., 2011; von Gise et al., 2012). This supports the idea that YAP-TEAD interaction is crucial for YAP tissue growth promoting activity and genome-wide studies corroborated the importance of this interaction, since most of YAP and TEAD genomic loci are in common (Stein et al., 2015; Zanconato et al., 2015).

As mentioned at the beginning of this section, Yki has two mammal orthologs, YAP and TAZ. Both proteins are regulated by the Hippo signaling and function as downstream co-transcriptional factors. TAZ structure is quite similar to the one of YAP, reaching a 46% identity in their aminoacidic sequence (Zhao et al., 2008). Nevertheless, differences exist (**Figure 10**), which can partially explain the different phenotypes displayed by total YAP KO mice versus total TAZ KO mice (discussed in the following section), suggesting that YAP and TAZ do not compensate for each other's functions.

1.3.3 YAP and the Hippo pathway in mammals: regulators of development, tissue homeostasis, tissue regeneration, and cancer

Given the importance of Yki and Hippo signaling pathway in regulating cell proliferation, apoptosis and organ growth in D*. melanogaster* (Huang et al., 2005), it is not surprising that researchers began to extensively characterize the role of YAP and of the Hippo core components in mammals. Studies on total YAP KO mice revealed that mutated embryos die around E8.5, due to defects in chorioallantoic

fusion, yolk sac vasculogenesis and body axis elongation (Morin-Kensicki et al., 2006), reinforcing the idea that YAP is required for proper control of tissue growth at early stage development. Conversely, total TAZ KO mice were only partially embryonic lethal, with survivors showing polycystic kidneys and lung emphysema (Tian et al., 2007). Thus, YAP and TAZ functions are required for proper embryo development and they cannot fully compensate for each other's biological activities.

In order to avoid embryonic lethality and to better characterize how YAP controls organ size, two independent groups analyzed YAP biological functions in mammals by utilizing inducible liver-specific YAP overexpression approaches (Camargo et al., 2007; Dong et al., 2007). Both studies showed that overexpression of YAP caused liver overgrowth due to a boost in cell proliferation rather than an increase in cell size. The observed phenotype was due to YAP aberrant activity that promoted resistance to apoptosis, and could be rescued after hampering YAP overexpression, thus indicating that YAP contributes to regulate liver size. Notably, following reports on *loss-of-function* mutations in the Hippo core components resulted in a similar phenotype (Lu et al., 2010; Nishio et al., 2016; Zhou et al., 2009). These seminal works showed that YAP is a key regulator of liver growth. Shortly after, other studies showed that a correct YAP activity is required for proper tissue growth in skin (Schlegelmilch et al., 2011), pancreas (Zhang et al., 2013) and neural tube (Cao et al., 2008).

Conversely, depletion of YAP expression specifically in the gut did not alter normal intestinal development or homeostasis (Cai et al., 2010). This study, instead, pointed YAP as an important regulator of intestinal tissue regeneration following injury. Moreover, in the heart, where cardiomyocytes stop proliferating a week right after birth and cardiac injuries are healed through the formation of fibrotic scars rather than through cardiomyocyte proliferation, YAP has been found to promote cardiomyocyte proliferation following heart injury (von Gise et al., 2012; Xin et al.,

2013). This finding not only define a prominent role for Hippo and YAP in cardiac tissue regeneration, but also opened up novel possible ways to improve heart regeneration after injury. The biological functions of YAP in mammals, thus, seem to be tissue and context-specific and further studies are required to better define its role in different mechanisms. Yet YAP is emerging as an important regulator of many biological processes required for proper tissue development and homeostasis, making it a very interesting clinical target in a variety of disorders.

Consistently with its pro-proliferative and anti-apoptotic effects, the activity of YAP has also been linked to cancer development and tumor progression. Indeed, overexpressing YAP in liver results in hepatocellular carcinoma development already after 3-10 weeks (Camargo et al., 2007; Dong et al., 2007). It should be noted that hepatocellular carcinoma can also arise upon *loss-of-function* mutation in the Hippo core components, even if this takes much longer to develop. Hence, other pathways along with the Hippo pathway seem to be required to finely control YAP localization and transcriptional activity, as it will be better explained in the section 1.3.4. Further studies have shown that overexpression of YAP in MCF10A cells caused hyperproliferation and loss of contact-inhibition growth (Overholtzer et al., 2006). Moreover, these mutated cells became more invasive and migratory and showed altered expression of epithelial markers, letting the authors conclude that YAP actively promotes EMT and cellular transformation. As discussed in section 1.2.1, EMT is emerging as a key regulatory mechanism that drives tumor development and metastatic dissemination. Thus, one way through which YAP can contribute to tumor progression is being a positive EMT regulator. Subsequent similar findings supported this hypothesis (Pei et al., 2015; Yuan et al., 2016; Zhao et al., 2009) and, more importantly, it was demonstrated that silencing of YAP can rescue the EMT phenotype of certain cell systems (Wang et al., 2016b). From the molecular point of view, YAP stimulates an EMT response by inducing the

expression of EMT markers and driving factors, like Snai1 and Snai2, and ZEB1 (Shao et al., 2014; Wang et al., 2016b; Xiao et al., 2015). Although these indications support the idea that YAP works as an oncogene, the underlying mechanisms are not yet fully elucidated and seem to be tissue- and context-specific. Indeed, in breast cancer, YAP was found to play a tumor-suppressive rather than a tumor-promoting role (Yuan et al., 2008). Hence, more detailed and tumor-specific studies are required.

Moreover, *Yap* gene is often found amplified in a variety of human cancers, such as medulloblastomas, esophageal squamous carcinomas and hepatocellular carcinomas (Fernandez et al., 2009; Overholtzer et al., 2006; Snijders et al., 2005; Zender et al., 2006). Interestingly, YAP expression is found upregulated in cancers prone to metastasize to lymph-nodes (Liang et al., 2014; Wang et al., 2010; Zhou et al., 2013). While in the primary sites of these tumors YAP expression is upregulated, the sub-cellular localization and activity of YAP in metastasis are even more altered. However, an exhaustive analysis of YAP sub-cellular localization and expression in different malignancies is missing and should distinguish between primary and secondary sites in order to better identify in which biological processes YAP is involved.

While YAP is considered an oncogene and is often found amplified in cancer, the expression and activity of Hippo pathway components are not dysregulated as often as YAP in human cancer. This suggests that other pathways along with the Hippo signaling likely contributes to regulate YAP activity and will be discussed in the following section.

1.3.4 Upstream regulators of Hippo pathway and other YAP regulatory pathways

The spatial regulation of YAP within a cell is mainly determined by its phosphorylation status at Ser127 (Basu et al., 2003). Indeed, once YAP is phosphorylated at Ser127 (pYAP S127), is recognized and bound by 14-3-3 protein, ultimately resulting in cytoplasmic retention and nuclear exclusion. pYAP S127 is primarily mediated by LATS 1/2 kinases, belonging to the canonical Hippo signaling module (Hao et al., 2008). As a result, when the Hippo signaling cascade is turned ON, YAP is phosphorylated and segregated in the cytoplasm. On the contrary, when the Hippo pathway is shut OFF, YAP phosphorylation is terminated and so YAP is free to shuttle to the nucleus (**Figure 11**).

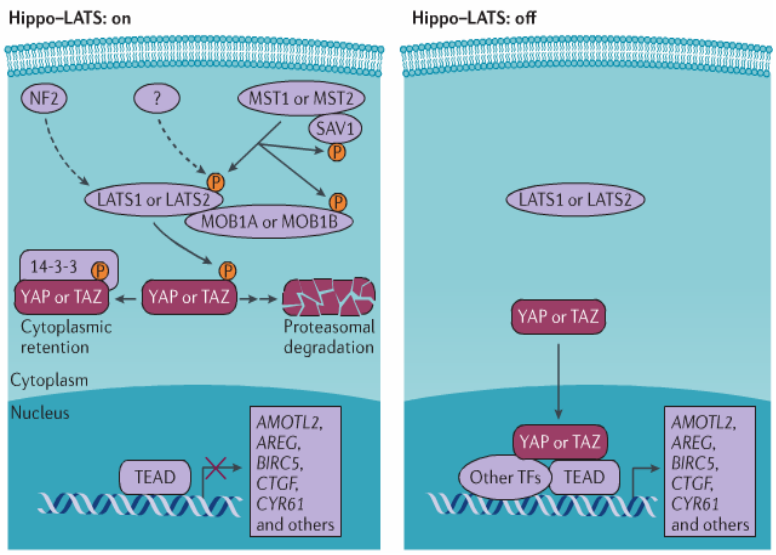

Figure 11. Canonical Hippo pathway overview. When the Hippo signaling is activated (Hippo ON), LATS1/2 are phosphorylated and activated by MST1/2. Subsequently, phosphorylated LATS1/2 trigger YAP or TAZ phosphorylation at Ser 127 or Ser 89, respectively, and cause their binding to 14-3-3 protein and cytoplasmic retention. Further post-translational modifications lead to YAP or TAZ proteosomal degradation. When the Hippo signaling cascade is prevented (Hippo OFF), YAP and TAZ are no longer phosphorylated and thus they can shuttle to the nucleus where they drive the expression of target genes, such as connective tissue growth factor (CTGF), Cysteine-rich angiogenic inducer 61 (CYR61), Inhibin beta A (INHBA) and others. *Taken from: Moroishi T. "The emerging roles of YAP and TAZ in cancer", Nat Rev Cancer. 2015;15(2):73-9.*

Although nowadays the Hippo core components along with their functions have been extensively characterized, much effort is still needed to properly define their upstream regulators. That said, researcher have already found a plethora of Hippo regulatory mechanisms, whose common characteristics are that they sense the extracellular environment and that their final output is to determine YAP localization and activity.

1.3.4.1 Cell density and cell polarity

In several studies, one recurrent observation is that YAP S127 phosphorylation and sub-cellular localization reflect cellular density (Giampietro et al., 2015; Varelas et al., 2010; Zhao et al., 2007). Indeed, while in sparse cultured cells YAP is mostly confined to the nucleus, with increasing cells density YAP gets phosphorylated at S127 and sequestered in the cytoplasm by interacting with 14-3-3 protein (Zhao et al., 2007). Thus, YAP sub-cellular localization depends on cell density. Moreover, while the cellular density increases, cells begin to interact with each other by forming AJs, and originate a polarized stratum of cells.

It is not surprising, then, that both junctional and polarity complexes are involved in regulating YAP sub-cellular localization. In confluent epithelial cells, indeed, clustering of E-cadherin activates the Hippo signaling pathway to phosphorylate YAP and sequesters it in the cytoplasm (Kim et al., 2011). In this way, formation of epithelial AJs prevents YAP pro-proliferative activity and controls contact-inhibition growth (**Figure 12, panel A**). Moreover, two independent studies demonstrated that the E-cadherin binding partner α-catenin binds to pYAP S127 and prevents its nuclear accumulation in confluent epithelial cells (Schlegelmilch et al., 2011; Silvis et al., 2011). Although these studies reported that YAP is phosphorylated at S127 by either LATS1/2 or by an unknown kinase upon clustering of epithelial AJs, both reports agreed on the importance of AJs in preventing YAP nuclear accumulation

and YAP-mediated cell proliferation. Thus, when cells are in a confluent state, they adhere with each other by forming homophilic E-cadherin-E-cadherin interactions that, in turn, trigger Hippo pathway activation and YAP nuclear exclusion and prevent uncontrolled cell-proliferation.

Additionally, Merlin/NF2, a membrane-associated protein that connects to the cytoskeleton (McClatchey and Giovannini, 2005), was shown to potently induce the canonical Hippo signaling cascade and thus repress YAP activity (**Figure 12, panel A**) (Striedinger et al., 2008; Zhang et al., 2010). Accordingly, Merlin is a tumor suppressor, whose inactivation results in the development of the benign tumor Neurofibromatosis Type II (Rouleau et al., 1993). Merlin was also found to interact and be activated by Angiomotin (AMOT) protein family at TJs (Li et al., 2015; Yi et al., 2011). AMOT are important regulators of cell polarity and cytoskeleton stability, that were found to regulate YAP activity at different levels and both in a positive and negative manner (**Figure 12, panel B**). Indeed, AMOT can function as YAP co-factor (Yi et al., 2013), but can also trigger LATS activation to restrict YAP transcriptional activity (Adler et al., 2013; Paramasivam et al., 2011). Interestingly, AMOT can retain YAP in the cytoplasm by directly interacting with it (Chan et al., 2011; Mana-Capelli et al., 2014; Zhao et al., 2011). This association is mediated by AMOT PPxY motif and YAP WW domains and thus it is independent of YAP phosphorylation at S127 (Chan et al., 2011; Zhao et al., 2011). Consequently, AMOT can control YAP sub-cellular localization and activity independently from LATS-induced phosphorylation at S127, opening up a novel additional mechanism that coordinates YAP nuclear translocation. In addition, YAP and F-actin compete for binding to AMOT (Chan et al., 2011; Zhao et al., 2011). Upon LATS1/2 phosphorylation of AMOT, F-actin dissociates from AMOT, favoring the interaction between YAP and AMOT and YAP cytoplasmic sequestration. Hence, AMOT inhibits YAP nuclear activity through several mechanisms, which can be either

dependent or not by LATS and further studies will better explain its mode of action under specific cellular contexts. Along with AMOT, other cell polarity proteins, such as Crumbs, Pals and Patj can inhibit YAP nuclear localization and activity (**Figure 12, panel A**) (Varelas et al., 2010). Thus, cell polarization is emerging as an important process that restricts YAP transcriptional activity.

Collectively these studies showed that both cell density and cell polarity contribute to tissue homeostasis by properly balancing YAP localization and nuclear activity. Conversely, their alteration results in an increased YAP nuclear localization, and this can likely contribute to EMT and cancer development.

1.3.4.2 GPCR receptors

Another recently discovered YAP regulatory mechanism takes place through the G-protein coupled receptors (GPCR) (**Figure 12, panel A**). This large family of receptors senses the extracellular signals and, upon ligand binding, triggers a signaling cascade through their cognate G-proteins. Depending on the G-protein coupled to the receptor, the Hippo signaling pathways is either inhibited or triggered. For example, lysophosphatidic acid, thrombin and sphingosine-1-phosphate (S1P) ligands signal through GPCRs coupled to Gα12/13 or Gαq/11 and function as potent activators of YAP by inducing assembly of the actin cytoskeleton (Miller et al., 2012; Mo et al., 2012; Yu et al., 2012). Conversely, epinephrine and glucagone ligands, which signal through Gαs-coupled receptors, promote pYAP S127 and thus repress its target gene activation (Yu et al., 2012).

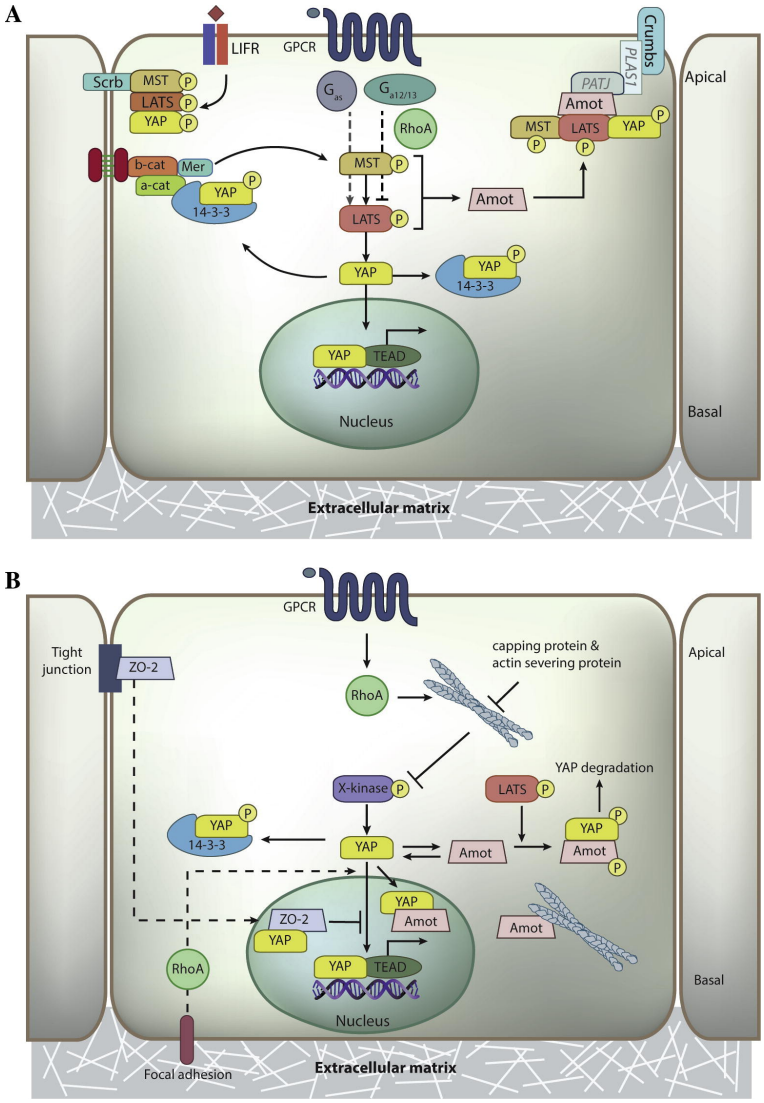

Figure 12. Upstream regulators of YAP. YAP upstream regulators can be divided in those that activate the canonical Hippo pathway to restrict YAP nuclear localization and activity (upper panel, A) from those that directly control YAP (lower panel, B).

A) Hippo can be activated by clustering of AJs, by cell polarization and by GPCRs acting through Gαs, whereas it is turned off in response to GPCRs coupled to Gα12/13 or Gαq/11.

B) YAP nuclear/cytoplasmic shuttling and activity is also under the control of mechanisms independent from the Hippo signaling pathway. Rho GTPases activity in response to mechanical stress signaling induces actin stress fiber formation, that, in turn, promote YAP nuclear localization and activity by deactivating unknown kinases responsible for YAP phosphorylate. F-actin competes with YAP for AMOT binding and thus favors its nuclear translocation. AMOT can directly bind to YAP PPxY motif through its WW domains and retain in the cytoplasm. However, the p130 isoform of AMOT can engage with YAP in the nucleus and act as a transcriptional co-activator of YAP-TEAD. *(continues on the next page)*

(continues from the previous page) Additionally, AMOT phosphorylation by LATS kinase promote YAP protesomal degradation. For detailed explanations, please refer to the main text. *Taken from: Low BC "YAP/TAZ as mechanosensors and mechanotransducers in regulating organ size and tumor growth." FEBS Lett. 2014;588(16):2663-70*

1.3.4.3 Mechanotransduction

Along with soluble factors, cells can covert mechanical signals into intracellular biochemical inputs - a process referred as mechanotransduction (Wang et al., 2009b) - by sensing changes in the extracellular environment that affect cell shape, cell size and the rigidity of the ECM (Dupont et al., 2011). All these mechanical inputs translate in a dynamic regulation of the actin cytoskeleton, that, in turn, control YAP nuclear localization (**Figure 12, panel B**). The activity of Rho GTPase and the formation of actin stress fibers, indeed, were shown to sustain YAP nuclear accumulation and target gene regulation. Conversely, YAP nuclear activity was prevented in response to inhibitors of tension-related proteins. Thus, cells grown in soft extracellular matrix or in a confined area display a high level of YAP in the cytoplasm, while cells grown in stiff ECM or allowed to spread show a predominant YAP nuclear localization (Dupont et al., 2011; Halder et al., 2012). Controversies about the kinase responsible for pYAP S127 have been reported. Piccolo's group excluded LATS1/2, since they observed that YAP activity could not be restored after LATS1/2 silencing when actin fibers formation is inhibited (Aragona et al., 2013). On the contrary, Guan and Sasaki's groups reported that LATS activity is shut off by the formation of stress fibers, leading ultimately to YAP target gene expression (Wada et al., 2011; Zhao et al., 2012). Mechanical signals, therefore, have emerged as novel regulator of YAP localization and activity, but clearly more studies are required to better elucidate how the actin cytoskeleton modulates YAP.

1.3.5 Crosstalk with other signaling pathways

1.3.5.1 YAP and canonical Wnt signaling

The Wnt pathway is a fundamental signaling cascade required for the polarity of the primary body axis and for proper embryo development, as well as for tissue homeostasis in adults (reviewed in (Nusse and Clevers, 2017)). Upon Wnt stimulation, the downstream effector β-catenin is activated, translocates from the cytoplasm to the nucleus, and drives the transcription of target genes. In a "Wnt OFF" situation, instead, β-catenin protein levels are kept under tight control by the combined effort of several proteins clustered together in a multimeric complex known as β-catenin destruction complex (DC) (**Figure 13, left panel**). DC is composed of the scaffolding proteins Disheveled (Dvl) and Axin, of APC, of two constitutively active kinases, GSK3 and CK1, and of the E3 ubiquitin ligase βTrCP. In the DC, Axin binds to β-catenin, while GSK3 and CK1 phosphorylate it in a sequential manner in Ser45, Thr41, Ser37 and Ser33. This phospho degron-motif is then recognized by βTrCP, targeting β-catenin for proteosomal degradation. In this way, the DC complex finely controls β-catenin protein levels and prevents its nuclear translocation. In a "Wnt ON" scenario, a seven-transmembrane receptor called Frizzled (Fz) recognizes and binds to Wnt ligands to initiate the signaling cascade (**Figure 13, right panel**). In particular, Fz forms a heterodimer with Lrp5/6 co-receptors, engages to the DC and interrupts its activity, ultimately restricting β-catenin degradation and promoting its nuclear translocation (**Figure 13, right panel**). Once in the nucleus, β-catenin interacts with T-cell factor/lymphoid enhancer-binding-factor-1 (TCF) or LEF to drive the expression of target genes, such as *Axin1*, *Cyclin D1* and *c-Myc*.

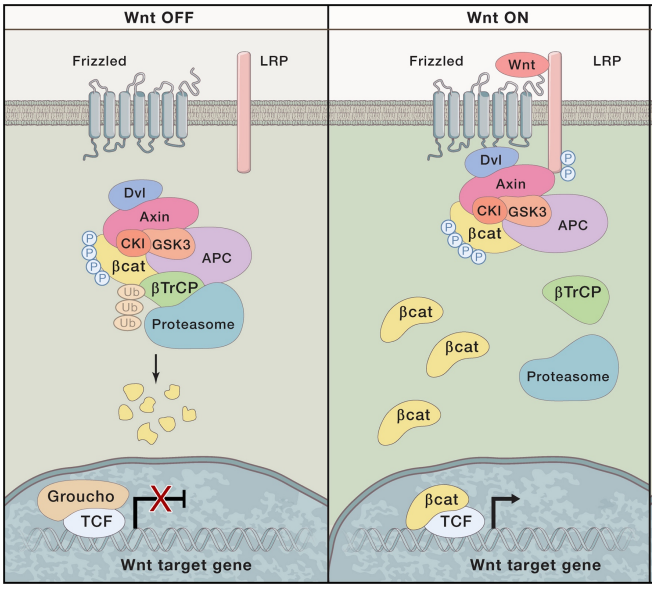

Figure 13. Canonical Wnt signaling overview. When a Wnt ligand is not present (Wnt OFF), a destruction (DC) complex formed by Dvl, Axin, APC, two constitutively active kinases, GSK3 and CK1, and the E3 ubiquitin ligase βTrCP bind to β-Catenin and target it to proteosomal degradation. Upon ligand binding (Wnt ON), Frizzled receptor complex with Lrp co-receptor and together recruit the DC to the cytosolic membrane. This causes conformational changes in the DC, which ultimately lead to β-Catenin release and nuclear accumulation, where it drives gene transcription. *Taken from: Nusse R "Wnt/beta-Catenin Signaling, Disease, and Emerging Therapeutic Modalities." Cell. 2017;169(6):985-99.*

In the past years, Wnt/β-catenin and Hippo signaling pathways have been shown to modulate each other at different levels. Initially, heart-specific Sav1 KO mice showed an increased cardiomyocyte proliferation due to high nuclear YAP and, concomitantly, an up-regulation of the Wnt target genes Sox2, Snai2 and Survivin (Heallen et al., 2011). More in-depth analysis revealed that these mice had an enhanced β-catenin nuclear-staining and their crossing with heterozygous β-catenin mice (Salv/β-cat$^{f/+}$ cKO) rescued target gene expression levels as well as cell proliferation rate. Moreover, immunoprecipitation analysis showed that β-catenin binds to total YAP but not to pYAP, suggesting that their interaction occurs in the nucleus. Indeed, β-catenin and YAP were able to drive Sox2 and Snai2 gene expression together, as shown by sequential chromatin immunoprecipitation (ChIP)

analyses. Intriguingly, a 2014 study by Piccolo's group has demonstrated that, in a "WNT OFF" situation, YAP is incorporated in the DC, where it sustains β-catenin degradation by serving as βTrCP docking site (**Figure 14D-E**) (Azzolin et al., 2014). Moreover, the authors showed that Axin directly binds to YAP and proposed that the DC functions as a cytoplasmic "trap" for YAP, restraining its nuclear activity. Conversely, DC disassembly upon WNT stimulation or by APC silencing led to β-catenin stabilization and YAP nuclear accumulation. However, the study did not investigate whether pYAP S127 is dispensable for YAP recruitment to the DC and whether nuclear YAP functions either as β-catenin co-transcriptional factor upon Wnt stimulation or drives the expression of a parallel set of genes. Collectively, these results set YAP as an important modulator of the Wnt/β-catenin signaling and reveal a dual-mode of action that depends both on the cellular compartment and on the presence/absence of the Wnt signal. In the cytoplasm of unstimulated cells, YAP contributes to β-catenin degradation and limits its transcriptional program; nuclear YAP, instead, works as β-catenin co-transcriptional factor. Although further studies are required to better elucidate how Wnt/β-catenin and Hippo signaling pathways cross-talks, it is becoming more and more clear that YAP and β-catenin signaling are intertwined, and clarifying their role will help unravelling molecular mechanisms often altered in pathological disorders.

1.3.5.2 YAP and canonical TGFβ and BMP signaling

Interplays between Hippo and Wnt signaling are not elusive, since YAP and the TGFβ-effectors SMADs have repeatedly shown to interact with each other. The first described evidence of a possible pathway crosstalk reported that YAP interacted with the inhibitory SMAD7, but not SMAD6 (**Figure 14B**) (Ferrigno et al., 2002). This interaction was partly mediated by the PY motif found on SMAD7, since mutation in

this site did not fully abolished YAP-SMAD7 complex formation, and thus suggesting that other domains are required for their binding. Moreover, the authors reported that YAP and SMAD7 act synergistically to repress TGFβ signaling, likely because the presence of full-lenght YAP reinforced SMAD7- TGFβRI complex formation. Thus, the author concluded that YAP is a negative regulator of the TGFβ signaling. Later on, YAP and SMAD7 structural interactions were unraveled, showing that YAP binds to SMAD7 PY motif through its WW1 domain (Aragon et al., 2011).

Furthermore, Alarcón and colleagues showed that YAP binds to SMAD1 in response to BMP2, and it functions as SMAD1 transcriptional co-activator to drive the expression of *Id1* and *Id2* (Alarcon et al., 2009). Interestingly, phosphorylation in the SMAD1 linker region was required for YAP and SMAD1 association, and it was observed around 20 minutes after BMP2 stimulation, preceded by SMAD1 C-terminal phosphorylation. Hence, the authors concluded that YAP promotes BMP-regulated target genes expression by acting as SMAD1 co-transcriptional factor. Of note, they also observed a weak YAP-SMAD3 interaction, which did not however require TGFβ-mediated SMAD3 linker phosphorylation. A subsequent study from the same group showed that S206 phosphorylation in SMAD1 linker site, mediated by CDK8/9, served as a docking site for YAP WW1 domain, while SMAD1 PY motif was recognized and bound by YAP WW2 domain (Aragon et al., 2011). By binding to pS206 SMAD1, YAP hindered the subsequent GSK3-mediated phosphorylations at T202 and S210, therefore impeding SMURF1 binding to SMAD1 and SMAD1 degradation. In conclusion, the authors proposed a model where YAP binds to pS206 SMAD1 in the nucleus and sustains SMAD1-driven target gene expression by working as a transcriptional co-factor. At the same time, binding of YAP to SMAD1 prevented additional SMAD1 phosphorylations and proteosomal degradation.

By attempting to clarify how cell density and cell polarity complexes impact on Hippo and TGFβ signaling, Varelas and colleagues have demonstrated that YAP/TAZ are required for SMAD2/3 nuclear accumulation and gene expression in response to TGFβ, in a cell-density dependent manner (**Figure 14I**) (Varelas et al., 2010). Confluent Eph4 cells, indeed, not only displayed high levels of YAP/TAZ but also of SMAD2/3 in the cytoplasm, even after TGFβ stimulation. The high density of the cells negatively affected SMAD2/3-driven target gene expression too. Conversely, stimulating sparse cells with TGFβ caused SMAD2/3 nuclear accumulation and target gene expression. Of note, YAP/TAZ were mainly localized in the nucleus of sparse cells, likely because of low Hippo pathway activation. Indeed, depletion of LATS1/2 (the kinase responsible for YAP and TAZ cytoplasmic sequestration) coupled with TGFβ treatment in confluent cells resulted in SMAD2/3 and YAP/TAZ re-localization to the nucleus and increased Ctgf and PAI-1 expression. Interestingly, Varelas showed that formation of cell-cell AJs and polarity complexes prevented YAP/TAZ and SMAD2/3 nuclear accumulation, as well as down-stream target genes expression. Taken together, these results showed for the first time that cytoplasmic YAP/TAZ prevent SMAD2/3 nuclear accumulation, while sustaining SMAD2/3-driven target gene expression. Somehow, cytoplasmic YAP/TAZ impacted on SMAD2/3 nuclear accumulation, probably by retaining SMAD2/3 in the cytoplasm, but the mechanism was not fully clarified by the authors. Moreover, pYAP S127 (cytoplasmic YAP) interacted with SMAD2 only in response to TGFβ, leaving unsolved how cytoplasmic YAP could retain SMAD2 in basal conditions of high dense cultured cells. Whether YAP/TAZ are required for SMAD2/3 nuclear import or nuclear retention or whether YAP/TAZ play different roles in different cell-compartments was not investigated. In support to this work, another group observed a very weak SMAD2 and SMAD3 nuclear translocation in response to TGFβ in confluent HT29 and HaCaT cells (Grannas et al., 2015).

Proximity ligation assays showed also that YAP and SMAD2/3 form few complexes in the cytoplasm of both sparse and dense cultured cells; however, after treatment, an increased association at the level of the nucleus was observed only in sparse cells, supporting the idea that cell density play a role both in TGFβ and in YAP/TAZ signaling. Yet, conflicting data were subsequently reported (Nallet-Staub et al., 2015), raising the need to better clarify how TGFβ, YAP/TAZ and cell density modulate each other as well as better elucidating whether cytoplasmic YAP/TAZ versus nuclear YAP/TAZ can have different functions.

YAP and SMAD3 were also shown to form a transcriptionally active complex together with TEAD4 and p300, driving CTGF expression and thus fostering mesothelioma progression (Fujii et al., 2012). Not only, YAP/TAZ and TEAD, together with SMAD2/3 and OCT4 were also found to balance the expression of pluripotency genes and inhibit the differentiating program of human embryonic stem cells (hESC) (Beyer et al., 2013). Notably, this study proposed for the first time that YAP/TAZ can also repress target genes expression. YAP/TAZ-TEAD and SMAD2/3 complex formation was also observed in a metastatic breast cancer cell line, where it promoted cell migration and cell transformation in response to TGFβ (Hiemer et al., 2014). While both nuclear and cytoplasmic interactions occurred in untreated conditions, an increased nuclear localization and complex formation was observed in stimulated cells. Of note, YAP/TAZ-TEAD and SMAD2/3 were shown to drive gene expression both together and in separate complexes as well as in both positive and negative manner, adding further complexity to the already multifaceted molecular situation.

Following studies have added further complexity on how YAP and SMAD signaling are inter-regulated. A study performed in hESC reported that YAP competes with SMAD to prevent activation of the differentiation program sustained by β-catenin/LEF-1 (Estaras et al., 2015). Moreover, in breast tumor initiating cells,

the expression of YAP negatively correlated with that of SMAD3 (Sun et al., 2016). Conversely, liver-specific deletion of MOB1a/1b (LATS1/2 co-activators), resulted in liver hyperplasia and early lethality due to enhanced YAP and SMAD2/3 nuclear translocation and TGFβ2/3 growth factor release (Nishio et al., 2016). The authors could greatly rescue the phenotype by crossing liver-specific MOB1a/1b mice with YAP floxed/floxed ($YAP^{f/f}$) or $TAZ^{f/f}$ or $Tgfbr2^{f/f}$ mice, thus further showing an inter-pathways regulation.

A recent report showed that, similarly to YAP/TAZ, SMAD2/3 localization and signaling in response to TGFβ is also regulated by matrix stiffness (Szeto et al., 2016). By treating cultured fibroblasts with verteporfin, an inhibitor of YAP transcriptional activity, there was a significant reduction of YAP and TAZ protein levels, concomitant with SMAD2 and 3 down-regulation, resulting in a diminished SMAD2/3 transcriptional activity in response to TGFβ. Thus, the authors concluded that the reduced expression of YAP and TAZ observed upon verteporfin treatment contributed to lower SMAD2/3 nuclear accumulation and signaling, and proposed verteporfin as a novel inhibitor of renal fibrogenesis.

In conclusion, YAP and SMADs signaling have repeatedly reported to modulate each other, both in a positive and negative manner. This probably depends on the cellular context as well as on the sub-cellular localization of YAP and SMADs. Therefore, future studies will help clarifying this intricate, but certainly very important, pathway cross-talk.

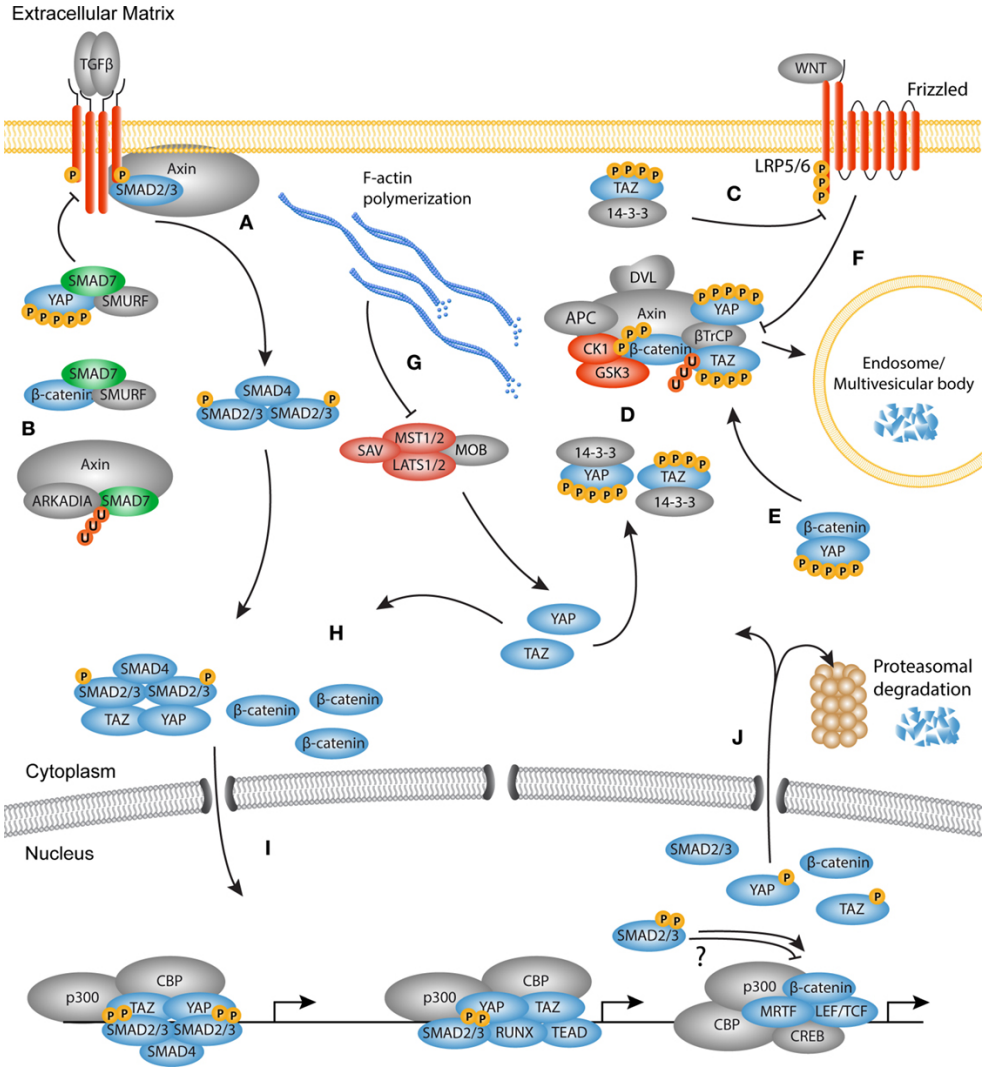

Figure 14. YAP regulates both Wnt and TGFβ signaling at different levels. YAP is involved in both TGFβ and Wnt signaling at different levels, which are schematically and synthetically presented here. Due to continuous expanding studies in the field, not all the molecular interactions so far described are depicted in this 2015 illustration. Thus, for more details, please refer to the main text. A) Upon TGFβ stimulation, SMAD3 is phosphorylated at the C-term, aided also by Axin B) YAP binds to SMAD7 and promote TGFβ-signaling inactivation. Instead, Axin can promote SMAD7 degradation, and thus TGFβ stimulated signaling C) Cytoplasmic TAZ was reported to inhibit Dvl phosphorylation and modulate Wnt signaling both in a positive and negative manner, depending on the ligand bound to the receptor D) YAP and TAZ are phosphorylated by the Hippo pathway kinases LATS1/2 and retained in the cytoplasm where E) YAP can take part to the β-catenin DC and contribute to β-catenin proteosomal degradation F) When Wnt binds to its receptor, the DC is inhibited and thus YAP and β-catenin are free to shuttle to the nucleus G) F-actin polymerization blocks the Hippo pathway kinase activity and, thus, favors YAP dephosphorylation and nuclear accumulation *(continues on the next page)*

(continues from the previous page) H) YAP, TAZ, SMAD2/3 and β-catenin can shuttle to the nucleus where I) YAP and TAZ can promote SMAD2/3 transcriptional activity along with other co-transcriptional partners J) YAP can also prevent SMAD1 proteosomal degradation. *Taken from: Piersma B "Signaling in Fibrosis: TGF-β, WNT, and YAP/TAZ Converge." Frontiers in Medicine. 2015;2:59.*

1.3.6 YAP in the vascular endothelium

1.3.6.1 Total-YAP and EC-specific YAP KO mice display vascular defects

The first hint that YAP is a key determinant for the vasculature development emerged from the generation of total-YAP KO mice ($YAP^{-/-}$), where genetic ablation of YAP caused embryonic lethality at E8.5 due to a lack of yolk-sac vascular organization, concurrent with defects in chorioallantoic fusion and embryo body axis development (Morin-Kensicki et al., 2006). Of note, yolk-sacs from $YAP^{-/-}$ mice were positive for the endothelial-marker CD31, but failed to form an organized vasculature, indicating that YAP is required for yolk-sac vasculogenesis but not for endothelial precursors formation. Conversely, vasculogenesis occurred both in the allantois and in the proper embryo of mutant mice, although vessels in the embryo were abnormally positioned. Taken together, these results suggested that YAP is a key regulator of early stage embryo development and of yolk-sac vasculogenesis.

8 years later, Zhang and colleagues generated a Tie2-Cre $YAP^{f/f}$ mouse reporter, which specifically ablates YAP both in endocardial and in vascular-endothelial cells in a constitutive manner (Zhang et al., 2014). Interestingly, these mice were embryonic lethal and only one homozygous mutant was retrieved out of 197 weaned mice. Clear morphological defects were already evident at E10.5. Indeed, while at E9.5 both the embryonic and the yolk-sac vascular plexuses did not show obvious differences between mutant and control mice, at E10.5 there was a striking growth delay of mutant mice, accompanied with defects in yolk-sac

vascular remodeling and maturation. To avoid vascular-dependent defects and to investigate the role of YAP in cardiac development, the authors then focused their attentions to E9.5 embryos. Interestingly, they found that YAP mutant mice had a significant reduced number of endocardial cells undergoing EndMT, partly because of a decreased endocardial proliferation, but also due to impaired mesenchymal transformation of endocardial cells. As a result, Tie2-Cre $YAP^{f/f}$ mice showed defects in the endocardial-cushion formation and heart valve development. To shed light on the molecular mechanism, the authors analyzed the expression of EndMT markers in the heart cushion and found that genetic depletion of YAP caused a marked down-regulation of Snai1, Snai2, Twist1, Msx1 and Msx2, whereas the expression of EndMT-triggering growth factors such as BMP2, TGFβ2 and Notch was not altered. Nonetheless, they also showed that YAP is required for TGFβ-mediated EndMT in *in vitro* cultured cells, by favoring SMAD2/3 but not SMAD1 nuclear localization, and Snai1 and Snai2 transcription. Thus, Zhang and colleagues proposed for the first time that YAP is required for the endocardial-cushion formation by sustaining cardiac EndMT during the embryonic development.

Collectively, these studies showed for the first time that YAP is a key player in vascular biology by contributing to physiological vasculogenesis and to heart-cushion EndMT, stimulating researchers to further investigate the role and the regulatory mechanisms of YAP in ECs.

1.3.6.2 YAP is regulated differently in static and under-flow conditions

A striking observation that prompted us and others to characterized YAP regulatory pathway in ECs, was that YAP sub-cellular localization and transcriptional activity was greatly dependent on cell-confluency state (Choi et al., 2015; Giampietro et al., 2015). Indeed, increasing cell density paralleled increasing pYAP S127 and YAP nuclear exclusion, while sparse ECs showed a marked

accumulation of YAP in the nucleus and intensive transcriptional activity (Figure 15). Thus, we and others hypothesized that YAP sub-cellular localization and activity is regulated by cell-cell contact. Results confirmed that disruption of VE-cadherin mediated cell-cell adhesion led to YAP nuclear translocation and target genes expression (*Ctgf, Cyr61, Inhba and Ankrd*). We also noticed that YAP sub-cellular localization and activity negatively correlated with a newly-identified VE-cadherin partner, EGF-receptor kinase substrate 8 (EPS8). EPS8 bound to the β-catenin binding domain of VE-cadherin in sparse and early-confluent ECs and contributed to enhance VE-cadherin turnover. In long-confluent cells, instead, its expression and localization at the cell membrane were strongly reduced. Notably, the β-catenin binding domain of VE-cadherin mediates binding to α-catenin too, and previous studies had already reported that α-catenin binds to YAP-14-3-3 complex to restrain it in the cytoplasm (Schlegelmilch et al., 2011; Silvis et al., 2011). We therefore envisioned a competitive binding of EPS8 with YAP-14-3-3 complex for α-catenin, and observed indeed that in EPS8-null ECs YAP could be immunoprecipitated together with VE-cadherin and α-catenin, but not in EPS8+ ECs. This suggested that EPS8 expression in sparse cells restricts the interaction of YAP-14-3-3 with α-catenin, and thus favors YAP nuclear translocation and transcriptional activity. Intriguingly, pYAP S127 was strongly increased in EPS8-null compared to EPS8+ ECs, but surprisingly not mirrored by an augmented MST1 and LATS1 phosphorylation and activation, suggesting that the Hippo pathway did not take part in regulating YAP phosphorylation and localization in static confluent ECs. We then moved to identify the kinase responsible for pYAP S127 in ECs and found that Akt kinase is activated upon AJ clustering, triggering, in turn, YAP phosphorylation and nuclear exclusion. We also observed that, where junctions are better organized, YAP colocalizes together with VE-cadherin *in vivo*, like in brain and retina vessels,

while it did not in more-fenestrated vessels, like in the kidney and spleen. In conclusion, our results showed for the first time that YAP sub-cellular localization and activity are regulated by other mechanisms than the Hippo pathway, and depend on several mechanisms like EPS8-induced exclusion to α-catenin binding and confluency-activated Akt-mediated phosphorylation (**Figure 15**). In agreement with our results, Choi and colleagues also reported that YAP is phosphorylated by Akt and retained in the cytoplasm of confluent ECs.

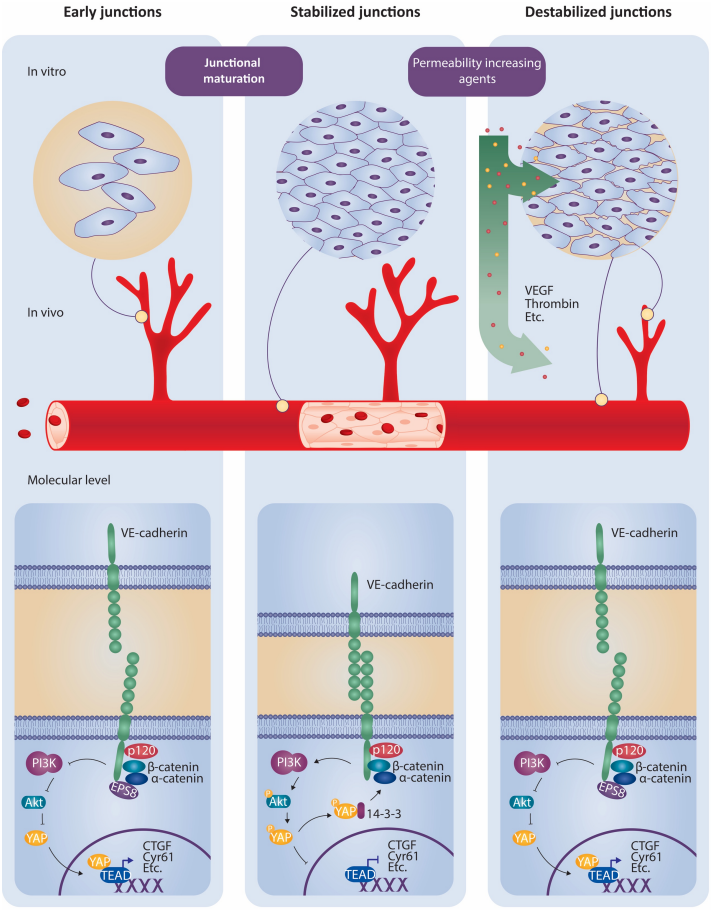

Figure 15. YAP regulatory mechanisms during junctional maturation and increasing cell density. When ECs are sparse, the PI3K/Akt pathway is prevented and so YAP translocates to the nucleus to sustain transcriptional activity. Instead, clustering of VE-cadherin in confluent ECs triggers PI3K/Akt pathway, which, in turn, stimulates YAP phosphorylation at Ser127. pYAP S127 is then bound by 14-3-3, and this complex is retained at the cytoplasmic membrane thanks to α-catenin mediated-binding to VE-cadherin. Exposure of ECs to permeability promoting factors causes junctional destabilization and, thus, YAP nuclear translocation and signaling. *Taken from: Giampietro C. "VE-cadherin complex plasticity: EPS8 and YAP play relay at adherens junctions." Tissue Barriers. 2016;4(4):e1232024.*

Very recently, Nakajima and colleagues have reported that YAP nuclear localization in ECs is positively regulated by laminar shear stress *in vitro* and by blood flow *in vivo* (**Figure 16**) (Nakajima et al., 2017). Strikingly, they found that shear stress did not alter either pYAP S127 levels or LATS1/2 phosphorylation, suggesting that, under flow, ECs stimulates YAP nuclear translocation through a Hippo- and phosphorylation-independent mechanism. Moreover, laminar shear stress enhanced actin bundling in ECs, while its inhibition resulted in decreased YAP nuclear accumulation. Thus, actin bundling stimulated YAP nuclear localization in response to shear stress. Indeed, formation of F-actin bundles in response to shear stress promoted F-actin binding to AMOT and consequent YAP release from AMOT in the cytoplasm, leading ultimately to YAP nuclear translocation. Furthermore, all the three AMOT family members were found to negatively regulate YAP nuclear translocation in cultured ECs, also in static conditions. However, after 6-24 hours of shear stress stimulus the nuclear accumulation of YAP decreased, suggesting that YAP localization and activity are regulated by shear stress

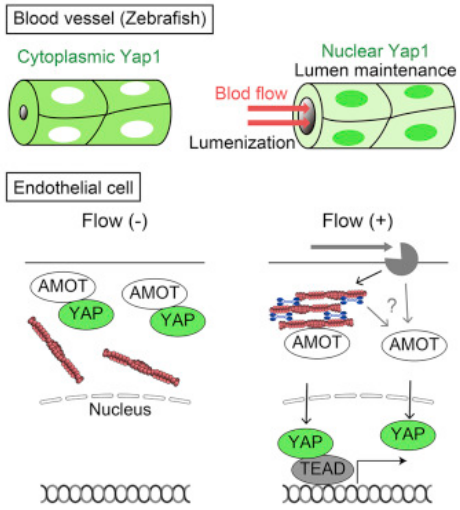

Figure 16. YAP is regulated by F-actin bundling and AMOT under laminar shear stress in ECs. Under resting condition, AMOT binds and sequesters YAP in the cytoplasm, thus preventing its nuclear activity. Under laminar shear stress, instead, F-actin bundles bind to AMOT, causing YAP release and nuclear accumulation. *Taken from: Nakajima H "Flow-Dependent Endothelial YAP Regulation Contributes to Vessel Maintenance." Dev Cell. 2017;40(6):523-36 e6.*

transiently and other mechanisms modulate them under different stimuli. In agreement with the *in vitro* results, *in vivo* analyses showed that the Amotl2a family member is necessary for preventing YAP nuclear accumulation in not-lumenized vessels, while its inhibitory effect is partly reduced by blood flow. Collectively, these results have shown for the first time that YAP nuclear localization in vascular ECs is transiently stimulated by laminar shear stress, likely due to F-actin fiber formation that binds to AMOT and releases YAP from its AMOT-mediated cytoplasmic segregation (Nakajima et al., 2017).

Thus, in ECs, YAP localization and activity is finely controlled by different mechanisms depending on cell confluency, clustering of AJs, shear stress and lumen formation and, so far, they appeared to be modulated by other mechanisms along with the Hippo signaling pathway.

1.3.6.3 YAP contributes to different biological processes to determine a proper vascular network formation

As already mentioned in the previous sections, YAP is emerging as an important regulator of several vascular biology processes. Initially, YAP was identified as a key determinant of yolk-sac vasculogenesis, since total YAP KO mice failed to formed an organized vascular plexus in the yolk-sac (Morin-Kensicki et al., 2006). Moreover, YAP localized at the nuclei of invading ECs in the retina vessels, suggesting a role of YAP in ECs migration and sprouting (Choi et al., 2015). These observations were supported by *in vitro* analyses where silencing of YAP in resulted in defective HUVEC cells tubular network formation and impaired aortic ring sprouting. Notably, the authors reported no significant alteration in ECs viability and proliferation upon YAP siRNA transfection. Moreover, transient down-regulation of YAP by siRNA injection in mouse retina vessels led to a reduced vessel density and a decreased number of branching points. The authors identified Angiopoietin-2

(ANG-2) as a YAP transcriptional target gene, whose expression was required for YAP-mediated ECs sprouting and angiogenesis. Thus, the authors revealed for the first time that YAP contributes to ECs sprouting and angiogenesis, partly via up-regulating ANG-2 (Choi et al., 2015). In agreement with these observations, generation of YAP/TAZ double EC-specific KO mice confirmed that these co-transcription factors are essential players in both developmental and pathological angiogenesis (Kim et al., 2017). Indeed, double mutant mice exhibited a markedly decreased retinal vessel growth in terms of vascular density, radial length and number of branching points at P5 (post-natal day 5). Interestingly, the front vascular region of mutant mice presented a blunted-end, with tip ECs forming shorter and significantly less filopodia. The tip EC protrusions, moreover, showed a disorganized F-actin bundle and led to a defective lumen formation, suggesting that YAP/TAZ expression is crucial for sustaining sprouting angiogenesis and vascular growth during retinal development by controlling F-acting rearrangements and proper lumen formation. Defects in vascular sprouting and growth in YAP/TAZ double KO mice were in part due to a decreased number of proliferating ECs. Interestingly, these phenotypes were greatly rescued by crossing YAP/TAZ double KO mice with LATS1/2 KO mice. Thus, YAP/TAZ promote sprouting angiogenesis in the developing retina by tuning different biological mechanisms, and their angiogenic activity is under the control of the canonical Hippo pathway. At P12, double mutant mice exhibited severe retinal and brain hemorrhages, due to reduced tight (ZO1 and Claudin-5) and adherens (VE-Cadherin) junction protein expression, and consequent vascular leakage increase. Notably, no difference in terms of pericyte coverage in both retina and brain vessels was detected. Strikingly, the authors have shown for the first time that YAP/TAZ are required for BBB formation and integrity, since double KO mutants contained fewer vessels in the brain, with a tortuous and enlarged morphology, and displayed altered BBB markers expression

(increased PLVAP and TfR, while no change in GLUT1). Mutant mice eventually died, probably due to extensive brain hemorrhages and growth delay. Remarkably, the authors showed that YAP/TAZ are not required for everyday BBB and BRB integrity, but they are required for vascularization post-injury, showing for the first time that YAP/TAZ are required for pathological angiogenesis in adult mice. Furthermore, they showed that VEGF elicits YAP/TAZ nuclear translocation, and induces LATS1 and YAP dephosphorylation. VEGF treatments of HUVEC cells silenced for YAP/TAZ revealed that YAP/TAZ are important for EC migration and formation of both filopodia and lamellipodia. In addition, EC proliferation was negatively affected by YAP/TAZ KD due to G_1 phase arrest, partly explained by reduced MYC expression and signaling.

Interestingly, under blood flow, YAP accumulates in the nucleus and is required for the maintenance of the lumen structure of certain blood vessels, as recently shown by Nakajima (Nakajima et al., 2017). YAP null zebrafish reporters displayed normal vasculature development until 7 days post fertilization, although frequent vessel stenosis and vessel retraction were observed. Conversely, vessel regression was observed in YAP or TAZ overexpressing zebrafish mutants already at 48 hours post fertilization, during the segmentation of the dorsal part of the caudal vein plexus (dCVP) (Nagasawa-Masuda and Terai, 2017). Sustained nuclear YAP localization and activity, indeed, induced Ctgf expression and release, that in turn contributed to dCVP regression. Thus, YAP and TAZ activity are involved in the maintenance of the lumen structure, but the exact mechanisms need to be better clarified.

Moreover, YAP and TAZ nuclear localization is stimulated by 24 hours of disturbed flow, resulting in ECs proliferation and activation of a pro-inflammatory program that contributes to atherosclerotic plaque formation (Wang et al., 2016a). Interestingly, the authors have also shown that YAP nuclear activity and the pro-inflammatory response is attenuated by statins treatments, setting YAP and TAZ as

novel therapeutic targets to counteract atherosclerotic lesion development. Accordingly, Nakajima and colleagues have also observed that YAP driven gene transcription was more sustained in vessels where the flow was disturbed compared to the ones under laminar shear stress (Nakajima et al., 2017). Taken together, these results showed that flow contributes to define YAP sub-cellular localization and activity.

In addition, by generating Tie2-Cre $YAP^{f/f}$ mice, Zhang has pointed YAP as a crucial regulator of physiological EndMT that occurs during the development of the heart cushion (Zhang et al., 2014). Whether YAP is also required for pathological EndMT is still an open question that would help identifying YAP as a novel therapeutic target to prevent mesenchymal and malignant transformation and, possibly, tumor dissemination.

Collectively, these studies have shown that YAP is an important regulator of many physiological vascular processes and it is finely tuned by several up-stream regulatory mechanisms. Alterations of YAP localization and activity impinges on proper vascular development under physiological development and, likely, also under pathological conditions. It would be now important to investigate whether and how YAP activity is deregulated in vascular pathologies and in tumor angiogenesis, in order to better define its role in vascular biology and possibly provide novel molecular mechanisms that could be targeted for the treatment of vascular pathologies.

Chapter 2 - Materials and Methods

2.1 Cell culture

2.1.1 ECs isolation and culture

Lung ECs were isolated and immortalized as previously described (Dong et al., 1997) from a $YAP^{f/f}$ mouse (Xin et al., 2011). Briefly, mouse lungs were removed under sterile conditions, washed two times with PBS and minced finely with scalpels. Organ disaggregation was carried out by incubating minced lungs with collagenase A (1.5 mg/ml; Roche) and DNAse (25 µg/ml; Roche) in DMEM (37 °C for 3 hours (h)). After filtering through nylon screen, cells were collected, centrifuged at 1,200 rpm for 10 minutes and then seeded in gelatin 0.1% coated 24 wells. 48 h afterwards, ECs were washed with PBS and infected with *polyoma middle* T antigen supernatant in order to specifically select and immortalize only ECs. Supernatant was then replaced with complete medium after 8 h. After 3 months in culture, we obtained a homogeneous population of ECs, whose purity was analyzed by performing extensive stainings for endothelial specific molecules. *Yap* floxed alleles were deleted by treating pure ECs *in vitro* with TAT-Cre recombinase using Hyclone ADCF-Mab medium (ThermoScientific), as previously described (Liebner et al., 2008), thus generating YAP wild-type (WT) and KO immortalized lung EC lines. Lung ECs were grown on 1% gelatin coated plates in complete medium, containing MCDB-131 (GIBCO) supplemented with 20% South American (SA) fetal bovine serum (FBS) (HyClone), penicillin/streptomycin (100 units/L; Sigma), sodium pyruvate (1mM), L-glutamine (2mM; Sigma), heparin (100 µg/ml; Sigma) and EC growth supplement (5 µg/ml; Sigma).

2.1.2 Culture of HEK 293T

293T packaging cells were provided by IFOM Cell Culture facility and cultured in DMEM medium (GIBCO) supplemented with 10 % SA FBS (Hyclone), and L-glutamine (2 mM, Sigma).

2.2 Cell treatments

For 5 days TGFβ/BMP6 stimulation, ECs were seeded at $0.75*10^6$ cells/21 cm^2 density. The day after plating, cells were starved overnight (O/N) with starving medium (MCDB-131, 1% bovine serum albumin (BSA)), followed by either 5 ng/ml TGFβ1 (PeproTech) or 100 ng/ML BMP6 (R&D) treatment. Fresh TGFβ/BMP6 in starving medium were added every day for 5 consecutive days.

For TGFβ stimulation, WT ECs were seeded at $0.4*10^6$ cells/9.5 cm^2 density and KO ECs at $0.5*10^6$ cells/9.5 cm^2. Confluent monolayers of ECs were incubated with starving medium O/N, followed by treatment with 5 ng/ml TGFβ in starving medium for the indicated time points.

For LiCl treatment, cells were grown till confluency and then incubated O/N with starving medium containing either 60 mM LiCl (Sigma Aldrich) or 60 mM NaCl (Sigma Aldrich). The day after, cells were stimulated for the indicated time points with 5 ng/ml TGFβ, dissolved in starving medium together with either 60 mM LiCl or NaCl.

2.3 siRNA transfection

For siRNA transfection, cells were plated at $0.6*10^6$ cells/10 cm^2 density in complete medium and transfected with either scrambled (scr) siRNA (ON-TARGET plus Non-targeting pool; GE Healthcare), or SMAD3 siRNA (ON-TARGET plus L-040706-00; GE Healthcare), or TEAD1 (ON-TARGET plus L-048419; GE

Healthcare). Transfection was performed with Lipofectamine 2000 (Invitrogen) in accordance with the manufacturer's instructions.

2.4 Lentiviral infections

Constitutively active YAP lentiviral plasmid (YAP 5SA) was a kind gift of Prof. Stefano Piccolo (Padua University, Italy) (Dupont et al., 2011), wherein a human Flag-YAP 5SA was inserted in a CSII-CMV-MCS-IRES2-Bsd lentiviral backbone plamid using EcoRI and NotI restriction sites. The lentiviral particles were produced in HEK 293T cells using a three-plasmid transfection system mediated by Lipofectamine 2000. 24 h before transfection, $2x10^6$ HEK 293T cells were plated in 57 cm^2 petri dishes. The following day, cells were transfected with a 3 mL OptiMEM solution containing 4.5 μg psPAX2 (packaging plasmid encoding for Gag, Pol, Rev, and Tat), 1.5 μg of pMD2.G (envelope plasmid encoding for VSV-G), 6 μg of either empty or YAP 5SA lentiviral vector, and 36 μl of Lipofectamine 2000 per petri dish. This solution was kept 30 minutes at room temperature (RT), applied drop by drop on cells and left O/N for transfection. The day after, transfected HEK 293T medium was replaced with DMEM 10 % SA FBS and L-glutamine. In parallel, $2x10^6$ of YAP WT and KO cells were seeded in 57 cm^2 petri dishes. Lentivirus-containing supernatants were collected 48 and 72 h after cell transfection, passed through a 0.45 μm filter and applied to YAP WT and KO cells using polybrene for 24 h. YAP WT and KO infected cells were then grown till confluency using complete culture medium, and then seeded for cell treatments as described.

2.5 Western Blotting

Western blot (WB) analysis was performed according to standard protocols. Confluent monolayers of ECs were lysed in boiling Laemmli sample buffer (SB) (2%

sodium dodedyl sulfate (SDS), 20% glycerol, and 125 mM Tris-HCl, pH 6.8). Protein concentration was determined using a BCA Protein Assay kit (Thermo Fisher Scientific). Equal amounts of proteins were loaded on gel, separated by SDS-PAGE and transferred to a Protran Nitrocellulose Membrane (Whatman). After blocking and incubation with primary and horseradish peroxidase-linked secondary antibodies, specific bindings were detected by a chemiluminescence system (GE Healthcare). WB bands have been quantified using optic densitometry software and normalized to the relative housekeeping.

2.6 Nuclear-cytoplasmic (N/C) fractionation

Confluent monolayers of ECs were lysed in pre-chilled cytosol buffer (20 mM Hepes pH 7.9 and 1 mM EDTA pH 8.0 and protease/phosphatase inhibitors). After centrifugation, the surnatant was collected (cytosolic fraction) while the pellet was washed three times with cytosol buffer, lysed in cold nuclear buffer (20 mM Hepes pH 7.9, 1 mM EDTA pH 8.0, 10% glycerol and 420 mM NaCl and protease/phosphatase inhibitors), followed by ultracentrifugation for 30 minutes at 50000 g. The obtained surnatant was collected as nuclear fraction.

2.7 Immunoprecipitation (IP)

Following O/N starvation and treatment with TGFβ, confluent monolayers of ECs were solubilized in cold IP lysis buffer (50 mM Tris-HCl pH 7.4, 150 mM NaCl, 2 mM $CaCl_2$, 0.1% Triton X-100, 0.1% NP-40 and protease/phosphatase inhibitors) and incubated on ice for 15 min. The protein lysate was then precleared with Protein A- or G- Sepharose beads (GE Healthcare) for 2 h at +4°C. Subsequently, protein concentration was determined with BCA Protein Assay Kit, and equal amounts of protein were incubated with immune antibodies and captured by protein A- or G-Sepharose beads O/N at +4°C. As a control, immune antibodies were incubated

with IP lysis buffer and protein A- or G- Sepharose beads O/N at +4°C. The following day, beads were washed several times with IP lysis buffer and boiled in an appropriate volume of SB. Immunoprecipitated material was analyzed through standard WB analysis.

2.8 IP from N/C fractionation

Cells were lysed with cold subcellular fractionation buffer (250 mM sucrose, 20 mM HEPES pH 7.4, 10 mM KCl, 1.5 mM $MgCl_2$, 1mM EDTA, 1mM EGTA and protease/phosphatase inhibitors). Cytosolic membranes were disrupted by passing the lysate through a 22 Ga needle, followed by 5 minutes centrifugation at 720 G. The surnatant was collected as cytosolic fraction, further centrifuged at 10000 G for 10 minutes and immunoprecipitated as previously described. The nuclear pellet was resuspended in cold IP lysis buffer and kept for an hour at 4°C under constant rotation. After a centrifugation at 13200 rpm for 20 minutes the surnatant containing the nuclear fraction was subjected to IP.

2.9 Transcription factor binding site analysis

The identification of putative TEAD or SMAD binding sequences on genomic DNA was performed using the software MatInspector (Genomatix), which predicts the transcription factor binding sites (TFBS) by using a large library of weight matrices. Using the RSAT software (http://rsat.sb-roscoff.fr/) we retrieved a sequence spanning from 5000 bp upstream and 1000 bp downstream the transcription start site (TSS) of *Fn1*, *Serpine1*, *Snai1, Cdh2* and *Acta2* genes.

2.10 Chromatin Immunoprecipitation (ChIP)

ChIP assays were performed as described elsewhere (Nakae et al., 2003). Briefly, cells were starved O/N and cross-linked with 1 % formaldehyde for 10

minutes at RT. 125 mM glycine for 5 minutes at RT was then added in order to inactivate formaldehyde. After two washes with ice-cold PBS ECs were lysed by scraping on ice-cold SDS buffer (NaCl 100 mM, Tris HCl pH 8.1 50 mM, EDTA 5mM, NaN3 0.2 %, SDS 0.5 %). The lysate was then collected and centrifuged at 1,300 rpm for 5 minutes at 4°C. After removal of the supernatant, the pellet was resuspended with Immunoprecipitation buffer (1 volume of SDS Buffer + 0.5 volume of Triton Dilution Buffer [NaCl 100 mM, Tris HCl pH 8.6 100 mM, EDTA 5 mM, NaN3 0.2 %, Triton X-100 5 %]). Sample sonication in microTUBE (COVARIS) was performed after 10 minutes of incubation using a COVARIS S220 according to the following conditions: Peak Incident Power 175.0 Watt, Duty Factor 10 %, 200 Cycles/Burst. Sonicated chromatin was loaded on 1 % agarose gel to evaluate the size of the sonicated chromatin fragments. 0.5 mg (for YAP) or 0.3 mg (for SMAD3) of DNA fragments with an average size of 500 base pairs (bp) were incubated with either 8 μg of YAP (NB110-58358) or 1.5 μg SMAD3 (cs#9523) directed antibodies or rabbit IgG control O/N at 4 °C in the presence of protein G covered magnetic beads (Life Technologies). The following day, beads were recovered and washed three times with Mixed Micelle Washing Buffer (NaCl 150 mM, TrisHCl pH 8.1 20 mM, EDTA 5 mM, Sucrose 5.2 % w/v, NaN_3 0.02%, Triton X-100 1 %, 0.2 % SDS), 500 Buffer (Deoxycholic acid 0.1 % w/v, NaCl 500 mM, HEPES pH 7.5 25 mM, EDTA 1 mM, NaN_3 0.02 %, Triton X-100 1 %), LiCl Detergent Washing Buffer (Deoxycholic acid 0.5 % w/v, LiCl 250 mM, EDTA 1 mM, NP-40 0.5 % v/v, NaN_3 0.02 %, Tris HCl pH 8.0 10 mM). Proteins/DNA complexes were detached from beads by heating the samples at 65 °C for 10 minutes. De-crosslinking was performed at 65 °C O/N. DNA was precipitated and purified using phenol/cloroform and amplified by quantitive real-time polymerase chain reaction (qPCR) using oligonucleotides flanking the assayed promoter regions (listed below). Primers were designed using Primer3 software and always tested before, in order to avoid "auto-

amplification" due to self-complementarity. qPCR reactions were carried out by diluting DNA in the presence of specific primers (0.4 µM each) to a final volume of 25 µl in SYBR Green Reaction Mix (Perkin Elmer). S.D.S 2.2.1 software was used to convert qPCR curves in C_t values. For each region, the mean of the C_ts of the inputs was calculated and subtracted to the C_t values of the immune samples (ΔCt). Then, the % of enrichment of input for the immune samples was obtained as 2^-ΔCt and multiplied by the % of input taken during the experiment. The same calculation was performed for the non-immune (IgG control) immunoprecipitated samples. To remove unspecific signal, the non-immune values were subtracted from the immune samples.

Gene	Position	Forward	Reverse
Fn1	-0.3 KB	5'-GTAAGCCTTACCACCCCAGG	3'-GGGATGGGAAACGGCTGTAA
Serpine1	-0.5 KB	5'-CAAAACCCAGCCGCACAAG	3'-GCATGTCTGACTCCCCACAT
	-4.3 KB	5'-CCCAGCTCTCCCAGTGAAAT	3'-GGTCAGCCTCCTTCCAGTTAC

Table 1. List of primers used for ChIP

2.11 Antibodies

For WB, IF, IP and ChIP the following antibodies were used: phospho-SMAD3 rabbit (9520, Cell Signaling; WB), SMAD3 rabbit (9523, Cell Signaling; WB), SMAD3 mouse (sc-101154, Santa Cruz; WB), SMAD3 mouse (MA5-15663, Thermofisher; WB) phospho-SMAD1/5 rabbit (9516, Cell Signaling; WB), SMAD1 rabbit (9743, Cell Signaling; WB), phospo-SMAD2 (3108, Cell Signaling; WB), SMAD2 (ab33875, Abcam; WB and IF), SMAD4 (sc-1909, Santa Cruz; WB, IF and IP), YAP mouse (sc-101199, Santa Cruz; WB), YAP mouse (sc-271134, Santa Cruz; IF and IP), YAP rabbit (sc-15407, Santa Cruz; WB), TEF-1 mouse (610923, BD Bioscience; WB), Fn1 (ab23750, Abcam; WB), Snai1 (sc-10432, Santa Cruz), Tubulin mouse (T9026,

Sigma), Vinculin mouse (V9264, Sigma), Lamin B goat (sc-6216, Santa Cruz; WB); HRP-linked anti-mouse and anti-rabbit (Cell Signaling); HRP-linked anti-goat (Promega); AlexaFluor 555-conjugated donkey anti-goat (Invitrogen); AlexaFluor 488-conjugated donkey anti-rat (Invitrogen).

2.12 Quantitative real-time PCR (qPCR) analysis

Total RNA was isolated using either the RNeasy micro kit (QIAGEN) for samples treated for 5 days with TGFβ/BMP or with Maxwell® RSC simplyRNA Tissue Kit (Promega) for all the other samples. Subsequently, 1 µg was reverse transcribed with random hexamers (High Capacity cDNA Archive kit; Applied Biosystems). cDNA was amplified with the TaqMan Gene Expression assay (Applied Biosystems) and a thermocycler (ABI Prism 7900HT; Thermo Fisher Scientific). For any sample, the expression level, normalized to the housekeeping genes encoding either *Actb*, *Hrpt1*, *B2m* was determined by the comparative threshold cycle method as described previously (Spagnuolo et al., 2004).

2.13 Immunofluorescence (IF)

Cells were fixed with 4% paraformaldehyde (PFA), permeabilized for 10 minutes with PBS 0,5% Triton-X, and incubated for 1h in a blocking solution of PBS with 2% BSA. Subsequently, samples were incubated with primary antibodies diluted in blocking buffer for 1h at RT, washed with PBS, followed by appropriate secondary antibodies incubation for 1h at RT, and mounted with VECTASHIELD with DAPI (Vector Biolabs). Confocal microscopy was performed at RT with a confocal microscope (TCS SP2AOBS; Leica) equipped with violet (405-nm laser diode), blue (488 nm; Argon), yellow (561 nm; solid state), and red (633 nm; HeNe) excitation laser lines before processing with ImageJ. Only adjustments of brightness and contrast were used in the preparation of the figures. For comparison purposes,

different sample images of the same antigen were acquired under constant acquisition settings. Image acquisition was performed using a 63×/1.4 NA oil immersion objective (HCX PL APO 63× Lbd BL; Leica) with spectral detection bands and scanning modalities optimized for removal of channel cross talk. Confocal software (Leica) and ImageJ version 1.33 were used for data analysis. Quantification of nuclear accumulation was made measuring the intensity of SMAD staining with ImageJ, using DAPI nuclear staining as a region of interest to identify cell nuclei.

3.1 Generation of immortalized lung YAP WT and KO ECs

In order to study the role of YAP in the vascular endothelium, and, in particular, characterize how it contributes to EndMT, we generated an *in vitro* cell culture model system by isolating ECs from lungs of a $YAP^{f/f}$ mouse, as described in materials and methods section 2.1.1. Once the cells have been immortalized with *polyoma middle-T*, we performed genetic recombination by means of TAT-Cre enzyme, which cut at the level of loxP sites flanking the third exon of *Yap* gene and created a STOP codon in the corresponding YAP transcript (Xin et al., 2011). As a result, *Yap* mRNA is no longer transduced in recombined cells. In this way, we obtained two immortalized EC lines coming from the same genetic background, one harbouring a WT *Yap* gene and one that no longer expressed YAP. WB analyses verified YAP recombination and genetic deletion (KO) (**Figure 17**). Thus, YAP WT and KO immortalized ECs were then cultured and used for subsequent *in vitro* experiments.

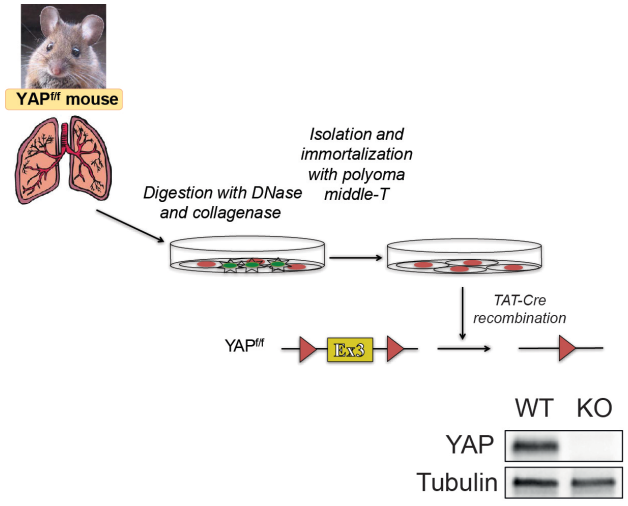

Figure 17. Generation of lung immortalized YAP WT and KO ECs. The drawing schematically represents how YAP WT and KO ECs were generated. Three months after isolation and immortalization of cells, WB analyses confirmed YAP recombination. Tubulin was used as a loading control.

3.2 YAP positively modulates TGFβ-mediated EndMT

Previous studies have reported YAP as an important promoter of EMT (Overholtzer et al., 2006; Yuan et al., 2016), while, at the beginning of my PhD studies, no scientific evidence proving a positive correlation between YAP expression and EndMT were yet provided. Interestingly, we and other have shown that prolonged exposure to TGFβ/BMP family of ligands is strongly correlated to physiological and pathological EndMT (Azhar et al., 2009; Maddaluno et al., 2013; Medici et al., 2010). We thus moved to investigate whether YAP contributes to EndMT in response to TGFβ/BMP family of ligands, by chronically treating YAP WT and KO ECs with either 100 ng/mL BMP6 or 5 ng/mL TGFβ for 5 consecutive days in order to stimulate an EndMT response. As shown in **Figure 18**, we observed that both BMP6 and TGFβ triggered the expression of EndMT marker genes in WT cells, as expected, in particular of *Klf4*, Stem-cells antigen 1 (*Sca1*) and *Fsp1* in response to BMP6 (**Figure 18 A**) and of *Acta2*, *Fn1*, *Cdh2* and *Snai1* after TGFβ stimulation (**Figure 18 B**). Interestingly, genetic loss of YAP negatively affected the EndMT response induced by TGFβ, since KO cells showed a significantly impaired mRNA up-regulation of *Acta2*, *Fn1*, *Cdh2* and *Snai1* compared to WT treated cells (**Figure 18 B**).

In order to verify that the genetic ablation of YAP specifically affects the EndMT markers expression induced by TGFβ, we analyzed the EndMT proteins expression through WB in WT and KO treated cells.

TGFβ chronic stimulation strongly induced Fn1, N-cadherin (encoded by *Cdh2*) and Snai1 protein expression in WT but not in KO cells, further suggesting that in ECs YAP is required for proper EndMT markers expression in response to TGFβ and set YAP as a positive regulator of TGFβ-mediated EndMT (**Figure 19**).

Moreover, these results are in line with what observed by Zhang and colleagues in other EC line systems (Zhang et al., 2014).

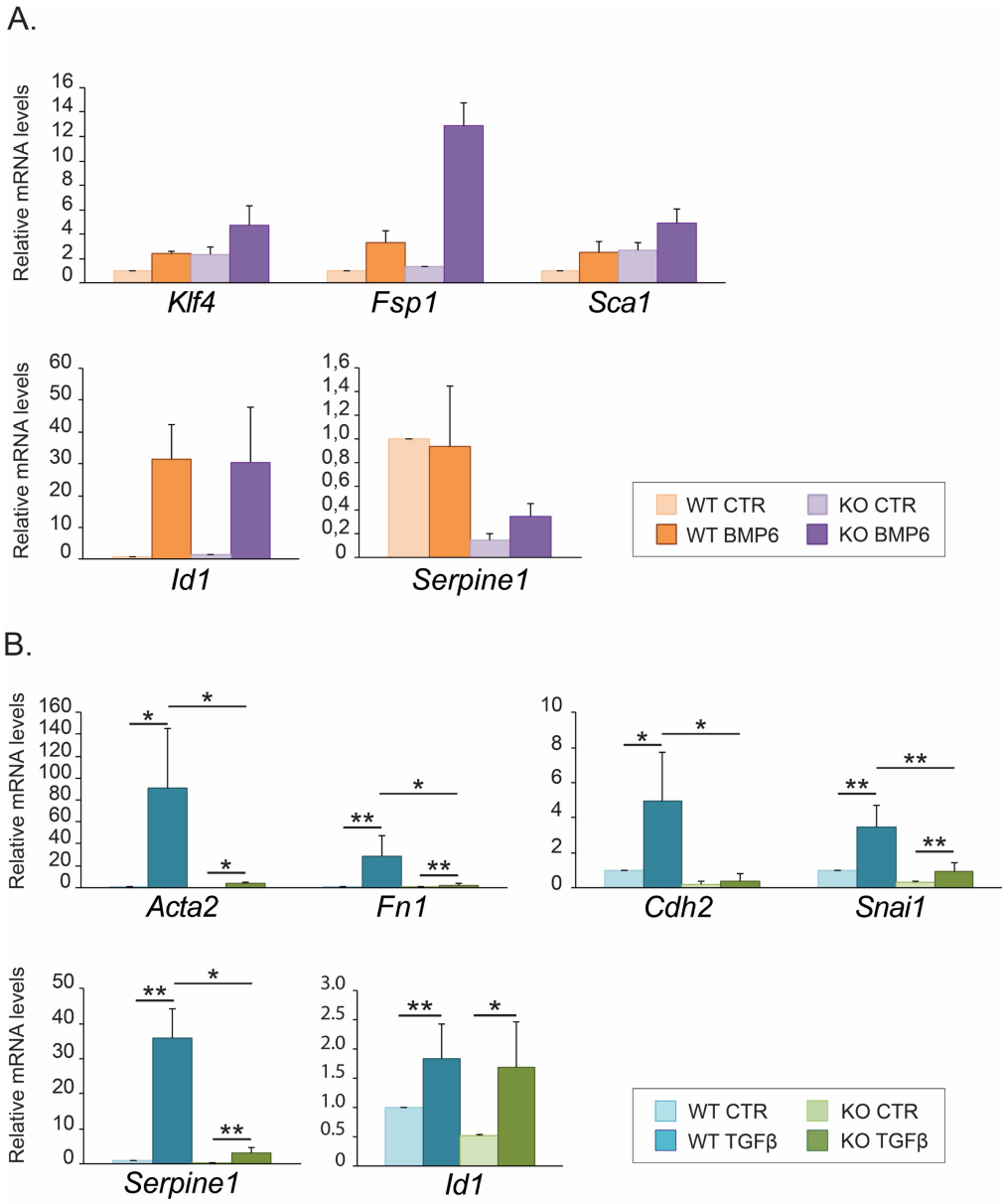

Figure 18. Loss of YAP negatively affects EndMT genes expression. qPCR analysis of the EndMT markers: A) *Klf4*, *Fsp1* and *Sca1* and of canonical targets of ALK1/SMAD1 and ALK5/SMAD3, *Id1* and *Serpine1*; B) *Acta2, Fn1, Cdh2* and of the EndMT- driving transcriptional factor *Snai1, Id1* and *Serpine1*. Cells were treated with A) 100 ng/mL BMP6 or B) 5 ng/mL TGFβ for 5 days. Unstimulated cells (CTR) were kept in starving medium for 5 days without addition of TGFβ. Data are mean ± standard deviation (SD) of A) two independent experiments (n=2) and B) n=4. Beta-2 microglobulin (b2m) was used as housekeeping gene. *p<0.05, **p<0.01, t-test.

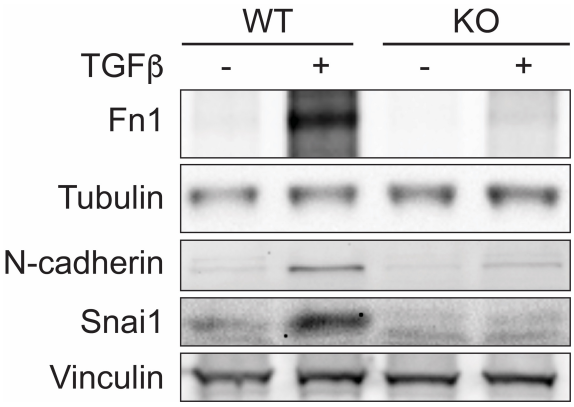

Figure 19. YAP positively regulates TGFβ-induced EndMT marker expression. WB of WT and KO cells treated with TGFβ for 5 consecutive days. The blot is representative of n=3 independent experiments. Tubulin and Vinculin were used as loading controls.

3.3 YAP contributes to TGFβ-induced SMAD3- but not SMAD1-signaling

Considering that YAP KO affected the EndMT markers up-regulation upon 5 days of TGFβ treatment and that TGFβ primarily signals through R-SMADs, we sought of characterizing whether loss of YAP might impact on SMAD3 and/or SMAD1 signaling activation in response to TGFβ in ECs. SMAD3 is considered the canonical effector of TGFβ, while SMAD1 the one of BMP growth factors (Goumans and Ten Dijke, 2017). Nevertheless, SMAD1 activation and transcriptional activity can also occur in response to TGFβ in ECs (Goumans et al., 2002). We thus checked for the mRNA expression levels of *Id1* and *Serpine1*, canonical targets of ALK1/SMAD1 and ALK5/SMAD3 signaling respectively, to assess whether YAP is required for R-SMAD signaling (Dennler et al., 1998; Goumans et al., 2002).

Results showed that 5 days of TGFβ treatment induced *Id1* up-regulation both in WT and in KO treated cells at a similar level (**Figure 18B**). On the contrary, *Serpine1* expression, which is known to be driven by SMAD3 (Dennler et al., 1998),

was significantly lower in KO compared to WT treated cells. Of note, prolonged BMP6 treatment resulted in a marker *Id1* upregulation both in WT and KO treated cells too, while *Serpine1* expression was not induced in response to this growth factor (**Figure 18A**).

Given that the phosphorylation and activation of the signaling cascade in response to TGFβ occurs around 45 minutes from the beginning of the treatment (Rudini et al., 2008), we evaluated whether SMAD1 and SMAD3-driven signaling activities were already activated and modulated 2 h after stimulation.

Interestingly, in line with the chronic TGFβ stimulation, 2 h of treatment induced *Id1* up-regulation at a similar level in both cell lines, while *Serpine1* expression was significantly affected upon loss of YAP (**Figure 20**).

We therefore concluded that TGFβ down-stream signaling is affected in YAP KO ECs and that YAP is specifically required for SMAD3 but not SMAD1 signaling in ECs.

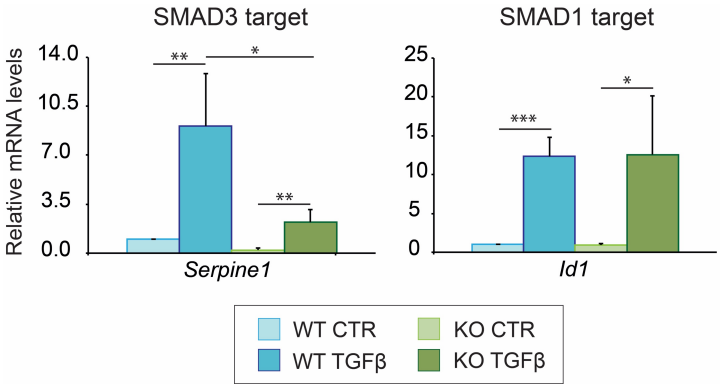

Figure 20. YAP specifically contributes to SMAD3-driven gene expression. qPCR analysis of *Serpine1* and *Id1* mRNA expression levels in YAP WT and KO cells treated with 5 ng/mL TGFβ for 2 h. Samples are normalized to WT untreated cells. Data are mean ± SD of n=3 independent experiments. *p<0.05 **p<0.01 ***p<0.001, t-test.

3.4 YAP is not required for SMAD3 and SMAD1 C-term phosphorylation

TGFβ-family of ligands signals by binding to an heteromeric complex formed by two TβRI and two TβRII, leading to R-SMADs phosphorylation and downstream signaling cascade activation. Since we observed that YAP is required for TGFβ-induced EndMT and for SMAD3-driven signaling activity, we next aimed at investigating at which step of the TGFβ signaling cascade YAP contributes to.

First, we looked at whether there was a differential activation of the TGFβ signaling pathway between the two cell lines, which could be the result of a decreased expression of components of the TβRI family of receptors or due to an impaired phosphorylation activity of the receptors. We tested the mRNA expression levels of ALK5 receptor (or *Tgfbr1*), responsible for SMAD2 and -3 phosphorylation and activation, and ALK1 (or *Acvlr1*), responsible for SMAD1 -5 and -8 in ECs (Goumans and Ten Dijke, 2017). Quantitative analysis of the expression levels of *Tgfbr1* and of *Acvlr1* did not reveal any significant difference between WT and KO cells (**Figure 21**), suggesting that genetic loss of YAP had no effect on the two main TβRI expression.

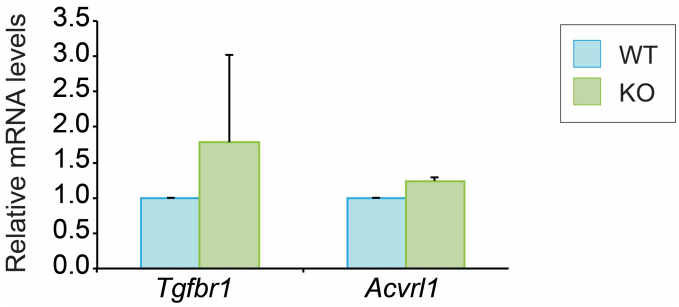

Figure 21. Genetic ablation of YAP in ECs does not affect TβRI expression levels. qPCR analysis of mRNA expression of *Tgfbr1* (ALK5) and *Acvlr1* (ALK1) in untreated conditions. B2m was used as house keeping gene. n=3 ± SD.

Upon TGFβ stimulation TβRI phosphorylates R-SMADs in a specific SSxS consensus-motif lying at their C-term. In particular, activated ALK1 phosphorylates SMAD1 at S463 and S465 (pSMAD1), while ALK5 phosphorylates SMAD3 at S423 and S425 (pSMAD3) (Goumans and Ten Dijke, 2017). By means of WB analyses, we then tested whether exposing WT and KO cells to TGFβ for 45 minutes could induce SMAD3 and SMAD1 C-term phosphorylation at a similar level in both cell lines.

Results clearly showed that 45 minutes TGFβ treatment induced a strong and significant C-term phosphorylation of SMAD3 and SMAD1 in both WT and KO cells, indicating that YAP expression is not necessary for TGFβ signaling activation (**Figure 22**).

Interestingly, loss of YAP in ECs caused a significant reduction of SMAD3 and SMAD1 total protein levels. Nevertheless, our previous data showed that SMAD1 signaling activity is not affected by YAP KO (**Figure 20**), indicating that SMAD1-reduced levels in KO cells are not enough to prevent downstream signaling activation. YAP, instead, was required for SMAD3 protein accumulation and relative signaling activity (**Figure 20** and **Figure 22**), suggesting that YAP specifically contributes to SMAD3 but not SMAD1 signaling activity in response to TGFβ. Of note, others have instead reported that silencing of YAP in HUVEC cells did not significantly affect SMAD3 and SMAD1 expression (Zhang et al., 2014).

In order to test whether the absence of YAP might result in a faster SMAD3 C-term dephosphorylation and, thus, in a quicker SMAD3 signaling activity switch off, we performed a TGFβ time course in both cell lines and checked for the C-term phosphorylation levels of SMAD3 over time. Results showed that SMAD3 C-term phosphorylation occurred at comparable levels between the two cell lines and that, 2 h after stimulation, the signal was not significantly decreased in KO cells compared

to WT cells, suggesting that loss of YAP did not influence SMAD3 C-term phosphorylation kinetic up to 2 h from TGFβ stimulation (**Figure 23**).

Collectively these results showed that loss of YAP did not decrease the expression of the two main TβRI in ECs, and that TGFβ signaling is activated at the

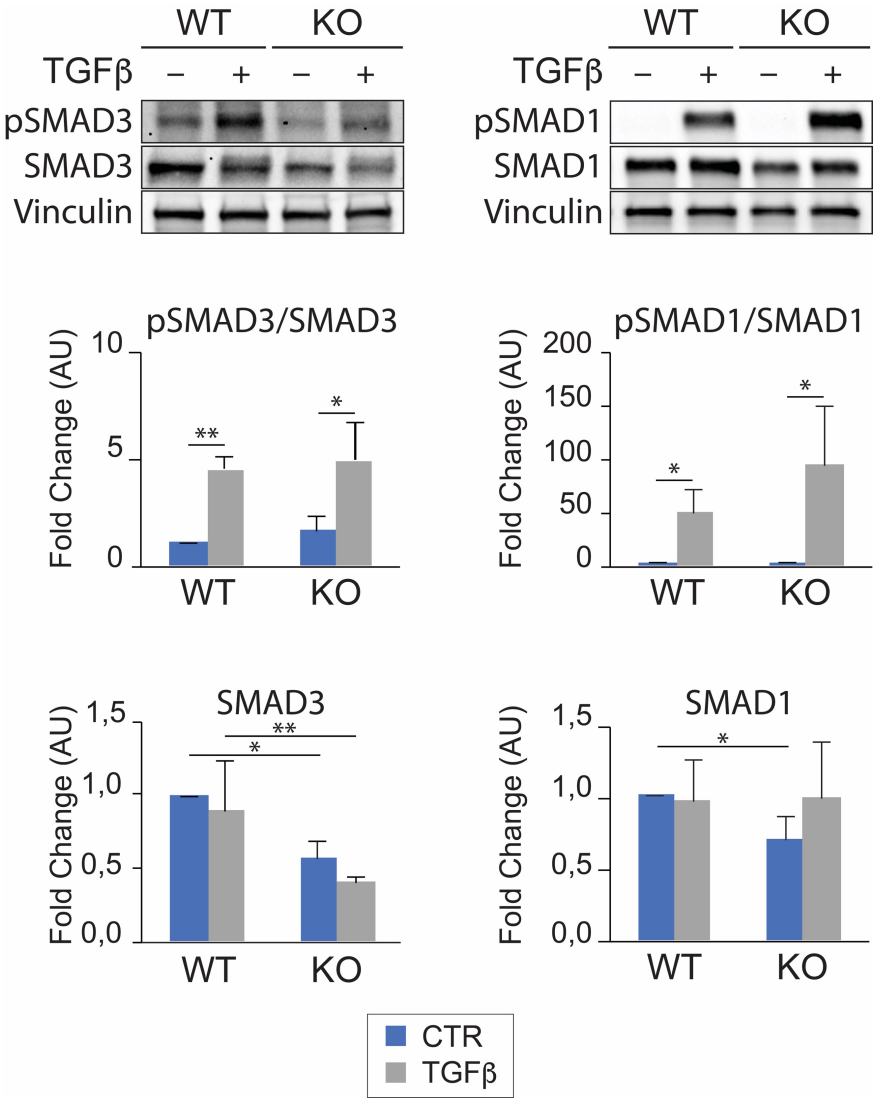

Figure 22. Expression of YAP in ECs does not influence SMAD3 and SMAD1 C-term phosphorylation. Representative WB of C-term phosphorylated SMAD3 and SMAD1 (pSMAD3 and pSMAD1) protein in WT and KO cells treated with TGFβ for 45 minutes, and relative total SMAD3 and SMAD1 expression levels. WB bands have been quantified using optic densitometry software and normalized to the relative Vinculin band (housekeeping). The ratio between normalized pSMAD3/1 and SMAD3/1 levels were then calculated for each sample, and expressed as fold change referred to WT untreated cells (arbitrary units, AU). Data are mean of n=3 independent experiments ± SD. *p<0.05, **p<0.01, t-test.

same level both in WT and KO cells in terms of R-SMADs phosphorylation, thus indicating that YAP is not required for the first steps of signaling activation. Of note, YAP expression is necessary for SMAD3 and SMAD1 protein expression.

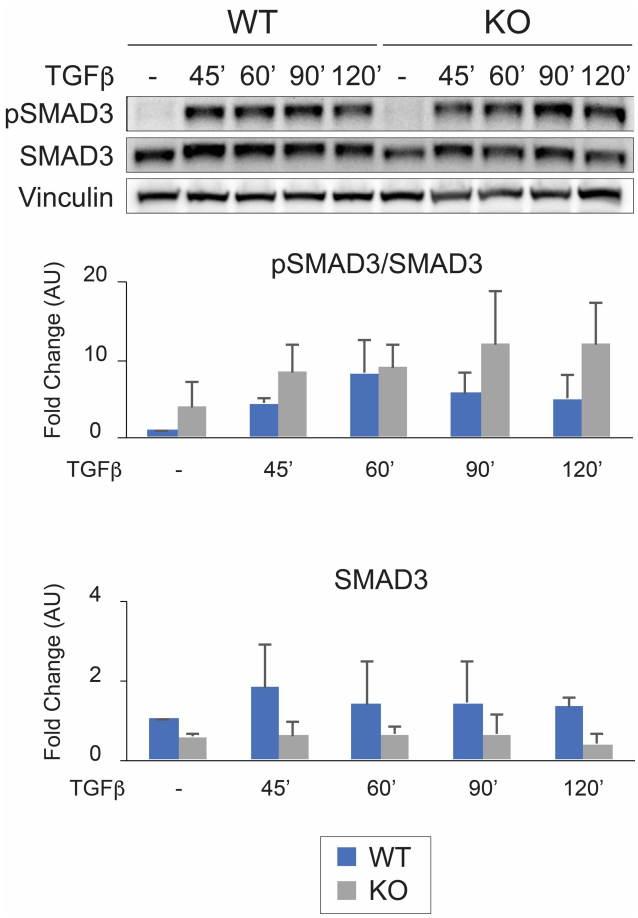

Figure 23. Loss of YAP does not influence SMAD3 C-term phosphorylation kinetic. Representative WB of YAP WT and KO cells treated with TGFβ for the indicated times. WB bands have been quantified using optic densitometry software and normalized to the relative Vinculin band (housekeeping). The ratio between normalized pSMAD3 and SMAD3 levels were then calculated for each sample, and expressed as fold change referred to WT untreated cells in AU. Data are mean of n=3 independent experiments ± SD.

3.5 YAP is required for SMAD3 nuclear accumulation

Following receptor-mediated phosphorylation, R-SMADs form a complex with SMAD4 and together shuttle to the nucleus (Goumans and Ten Dijke, 2017). Since our data showed that YAP is necessary for SMAD3-driven signaling activity (**Figure 20**), but not for TGFβ-induced cascade activation (**Figure 22**), we next moved to

investigate whether YAP is involved in the downstream R-SMADs nuclear accumulation.

First, we assessed whether SMAD3 can form a complex together with SMAD4 even in the absence of YAP. To address this question, we performed IP of SMAD3 from total cell extracts of WT and KO ECs, and observed that SMAD3 co-immunoprecipitated together with SMAD4 at a similar level in both cell lines, suggesting that loss of YAP does not affect SMAD3-SMAD4 complex formation (**Figure 24**). Moreover, these analyses revealed that SMAD3 formed a protein complex together with YAP both in control and stimulated conditions.

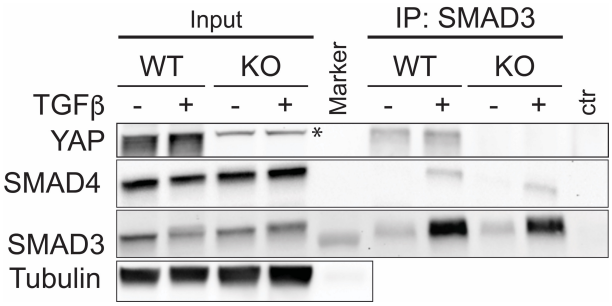

Figure 24. SMAD3 co-immunoprecipitates with SMAD4 in response to TGFβ. Representative WB of SMAD3 IP (right side) from total cell lysate (input, left side). Cell were treated with TGFβ for 45 minutes before performing IP as described in materials and methods section. SMAD3 sc-101154 was used for IP, while SMAD3 cs-9523 for detecting WB bands, Asterisk (*) indicate an unspecific band detected in KO cells. Tubulin was used as input loading control. N=3 independent experiments.

We then treated WT and KO cells for 2 h with TGFβ and analyzed R-SMAD sub-cellular localization, in order to determine whether YAP is important for R-SMADs nuclear accumulation in response to TGFβ.

N/C fractionation assays showed that ECs stimulation with TGFβ induced a marked SMAD3, -1, -2 and -4 nuclear accumulation in WT and KO cells. However, while SMAD1, -2 and -4 nuclear translocation occurred at comparable levels in both cell lines, loss of YAP significantly affected SMAD3 nuclear accumulation (**Figure 25**). Thus, we concluded that YAP specifically contributes to SMAD3 nuclear

accumulation upon TGFβ treatment and our results are in agreement with what previously described (Zhang et al., 2014). Moreover, despite SMAD1 protein levels are down-regulated in KO cells (**Figure 22**), we observed similar nuclear SMAD1 accumulation levels in the two cell lines, which could partly explain why we did not detect a reduced SMAD1 signaling activity in KO cells compared to WT cells (**Figure 20**). On the other hand, our data showed that YAP is required for both SMAD3 protein accumulation (**Figure 22**) and nuclear translocation (**Figure 25**), and, overall, for SMAD3 signaling activity (**Figure 20**), further suggesting that YAP and SMAD3 cooperate to drive TGFβ-induced signaling in ECs.

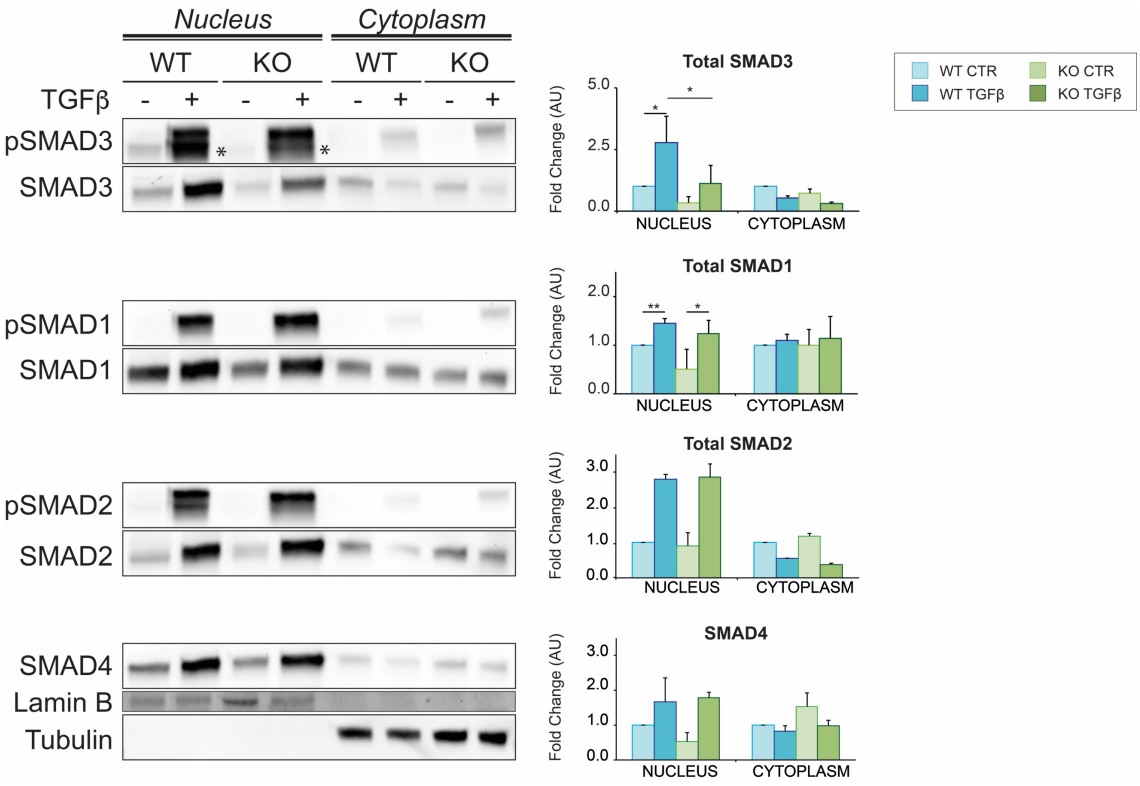

Figure 25. YAP is required for SMAD3 nuclear accumulation. Representative WB of N/C fractionation after 2 hours of TGFβ treatment. Asterisks in the blot indicate pSMAD3 C-term specific band. Right: Data are mean of at least n=3 independent experiments ± SD *p<0.05 **p<0.01. Fold changes are referred to either nuclear or cytoplasmic WT untreated cells. Lamin B is used as loading control for the nuclear fraction. Tubulin is used as loading control for the cytoplasmic fraction and to verify the purity of the nuclear fraction.

To further confirm these data, we performed IF stainings of SMAD3, -1, -2 and -4 in WT and KO treated cells (**Figure 26**). In line with N/C fractionation analyses, results showed that SMAD1, -2 and -4 nuclear relocalization upon TGFβ treatment occurred at a comparable level between the two cell lines, while SMAD3 nuclear accumulation was reduced in YAP KO cells.

In conclusion, loss of YAP did not impair SMAD3 and SMAD4 complex formation, but it strongly reduced the amount of SMAD3 that shuttles to the nucleus upon TGFβ treatment. Moreover, we observed a protein interaction between YAP and SMAD3 both in basal and stimulated conditions, but how YAP contributed to SMAD3 nuclear accumulation was still unknown.

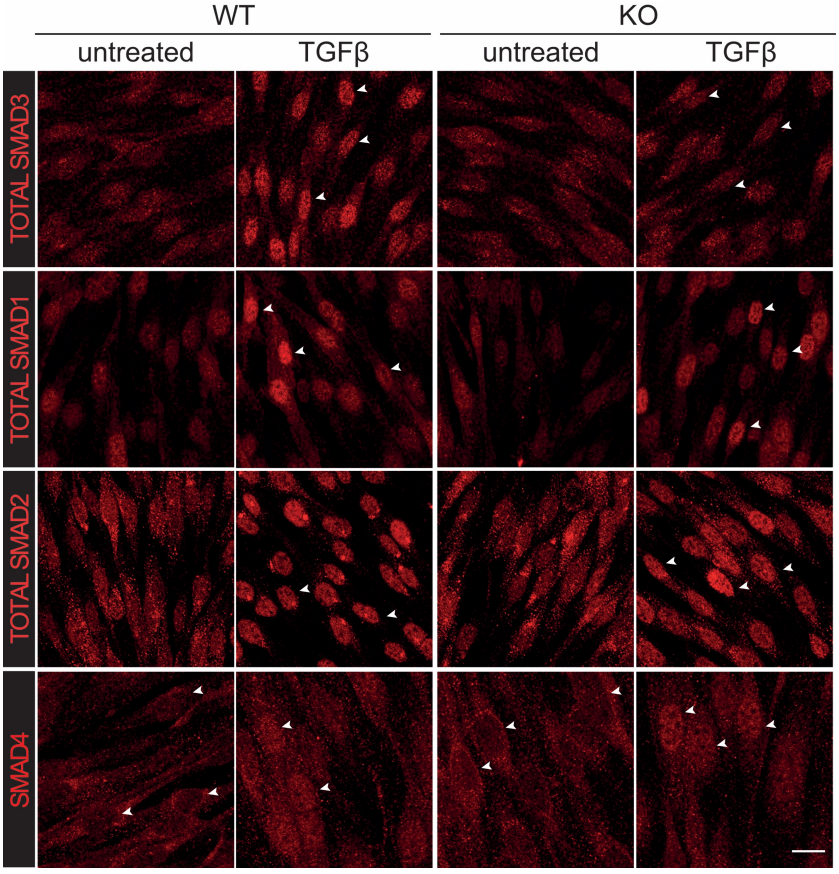

Figure 26. SMAD3 nuclear accumulation is impaired in absence of YAP. Representative IF stainings of total SMAD3, -1, -2 and -4 in WT and KO cells treated with TGFβ for 2 h. Arrowheads point to nuclei. Scale bar = 20 μm. n=5 for SMAD3 and SMAD1 and n=2 for SMAD2 and SMAD4.

3.6 YAP does not shuttle to the nucleus in response to TGFβ

In confluent epithelial cells, YAP binds and sequesters SMAD3 in the cytoplasm, thereby preventing SMAD3 nuclear translocation and transcriptional activity upon TGFβ stimulation (Grannas et al., 2015; Varelas et al., 2010). In confluent ECs, instead, SMAD3 translocated to the nucleus in response to TGFβ despite YAP expression, while SMAD3 nuclear accumulation was significantly reduced when YAP expression was lost (**Figure 25** and **Figure 26**).

In order to define how YAP contributed to SMAD3 nuclear accumulation, we first checked whether YAP sub-cellular localization varied upon TGFβ treatment. To do so, we performed TGFβ time-course treatment of YAP WT cells and analyzed pYAP Ser127 levels over-time, since 14-3-3 protein recognizes and causes pYAP Ser127 cytoplasmic retention (Basu et al., 2003). Interestingly, we found that TGFβ did not affect phosphorylation of YAP at Ser127 at any time point tested (**Figure**

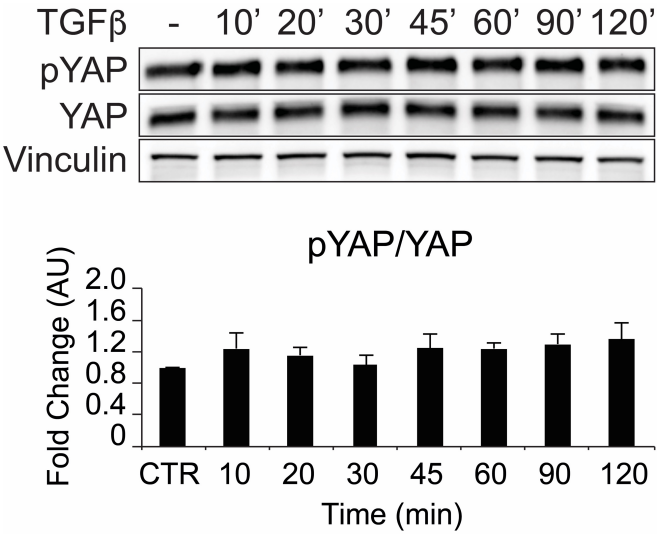

Figure 27. pYAP Ser127 levels are not modulated by TGFβ. Representative WB of YAP WT cells treated with TGFβ for the indicated times. WB bands have been quantified using optic densitometry software and normalized to the relative Vinculin band (housekeeping). The ratio between normalized pYAP Ser127 and YAP levels were then calculated for each sample, and expressed as fold change referred to WT untreated cells in AU. The chart represents quantification of n=4 independent experiments ± SD.

27), suggesting that YAP does not shuttle to the nucleus in response to TGFβ stimulation.

In order to exclude a possible YAP nuclear translocation, we then performed both N/C and IF analyses and checked YAP sub-cellular localization in presence of a TGFβ stimulus (**Figure 28**). In line with our previous observations and with what described in other cells systems (Giampietro et al., 2015; Varelas et al., 2010), YAP predominantly localizes in the cytoplasm of confluent ECs, although a small amount of YAP is anyway present in the nucleus. By treating WT cells with TGFβ for 2 h, we did not detect any YAP nuclear accumulation, and therefore we concluded that TGFβ did not modulate YAP sub-cellular localization.

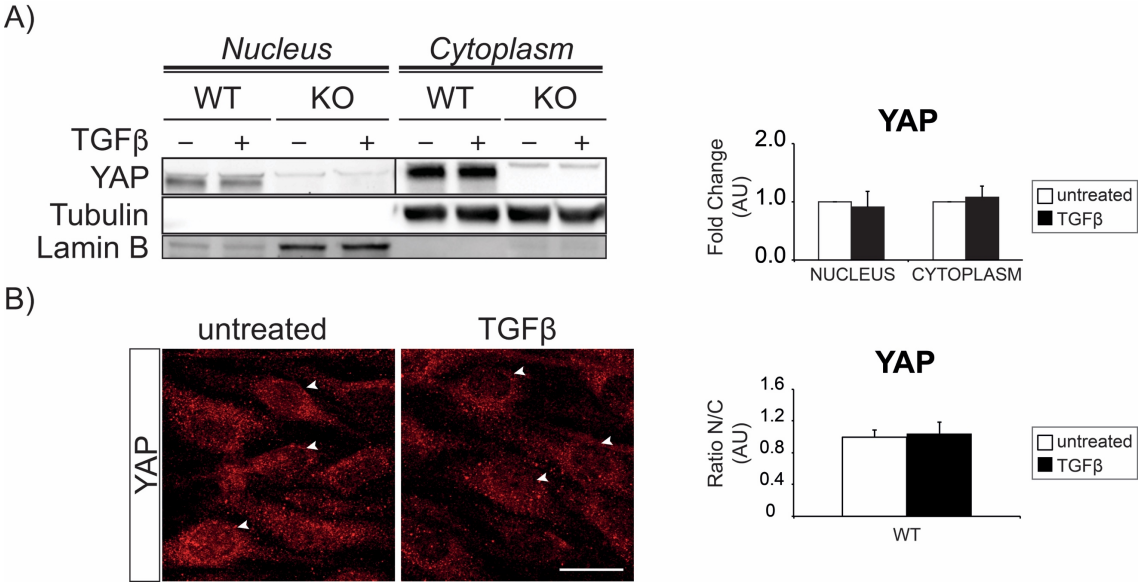

Figure 28. YAP subcellular localization is not influenced by TGFβ. A) Left: representative WB of N/C fractionation after 2 h of TGFβ treatment. Right: mean quantification of n=3 independent experiments ± SD. Fold changes are referred to either nuclear or cytoplasmic YAP WT untreated cells. Lamin B is used as a loading control for the nuclear fraction. Tubulin is used as a loading control for the cytoplasmic fraction and to verify the purity of the nuclear fraction. B) Left: IF staining of YAP in WT confluent cells after 2 h of TGFβ treatment. Arrowheads point to nuclei. Scale bar = 10 μm. Right: quantification of the ratio between the nuclear and the cytoplasmic intensity of the staining. Samples are normalized to YAP WT untreated cells. Data are mean of n=3 independent experiments ± SD.

Interestingly, by performing IP of SMAD4 from total cell lysate in presence or absence of a TGFβ stimulus, we could not observe an interaction between SMAD4 and YAP (**Figure 29**), suggesting that SMAD3 binds to YAP or to SMAD4 under different conditions and they do not form a trimeric complex that together shuttles to the nucleus.

Collectively, these data showed for the first time that YAP sub-cellular localization is not modulated by TGFβ stimulus and that YAP does not take part into SMAD4-mediated SMAD3 nuclear translocation. Thus, how YAP contributed to SMAD3 nuclear accumulation and why YAP formed a complex with SMAD3 was yet to be elucidated.

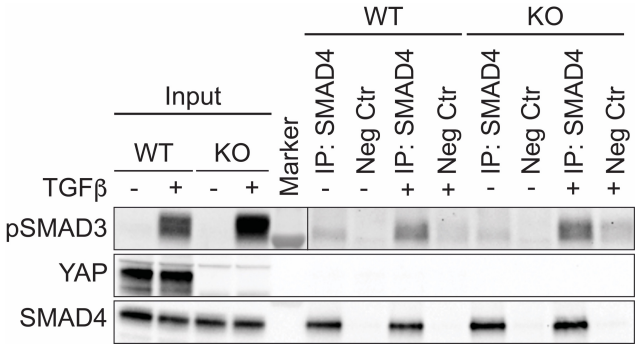

Figure 29. SMAD4 does not form a complex together with YAP. WB showing of SMAD4 IP (right side) from total cell lysate (input, left side). Cell were treated with TGFβ for 2 h before performing IP as described in materials and methods section. As a negative control (Neg Ctr) we used a species-matching antibody. N=3

3.7 TGFβ induces a dissociation of SMAD3 from cytoplasmic YAP, while inducing a nuclear YAP-SMAD3 complex formation

Since our previous observations showed that YAP and SMAD3 can form a protein complex and that the absence of YAP negatively impacts on SMAD3 nuclear accumulation, we then wondered whether YAP can play a role in SMAD3 nuclear accumulation by binding it in the nucleus in response to TGFβ. In order to address

this question, we performed IP of YAP both from nuclear and cytosolic cell fractions in response to 45 minutes TGFβ stimulation.

Very interestingly, we observed that YAP and SMAD3 interacted with each other in the nucleus and their binding was further increased in response to TGFβ treatments (**Figure 30**). At the same time, cytoplasmic YAP formed a complex together with SMAD3 in basal conditions, while exposure to TGFβ induced their dissociation.

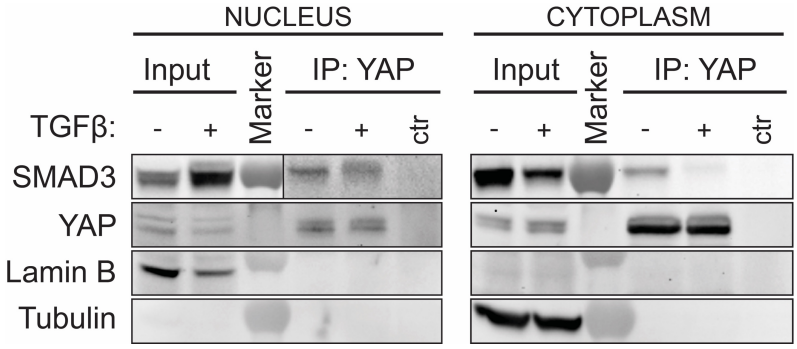

Figure 30. TGFβ induces a dissociation of SMAD3 from cytoplasmic YAP, while inducing a nuclear YAP-SMAD3 complex formation. Representative WB of WT cells immunoprecipitated for YAP (sc-271134) from either nuclear or cytosolic cell fraction. Cells were treated with TGFβ for 45 minutes. Input represent either nuclear (left) or cytoplasmic (right) protein pools. YAP sc-15407 was used to detect the corresponding WB band. N=3 independent experiments.

In conclusion, our data showed that YAP acted by sustaining TGFβ-mediated EndMT, SMAD3-driven signaling, SMAD3 protein and nuclear accumulation, and, also, that TGFβ reinforced SMAD3 binding to nuclear YAP in ECs. In light of these results, we hypothesized that YAP could bind to SMAD3 in the nucleus, strengthens SMAD3 binding to DNA and regulate together EndMT genes expression, while at the same time preventing SMAD3 nuclear exit by acting as a transcriptional cofactor.

3.8 EndMT genes contain putative binding sites for TEAD and SMAD3

Previous studies have described YAP as a SMAD3 transcriptional cofactor in a variety of cell systems, including ECs (Beyer et al., 2013; Fujii et al., 2012; Hiemer et al., 2014; Zhang et al., 2014). In order to determine whether YAP and SMAD3 can function as transcriptional cofactor in driving EndMT genes expression, we analyzed the promoter region of several EndMT genes, spanning -5.0 KB to +1.0 KB around the TSS. We looked for either SMAD3 or TEADs putative binding sites, as TEAD family of transcription factor is known to cooperate together with YAP in driving gene transcription (Vassilev et al., 2001; Zhao et al., 2008), and also because previous reports have already shown that YAP/SMAD/TEAD complex work together to regulate gene expression in human embryonic stem cells and cancer cells (Beyer et al., 2013; Fujii et al., 2012; Hiemer et al., 2014).

Analyses revealed that the EndMT genes *Fn1*, *Acta2* and *Cdh2*, along with the EndMT-driving transcription factor *Snai1* contain SMAD3 putative binding sites, while TEAD binding sites are found only on *Acta2* and *Cdh2* promoter regions (**Figure 31**). As internal control, we analyzed also *Serpine1* promoter and found that contains one TEAD and four different SMAD3 binding sites. We then focused our attention on *Fn1* and *Serpine1*, since preliminary studies (not shown) showed that their expression is up-regulated at early time points (within 24h).

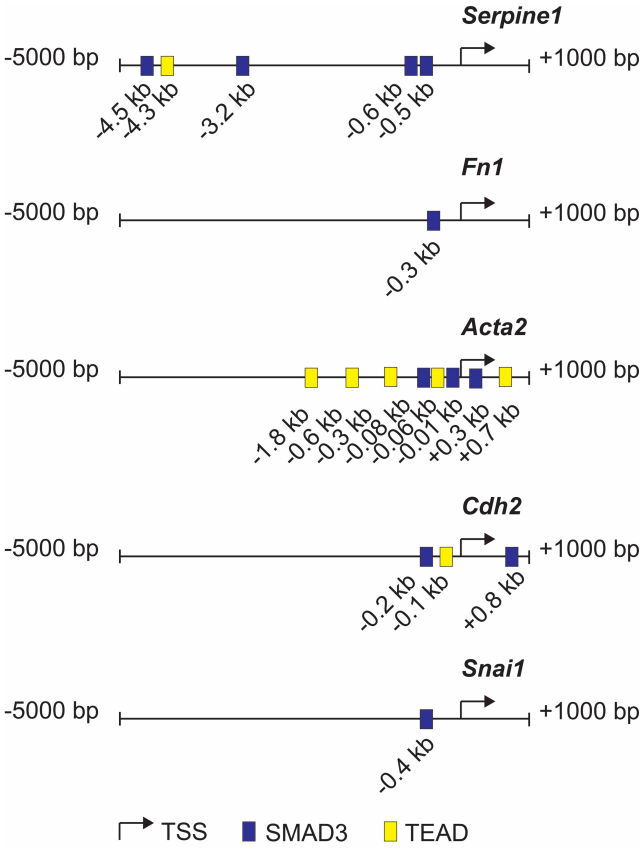

Figure 31. EndMT genes promoter analysis. The above figure schematically illustrates the promoter regions spanning - 5.0 KB to + 1.0 KB around the transcription start site (TSS) of *Serpine1*, *Fn1*, *Acta2*, *Cdh2* and *Snai1*. Boxes represent either SMAD3 (blue) or TEAD (yellow) putative binding site. Analysis has been performed retrieving the sequence from RSAT and then searching for putative binding sites using MatInspector software.

3.9 Silencing of TEAD1 does not impair EndMT genes expression

Since previous studies have reported that YAP/SMAD/TEAD complex work together to regulate gene expression (Beyer et al., 2013; Fujii et al., 2012; Hiemer et al., 2014), we evaluated whether YAP, SMAD3 and TEAD1 can form a protein complex in our cell system and together induce gene expression upon TGFβ treatment. By performing SMAD3 pull-down assays in WT and KO treated cells, we observed that TGFβ strengthened SMAD3-TEAD1 interaction in both WT and KO cells, although this effect was partially reduced in absence of YAP (**Figure 32**). This

suggested that probably a portion of total SMAD3 requires YAP to interact with TEAD1, while other SMAD3 molecules might engage with other interactors to form a complex together with TEAD1, like TAZ, or SMAD3 might directly bind to TEAD1 without the aid of YAP.

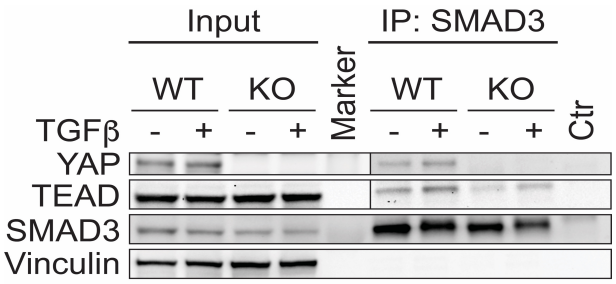

Figure 32. SMAD3 co-immunoprecipitates together with TEAD1. WB showing IP of SMAD3 (cs#9523) from total cell lysate of WT and KO cells treated with TGFβ for 45 minutes. Blot for: YAP (sc-271134), TEAD1 (BD 610923) and SMAD3 (MA5-15663). N=3 independent experiments. Vinculin was used a loading control of inputs (total cell lysate).

Although *Fn1* does not contain TEAD putative binding sites, while *Serpine1* bears only one of them (**Figure 31**), we wanted to investigate whether YAP/TEAD1/SMAD3 can cooperate to drive the transcription of these genes, as we couldn't exclude that YAP/TEAD could function at distal sites (enhancers) to modulate SMAD transcriptional activity (Stein et al., 2015; Zanconato et al., 2015).

If TEAD1 is involved in *Fn1* and *Serpine1* expression, its removal would then result in a decreased expression of the analyzed genes in YAP WT stimulated cells. However, by silencing TEAD1 through siRNA approach, we could not detect a significant down-regulation in *Fn1* and *Serpine1* expression neither at 6 nor at 24 h after TGFβ stimulation (**Figure 33**), suggesting that TEAD1 is not involved in the regulation of these genes.

Hence, these results indicated that SMAD3 can form a protein complex together with TEAD1 and that YAP might partly contribute to their interaction. TEAD1, however, is not required for *Fn1* and *Serpine1* expression, suggesting that YAP and

SMAD3 are likely responsible for the expression of these genes by forming a complex that does not comprise TEAD1. Whether other components of TEAD family are involved in EndMT genes expression remains yet to be elucidated.

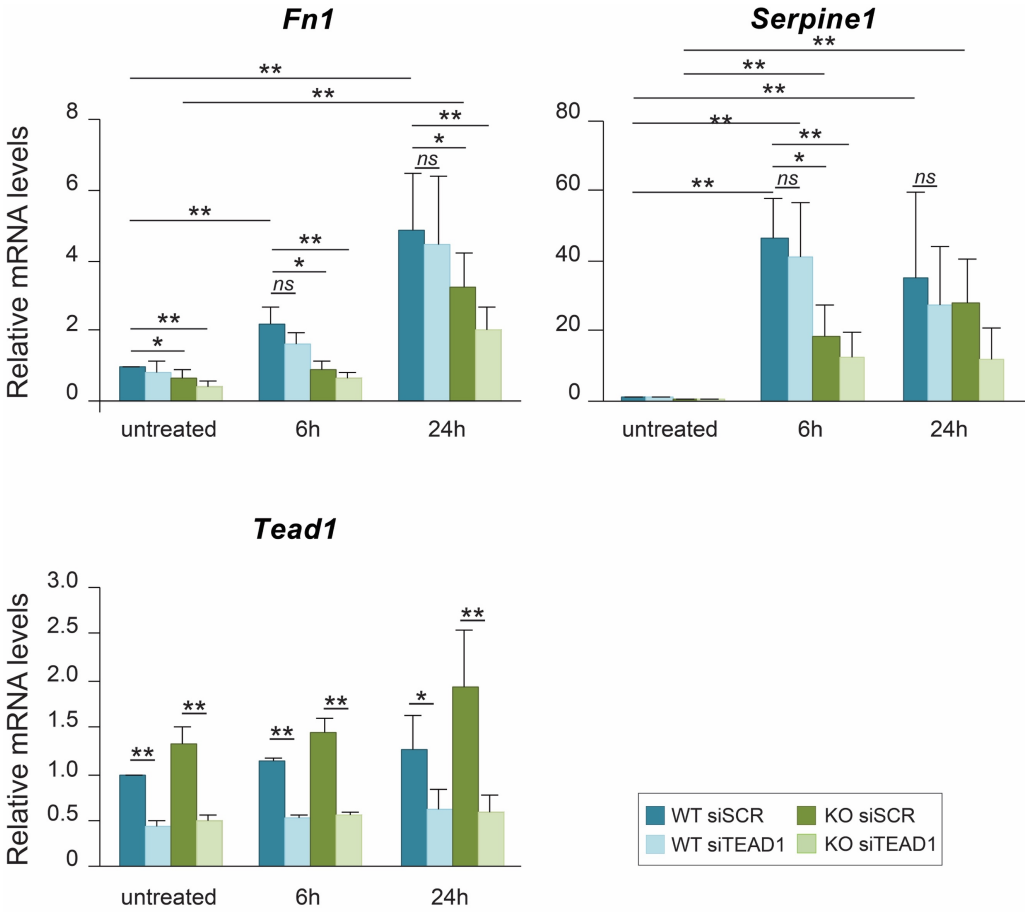

Figure 33. TEAD1 is not required for Fn1 and Serpine1 expression. qPCR analysis of *Fn1, Serpine1* and *Tead1* mRNA expression levels in YAP WT and KO cells treated with 5 ng/mL TGFβ for either 6 h or 24 h. Samples are normalized to WT untreated cells. Data are mean ± SD of n=3 independent experiments. *p<0.05 **p<0.01, ns= not significant, t-test.

3.10 YAP and SMAD3 bind to the same *Fn1* binding site

Having established that *Serpine1* and *Fn1* contain several SMAD3 putative binding sites, we next assessed whether YAP and SMAD3 act as transcriptional regulators of TGFβ-induced EndMT genes by binding to their identified putative binding sites (**Figure 31**). Interestingly, it was previously reported that YAP and SMAD3 directly mediate *Snai1* transcription by binding to its promoter region in

response to TGFβ stimulus (Zhang et al., 2014), prompting us to focus our attention to other genes, that is *Fn1* and *Serpine1*. In order to assess whether YAP and SMAD3 binds to *Fn1* and *Serpine1* promoter regions, we performed ChIP assays of WT and KO cells stimulated with TGFβ for 6 h, because preliminary data have shown that is the earliest time point at which *Fn1* expression is significantly up-regulated (data not shown).

Interestingly, we found that both YAP and SMAD3 bound to *Fn1* promoter region at the level of a SMAD3 putative binding site, suggesting that they possibly work as *Fn1* transcriptional regulators (**Figure 34**). However, we did not retrieve any YAP or SMAD3 bound to *Serpine1* promoter region #A1 (SMAD3 putative binding site, -0.5 KB from TSS, **Figure 31**) nor to region #C (TEAD putative binding site, -4.3 KB from

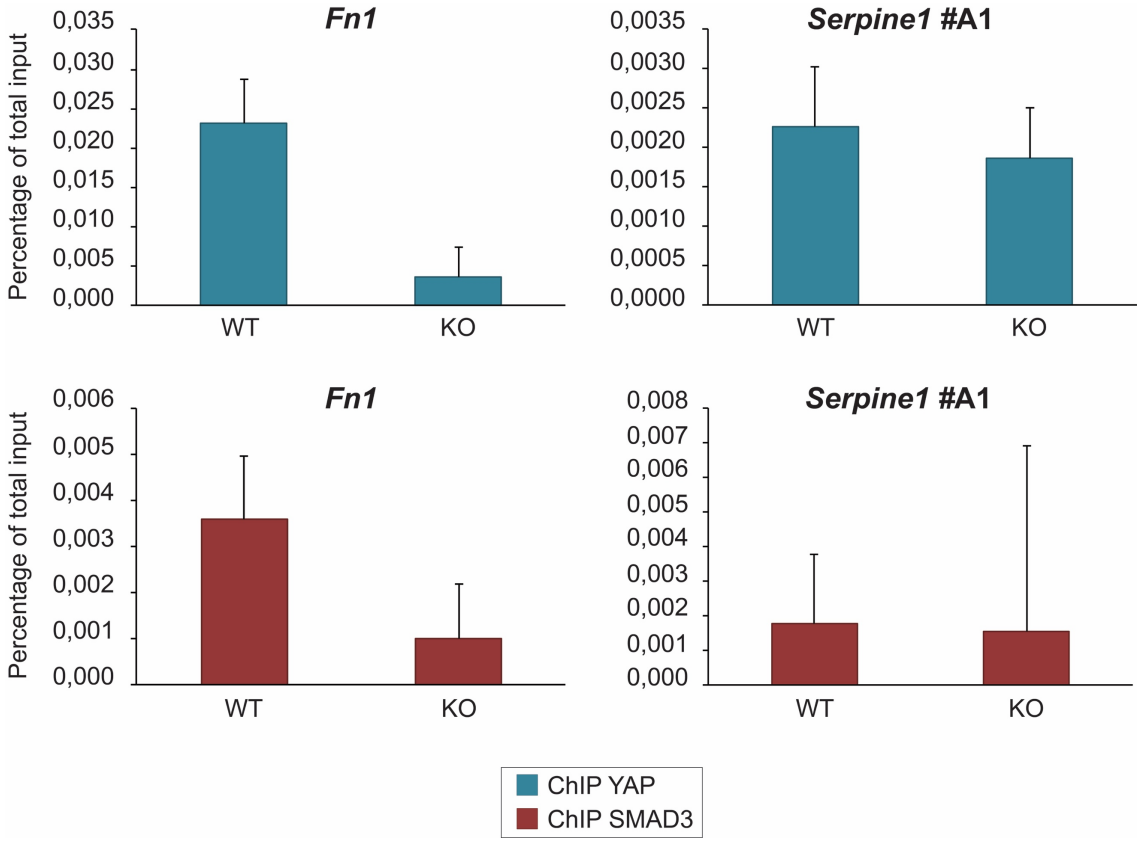

Figure 34. YAP and SMAD3 bind to *Fn1* promoter. ChIP analysis of YAP (blue) and SMAD3 (red) binding to *Fn1* and *Serpine1* promoters. WT and KO cells were treated for 6 h with TGFβ. DNA levels are normalized to the relative inputs. Columns are mean ±SD of triplicates from a representative experiment out of three with comparable results.

TSS, **Figure 31**) (**Figure 34** and data not shown). Unfortunately, due to technical problems, we could not amplify the other putative binding sites shown in **Figure 31** and thus we could not investigate whether YAP and/or SMAD3 bind to *Serpine1* promoter region at these sites.

In order to verify that SMAD3 is required for the expression of both *Fn1* and *Serpine1*, we silenced SMAD3 in both WT and KO cells and analyzed the expression of EndMT genes in response to TGFβ treatment. As shown in **Figure 35**, we found that SMAD3 is necessary for inducing *Fn1* and *Serpine1* expression upon TGFβ stimulation, further indicating that this transcriptional factor is important for driving EndMT genes transcription. Interestingly, in KO cells, *Fn1* and *Serpine1* expression tend to be even more reduced upon SMAD3 silencing, suggesting that, in absence of both YAP and SMAD3, the transcription of these genes is strongly reduced compared to WT treated cells.

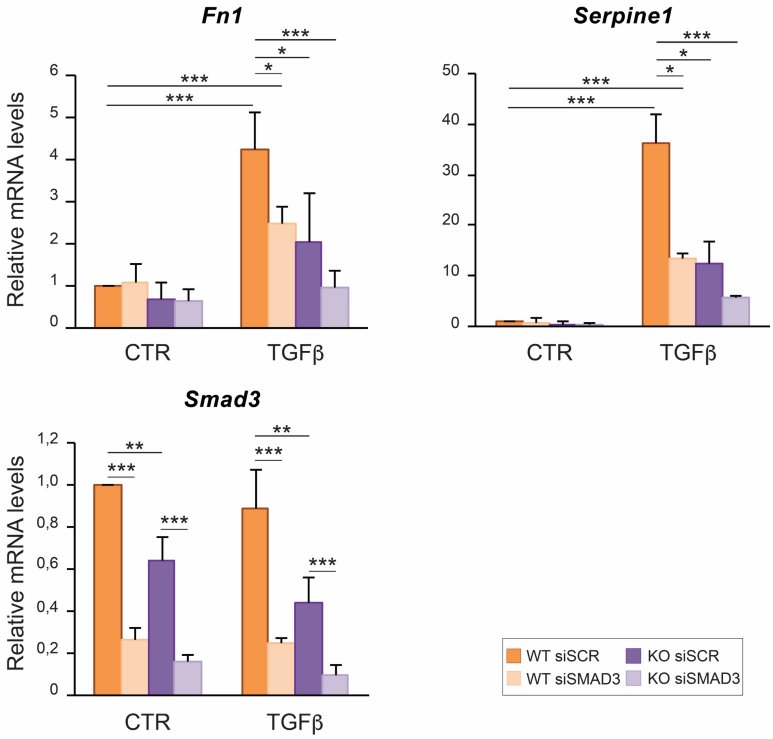

Figure 35. SMAD3 is required for *Fn1* and *Serpine1* expression. qPCR analysis of *Fn1, Serpine1* and *Smad3* mRNA expression levels in YAP WT and KO cells treated with 5 ng/mL TGFβ for 24 h. Samples are normalized to WT untreated cells. Data are mean ± SD of n=4 independent experiments. *p<0.05 ***p<0.001, t-test.

Of note, we observed also that SMAD3 mRNA expression is significantly lower in KO compared to WT cells, already at a basal level, partly explaining the reduced amount of total SMAD3 observed upon loss of YAP (**Figure 22**).

Collectively, these results showed that both YAP and SMAD3 bind to *Fn1* promoter region and probably act as transcriptional regulators, suggesting that YAP can function as SMAD3 co-transcriptional factor to drive EndMT genes expression in response to TGFβ stimulation.

3.11 YAP *gain-of-function* partially restores EndMT genes expression

Our previous data have so far demonstrated that loss of YAP in ECs resulted in an impaired EndMT response induced by TGFβ, and that YAP specifically contributed to SMAD3 expression and signaling activity. We thus assessed whether reintroducing a constitutively and transcriptionally active form of YAP, that cannot be phosphorylated in any of the 5 crucial serine residues required for YAP cytoplasmic retention and therefore localizes predominantly in the nucleus (YAP 5SA) (Dupont et al., 2011; Zhao et al., 2007), could restore the ability of KO cells to undergo EndMT upon TGFβ treatments. To do so, we infected WT and KO cells with lentiviral vectors expressing YAP 5SA, stimulated them with TGFβ for 24 h and analyzed the EndMT genes expression profile.

By observing the morphology of infected cells at phase-contrast microscope, we noticed that the overexpression of constitutively active YAP led to the formation of clusters of cells growing on top of the EC monolayer, as if the cells had lost contact-inhibition of growth (**Figure 36**). This phenotype resembled what previously described in other cell systems and, *per se,* showed that controlling the correct subcellular localization of YAP is useful to maintain a quiescent EC monolayer.

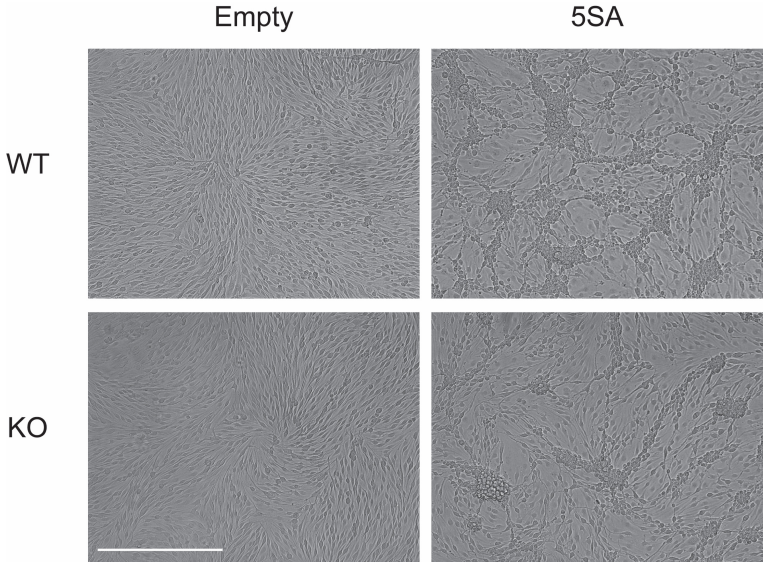

Figure 36. Expression of YAP 5SA abolishes contact-inhibition of growth in WT and KO cells. Representative pictures of WT and KO cells infected with either empty or YAP 5SA expressing lentiviral vectors as described in materials and methods section. Pictures have been acquired through transmitted light microscope (EVOS, ThermoFisher). Scale bar = 400 μm

We then stimulated infected cells with TGFβ for 24 h and assessed the EndMT response in terms of *Fn1* and *Serpine1* mRNA and protein expression. Interestingly, qPCR analyses revealed that YAP 5SA strongly induced *Fn1* and *Serpine1* expression in both WT and KO cells already at basal levels, suggesting that active nuclear YAP is important for the transcription of these genes. Moreover, TGFβ treatment further increased *Fn1* and *Serpine1* expression in WT and KO YAP *gain-of-function* cells, leading to comparable EndMT genes transcription levels between KO 5SA and WT empty treated cells (**Figur**). Of note, YAP 5SA expression in KO cells did not upregulate the expression of EndMT genes at the same levels as in WT 5SA treated cells. Accordingly, Fn1 protein expression was strongly up-regulated in KO YAP 5SA cells, yet not as much as in WT 5SA treated cells (**Figure**), suggesting that nuclear YAP activity is not enough to fully rescue SMAD3-driven signaling.

Along with EndMT genes expression, we also analyzed whether YAP 5SA expression is sufficient to restore SMAD3 mRNA and protein expression.

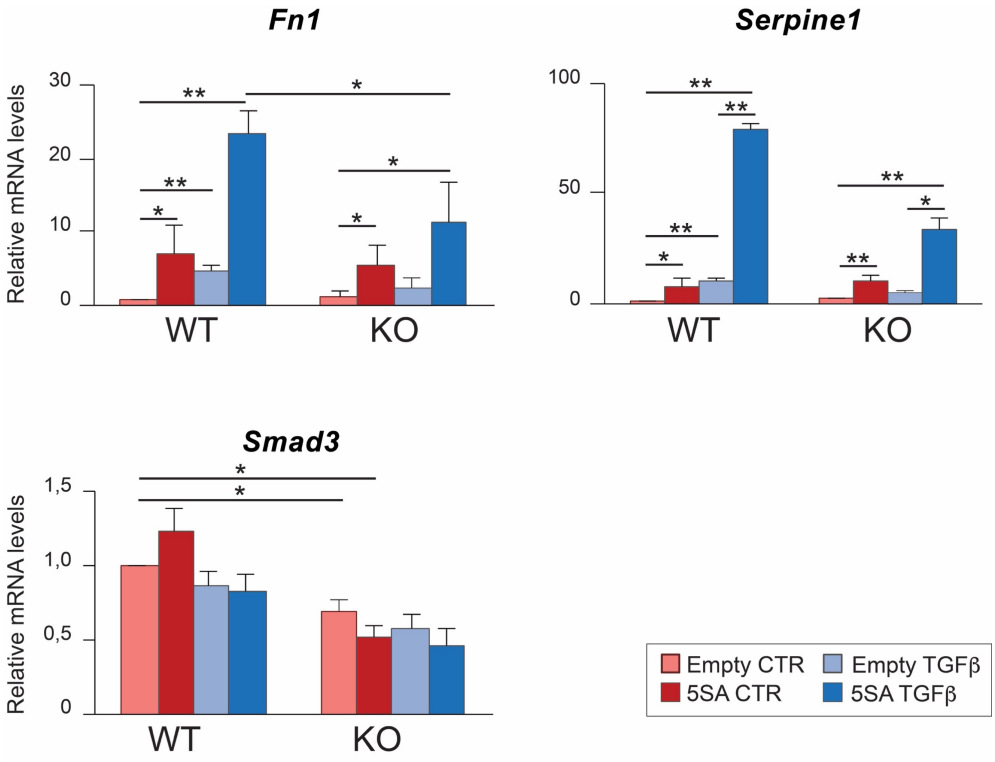

Figure 37. YAP 5SA partially restores *Fn1* and *Serpine1* mRNA expression. qPCR analysis of *Fn1, Serpine1* and *Smad3* mRNA expression levels in YAP WT and KO cells that were infected with either Empty or YAP 5SA lentiviral vectors and treated with 5 ng/mL TGFβ for 24 h. Samples are normalized to WT Empty untreated cells. Data are mean ± SD of n=3 independent experiments. *p<0.05 **p<0.01, t-test.

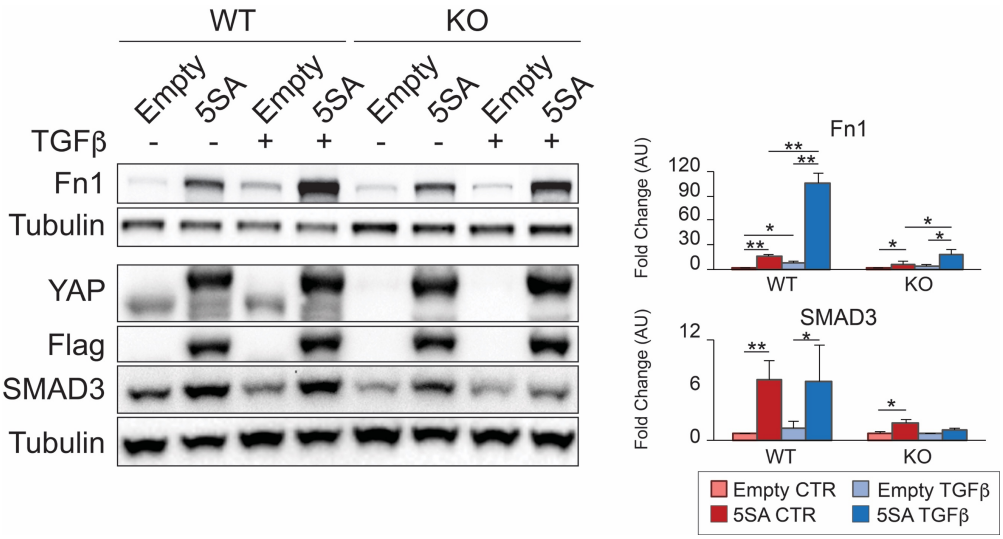

Figure 38. YAP 5SA partially restores Fn1 and SMAD3 protein expression. Representative WB of YAP WT and KO cells that were infected with either EMPTY or YAP 5SA lentiviral vectors and treated with 5 ng/mL TGFβ for 24 h. WB bands have been quantified using optic densitometry software and normalized to the relative Tubulin band (housekeeping). The fold change is referred to either WT or KO Empty untreated cells. Data are mean ± SD of n=3 independent experiments. *p<0.05 **p<0.01, t-test.

Interestingly, re-introducing a constitutively active form of YAP in KO cells did not rescue SMAD3 mRNA expression (**Figur**), while it strongly increased SMAD3 protein expression (**Figure**). These results indicated that YAP is not directly involved in *Smad3* gene transcription, rather YAP seems likely to be involved in SMAD3 protein stabilization.

Collectively, these results showed that reintroducing a constitutive form of YAP in KO cells partially restored EndMT genes expression both at mRNA and protein levels, adding further evidence that YAP is an important transcriptional regulator of these genes. Moreover, YAP 5SA expression in KO cells restored SMAD3 protein but not mRNA expression, opening up the possibility that YAP expression in ECs is important for SMAD3 protein stabilization and turnover.

3.12 YAP prevents SMAD3 phosphorylation at S204

Previous studies have reported that, upon BMP stimulation and subsequent C-term phosphorylation, SMAD1 is phosphorylated by CDK8/9 in its linker region at S206 and S214, which allows the binding of co-transcriptional factors such as YAP, and target genes transcription. Binding of co-transcription factors to SMAD1, moreover, prevents SMAD1 subsequent phosphorylation by GSK3β, thus impeding SMAD1 targeting to proteosomal degradation. In this way, while ensuring target genes transcription, binding of co-transcription factors to SMAD1 prevents its degradation (Alarcon et al., 2009; Aragon et al., 2011). A similar turnover pathway has been described concerning SMAD3, wherein CDK8/9 phosphorylates SMAD3 at T179 and S208, favoring co-transcriptional partners binding while priming SMAD3 to GSK3β-mediated phosphorylation at S204, and ultimately targeting SMAD3 to proteosomal degradation (Alarcon et al., 2009; Aragon et al., 2011). Nevertheless, it has never been suggested before that YAP might play this double role in case of SMAD3, that is sustaining SMAD3 transcriptional activity while preventing its

turnover. Since we observed that re-introducing a transcriptionally constitutively active form of YAP in ECs resulted in a marked SMAD3 protein accumulation in KO cells, we hypothesized that YAP might function as SMAD3 co-transcription factor to drive EndMT genes transcription while preventing phosphorylation at S204 and subsequent degradation.

In order to verify this hypothesis, we first analyzed whether lack of YAP expression in ECs might result in an increased phosphorylation of SMAD3 at S204. Remarkably, TGFβ time course treatment revealed that SMAD3 is phosphorylated at a higher level in KO versus WT cells already at basal conditions, suggesting that YAP expression prevents SMAD3 pS204 even in absence of a TGFβ stimulus (**Figure 39**). Very interestingly, 45 minutes TGFβ treatment led to a marked increase

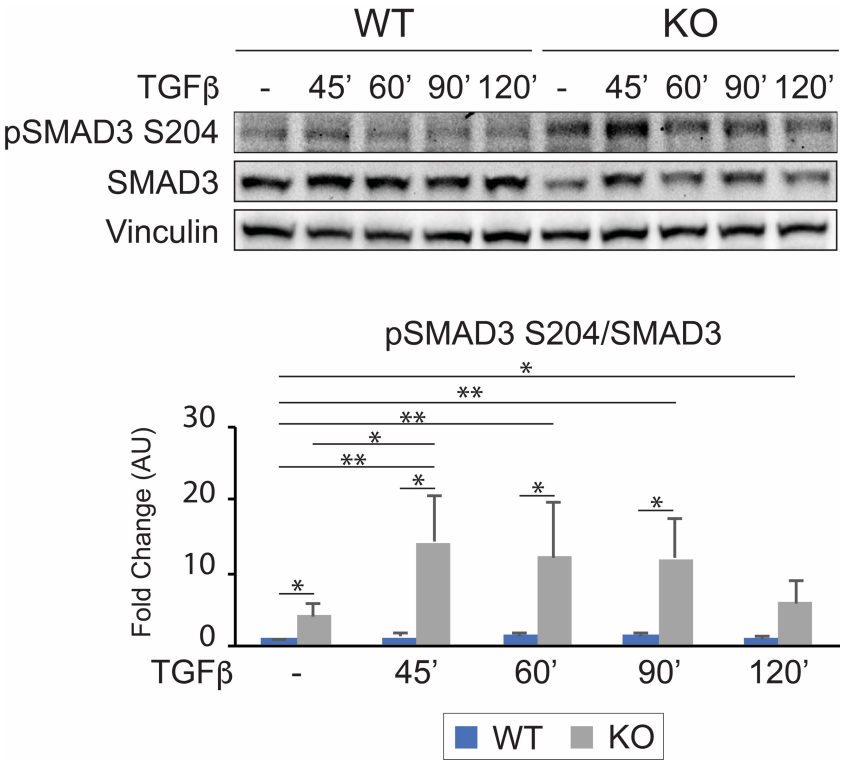

Figure 37. YAP prevents SMAD3 phosphorylation at S204. Representative WB of YAP WT and KO cells treated with TGFβ for the indicated times. WB bands have been quantified using optic densitometry software and normalized to the relative Vinculin band (housekeeping). The ratio between normalized pSMAD3 S204 and SMAD3 levels were then calculated for each sample, and expressed as fold change referred to WT untreated cells in AU. Data are mean of n=3 independent experiments ± SD. *p<0.05 **p<0.01, t-test.

in SMAD3 pS204 levels in KO cells, which lasted till about 90 minutes from the beginning of the treatment. Conversely, SMAD3 pS204 levels in WT cells were only slightly increased 45 minutes after TGFβ stimulation, and, over time, were kept at lower levels compared to KO cells.

Moreover, YAP 5SA expression in KO cells resulted in a marked decrease of pSMAD3 S204 compared to Empty KO cells (**Figure 40**), indicating that a transcriptionally active form of YAP contributed to prevent SMAD3 phosphorylation at S204, likely by engaging SMAD3 as a co-transcriptional factor and impeding phosphorylation at S204 involved in protein turnover.

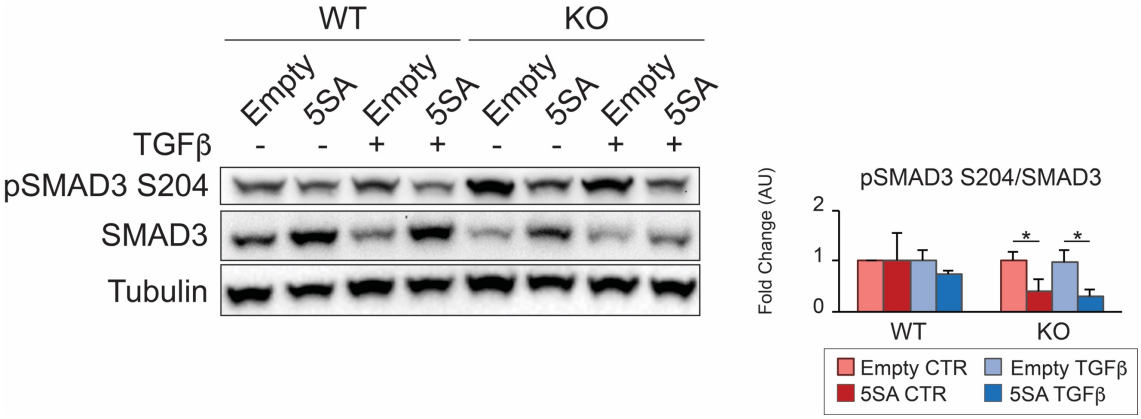

Figure 38. YAP 5SA reduces SMAD3 pS204 levels in KO cells. Representative WB of YAP WT and KO cells infected with either EMPTY or YAP 5SA lentiviral vectors and treated with 5 ng/mL TGFβ for 24 h. WB bands have been quantified using optic densitometry software and normalized to the relative Tubulin band (housekeeping). The fold change is referred to either WT or KO Empty untreated cells. Data are mean of n=3 independent experiments ± SD. *p<0.05, t-test.

In conclusion, these results showed for the first time that, upon genetic loss of YAP in ECs, SMAD3 undergoes extensive phosphorylation at S204 (**Figure 39**) and it is less expressed (**Figure 22**), indicating that YAP likely contributes to stabilize SMAD3 protein and prevent its degradation. Moreover, TGFβ treatments result in a stronger phosphorylation at SMAD3 S204 in cells lacking YAP expression while

expression of a transcriptionally active form of YAP decreases pSMAD3 S204 levels in KO cells, suggesting that YAP possibly prevents SMAD3 pS204 and subsequent degradation by engaging SMAD3 as a co-transcriptional factor.

3.13 SMAD3-GSK3β association is increased in absence of YAP

Previously, Wang and colleagues demonstrated that, in epithelial cells, the kinase responsible for SMAD3 pS204 is GSK3β (Wang et al., 2009a). Given that our former data clearly showed increased SMAD3 pS204 levels in ECs lacking YAP expression, we sought of investigating whether GSK3β is the kinase responsible for SMAD3 pS204 in ECs too.

We therefore performed pull-down assays to explore whether SMAD3 and GSK3β associated in YAP WT and KO ECs both at basal conditions and in response to TGFβ treatments. Results showed for the first time that SMAD3 and GSK3β form a complex in ECs (**Figure 41**). Moreover, we observed for the first time that genetic ablation of YAP in ECs led to an increased association between SMAD3 and GSK3β

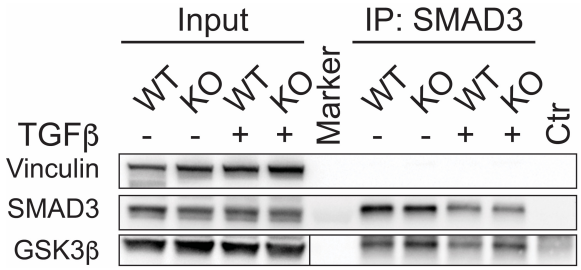

Figure 39. SMAD3-GSK3β binding increases in YAP KO cells. Representative WB of SMAD3 pull-down assay from total cell lysate. Cell were treated with TGFβ for 45 minutes before performing IP as described in materials and methods section. SMAD3 cs-9523 was used for IP, while SMAD3 MA5-15663 for detecting WB bands. Vinculin was used as input loading control.

at basal conditions, that was further increased in response to TGFβ treatments.

Hence, these results showed that GSK3β forms a complex together with SMAD3 in ECs and, very interestingly, the degree of their association is increased

upon genetic removal of YAP, suggesting that the expression of this co-transcriptional factor might hamper SMAD3-GSK3β interaction and possibly SMAD3 protein turnover.

3.14 GSK3β kinase activity is responsible for SMAD3 pS204 and protein turnover

Our previous data showed that, in YAP KO cells compared to WT cells, SMAD3 pS204 levels are increased (**Figure 39**) as well as SMAD3-GSK3β association (**Figure 41**). Since GSK3β is known to induce SMAD3 S204 phosphorylation in epithelial cells(Wang et al., 2009a), we investigated whether GSK3β is the kinase responsible for SMAD3 pS204 in ECs too and whether the phosphorylation at this site targets SMAD3 for proteosomal degradation.

To do so, we took advantage of an inhibitor of GSK3β activity, namely LiCl (Klein and Melton, 1996), and analyzed SMAD3 total protein and S204 phosphorylation levels in both WT and KO treated cells.

Interestingly, we observed a marked decrease in S204 phosphorylation upon LiCl treatment occurring both at basal and TGFβ-treated conditions in KO cells, suggesting that GSK3β kinase activity is required for SMAD3 pS204 in ECs (**Figure 42**). Moreover, exposure of KO cells to LiCl led to an increased SMAD3 protein expression, that reached levels similar to the ones observed in WT cells.

In light of these results, we also analyzed whether SMAD3 nuclear accumulation is restored in KO cells upon inhibition of protein degradation through LiCl and in response to TGFβ. Interestingly, we observed a significant increase in SMAD3 nuclear accumulation in KO cells treated with LiCl and TGFβ compared to control KO cells treated with TGFβ (**Figure 43** and **Figure 44**), suggesting that inhibition of

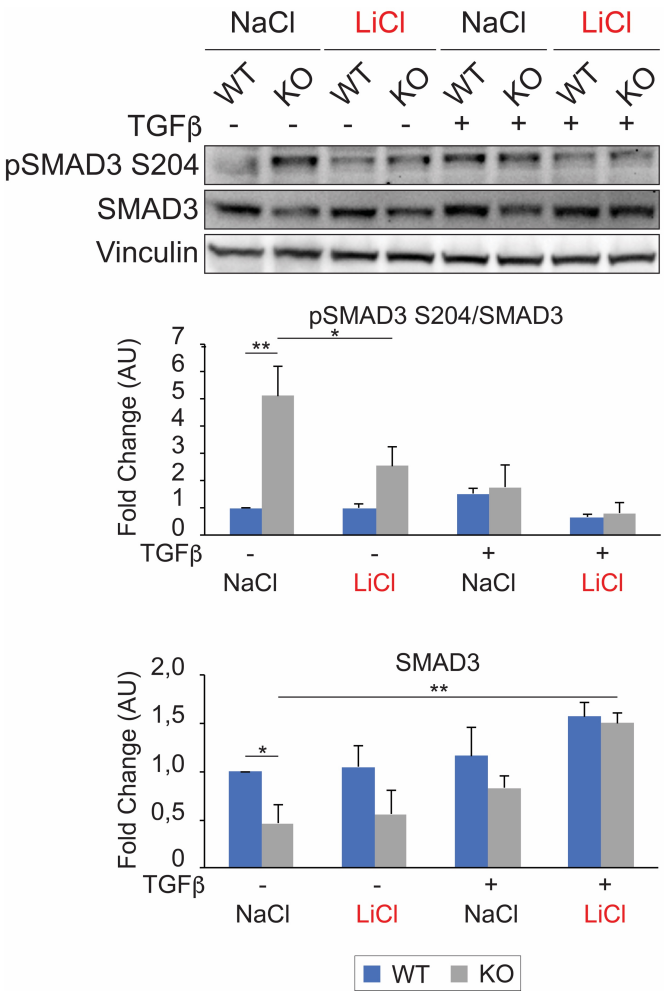

Figure 40. GSK3β phosphorylates SMAD3 and targets it to degradation. Representative WB and relative quantification of WT and KO cells treated with either 60 mM LiCl or NaCl (control) O/N in starving medium, followed by 2 h TGFβ stimulation (for further details see materials and methods section). Data are mean of n=4 independent experiments ± SD. *p<0.05, t-test.

GSK3β-mediated SMAD3 protein turnover is sufficient to restore SMAD3 nuclear accumulation in KO cells.

To conclude, these results showed for the first time that GSK3β is the kinase responsible for SMAD3 pS204 in ECs, targeting SMAD3 for protein degradation, and that GSK3β inhibition combined with TGFβ treatments results in increased SMAD3 nuclear accumulation in KO cells.

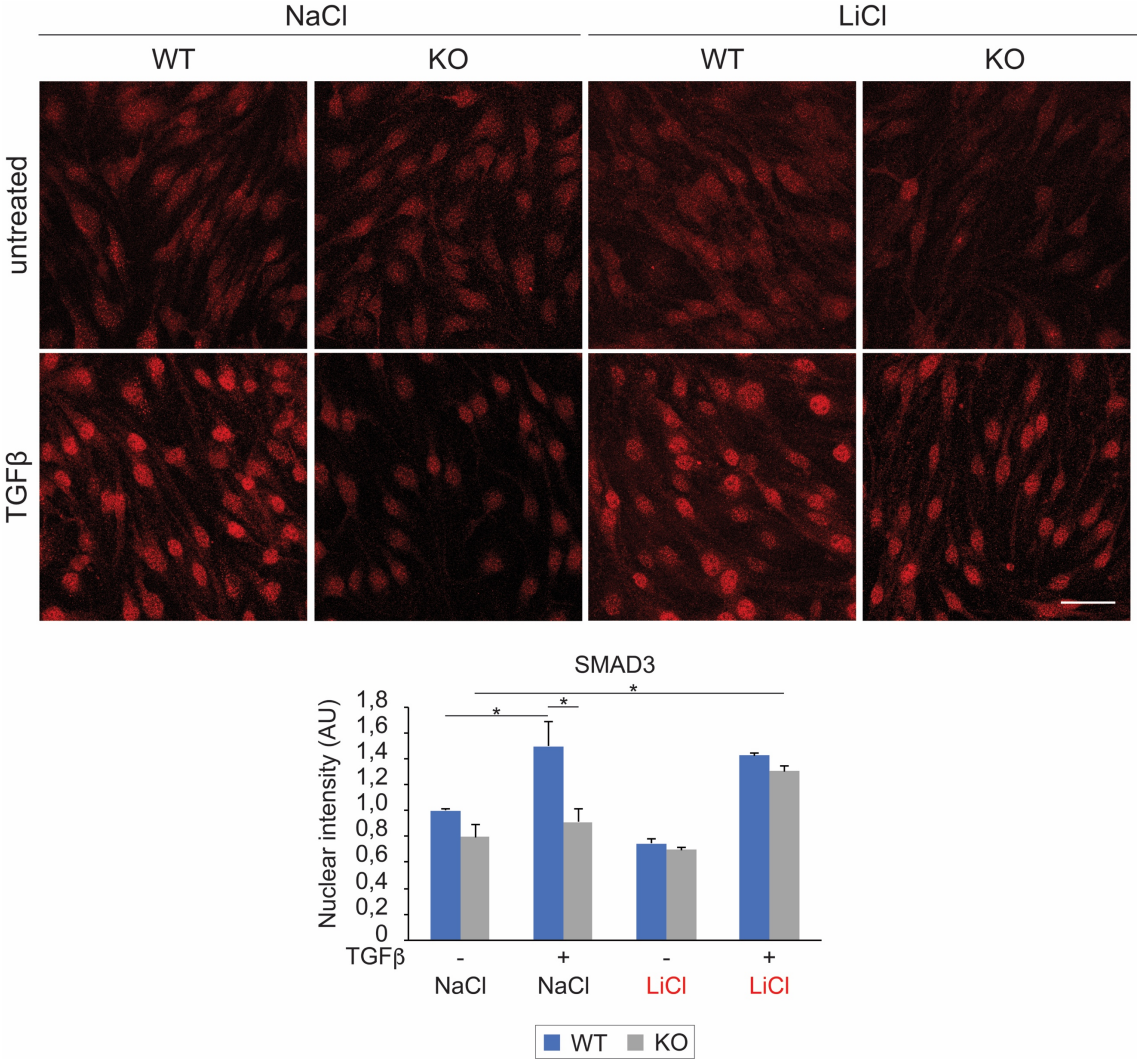

Figure 41. SMAD3 nuclear accumulation is restored in KO cells upon LiCl-mediated GSK3β inhibition. Representative IF stainings of total SMAD3 in WT and KO cells treated with either 60 mM LiCl or NaCl (control) O/N in starving medium, followed by 2 h TGFβ stimulation. Scale bar = 40 µm. The bottom chart represents the mean intensity of nuclear SMAD3 ± SD from n=3 independent experiments, expressed as a fold change referred to WT NaCl treated cells. *p< 0.05, t-test

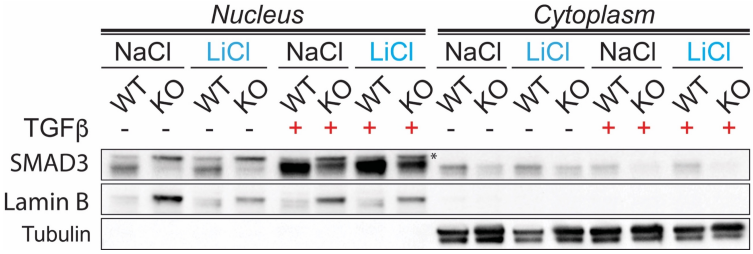

Figure 42. SMAD3 nuclear accumulation is restored in KO cells upon LiCl-mediated GSK3β inhibition. Representative WB of total SMAD3 in WT and KO cells treated with either 60 mM LiCl or NaCl (control) O/N in starving medium, followed by 2 h TGFβ stimulation. Asterisk (*) indicate unspecific bands. Lamin B was used as nuclear loading control, while tubulin as cytosolic housekeeping gene. N=2 independent experiments.

3.15 SMAD3 protein stabilization through GSK3β inhibition is not sufficient to restore TGFβ-induced EndMT in YAP KO ECs

Since GSK3β inhibition resulted in an increased SMAD3 protein stability and nuclear accumulation in KO cells, we wondered whether the defective EndMT response observed in KO cells was due to decreased levels in SMAD3 protein expression and nuclear accumulation or whether SMAD3 effectively requires YAP as a transcriptional co-factor that, at the same time, prevents protein turnover.

In order to address this question, we analyzed EndMT genes expression in WT and KO cells stimulated with TGFβ and LiCl. Interestingly, inhibition of GSK3β by LiCl significantly up-regulated *Fn1* and *Serpine1* mRNA expression in WT but not in KO cells in response to TGFβ (**Figure 45**). Moreover, LiCl treatments did not have any effect on SMAD3 mRNA expression levels, further indicating that GSK3β inhibition plays a role in SMAD3 protein stabilization rather than protein transcription.

Hence, we showed that the SMAD3 protein accumulation occurring upon LiCl-mediated GSK3β inhibition was not sufficient for restoring EndMT genes transcription in cells lacking YAP expression, while it significantly increased *Fn1* and

Serpine1 mRNA levels in WT cells. In conclusion, our results strongly suggested that the expression of YAP is required not only for SMAD3 expression, but also as a SMAD3 co-transcriptional regulator of EndMT genes.

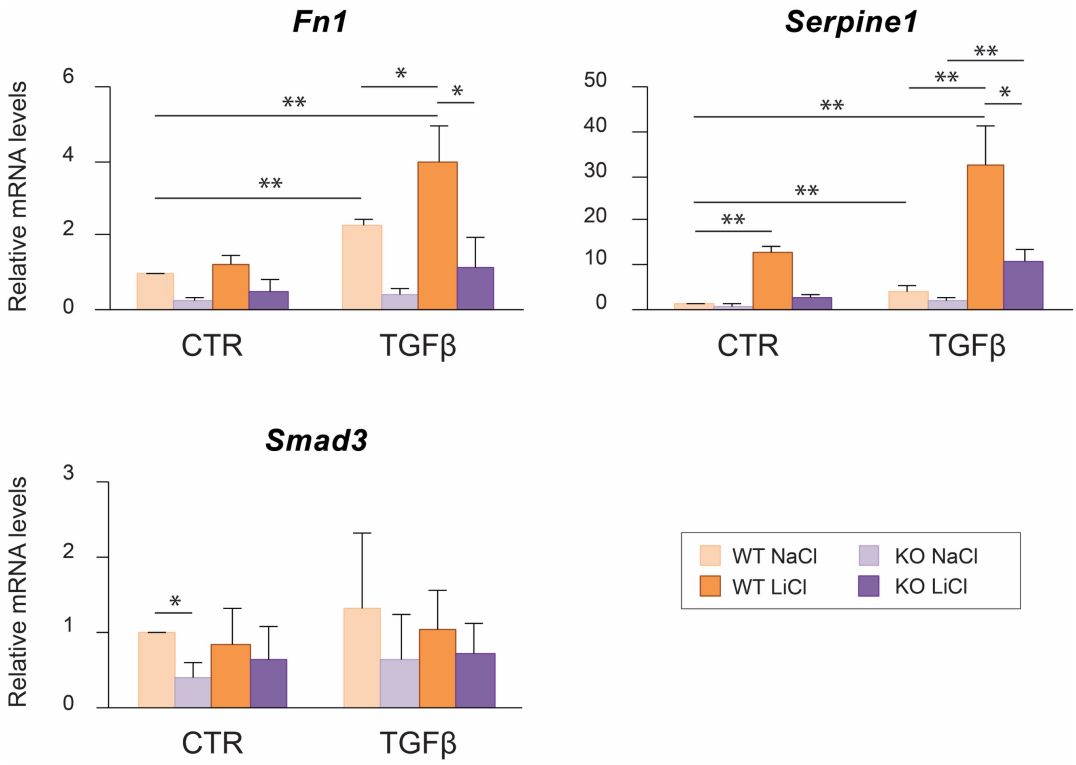

Figure 43. SMAD3 protein accumulation upon GSK3β inhibition is not enough to restore EndMT genes transcription in KO cells. qPCR of *Fn1, Serpine1* and *Smad3* mRNA expression levels in YAP WT and KO cells treated with either 60 mM LiCl or NaCl (control) O/N in starving medium, followed by 24 h TGFβ stimulation. Samples are normalized to WT NaCl untreated cells. Data are mean ± SD of n=4 independent experiments. *p<0.05 **p<0.01, t-test.

Chapter 4 - Discussion

EndMT refers to a biological process that allows the transdifferentiation of quiescent ECs into mesenchymal cells, thus originating cells capable of novel functions required to meet the needs of the surrounding environment (van Meeteren and ten Dijke, 2012). During this process, ECs lose their peculiar features and markers, like VE-cadherin, Claudin-5, CD31 and others, and begin to display mesenchymal-like characteristics, that is increased migration and invasiveness, and the expression of a plethora of markers such as Snai1, Snai2, αSMA, Fn1, FSP1, KLF4, N-Cadherin, and Serpine1. Physiologically, EndMT regulates endocardial cushion formation during embryo development, and it is stimulated by growth factors belonging to the TGFβ/BMP family of ligands. Conversely, EndMT does not generally occur in the adulthood, unless ECs are challenged with continuous inflammatory stimuli, leading to organ fibrosis, or during pathological conditions such as tumor progression and FOP. Besides, our group has been the first one to identify EndMT as a key biological mechanism that drives CCM pathology onset and progression, and revealed that, once again, TGFβ/BMP family of ligands are deeply involved in fueling this newly-characterized EndMT process (Maddaluno et al., 2013). Therefore, it is becoming more and more crucial to characterize the molecular regulators cooperating with TGFβ signaling in sustaining this fundamental biological process, in order to possibly provide novel therapeutic targets to treat these life-threatening conditions.

We focused our attention on YAP, a co-transcriptional regulator involved in many fundamental cell biology processes, like cell proliferation, cell migration, apoptosis, but also EMT (Overholtzer et al., 2006). This process shares some similarity with EndMT and occurs in epithelial cells in pathological conditions, such as tumor progression and metastasis, and during development (Kalluri and

Weinberg, 2009). Since EndMT is considered a “specialized” form of EMT, we hypothesized that YAP could also be an important regulator for EndMT. Additionally, over the last decade, YAP has been repeatedly shown to interplay with TGFβ/BMP signaling both in a positive and a negative manner in epithelial cells, suggesting a possible YAP-TGFβ crosstalk in ECs too.

Under theses premises, we hypothesized that YAP contributes to EndMT by modulating TGFβ/BMP signaling, and tested our hypothesis by generating lung immortalized ECs either WT or KO for YAP.

YAP WT and KO ECs were then chronically stimulated for 5 consecutive days with either BMP6 or TGFβ in order to elicit an EndMT response. Interestingly, BMP6 stimulated EndMT markers expression in WT ECs, and even more in KO cells, thus suggesting that YAP might play a protective role in BMP6-induced EndMT. Although we did not further investigate this aspect, we can hypothesize a role of YAP in CCM pathology, where BMP6 expression is strongly up-regulated (Maddaluno et al., 2013). On the other hand, loss of YAP in ECs resulted in a defective TGFβ-induced EndMT response. Chronic TGFβ treatment, indeed, induced a strong upregulation of the EndMT markers *Acta2*, *Fn1*, *Cdh2*, *Snai1* and *Serpine1* in WT cells, while their expression levels were significantly reduced in YAP KO ECs. Hence, our results support the idea that YAP is required for TGFβ-mediated EndMT. Accordingly, Zhang and colleagues have later on shown that endothelial-specific YAP KO mice resulted in defective EndMT during the atrioventricular cushion formation, and observed that cultured ECs silenced for YAP did not respond to TGFβ-mediated EndMT (Zhang et al., 2014). YAP is therefore emerging as a key player for the mesenchymal switch of both endothelial and epithelial cells, but very little is known about the underlying mechanism. We thus aimed at better defining the molecular mechanism through which YAP contributes to TGFβ-mediated EndMT, bearing in mind that this would also help identifying novel ways to target

pathological conditions where EndMT occurs, like CAFs generation or during organ fibrosis.

In ECs, TGFβ binds to two different TβRI, ALK5 and ALK1, and trigger parallel SMAD-mediated signaling cascades (Goumans and Ten Dijke, 2017). Binding of TGFβ to ALK5, indeed, stimulates SMAD2 and SMAD3 C-term phosphorylation, which, in turn, trigger the expression of target genes, like *Serpine1* (Dennler et al., 1998; Goumans et al., 2002). TGFβ-ALK1 binding, instead, induces SMAD1/5 C-term phosphorylation and leads to the expression of genes such as *Id1* (Goumans et al., 2003b). Interestingly, after 5 days of chronic TGFβ stimulation, we found that genetic loss of YAP in ECs negatively affected *Serpine1* up-regulation compared to WT cells, while *Id1* expression was increased at the same level in both cell lines. These findings were further supported by analyses performed in acute stimulation (2 h), strongly suggesting a positive role of YAP in mediating SMAD3, but not SMAD1, signaling activity.

Subsequently, we excluded that the differential SMAD3 signaling activation observed between the two cell lines could be due to differences in terms of ALK5 and ALK1 expression levels and in terms of SMAD3 C-term phosphorylation. Unexpectedly, by observing SMAD3 and SMAD1 total protein levels in the two cell lines, we found a significant SMAD3 and -1 reduction in KO versus WT cells, which could partly explain SMAD3 impaired signaling activity in YAP KO cells. SMAD1 reduced levels, however, did not impact on SMAD1-driven signaling in YAP KO cells. Of note, our results are in sharp contrast with a previous report, where the authors observed a negative correlation between YAP and SMAD3 expression in tumor-initiating breast cancer cells (Sun et al., 2016), and also with what Zhang and colleagues have reported in HUVEC cells (Zhang et al., 2014). These discrepancies could be due to the employment of different cell types (Sun et al., 2016), further stressing the importance of dissecting molecular mechanisms in specific biological

context, or could be due to different protein expression levels observed under acute (YAP KD) or chronic and total (YAP KO) silencing methods (Zhang et al., 2014). Nonetheless, our results clearly supported a role of YAP in sustaining SMAD3 protein levels and SMAD3-driven EndMT response.

SMAD3 mRNA levels were also significantly reduced in YAP KO cells, opening up the possibility that YAP could regulate SMAD3 transcription and, in this way, TGFβ-mediated EndMT. However, by reintroducing a transcriptionally active form of YAP (YAP 5SA) in KO cells, we did not observe an increase in SMAD3 mRNA transcription, rather YAP 5SA expression led to a significant up-regulation of SMAD3 protein levels. This very interesting finding suggested that nuclear YAP could play a double role in SMAD3 signaling activity, functioning at the same time as SMAD3 co-transcriptional factor while preventing its turnover in response to TGFβ.

Previous reports in epithelial cells have suggested that cytoplasmic YAP (pYAP) is capable of binding to SMAD2/3 in response to TGFβ, thus preventing SMAD2/3-mediated TGFβ signaling (Grannas et al., 2015; Varelas et al., 2010). Although our results showed that YAP specifically sustains SMAD3-driven target genes expression in ECs, we could not rule out the possibility that cytoplasmic YAP could prevent SMAD3 nuclear accumulation in ECs too. We therefore performed co-immunoprecipitation analyses from nuclear and cytosolic cell compartments and observed that, conversely to what described in epithelial cells, cytoplasmic YAP binds to SMAD3 in basal conditions, while exposure to TGFβ induces a dissociation of the observed complex. Moreover, we found that YAP genetic deletion did not impact on SMAD4-mediated SMAD3 nuclear translocation, still YAP was specifically required for SMAD3 nuclear accumulation, as shown by N/C fractionation analyses and IF stainings. Our results are in agreement with previously published findings

(Zhang et al., 2014) and, collectively, show once again the importance of YAP in supporting SMAD3-driven signaling activity in ECs.

Interestingly, TGFβ stimulation did not influence pYAP Ser127 levels – a marker for cytoplasmic YAP – as well as YAP nuclear accumulation, suggesting that TGFβ does not have a direct effect on YAP activation in ECs. Nevertheless, we found that TGFβ increased the levels of SMAD3 bound to YAP in the nucleus, indicating that SMAD3 and nuclear YAP form a complex in response to TGFβ treatments and likely work together as transcriptional regulators of EndMT genes.

We therefore investigated whether *Acta2*, *Fn1*, *Cdh2*, *Snai1* and *Serpine1* EndMT genes contain putative binding sites for SMAD3 and/or for TEAD, a family of transcriptional factors often bound by YAP that also contributes to EMT (Zhao et al., 2008). Moreover, it has been reported before that YAP/SMAD3/TEAD work together to regulate gene expression in different biological contexts where cells are undergoing differentiating or transforming processes, such as during development in human embryonic stem cells (Beyer et al., 2013) or in cancer model systems (Fujii et al., 2012; Hiemer et al., 2014), suggesting that YAP/SMAD3/TEAD complex controls the expression of genes involved in highly plastic processes. We therefore investigated whether the same occurred during EndMT. EndMT genes promoter analysis, indeed, revealed many putative binding sites for both TEAD and SMAD within a region spanning -5 KB to +1 KB around their TSS, while *Fn1* and *Snai1* presented only SMAD putative binding sites. Previously, Zhang and colleagues showed that YAP and SMAD3 are responsible for *Snai1* gene transcription (Zhang et al., 2014), and so we focused our attention on *Fn1* and *Serpine1*, whose expression increased already 24 h after TGFβ stimulation. Interestingly, we found that both SMAD3 and YAP bound to the same *Fn1* region, strongly suggesting that they work together as co-transcriptional factors driving the expression of this gene. We are currently cloning this *Fn1* region in a luciferase reporter plasmid and

transfect it along with YAP and SMAD3 expressing plasmids, so to further confirm that they work together as active *Fn1* transcriptional regulators in response to TGFβ. Unfortunately, we did not retrieve any YAP or SMAD3 bound to some identified putative binding sites on *Serpine1* promoter region. However, due to technical problems, we could not analyze all *Serpine1* putative binding sites, and will be analyzed in the next future. By means of siRNA approach, we also confirmed that SMAD3 is required for *Fn1* and *Serpine1* expression. Taken together, these results strongly indicate that YAP and SMAD3 work together as co-transcriptional factors that drive the expression of EndMT genes like *Fn1*, *Serpine1* and *Snai1* in response to TGFβ stimulation. Although these genes do not contain TEAD putative binding sites, apart from *Serpine1*, we could not exclude that YAP/TEAD could modulate SMAD3 transcriptional activity by binding to distal sites (enhancers), as previously reported by others (Stein et al., 2015; Zanconato et al., 2015). After observing an increased YAP-SMAD3-TEAD1 complex formation in both WT and KO cells upon TGFβ stimulation, we hypothesized that this complex might regulate the expression of EndMT genes. It has to be noted, however, that YAP KO did not fully prevent SMAD3-TEAD1 binding, suggesting that other co-transcriptional factors like TAZ could mediate their binding. Interestingly, we found that TEAD1 silencing in ECs did not significantly affect *Fn1* and *Serpine1* up-regulation induced by TGFβ, thus suggesting that TEAD1 is not required for the expression of these EndMT genes. Whether other TEAD family members are involved in EndMT genes transcription will be investigated in the next future.

Collectively, these results showed for the first time that YAP and SMAD3 are required for *Fn1* and *Serpine1* expression in ECs, likely working as EndMT genes transcriptional regulators in response to TGFβ stimulation.

Since our data showed that reintroducing a transcriptionally active form of YAP (YAP 5SA) in KO cells led to a significant up-regulation of SMAD3 protein levels, we

also tested the hypothesis that nuclear YAP could play a double role in SMAD3 signaling activity, that is sustaining SMAD3-mediated transcriptional regulation while preventing protein turnover. In support of this hypothesis, other reports have previously shown that, upon BMP stimulation, SMAD1 is phosphorylated in its linker region by CDK8/9, allowing the binding of co-transcriptional regulators like YAP that, at the same time, prevent the subsequent GSK3β-mediated phosphorylation and SMAD1 targeting to protein degradation (Alarcon et al., 2009; Aragon et al., 2011). Whether YAP could play a similar function for SMAD3 has never been reported before. We therefore decided to test if the levels of SMAD3 pS204 – the phosphorylation described to target SMAD3 for protein degradation (Aragon et al., 2011) – were more strongly increased after TGFβ treatments in cells lacking YAP expression compared to a WT situation. Remarkably, we found for the first time that SMAD3 pS204 levels are strongly increased in ECs lacking YAP expression while only slightly up-regulated in WT cells. YAP 5SA expression in KO cells, moreover, markedly reduced SMAD3 pS204 levels, further indicating that nuclear YAP prevents SMAD3 S204 phosphorylation in ECs treated with TGFβ.

Of note, we observed that SMAD3 pS204 levels were significantly increased in YAP KO cells compared to WT cells even without TGFβ stimulation, suggesting a novel function of YAP in protecting SMAD3 protein degradation already at basal conditions. Literature reports have previously shown that SMAD3 S204 can be phosphorylated either by Erk2 MAPK in unstimulated conditions (Alarcon et al., 2009) or by GSK3β in response to TGFβ (Wang et al., 2009a). We are therefore planning to investigate whether YAP inhibits SMAD3 pS204 mediated by Erk2 in basal conditions.

Considering that our primary goal was to better define the molecular mechanism through which YAP contributes to TGFβ-induced EndMT, we moved to identify the kinase responsible for the increased SMAD3 S204 phosphorylation levels observed

in KO cells in response to TGFβ. Interestingly, co-immunoprecipitation analyses revealed a higher amount of GSK3β bound to SMAD3 in ECs lacking YAP expression, that was further increased after TGFβ stimulation. Moreover, inhibition of GSK3β activity by LiCl cell treatments was capable of reducing the amount of SMAD3 pS204 in TGFβ-stimulated YAP KO cells, showing that GSK3β is the kinase responsible for SMAD3 pS204 occurring in TGFβ-treated ECs. Very interestingly, ECs treatments with LiCl led to total SMAD3 protein levels accumulation in response to TGFβ, which also resulted in an increased SMAD3 nuclear accumulation in KO stimulated cells. However, preventing SMAD3 protein turnover through LiCl-mediated GSK3β inhibition was not sufficient to restore EndMT genes transcription, strongly suggesting that SMAD3 requires YAP as a co-transcriptional factor in order to drive an effective EndMT response upon TGFβ stimulation. Accordingly, YAP 5SA strongly induced *Fn1* and *Serpine1* expression in KO treated cells, indicating that nuclear YAP is required for the expression of these EndMT genes in response to TGFβ.

We therefore propose here a novel mechanism through which YAP contributes to TGFβ-mediated EndMT (**Figure 46**). ECs respond to TGFβ stimulation by triggering C-term phosphorylation of SMAD3, which then shuttle to the nucleus to drive target genes transcription. To do so, SMAD3 binds to different co-transcriptional regulators, that not only increase SMAD3-DNA binding affinity, but also help modulating the type of response activated by SMAD3. Remarkably, we found that the co-transcriptional partner YAP works together with SMAD3 to induce EndMT genes transcription, and, at the same time, prevents GSK3β-mediated SMAD3 linker phosphorylation and subsequent proteosomal degradation.

In light of our *in vitro* results, we propose YAP as a possible candidate target to limit TGFβ-mediated EndMT occurring in pathological conditions. Although we have not yet investigated this aspect, several lines of evidence support our hypothesis.

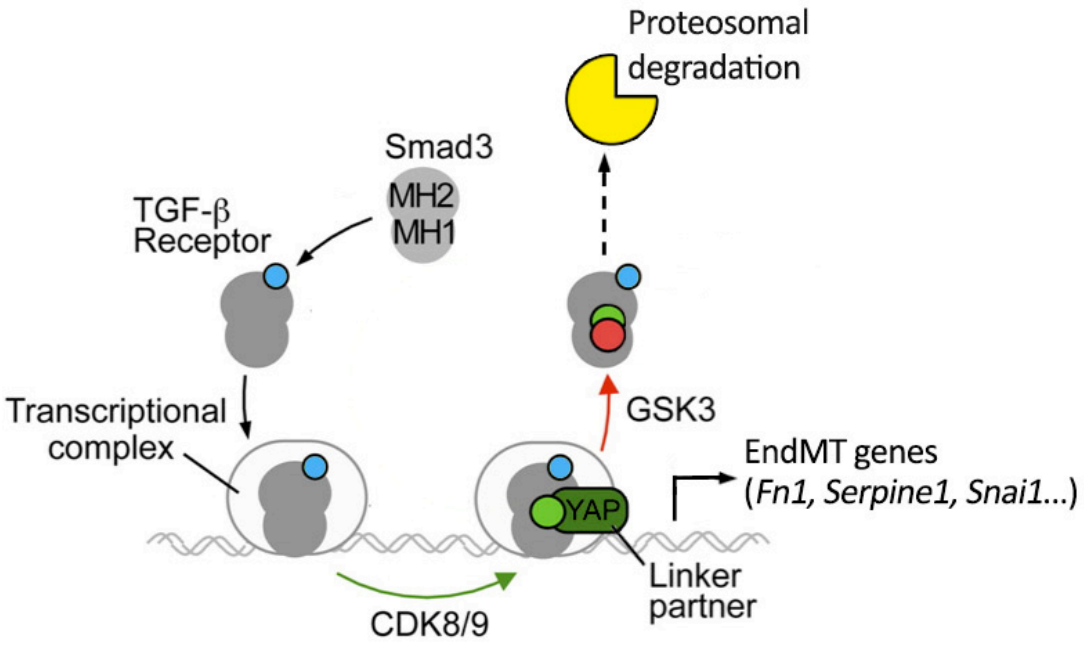

Figure 44. Proposed working model on how YAP regulates TGFβ-mediated EndMT. Binding of TGFβ to the TGFβ receptor complex stimulates SMAD3 C-term phosphorylation (blue dot). Subsequently, SMAD3 shuttles to the nucleus where it is phosphorylated likely by CDK8/9 kinases in two residues lying within SMAD3 linker region, T179 and S208 (green dot). Phosphorylation at these sites favors the recruitment of the co-transcriptional factor YAP, which contributes to SMAD3-driven EndMT target genes expression. Moreover, binding of nuclear YAP to SMAD3 inhibits SMAD3 S204 phosphorylation (red dot), mediated by GSK3β kinase, and so prevents targeting of SMAD3 to proteosomal degradation. *Modified from: Aragon, E., Goerner, N., Zaromytidou, A.I., Xi, Q., Escobedo, A., Massague, J., and Macias, M.J. (2011). A Smad action turnover switch operated by WW domain readers of a phosphoserine code. Genes Dev 25, 1275-1288.*

YAP can be pharmacologically targeted by different molecules, like Verteporfin (VP) or statins. Statins have been shown to promote YAP cytoplasmic retention, and thus interfere with YAP transcriptional activity (Sorrentino et al., 2014). VP, instead, was initially discovered as an inhibitor of YAP-TEAD interaction during a screening of a panel of clinically Food and Drug Administration- (FDA-) approved pharmacological compounds. VP is indeed currently used to treat neovascular macular degeneration

(Kawczyk-Krupka et al., 2015). Importantly, Liu-Chittenden and colleagues also tested VP anti-neoplastic activity in YAP transgenic mouse models, as YAP *gain-of-function* mutations were previously reported to cause oncogenic transformation in liver (Camargo et al., 2007; Dong et al., 2007). Remarkably, the authors greatly rescued the liver overgrowth observed in vehicle-treated mice, proving that VP could be a potential drug to prevent YAP-oncogenic activity (Liu-Chittenden et al., 2012). A 2016 report, moreover, has also proposed VP as therapeutic molecule to reduce *in vivo* kidney fibrosis, a pathological process known to be driven by continuous TGFβ exposure (Szeto et al., 2016). Interestingly, in this study, the authors have observed that YAP and TAZ protein expression were strongly reduced in cultured fibroblasts upon VP treatments. Strikingly, VP also decreased the expression of the TGFβ-downstream effectors SMAD2 and SMAD3 and this effect was further exacerbated in presence of TGFβ. As a result, TGFβ-induced SMAD3 transcriptional activity and, thus, profibrotic genes expression (*Col3A1*, *Col4A1* and *Acta2*) were markedly reduced after VP treatments. Finally, the authors observed that VP was capable of attenuating renal fibrosis in mouse models of unilateral ureteral obstruction (UUO), by reducing YAP/TAZ levels and thus their profibrotic activity. These results not only set VP as a putative therapeutic strategy to treat kidney fibrosis, but also suggest that YAP functions as a SMAD transcriptional cofactor, and its expression is required to prevent SMAD2 and -3 protein degradation, as also stated by the authors themselves (Szeto et al., 2016). This strongly indicates that our identified mechanism on how YAP regulates TGFβ-mediated EndMT does not only occur in ECs, but also in other cell systems, like in fibroblasts. Therefore, it would be now important to explore whether our identified mechanism is applicable also to other cell systems.

Previous studies have shown that EndMT is a source of activated (myo)fibroblasts that contribute to kidney fibrosis (Zeisberg et al., 2008).

Importantly, SMAD3-null mice display a reduced kidney fibrosis in UUO mouse models (Inazaki et al., 2004). Moreover, Li and colleagues have later shown that blocking SMAD3 with pharmacological agents led to reduced EndMT and, consequently, decreased diabetes-induced kidney fibrosis (Li et al., 2010). Taken together, these results clearly suggest that blocking TGFβ-mediated EndMT can be a valid therapeutic strategy to treat kidney fibrosis, and that YAP is emerging as a possible target to attenuate this pathological condition.

TGFβ-mediated EndMT can occur also in other fibrotic conditions, like in cardiac fibrosis (Zeisberg et al., 2007b). Although it has been proposed that YAP plays a role in promoting cardiac regeneration upon injury (Xin et al., 2013), it remains to be elucidated whether it is involved in pathological EndMT contributing to heart fibrosis.

Along with fibrotic conditions, EndMT was shown to contribute to the formation of CAFs in tumor mouse models of malignant melanoma and pancreatic tumors (Zeisberg et al., 2007a). In this study, the authors stated that the observed EndMT was specifically driven by TGFβ, and, although they did not clearly demonstrate that TGFβ was involved in the *in vivo* mechanism, results showed a locally increased TGFβ secretion in $FSP1^+$ fibroblasts areas. These very interesting findings need stronger *in vivo* validation, but clearly suggest EndMT as a key process contributing to cancer progression. Accordingly, the EndMT response occurring in endoglin mutant pancreatic tumor mouse models contributes to an increased metastatic dissemination (Anderberg et al., 2013). Intriguingly, this observed EndMT was partly driven by ALK5-mediated signaling. Thus, TGFβ is emerging as a leading growth factor that fosters tumor progression by promoting EndMT/EMT and chemotherapy resistance, thus rendering TGFβ an important therapeutic target to prevent cancer development (Colak and Ten Dijke, 2017). In this respect, several TGFβ targeting agents are currently under clinical trials (Colak and Ten Dijke, 2017). Since we and other have observed that EndMT is triggered by chronic TGFβ stimulation, tackling

possible common TGFβ-driven EMT and EndMT mechanisms would potentially help reducing tumor progression and, also, metastatic spread (Gasparics et al., 2016). In this regard, Krizbai and coworkers have recently proposed that TGFβ secreted by melanoma cancer cells (B16F10) is capable of inducing EndMT in brain endothelial cells, decreasing the expression of components of AJs and TJs while triggering EndMT markers expression. Importantly, they showed that blocking B16F10-secreted TGFβ strongly reduced the amount of melanoma cells adhering to ECs along with the number of cancer cells transmigrating through the EC monolayer (Krizbai et al., 2015). In light of these *in vitro* results, the authors proposed that endothelial transdifferentiation into mesenchymal cells is a process that favors metastatic extravasation by providing *de novo* expression of N-cadherin – and thus favoring circulating tumor cells attachment – as well as downregulating components of AJs and TJs to allow cancer cells extravasation. Clearly, these *in vitro* results need to be validated *in vivo*, but suggest that EndMT should be thoroughly investigated in tumor context too. On this basis, we are planning to study whether YAP is important for driving TGFβ-mediated EndMT *in vivo* by analyzing the EndMT response stimulated during cancer development, in order to possibly suggest YAP as a novel potential therapeutic target to counteract tumor progression. In parallel, we will also investigate whether YAP and YAP-driven TGFβ-mediated EndMT can possibly regulate tumor-associated angiogenesis (Welch-Reardon et al., 2015), since angiogenesis is essential for tumor growth and metastasis and its limitation is a promising approach to restrain cancer progression,

In conclusion, our results have set YAP as an important positive regulator of TGFβ-mediated EndMT by specifically sustaining SMAD3-driven signaling activity, providing a novel potential *in vivo* target to treat TGFβ-driven pathological conditions like tumor dissemination or organ fibrosis.

JCB: Article

The actin-binding protein EPS8 binds VE-cadherin and modulates YAP localization and signaling

Costanza Giampietro,[1,6] Andrea Disanza,[1] Luca Bravi,[1] Miriam Barrios-Rodiles,[2] Monica Corada,[1] Emanuela Frittoli,[1] Cecilia Savorani,[1] Maria Grazia Lampugnani,[1,7] Barbara Boggetti,[4] Carien Niessen,[4] Jeff L. Wrana,[2,3] Giorgio Scita,[1,5] and Elisabetta Dejana[1,6,8]

[1]FIRC Institute of Molecular Oncology, 20139 Milan, Italy
[2]Center for Systems Biology, Samuel Lunenfeld Research Institute, Mount Sinai Hospital, Toronto, Ontario M5G 1X5, Canada
[3]Department of Molecular Genetics, University of Toronto, Toronto, Ontario M5S 1A8, Canada
[4]Department of Dermatology, Cologne Excellence Cluster for Stress Responses in Ageing-Associated Diseases, Center for Molecular Medicine Cologne, University of Cologne, 50931 Cologne, Germany
[5]Dipartimento di Scienze della Salute and [6]Dipartimento di Bioscienze, Università degli Studi di Milano, 20122 Milan, Italy
[7]Istituto di Ricerche Farmacologiche Mario Negri, 20156 Milan, Italy
[8]Department of Immunology, Genetics and Pathology, Uppsala University, 751 05 Uppsala, Sweden

Vascular endothelial (VE)–cadherin transfers intracellular signals contributing to vascular hemostasis. Signaling through VE-cadherin requires association and activity of different intracellular partners. Yes-associated protein (YAP)/TAZ transcriptional cofactors are important regulators of cell growth and organ size. We show that EPS8, a signaling adapter regulating actin dynamics, is a novel partner of VE-cadherin and is able to modulate YAP activity. By biochemical and imaging approaches, we demonstrate that EPS8 associates with the VE-cadherin complex of remodeling junctions promoting YAP translocation to the nucleus and transcriptional activation. Conversely, in stabilized junctions, 14–3-3–YAP associates with the VE–cadherin complex, whereas Eps8 is excluded. Junctional association of YAP inhibits nuclear translocation and inactivates its transcriptional activity both in vitro and in vivo in Eps8-null mice. The absence of Eps8 also increases vascular permeability in vivo, but did not induce other major vascular defects. Collectively, we identified novel components of the adherens junction complex, and we introduce a novel molecular mechanism through which the VE-cadherin complex controls YAP transcriptional activity.

Introduction

Endothelial cells (ECs) form the inner lining of blood vessels, and one of their most important properties is to separate blood from underlying tissues. Their role as a selective permeability barrier is mainly achieved through the coordinated opening and closure of cell-to-cell junctions. In addition to maintaining adhesion between neighboring cells, junctions play crucial roles in transducing chemical and mechanical signals that regulate contact-induced inhibition of cell growth, apoptosis, gene expression, and vessel formation and stability (Vandenbroucke et al., 2008; Giampietro et al., 2012; Giannotta et al., 2013).

EC homotypic adhesion is mainly controlled by two types of adhesive structures: tight and adherens junctions (AJs; McCrea et al., 2009; Vestweber et al., 2009; Giannotta et al., 2013). The key component of AJs is transmembrane vascular endothelial (VE)–cadherin, an endothelial-specific member of the cadherin family. VE-cadherin is physically connected to a large number of intracellular partners that mediate its anchorage to the actin cytoskeleton and the transfer of signals essential to modulate endothelial functions (Vestweber et al., 2009; Dejana and Giampietro, 2012). Not surprisingly, changes in the structure and composition of AJs have profound effects on vascular permeability as well as on the overall vascular homeostasis (Vestweber et al., 2010).

Junctions are dynamic structures whose regulation and structural changes strongly impact adhesion strength and tissue plasticity. ECs from different types of vessels and also from different organs show differences in junction composition and organization (Orsenigo et al., 2012; Kluger et al., 2013).

Recent studies revealed that the cotranscriptional regulator YAP (Yes-associated protein), originally characterized as the molecular target of the size-controlling Hippo pathway (Varelas, 2014), is a key relay for the transmission of mechanical inputs into gene transcriptional programs (Dupont et al., 2011). Indeed, multiple signaling pathways integrating biophysical

Correspondence to Costanza Giampietro: costanza.giampietro@unimi.it; or Elisabetta Dejana: elisabetta.dejana@ifom.eu; or Giorgio Scita: giorgio.scita@ifom.eu

Abbreviations used in this paper: AJ, adherens junction; EC, endothelial cell; IF, immunofluorescence; IP, immunoprecipitation; Ni-NTA, nickel–nitrilotriacetic acid; qRT-PCR, quantitative RT-PCR; RL, Renilla luciferase; VE, vascular endothelial; WB, Western blot; WT, wild type; YAP, Yes-associated protein.

Supplemental material can be found at:
http://doi.org/10.1083/jcb.201501089

The Rockefeller University Press $30.00
J. Cell Biol.
www.jcb.org/cgi/doi/10.1083/jcb.201501089

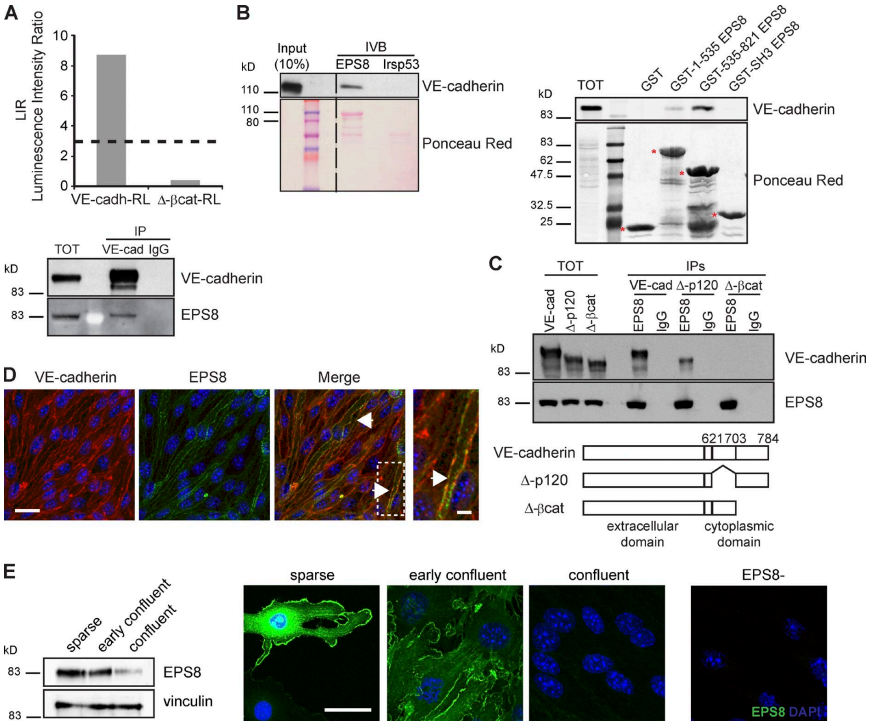

Figure 1. **EPS8 is a novel component of AJ complexes in ECs.** (A) Detection of full-length VE-cadherin–EPS8 interaction by LUMIER (top); the data are representative of five independent experiments. Association of EPS8 to full-length VE-cadherin (bottom). Coimmunoprecipitation and Western blot of endogenous VE-cadherin and EPS8 from extract of VE-Cadherin–positive ECs. The dashed line indicates an LIR of 3, a conservative LIR cutoff. (B) Analysis of VE-cadherin cytoplasmic tail and EPS8 full-length interaction in vitro by His-tag pull-down assay (left). Analysis of the interaction between VE-cadherin cytoplasmic tail and EPS8 deleted mutants (asterisks) in vitro by GST pull-down assay (right). (C) Association of EPS8 to VE-cadherin full-length (VE-cad), Δ-p120, and Δ-βcat mutants upon transient expression in COS-1 cells. Cells were transfected with the indicated constructs, immunoprecipitated with specific EPS8 antibody or isotype control IgG, and blotted as indicated. (D) IF microscopy of VE-cadherin–positive ECs in early confluent (24 h) conditions. Cells were double stained with anti–VE-cadherin (red) and anti-EPS8 (green) antibodies. Junctional EPS8 colocalizing with VE-cadherin (arrows) was detected. The dashed outline indicates the magnified area to the right. (E) WB analysis (left) of EPS8 expression levels in various stages of confluence conditions (see Materials and methods section). Vinculin is the loading control. IF microscopy (right) of WT lung–derived ECs in various stages of confluence conditions. The IF of Eps8^{-} ECs confirmed the specificity of the staining. Cells were stained with anti-EPS8 antibody (green) and DAPI (blue). Bars: (D and E) 20 µm; (magnification) 10 µm. IVB, in vitro binding; TOT, total cell lysate.

and biochemical cues converge to regulate the activity of YAP (Morgan et al., 2013). YAP, in turn, is essential to modulate cell proliferation and differentiation, apoptosis, organ size, and morphogenesis of various tissues (Zhao et al., 2011). In epithelial tissues, for example, YAP has been shown to be regulated by the formation of cell–cell contacts, to be required for contact inhibition of cell proliferation (Zhao et al., 2007), and to respond to mechanical perturbation of the epithelial sheet (Aragona et al., 2013). In all these situations, actin cytoskeletal–based mechanical forces have been shown to be the overarching regulator of the activity of YAP and its related molecule TAZ, setting responsiveness to a variety of key signaling axes, including the Hippo, WNT, and G protein–coupled receptor pathways. Notably, Yap$^{-/-}$ mice display an early embryonic lethal phenotype resulting from defects in yolk sac vasculogenesis, chorioallantoic fusion, and embryonic axis elongation (Morin-Kensicki et al., 2006), suggesting a role of this protein also in the control of endothelial morphogenetic processes. The molecular determinants through which ECs control YAP regulation remain, however, largely unexplored.

The EGF receptor kinase substrate 8 (EPS8) is a signaling adapter protein involved in the transduction of signal from RAS to RAC (Scita et al., 1999). EPS8 also directly binds to actin filaments controlling the rate of polymerization/depolymerization by capping the fast-growing ends of filaments (Croce et al., 2004; Disanza et al., 2004, 2006; Hertzog et al., 2010). Consistently, EPS8, in vivo, is required for optimal actin-based motility impacting migratory properties of different cells (Frittoli et al., 2011). Furthermore, EPS8 regulates the proper architectural organization of actin-based structures, including intestinal microvilli and stereocilia (Disanza et al., 2006; Hertzog et al., 2010; Tocchetti et al., 2010; Manor et al., 2011). One

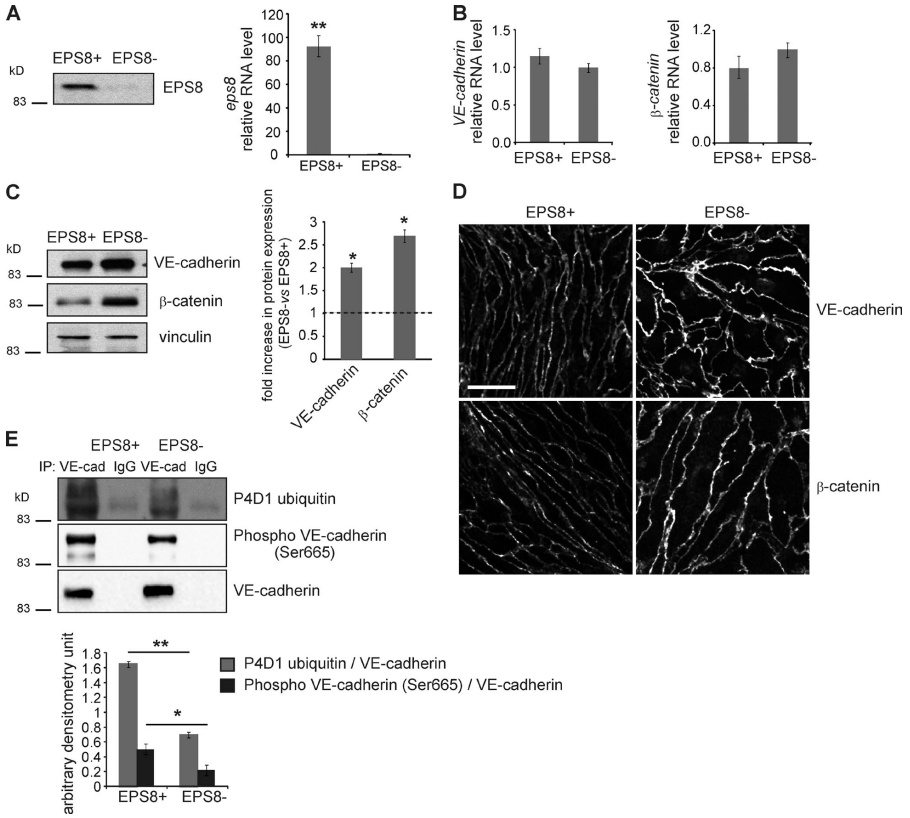

Figure 2. **Effect of EPS8 expression on AJ organization and dynamics.** (A) WB (left) and qRT-PCR (right) analysis of EPS8 reconstitution in *eps8*$^{-/-}$ lung–derived ECs. Cells were infected with either WT EPS8-GFP (EPS8^{+}) or control GFP (EPS8^{-}) lentiviral vectors. The gene expression level has been represented as fold changes ± SEM of three independent experiments. (B) qRT-PCR analysis of VE-cadherin ($P = 0.06$) and β-catenin ($P = 0.07$) in EPS8^{+} and EPS8^{-} ECs. For each tested gene, the expression level has been represented as fold changes ± SEM of four independent experiments. (C) WB analysis (left) of VE-cadherin and β-catenin expression in extracts of EPS8^{+} and EPS8^{-} ECs in confluent condition. Vinculin is shown as the loading control. The graph (right) represents the WB quantification. Columns are means ± SEM of three independent experiments. The dashed line indicates that relative levels for the Eps8^{+} cells were set to 1. (D) IF microscopy of confluent EPS8^{+} and EPS8^{-} cells stained with anti–VE-cadherin and –β-catenin antibody. An increase of junctional proteins' distribution is observed in the absence of EPS8. Bar, 20 µm. (E) IP of VE-cadherin from EPS8^{+} and EPS8^{-} cell extracts followed by WB analysis of phosphorylation on serine 665 residue and ubiquitin level (top). Quantifications of three independent experiments are shown as means ± SD at the bottom. *, $P < 0.05$; **, $P < 0.01$.

additional cellular process in which EPS8 is implicated is the regulation of intracellular trafficking of various membrane receptors (Lanzetti et al., 2000; Di Fiore and Scita, 2002; Auciello et al., 2013). EPS8 exerts this function either through its direct interaction with the GTPase-activating protein, RN-tre, which controls the activity of RAB5, a master regulator of early endosomes (Lanzetti et al., 2000; Di Fiore and Scita, 2002), or by interacting with the clathrin-mediated endocytosis machinery (Taylor et al., 2012; Auciello et al., 2013).

Here, we identified EPS8 as a novel partner of VE-cadherin at AJs. We also found that EPS8 regulates the dynamic organization of endothelial junctions and the transduction of intracellular signals by tuning YAP transcriptional activity.

Results

EPS8 is a novel component of AJ complexes

To identify novel components of the VE-cadherin signaling complex, we set up a LUMIER (luminescence-based mammalian interactome mapping) automated high throughput screening. This approach is designed for the systematic mapping of dynamic protein–protein interaction networks in mammalian cells (Barrios-Rodiles et al., 2005). Full-length VE-cadherin and Δ-βcat mutant, devoid of the C-terminal interaction domain with β-catenin (Fig. 1 C, bottom; Navarro et al., 1995), were fused to Renilla luciferase (RL) and coexpressed with a library

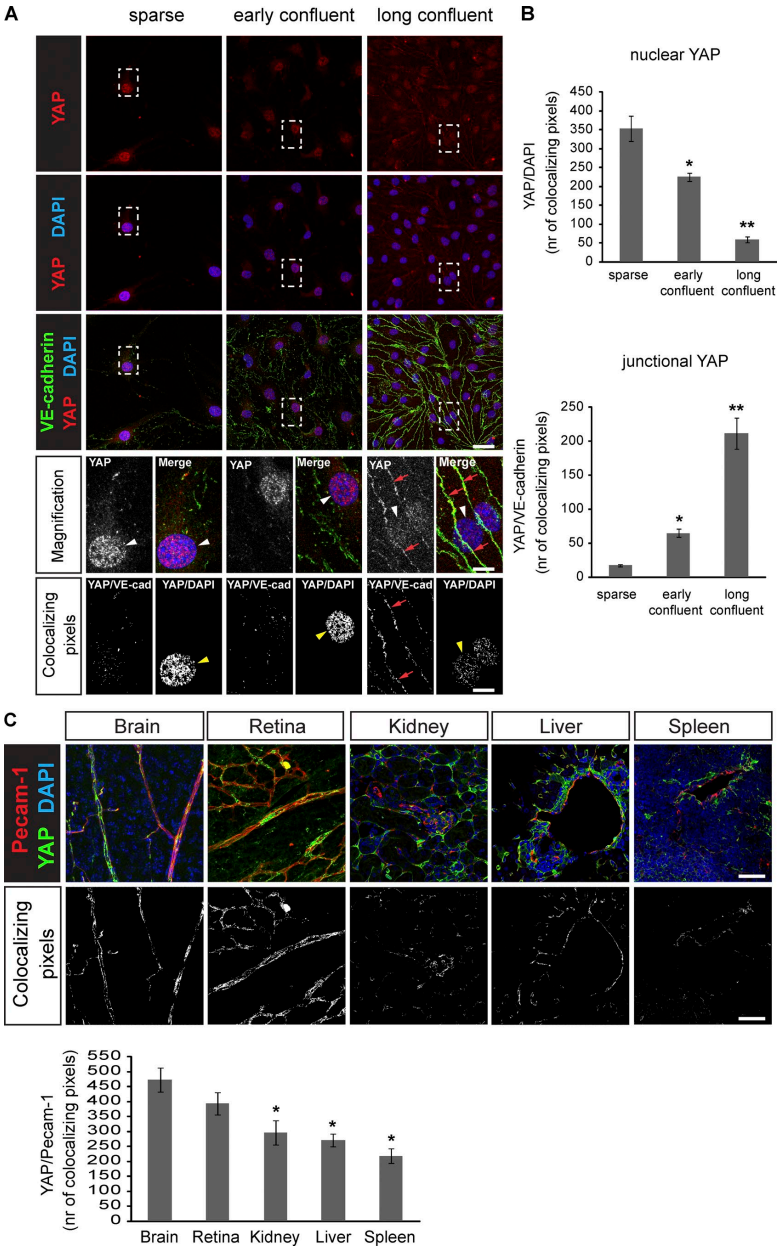

of individual Flag-tagged partners in mammalian HEK293T cells. We next assessed the association of VE-cadherin wild-type (WT) and mutant proteins with Flag-tagged proteins by performing a luciferase assay on anti-Flag immunoprecipitates. Among a variety of identified interactors, we focused our investigation on EPS8, which bound full-length VE-cadherin-RL, but not Δ-βcat-RL mutant (Fig. 1 A, top). We validated the physiological relevance of this association by coimmunoprecipitation of endogenous proteins from whole WT EC extracts (Fig. 1 A, bottom). In vitro pull-down experiments using recombinant purified proteins indicated that EPS8 binds directly, through its C-terminal domain, to the C-terminal region of the cytoplasmic tail of VE-cadherin (Fig. 1 B). Coimmunoprecipitation experiments between EPS8 and a set of deletion mutants of VE-cadherin corroborated the results obtained with LUMIER. EPS8 efficiently bound to WT and a VE-cadherin mutant devoid of the interaction domain with p120 (Δ-p120; Lampugnani et al., 1997) but failed to associate with a Δ-βcat VE-cadherin, which binds neither endogenous β-catenin nor α-catenin (Fig. 1 C, top), indicating that the region spanning amino acids 703–784 of VE-cadherin is indispensable for this interaction. Confocal analyses of early confluent WT (24 h) ECs showed that EPS8 was enriched along cell-to-cell junctions and largely colocalized with VE-cadherin (Fig. 1 D, arrows and magnification). Notably, EPS8 expression and junctional localization were down-regulated in long confluent WT EC culture (72 h; Fig. 1 E). To confirm the specificity of the staining, we also performed immunofluorescence (IF) analysis on early confluent *Eps8*-null ECs (EPS8$^-$) that consistently did not reveal any signal.

EPS8 increases the dynamic turnover of VE-cadherin

To gain functional cues into the role of EPS8 in ECs, we derived ECs from lungs of eps8-null mice, which were subsequently reconstituted with either WT EPS8-EGFP (EPS8$^+$ cells) or control EGFP (EPS8$^-$ cells) lentiviral vectors (Fig. 2 A; Menna et al., 2009). EC populations are characterized by high phenotypic heterogeneity (Ribatti et al., 2002); thus, we decided to use this approach to work with the same cell line, differing only for the expression of EPS8. The level of the EPS8 in EPS8$^+$ ECs is ∼30% more than WT ECs (Fig. S1 A), but this does not significantly impact the molecular mechanisms studied, as shown in the following paragraph. In the absence of EPS8, the major components of the AJ complexes were up-regulated (Fig. 2 C) at junctions (Fig. 2 D), but the corresponding mRNAs remained unchanged (Fig. 2 B), suggesting a posttranscriptional effect. VE-cadherin is internalized through clathrin-mediated pathways in a process that requires VE-cadherin phosphorylation and ubiquitination (Gavard and Gutkind, 2006; Orsenigo et al., 2012). Expression of EPS8 increased VE-cadherin phosphorylation on serine 665 and ubiquitination (Fig. 2 E), suggesting enhanced VE-cadherin turnover.

EPS8 and YAP localization at junctions is mutually exclusive

Cadherin complexes can either repress or stimulate gene transcription. Considering the role of EPS8 in cytoskeletal organization, we asked whether the association of EPS8 with VE-cadherin might influence signaling pathways modulated by actin remodeling. We focused on the transcriptional cofactor YAP because its nuclear-cytoplasmic shuttling and activity may be regulated by cadherin-mediated cell–cell contacts (Kim et al., 2011) and cytoskeletal-dependent mechanical forces (Dupont et al., 2011). YAP was, as shown in other cell types (Aragona et al., 2013), almost entirely localized in the nucleus of sparse WT ECs (Fig. 3, A and B). Conversely, in early confluent and long confluent WT endothelial monolayers, it was gradually excluded from the nuclei (Fig. 3, A and B) and redistributed along cell-to-cell junctions, where it colocalized with VE-cadherin (Fig. 3, A and B). To detect the junctional localization of YAP, cells have been fixed with 1% PFA in 2.5-mM triethanolamine (see Materials and methods section IF microscopy). In vivo, YAP localization at cell–cell junctions was detectable in the vessels of the brain and the retina of neonatal mice. Conversely, in vessels of other organs such as spleen, kidney, and liver, where the junctions are loose, YAP expression at junctions was decreased (Fig. 3 C).

Overall, these in vitro and in vivo data suggest that EPS8 and YAP localize at junctions in a mutually exclusive and temporally distinct manner. In particular, EPS8 is a marker of early and dynamic junctions, whereas YAP is mostly recruited at stable junctions.

We then asked whether EPS8 might regulate YAP signaling. To this end, we compared EPS8$^+$ to EPS8$^-$ ECs in early confluent conditions when EPS8 is prominently localized at intercellular junctions in WT ECs (Fig. 1 E). Under these conditions, we found that in EPS8$^-$ ECs, YAP phosphorylation on serine 127, an inhibitory posttranslational modification (Zhao et al., 2007), was increased (Fig. 4 A), and YAP nuclear fraction was diminished (Fig. 4, B and C) as well as the expression of its target genes (Fig. 4 D), whose mRNAs are reduced by ∼10-fold. Of note, as reported in Fig. S1 B, the expression of YAP target genes was significantly high in sparse conditions, and it was not affected by the presence or absence of EPS8. YAP target gene expression was strongly reduced by early cell confluence as previously published (Schlegelmilch et al., 2011), but the reductions were significantly less in the absence of EPS8, supporting the idea that EPS8 sustained YAP transcriptional activity only when it was localized at AJs (Fig. 1 E).

Inhibition of YAP transcriptional activity is mediated by the activation of the PI(3)K–Akt pathway upon VE-cadherin clustering at AJs

A phosphorylation-dependent "shuttling" between the cytoplasm and the nucleus regulates the transcriptional activity of

Figure 3. **YAP is localized at junctions in long confluent monolayers in vitro and in the more stabilized vessels in vivo.** (A, top) Confocal microscopy analysis of YAP (red) colocalization with VE-cadherin (green) and nuclei (DAPI, blue) in WT lung–derived ECs at different stages of confluence conditions (see Cell lines in the Materials and methods section). Bar, 20 µm. (A, bottom) Pixels presenting the colocalization of VE-cadherin and YAP are highlighted in white. Bars, 10 µm. Nuclei are highlighted with arrowheads, and junctions are highlighted with arrows. (B) Quantification of the number of colocalizing pixels between YAP and DAPI (top) or VE-cadherin (bottom) is shown. Data are means ± SEM of three independent experiments. *, $P < 0.05$; **, $P < 0.01$. (C) Confocal microscopy analysis of Pecam-1 (red) and YAP (green) localization in different organs of P9 mice (top). Bars, 50 µm. Pixels presenting the colocalization of Pecam-1 and YAP are highlighted in white. Quantification of the number of colocalizing pixels between YAP and Pecam-1 (bottom). Data are means ± SEM of five mice analyzed. *, $P < 0.05$ for retina, kidney, liver, and spleen versus brain.

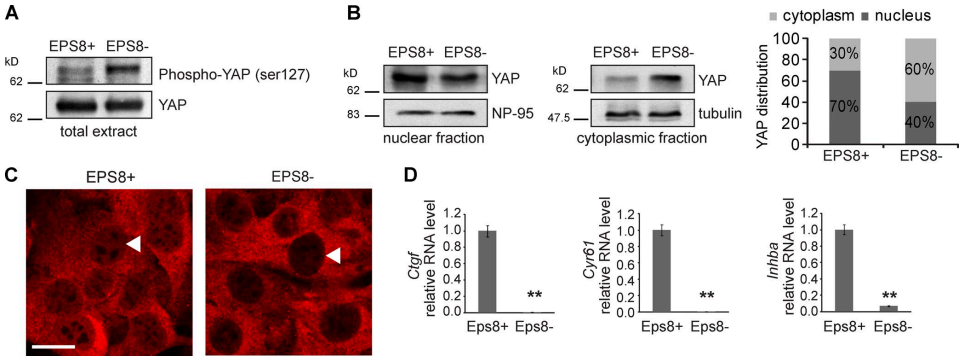

Figure 4. **EPS8 expression modulates YAP phosphorylation, localization, and transcriptional activity in confluent ECs.** (A) YAP phosphorylation (Phospho-YAP serine 127) in confluent EPS8$^+$ and EPS8$^-$ cells. Total cell lysates were analyzed by WB for phosphorylated and total YAP expression by using specific antibodies. (B, left) WB analysis of nuclear/cytoplasmic distribution of YAP in confluent EPS8$^+$ and EPS8$^-$ cells. On EPS8 removal (right), YAP shifted from a preferentially nuclear to a preferentially cytoplasmic localization. NP-95 and tubulin were used as nuclear and cytoplasmic markers, respectively. The graph on the right represents the quantification of four independent experiments. (C) IF microscopy of YAP (red) nuclear localization (arrowheads) in EPS8$^+$ and EPS8$^-$ ECs. Bar, 20 µm. (D) qRT-PCR analysis of *connective tissue growth factor* (*Ctgf*), *Cysteine-rich angiogenic inducer 61* (*Cyr61*), and *Inhibin β A* (*Inhba*) in EPS8$^+$ and EPS8$^-$ ECs to measure YAP transcriptional activity. The absence of EPS8 strongly inhibited YAP transcriptional activity. For each tested gene, the expression level has been represented as fold changes ± SEM of three independent experiments. **, $P < 0.01$.

YAP (Varelas, 2014). We found that VE-cadherin expression and clustering was important to limit YAP transcriptional activity. As reported in Fig. S2 A, and consistent with previously published literature (Choi et al., 2015), the up-regulation of YAP target genes was severely inhibited in VE-cadherin–positive as compared with VE-cadherin–null ECs in confluent conditions. VE-cadherin clustering is known to activate Akt through PI(3)K (Carmeliet et al., 1999; Taddei et al., 2008). Akt, in turn, was shown to be able to phosphorylate YAP in serine 127 in vitro and in ECs (Basu et al., 2003; Choi et al., 2015). We therefore investigated whether EPS8 localization at AJs might affect Akt activation and Akt-dependent YAP phosphorylation. Both Akt and YAP phosphorylation were increased in EPS8$^-$ cells as compared with EPS8$^+$ cells (Fig. 5 A). Pharmacological inhibition of PI(3)K with LY294002 reduced both Akt and YAP phosphorylation in EPS8$^+$ and EPS8$^-$ cells to a comparable level. LY294002 treatment also restored the expression of YAP-dependent genes in EPS8$^-$ ECs to levels similar to those observed in EPS8$^+$ cells (Fig. 5 B). Conversely, the ectopic expression of myr-Akt, a constitutively active form of Akt (Brown et al., 2005), increased the phosphorylation of YAP in EPS8$^+$ but not in EPS8$^-$ ECs. This lack of effect is likely a result of an already high basal AKT phosphorylation in the latter cell type (Fig. 5 C). myr-Akt infection was also able to reduce YAP target gene expression in EPS8$^+$ but not EPS8$^-$ ECs (Fig. 5 D).

In epithelial cells, YAP transcriptional activity is reduced by the organization of E-cadherin–based AJs through the activation of the Hippo signaling pathway (Kim et al., 2011) and by the activity of small GTPases that act primarily through regulation of the actin cytoskeleton (Dupont et al., 2011). Of note, in ECs small GTPase activity is controlled by VE-cadherin clustering (Pannekoek et al., 2011; Giannotta et al., 2013; Goddard and Iruela-Arispe, 2013). However, neither the Hippo pathway (Fig. S3 A) nor the activity of RHO (Fig. S3 B) and RAC1 (Fig. S3 C) was altered by removal of EPS8.

Collectively, these data suggest that in ECs inhibition of PI(3)K–Akt is the prominent pathway through which EPS8 increases YAP activity.

Inhibition of YAP transcriptional activity is mediated by YAP sequestration by α-catenin at AJs

The association of YAP with α-catenin limits its transcriptional activity (Silvis et al., 2011). α-Catenin sequesters YAP in the cytoplasm, thus preventing its dephosphorylation and nuclear translocation (Schlegelmilch et al., 2011; Silvis et al., 2011). We investigated whether EPS8 might play a role in the regulation of this pathway. An endogenous YAP–α-catenin complex could be detected by coimmunoprecipitation only in EPS8$^-$, but not in EPS8$^+$ ECs (Fig. 5 E). This complex associated with VE-cadherin as revealed by coimmunoprecipitation experiments (Fig. 5 F), and α-catenin was required for YAP–VE-cadherin interaction. Notably, removal of the VE-cadherin binding surface for β-catenin, which is required for α-catenin binding but not for p120, reduced, as expected, YAP phosphorylation (Fig. S4 A), prevented YAP binding to VE-cadherin (Fig. S4 B), and enhanced YAP transcriptional activity (Fig. S4 C). Finally, silencing of α-catenin impaired YAP localization at AJs (Fig. 5 F), reduced YAP phosphorylation (Fig. 5 G), and increased its transcriptional activity (Fig. 5 H) in a way more marked in the absence than in the presence of EPS8. These results suggest that EPS8 restrains the interaction of YAP with α-catenin. As a consequence, upon removal of EPS8, YAP is more efficiently sequestered into junctional complexes that prevent its nuclear translocation and transcriptional activity. Of note, and in line with what has been previously published (Schlegelmilch et al., 2011; Silvis et al., 2011), we were unable to detect a complex between TAZ, the related protein of YAP, and α-catenin, suggesting that TAZ activity may be regulated by different mechanisms, but specific studies are required to test this hypothesis.

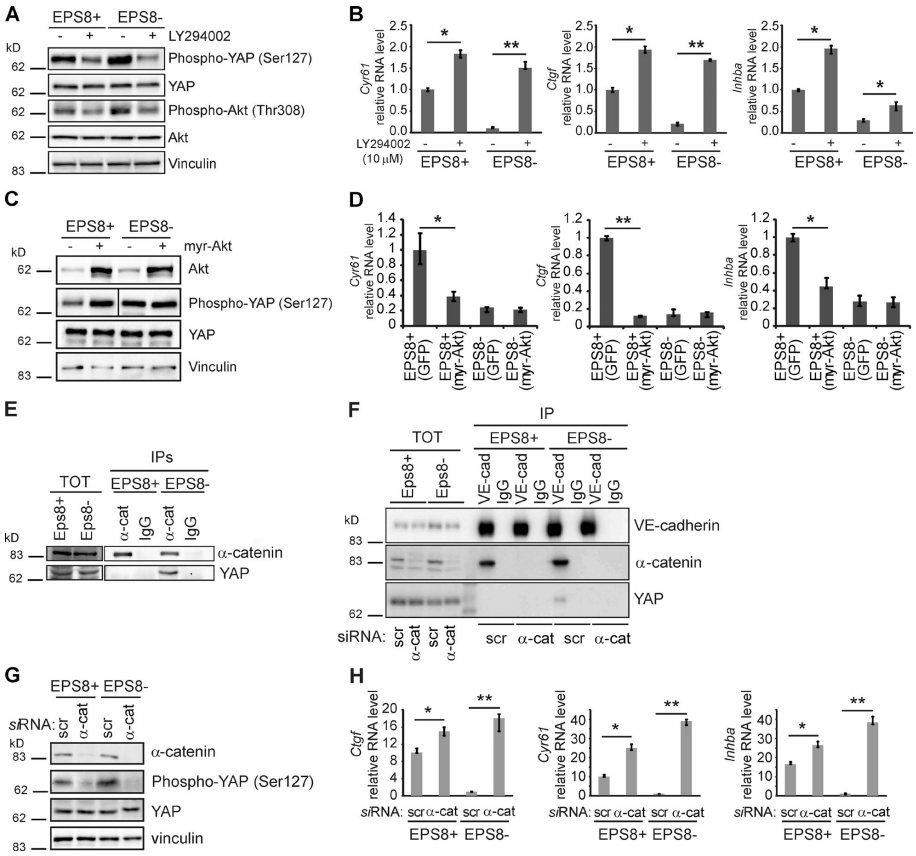

Figure 5. **YAP phosphorylation and transcriptional activity are regulated through differential PI(3)K–Akt pathway activation and binding to α-catenin.** (A) WB analysis of YAP and Akt phosphorylation upon inhibition of the PI(3)K–Akt pathway. Cells were grown to 90% confluence, starved for 24 h, and incubated overnight in complete medium with the PI(3)K inhibitor LY294002 (10 µM). Vinculin is shown as a loading control. (B) qRT-PCR analysis of *Cyr61*, *Ctgf*, and *Inhba* to measure YAP transcriptional activity upon inhibition of PI(3)K in EPS8$^+$ and EPS8$^-$ ECs. (C) WB analysis of YAP phosphorylation upon overexpression of constitutively active Akt (myr-Akt) in EPS8$^+$ and EPS8$^-$ ECs. Vinculin is shown as a loading control. (D) qRT-PCR analysis of *Cyr61*, *Ctgf*, and *Inhba* to measure YAP transcriptional activity upon myr-Akt expression in EPS8$^+$ and EPS8$^-$ ECs. (E) Coimmunoprecipitation and WB analysis of the YAP–α-catenin complex in EPS8$^+$ and EPS8$^-$ ECs. (F) IP of VE-cadherin and WB analysis of the YAP–α-catenin complex localization at cell–cell contacts in EPS8$^+$ and EPS8$^-$ cells upon specific siRNA of α-catenin. (G) WB analysis of YAP phosphorylation upon specific siRNA of α-catenin in EPS8$^+$ and EPS8$^-$ ECs. Vinculin is shown as a loading control. (H) qRT-PCR analysis of *Ctgf*, *Cyr61*, and *Inhba* to measure YAP transcriptional activity upon siRNA of α-catenin. For each tested gene, the expression level has been represented as fold changes ± SEM of three independent experiments. *, $P < 0.05$; **, $P < 0.01$. TOT, total cell lysate.

EPS8 and the 14-3-3-YAP complex compete for binding to α-catenin

A common mechanism of cytoplasmic retention of nuclear proteins is mediated by the binding of 14–3-3 proteins, which interact with phosphorylated serine and threonine residues (Muslin and Xing, 2000). Consistently, YAP phosphorylated on serine 127 interacts with 14–3-3 proteins (Zhao et al., 2007), which were also shown to mediate its association with α-catenin (Schlegelmilch et al., 2011) in keratinocytes. To assess whether a similar complex could be detected in WT ECs, we immunoprecipitated YAP from EC extracts (36 h of culture). We were able to detect a VE-cadherin–α-catenin–14–3-3–YAP complex from which EPS8 was excluded (Fig. 6 A). In contrast, α-catenin and VE-cadherin, but neither YAP nor 14–3-3 proteins, were recovered in EPS8 immunoprecipitates. These results support the idea of two different, mutually exclusive pools of VE-cadherin. EPS8 may compete with the 14–3-3–YAP complex for the interaction with α-catenin, ultimately controlling YAP activation by inhibiting its retention at AJs. We verified this hypothesis using recombinant purified proteins in in vitro pull-down

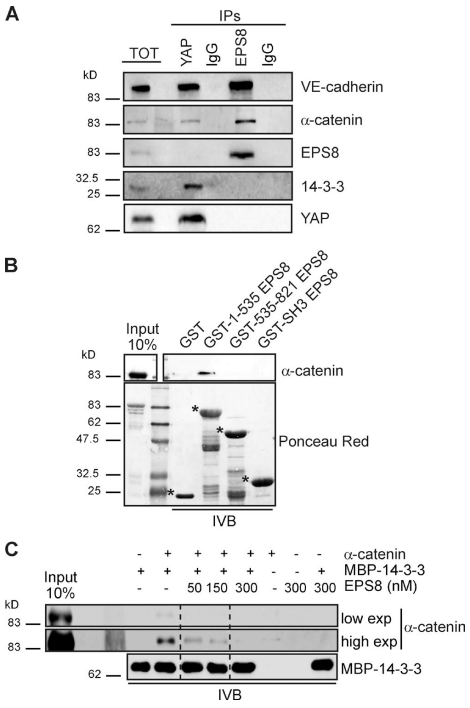

Figure 6. **EPS8 and 14–3-3–YAP complex compete for binding to α-catenin.** (A) IP of YAP or EPS8 from VE-cadherin–positive cell extracts followed by WB analysis of α-catenin, 14–3-3, and VE-cadherin association. EPS8 and YAP–14–3-3 are mutually exclusively bound to VE-cadherin and α-catenin. (B) Analysis of the interaction between α-catenin and EPS8-deleted mutants (asterisks) in vitro by GST pull-down assay. (C) In vitro competition assay between EPS8 and 14–3-3 for binding with α-catenin. 14–3-3 bound α-catenin in the absence of EPS8, and EPS8 reduced this direct interaction in a dose-dependent manner. The dashed lines indicate the blot has been cropped. IVB, in vitro binding; TOT, total cell lysate.

experiments. We found that EPS8 directly bound α-catenin through its N-terminal domain (Fig. 6 B). This latter observation suggested that EPS8 and the 14–3-3–YAP complex may compete for binding to α-catenin. By monitoring the direct association of purified α-catenin to immobilized 14–3-3 proteins (Schlegelmilch et al., 2011), we found that this interaction was abrogated in the presence of an equimolar amount of EPS8 (Fig. 6 C), supporting the idea of a competition between EPS8 and 14–3-3–YAP for α-catenin binding.

A critical role of YAP is to release epithelial cells from contact inhibition of cell growth (Zhao et al., 2011). This latter phenomenon is induced by the formation of cadherin junctional complexes that, in addition to physically sequestering YAP at junctions (Zhao et al., 2011), also promote YAP phosphorylation, further impairing YAP nuclear translocation and transcriptional activity (Dupont et al., 2011). The growth inhibitory function was ascribed to VE-cadherin in ECs (Caveda et al., 1996; Giampietro et al., 2012), suggesting that EPS8 may contribute to this effect through the regulation of VE-cadherin stability at junctions (Fig. 2) and the consequent modulation of YAP localization and activity (Fig. 4).

To provide evidence in this direction, we monitored contact inhibition of cell growth in WT ECs, and we found that with the establishment of cell confluence, both Akt and YAP increased their phosphorylation level (Fig. 7 A), and in parallel YAP transcriptional activity was reduced (Fig. 7 B). Consistently, the removal of EPS8, which both dampens YAP activity and increases VE-cadherin localization at junctions, significantly reduced the number of confluent cells needed to achieve growth arrest (Fig. 7 C).

A correct control of proliferation and the proper establishment of junctional complexes are the crucial steps for the fine regulation of permeability exerted by ECs. Thus, we analyzed whether the absence of Eps8 and the consequent alteration in the transcriptional activity of YAP could impact the regulation of permeability. We found that Eps8$^-$ ECs displayed increased permeability compared with Eps8$^+$ ECs (Fig. 7 D). EPS8 is therefore emerging as a key inductor of YAP activity that acts both by preventing Akt-dependent phosphorylation of YAP, as well as by restraining the binding of the 14–3-3–YAP complex to α-catenin, allowing YAP nuclear translocation.

These EPS8 activities are novel and unrelated to its well-established role in remodeling actin cytoskeleton. Indeed, ECs expressing an EPS8 mutant devoid of actin capping and bundling functions (Hertzog et al., 2010) showed a YAP activity almost equal to EPS8$^+$-expressing cells as measured by serine 127 phosphorylation levels (Fig. 8 A) and by the induction of target gene expression (Fig. 8 B). So far, we have deciphered a new molecular mechanism (Fig. 8 C) through which EPS8, a novel partner of VE-cadherin, is able to modulate YAP transcriptional activity.

The absence of EPS8 alters YAP activity in vivo

To confirm the in vivo relevance of the mechanisms described in the previous paragraphs, we analyzed YAP nuclear localization in vessels of WT and *eps8*-null mice. Consistent with what we previously observed, YAP nuclear localization was increased in the vasculature of *eps8*-null mice (Fig. 9, A and B). Furthermore, freshly isolated ECs obtained from *eps8*-null mice showed ∼30% reduction of YAP target gene expression compared with WT mice (Fig. 9 C). Finally, in agreement with cultured cells, the absence of *eps8* increased VE-cadherin localization at AJs in vivo too (Fig. 10 A).

To test whether the observed defects in permeability shown in cultured ECs were also present in vivo, we tested small- and large-size tracers (cadaverine–Alexa Fluor 555 and 0.1-µm-diameter green fluorescent microsphere, respectively) in WT and eps8-null mice (Figs. 10 B and S5). The analysis revealed a specific increase (∼30%) in the accumulation of cadaverine in the parenchyma of brain and lungs in *eps8*-null mice (Fig. 10 B), whereas no difference in the extravasation of the high-size green fluorescent microspheres was found (Fig. S5).

Collectively, these findings support the idea that the signaling mechanisms uncovered by in vitro analyses are present also in vivo, and Eps8 plays a role in controlling permeability, but only to small molecular size tracers.

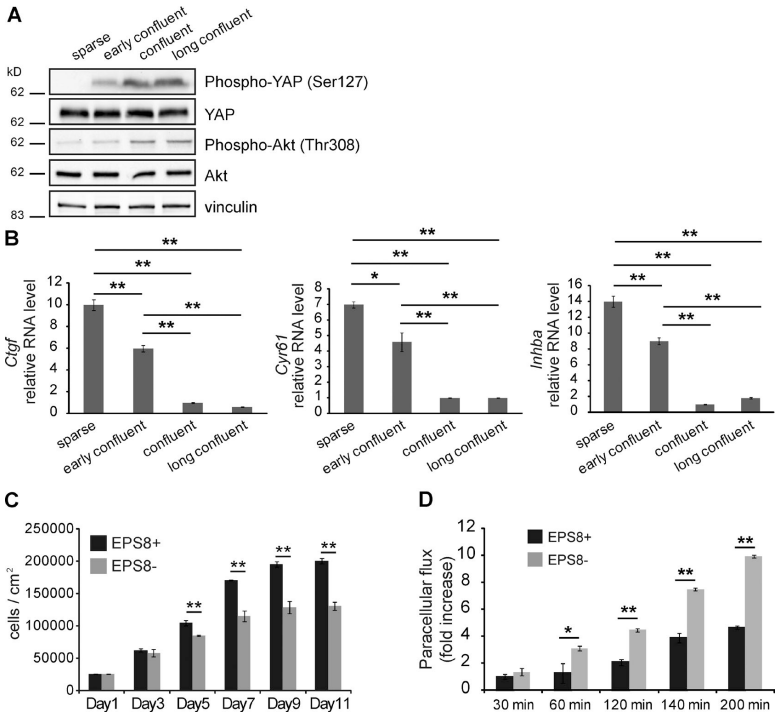

Figure 7. **The absence of EPS8 induces earlier contact inhibition of cell growth and impairs EC permeability.** (A) WB analysis of Phospho-YAP, YAP, Phospho-Akt, and Akt in WT lung–derived ECs at different stages of confluence conditions. Vinculin is the loading control. (B) qRT-PCR analysis of YAP target genes in WT lung–derived ECs at different stages of confluence conditions. Data are means ± SEM of four independent experiments. (C) Cell density analysis performed on EPS8$^+$ and EPS8$^-$ ECs. Equal numbers of cells were seeded at day 1 and subsequently counted at set time points. In the absence of EPS8, VE-cadherin localization is higher, and, consequently, cell–cell contact inhibition of proliferation is increased. Data are means ± SEM of eight independent experiments. (D) Paracellular tracer flux assay. Permeability to FITC-dextran (70 kD) was assayed. Data are means ± SEM of three independent experiments. At all time values from 60 min onward, Eps8$^+$ ECs were statistically lower than Eps8$^-$ ECs. *, $P < 0.05$; **, $P < 0.01$.

Discussion

Endothelial cell-to-cell junctions not only maintain intercellular adhesion but also transfer multiple intracellular signals that modulate contact inhibition of cell growth, cell polarity, lumen formation, and permeability (Dejana et al., 2009; McCrea et al., 2009). The complexity of VE-cadherin signaling is a result of the large number of identified intracellular partners that have been shown to be directly or indirectly associated with AJs in the endothelium (Dejana and Vestweber, 2013).

These signaling proteins can assemble into distinct types of complexes, which would vary in composition in the different vessels, stages of development, and even within the same cell. Furthermore, VE-cadherin association with one or another partner is reversible and can be spatially and temporally regulated.

We report here the identification of EPS8 as a new partner of the VE-cadherin complex in ECs that mediates the transduction of signals impinging on the regulation of the transcriptional coactivator YAP. EPS8 promotes VE-cadherin phosphorylation and ubiquitination. These posttranslational modifications invariably associate with increased internalization and enhance cell surface turnover of VE-cadherin (Gavard and Gutkind, 2006; Orsenigo et al., 2012). Notably, EPS8 is not a stable component of VE-cadherin junctions, but it is transiently and rapidly recruited at cell-to-cell contacts during dynamic remodeling of junctions in early stages of confluency It is likely, therefore, that EPS8 contributes to increase junction dynamics. Conversely, EPS8 loss reduces the turnover of VE-cadherin and favors its clustering, a condition previously shown to promote the activation of the PI(3)K–Akt pathway (Carmeliet et al., 1999; Taddei et al., 2008). Consistent with our results, Choi and Kwon (2015) recently found that YAP subcellular localization and activity in ECs are regulated by the VE-cadherin–mediated PI3K–Akt pathway. In keeping with these notions, we showed that the removal of EPS8 correlates with an increased localization of VE-cadherin at AJs and increased activation of the PI(3)K–Akt pathway.

YAP has long been shown to be a direct downstream target of Akt (Basu et al., 2003). This posttranslational modification creates binding sites for 14–3-3 proteins, a family of

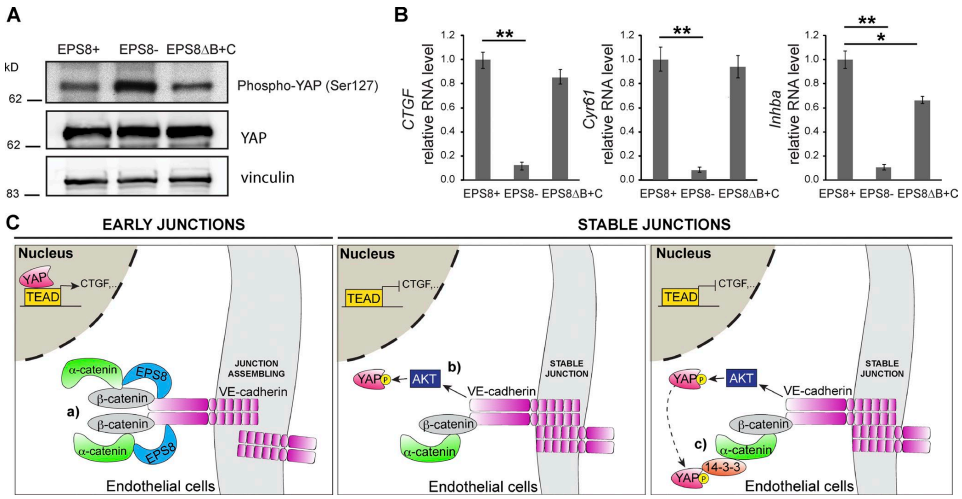

Figure 8. **EPS8 modulation of YAP phosphorylation and transcriptional activity is independent from its actin capping and bundling functions.** (A) WB analysis of YAP phosphorylation in EPS8$^+$, EPS8$^-$, and EPS8ΔB+C ECs. Vinculin is shown as a loading control. (B) qRT-PCR analysis of *Ctgf*, *Cyr61*, and *Inhba* in confluent EPS8$^+$, EPS8$^-$, and EPS8ΔB+C cells. Significant differences in YAP transcriptional activity has been detected only in EPS8$^-$ ECs. For each tested gene, the expression level has been represented as fold changes ± SEM of three independent experiments. *, $P < 0.05$; **, $P < 0.01$. (C) Suggested model for the regulation of YAP phosphorylation, localization, and transcriptional activity. EPS8 transiently binds VE-cadherin during junctional remodeling a) while YAP is localized in the nuclei of ECs; b) when junctions are stabilized, VE-cadherin clustering induces PI(3)K–Akt–YAP phosphorylation and, c) consequently, YAP is sequestered at the plasma membrane. a) The transient direct bond of Eps8 to α-catenin prevents that of 14–3-3–phospho-YAP.

phosphoserine-binding proteins, that may retain YAP in the cytoplasm, preventing its nucleocytoplasmic trafficking and transcriptional activity (Zhao et al., 2007). By associating with 14–3-3, YAP was shown to bind α-catenin in epithelial cells (Schlegelmilch et al., 2011). We report here that this interaction also occurs in ECs, where the loss of EPS8 promotes the localization of hyperphosphorylated YAP at AJs in a trimeric complex with 14–3-3 and α-catenin.

We also found that EPS8 is able to bind directly to α-catenin, competing with the 14–3-3–YAP complex. Coimmunoprecipitation experiments show the existence of two different, mutually exclusive protein complexes of VE-cadherin at AJs: in one complex, VE-cadherin binds α-catenin and EPS8, whereas in the other, VE-cadherin binds α-catenin, 14–3-3, and YAP. As a consequence, elevation of EPS8 levels inhibits, by competition for binding to α-catenin, the formation of the YAP–14–3-3–α-catenin protein assembly, ultimately inducing YAP nucleocytoplasmic shuttling and transcriptional activity. The exclusion of YAP from cell junctions by EPS8 is of particular relevance under conditions of dynamic remodeling of junctions, when endothelial monolayers may not have yet committed to a full growth arrest.

It was shown that actin cytoskeleton and tensional forces can modulate YAP activity (Dupont et al., 2011; Aragona et al., 2013). EPS8 is an actin-capping and -bundling protein that influences actin dynamics in migratory cells. This function resides in the C-terminal effector region of EPS8. We show here that EPS8 can interact with α-catenin through its N-terminal domain at junctions in a topological arrangement that would enable EPS8 to execute its actin regulatory activity via its free effector C-terminal domain. However, the finding that an EPS8 mutant unable to interact with actin (Hertzog et al., 2010) is fully competent in restoring YAP translocation to the nucleus in EPS8-null ECs argues against this possibility. Our findings reveal, instead, an unexpected way of signaling of Eps8 that is apparently independent from its ability to control actin dynamics, but relies on a specific set of protein–protein interactions.

It will be important in future studies to determine the mechanism through which EPS8 is only transiently recruited to junctions. It is possible that increased tension across junctions is the key initiating cue that translates into the formation of a set of specialized complexes required to promote the necessary dynamics and plasticity of otherwise relatively stable structures and tissues.

Under in vitro and in vivo conditions, AJs are highly dynamic structures. Conditions that perturb this equilibrium might also perturb vascular permeability.

In *eps8*-null mice, VE-cadherin localization is increased at cell-to-cell contacts, likely through inhibition of turnover. As in cultured cells, *eps8*-null mice show an increase in vascular permeability, and the small-size tracer cadaverin accumulates in the parenchyma of different organs. However, large-size fluorescent beads did not cross the vessels more efficiently in the absence of eps8, suggesting a size-selective impairment of permeability. This result is consistent with the fact that *eps8*-null mice are viable and fertile and apparently devoid of macroscopic vascular abnormalities.

A possible explanation for the absence of a more dramatic phenotype is that inactivation of *Eps8* may be compensated for by other members of the family of related genes (Scita et al., 1999). Double and triple knockout of EPS8-related genes may clarify this aspect. Alternatively, it is possible that under

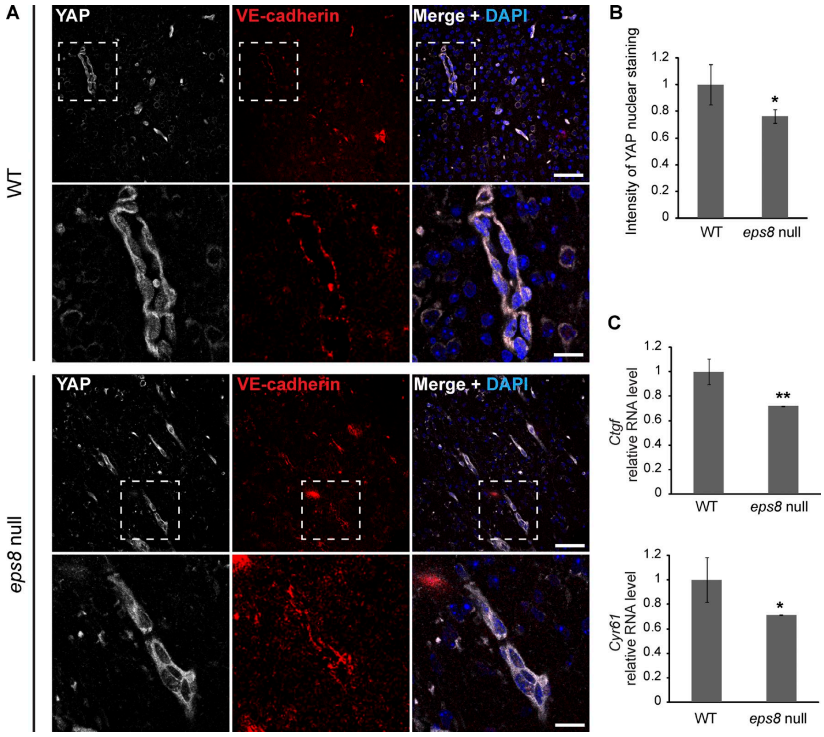

Figure 9. **EPS8 expression modulates YAP localization and transcriptional activity in vivo.** (A) Confocal microscopy analysis of YAP (white) and VE-cadherin (red) localization in paraffin sections of brains of WT and *eps8*-null P9 mice. Bars: (A) 50 µm; (magnification) 20 µm. The dashed outlines indicate the areas magnified below. (B) Quantification of the main intensity of YAP nuclear localization. Data are means ± SEM of six WT and six *eps8*-null mice analyzed. (C) qRT-PCR analysis of *Ctgf* and *Cyr61* expression levels in freshly isolated ECs from WT and *eps8*-null mice. Data are means ± SEM of five WT and five *Eps8*-null mice analyzed. The levels of *Ctgf* and *Cyr61* expression have been normalized on the amount of *VE-cadherin* gene expression. *, $P < 0.05$; **, $P < 0.01$.

specific pathological conditions, eps8-null mice present alterations that are undetectable in healthy conditions.

In conclusion, we show here that the transient localization of EPS8 at endothelial junctions modulates VE-cadherin organization and induces YAP nuclear translocation and transcriptional activity. Further studies are required to characterize in more detail the relevance of this novel molecular pathway in additional in vivo models.

Materials and methods

Cell lines

Murine ECs genetically ablated for *Cdh5* (VE-cadherin null) and modified to express the human WT VE-cadherin (VE-cadherin positive) or VE-cadherin Δ-p120 (lacking aa 621–702 of human VE-cadherin cDNA, which correspond to the p120-catenin–binding region) and Δ-βcat (lacking aa 703–784 of human VE-cadherin cDNA, which correspond to the β-catenin–binding region) were obtained and cultured as described previously (Giampietro et al., 2012). ECs isolated from lungs (Dong et al., 1997; Balconi et al., 2000) of *eps8*-null adult mice were lentivirally infected with EGFP alone or EGFP-EPS8 (Menna et al., 2009). For the experiments, 1,800 cells/cm^2 and 42,000 cells/cm^2 were seeded to obtain sparse and confluent cultures; and 40,000 cells/cm^2 were seeded and cultured for 24 h, 36 h, and 72 h to reach different stages of confluency (early confluent, confluent, and long confluent, respectively). For all ECs of murine origin, the culture medium was DMEM with 20% FCS, 2-mM glutamine, 100 U/liter penicillin/streptomycin, 1-mM sodium pyruvate, 100 µg/ml heparin (from porcine intestinal mucosa; Sigma-Aldrich), and 5 µg/ml EC growth supplement (made from calf brain; complete culture medium).

The starving medium was MCDB 131 (Invitrogen) with 1% BSA (EuroClone), 2-mM glutamine, 100 U/liter penicillin/streptomycin, and 1-mM sodium pyruvate.

The epithelial AD-HEK293 cell line (human embryonic kidney; American Type Culture Collection) used for adenoviral production was grown in DMEM (Cambrex Bioscience) supplemented with 10% FBS (HyClone), 2-mM glutamine, 100 U/liter penicillin/streptomycin, and 1-mM sodium pyruvate.

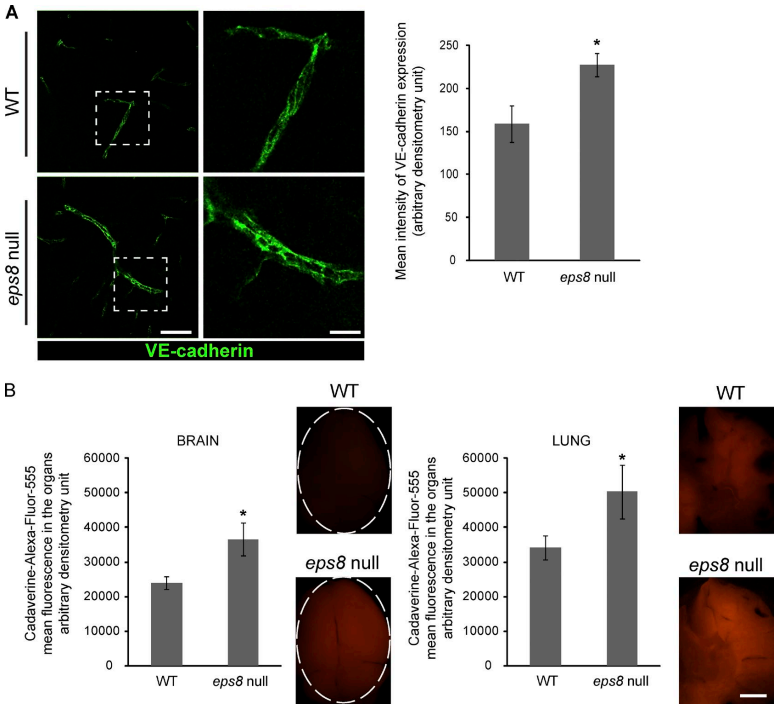

Figure 10. **The absence of EPS8 alters the AJ organization and impairs the correct control of permeability in vivo.** (A) Confocal microscopy analysis of VE-cadherin (green) localization in cryosections of brains of WT and *eps8*-null adult (2 mo old) mice (left). Quantification of the main intensity of VE-cadherin expression; data are means ± SEM of four WT and four *eps8*-null mice analyzed. Bars: (A) 50 µm; (magnification) 20 µm. The dashed outlines indicate the areas magnified on the right. (B) In vivo permeability assay. Mice were injected with 25 mg/kg cadaverine–Alexa Fluor 555, and 2 h later they were sacrificed and their organs were collected. Whole brains and lungs were photographed, and cadaverine was quantified. Bar, 500 µm. The presence of cadaverine in the organs was expressed in arbitrary units as mean fluorescence. $n = 4$ for WT and *eps8* null. The dashed outline highlights the brain area.*, $P < 0.05$.

The COS-1 cell line (monkey kidney fibroblast-like cells; American Type Culture Collection) used for transient transfection was grown in DMEM supplemented with 10% FBS and 2-mM glutamine. All cells were cultured at 37°C in a humidified atmosphere of 5% CO_2/air.

Antibodies

For IF, Western blotting, and immunoprecipitation (IP), the following antibodies were used: VE-cadherin (C-19) goat (sc-6458; Santa Cruz Biotechnology, Inc.); VE-cadherin rat BV13 (ab91064; Abcam; Corada et al., 2002); EPS8 mouse (610144; BD); α-tubulin mouse (T9026; Sigma-Aldrich); vinculin mouse (V9264; Sigma-Aldrich); Ub P4D1 mouse (sc-8017; Santa Cruz Biotechnology, Inc.); pY665-VE-cadherin rabbit (gift from J. Gavard, Institut Cochin, Paris, France; Gavard and Gutkind, 2006); YAP (63.7) mouse (sc-10199; Santa Cruz Biotechnology, Inc.; Western blot [WB]); phospho-YAP (serine 127) rabbit (4911; Cell Signaling Technology); Rac mouse (610650; BD); YAP (H-9) mouse (sc-271134; Santa Cruz Biotechnology, Inc.; IF); pan 14–3-3 (K-19) rabbit (sc-629; Santa Cruz Biotechnology, Inc.); α-catenin rabbit (C2081; Sigma-Aldrich; WB); α-catenin rabbit (2028–1; Epitomics; IP); β-catenin mouse (610154; BD); Mst1 rabbit (3682; Cell Signaling Technology); Mst2 rabbit (3681; Cell Signaling Technology); phospho-Mst1 (threonine 183)/Mst2 (threonine 180) rabbit (3681; Cell Signaling Technology); LATS1 (G-16) goat (sc-12494; Santa Cruz Biotechnology, Inc.); phospho-LATS1 (serine 909) rabbit (9157; Cell Signaling Technology); Akt rabbit (9271; Cell Signaling Technology); phospho-Akt (threonine 308) rabbit (9275; Cell Signaling Technology); Pecam-1 (CD31; ab28364; Abcam); HRP-linked anti-mouse, anti-rat, and anti-rabbit (Cell Signaling Technology); HRP-linked anti-goat (Promega); Alexa Fluor 555–conjugated donkey anti-mouse and anti-goat (Invitrogen); Alexa Fluor 488–conjugated donkey anti-mouse (Invitrogen); and GST (Z-5) rabbit (sc-459; Santa Cruz Biotechnology, Inc.).

Quantitative RT-PCR (qRT-PCR) analysis

Total RNA was isolated using the RNeasy mini kit (QIAGEN), and 1 µg was reverse transcribed with random hexamers (High Capacity cDNA Archive kit; Applied Biosystems). cDNA was amplified with the TaqMan Gene Expression assay (Applied Biosystems) and a thermocycler (ABI Prism 7900HT; Thermo Fisher Scientific). For any sample, the expression level, normalized to the housekeeping genes encoding *18S*, was determined by the comparative threshold cycle method as described previously (Spagnuolo et al., 2004).

Mice

All procedures involving animals and their care were performed in conformity with the guidelines established by the Italian Foundation for Cancer Research Institute of Molecular Oncology Foundation–European Institute of Oncology Campus Principles of Laboratory Animal Care (directive 86/609/EEC).

The generation of *eps8*$^{-/-}$ mice has been described previously by Scita et al. (1999). In brief, we isolated mouse genomic *eps*8 clones from a 129SV library (Agilent Technologies). We used a 7-kb XhoI–XhoI fragment for 5′ homology and a 2.5-kb EcoRV–NotI fragment for 3′ homology. A phosphoglycerate kinase–*neo* cassette replaced an exon-containing *eps*8 genomic 1.7-kb XhoI–EcoRV fragment. The *eps*8 SH3 domain is encoded by two exons, and the targeting construct excluded the first and part of the second of these exons. A genomic probe, flanking the targeting construct at the 5′ end, was used to detect the WT (2.6 kb) and targeted (9.5 kb) alleles. Of note, this genetic lesion resulted in the complete loss of the eps8 gene product as determined by mRNA analysis and immunoblotting with antipeptide serum raised against the N-terminal region of EPS8. Electroporation into mouse embryonic day 14 embryonic stem cell clones, and subsequent manipulations leading to mice heterozygous and homozygous for the mutant *Eps*8 allele, were performed as described previously (Levéen et al., 1994). A targeted embryonic stem cell clone was injected into C57BL/6 blastocysts, and germline chimeras and mice heterozygous and homozygous for the *eps8* mutant allele were derived. DNA analyses, derivation of chimeras, and subsequent identification of germline transmission, and mice heterozygous and homozygous for the mutant *eps8* allele, were described previously (Levéen et al., 1994). *eps8*-null mice were backcrossed for >20 generations to C57BL/6 mice. Age- and sex-matched C57BL/6 mice were used as controls.

Intravenous injection of lysine-fixable cadaverine conjugated to Alexa Fluor 555 and microsphere

Cadaverine conjugated to Alexa Fluor 555 (3.125 mg/ml in saline) was injected intravenously into the tail vein of adult (2 mo old) 25-mg/kg mice eps8 null and controls. The circulation time was 2 h. For in situ detection of cadaverine, the anesthetized mice were perfused for 1–2 min with HBSS, followed by 5 min of perfusion with 4% PFA in PBS, pH 7.2. The organs were then removed and postfixed in 4% PFA at 4°C for 5–6 h. Images of dissected organs were captured using a stereomicroscope (SZX16; Olympus) equipped with a fluorescence long-pass filter for RFP (excitation, 530–550 nm; emission, 575 nm). Image acquisition was performed using a 1× objective with a total magnification of 0.35×, supported by an RGB camera (Digital Sight DS-5Mc; Nikon). The ImageJ open-source software (National Institutes of Health) was used for data analysis. The mean fluorescence was calculated as the ratios of the total fluorescence signals to the number of pixels in the areas, expressed as arbitrary units.

For in situ detection of microspheres, the anesthetized mice were intravenously injected with green fluorescent microspheres (0.1-µm diameter; 50 ml; Duke Scientific) and then perfused for 1–2 min with HBSS, followed by 5 min of perfusion with 4% PFA in PBS, pH 7.2. The tracheas were then removed and postfixed in 4% PFA at 4°C for 1 h and then processed for IF analyses.

Histology and tissue IF

Mouse organs were embedded in optimal cutting temperature compound (Tissue-Tek; Sakura) and snap frozen or embedded in paraffin. 5-µm-thick sections were cut. Frozen sections were fixed in cold methanol or 4% PFA and subjected to IF. Paraffin sections were subjected to IF. Blocking (2 h), primary (overnight), and secondary (3 h) antibodies were diluted in PBS with 2% BSA. Sections were then counterstained with DAPI and mounted in Vectashield.

Retinal immunohistochemistry

Eyes from WT C57BL/6 postnatal day 9 mice were fixed in 2% PFA overnight before retinas were dissected. Retinas were incubated in 5% donkey serum, 1% BSA, and 0.5% Triton X-100 in PBS overnight and the day after, stained with primary antibodies overnight. Then retinas were incubated with fluorophore-conjugated antibodies and mounted with ProLong gold (Invitrogen).

IF microscopy

Cells were cultured and then fixed with 4% PFA or, if specified in the text, with 1% PFA in 2.5-mM triethanolamine, pH 7.5, containing 0.1% Triton X-100 and 0.1% NP-40 to optimize junctional staining. Fixed cells were permeabilized and incubated for 30 min in a blocking solution of PBS with 2% BSA.

Cells were then incubated overnight with primary antibodies diluted in blocking buffer. Appropriate secondary antibodies were applied on cells for 45 min at RT. Confocal microscopy was performed at RT with a confocal microscope (TCS SP2AOBS; Leica) equipped with violet (405-nm laser diode), blue (488 nm; Argon), yellow (561 nm; solid state), and red (633 nm; HeNe) excitation laser lines before processing with Photoshop (Adobe). Only adjustments of brightness and contrast were used in the preparation of the figures. For comparison purposes, different sample images of the same antigen were acquired under constant acquisition settings. Image acquisition was performed using a 63×/1.4 NA oil immersion objective (HCX PL APO 63× Lbd BL; Leica) with spectral detection bands and scanning modalities optimized for removal of channel cross talk. Confocal software (Leica) and ImageJ version 1.33 were used for data analysis.

LUMIER assay

The automated high throughput technology LUMIER to analyze dynamic protein–protein interaction networks in mammalian cells was performed as previously described (Barrios-Rodiles et al., 2005). Full-length human VE-cadherin and Δ-βcat mutant were C-terminally tagged with RL (VE-cadherin-RL and Δ-βcat-RL). In brief, HEK293T cells from a library of 640 3× Flag-tagged cDNAs that encode proteins comprised of diverse signaling-associated domains (Miller et al., 2009), plated in dishes, were robotically transfected using PolyFect (QIAGEN). After 48 h, cells were lysed and then immunoprecipitated using anti-Flag M2 monoclonal antibody (Sigma-Aldrich). Luciferase activity in immunoprecipitates and in aliquots of total cell lysates was determined using the Renilla Luciferase Assay system (Promega).

Lung EC isolation

Lungs were excised from mice and digested with collagenase type I (Roche) for 2 h at 37°C. The ECs were then separated using Dynabeads (Invitrogen) coated with Pecam-1 antibody (BD) according to the manual's instructions and immediately processed for RNA isolation. cDNA synthesis and qRT-PCR were performed as described in the Quantitative RT-PCR (qRT-PCR) analysis section.

Statistical analysis

A Student's two-tailed unpaired *t* test was used to determine statistical significance. The significance level was set at $P < 0.05$.

IP

Cells were incubated with 100 µg/ml dithiobis(succinimidyl)propionate (Thermo Fisher Scientific) for 20 min at 37°C and then solubilized in lysis buffer (100-mM Tris-HCl, pH 7.4, 150-mM NaCl, 1% Triton X-100, 1% deoxycholic acid, 0.1% SDS, 2-mM $CaCl_2$, and

protease/phosphatase inhibitors) on ice for 30 min. Precleared cell extracts were subjected to antibody precipitation overnight at 4°C, and immune complexes were captured by protein G–Sepharose beads (GE Healthcare). Immunoprecipitated material was separated on Tris-glycine SDS-PAGE, blotted onto nitrocellulose membrane, and analyzed by standard methodologies.

Western blotting

Confluent cells were lysed by boiling in a modified Laemmli sample buffer (2% SDS, 20% glycerol, and 125-mM Tris-HCl, pH 6.8). Equal amounts of proteins were loaded on gels, separated by SDS-PAGE, and transferred to a nitrocellulose membrane (Protran; Whatman). After incubation with primary and HRP-linked secondary antibodies, specific bindings were detected by a chemiluminescence system (GE Healthcare).

Gelatin-glutaraldehyde cross-linking

To enhance EC adhesion, slides were coated with glutaraldehyde–cross-linked gelatin as follows. The culture supports were incubated for 1 h at RT with 1% gelatin, followed by a cross-linking with 2% glutaraldehyde solution for 15 min at RT. The glutaraldehyde was replaced by 70% ethanol. After 1 h, five washes with PBS followed by overnight incubation with PBS containing 2-mM glycine were performed. Before cell seeding, slides were washed five times with PBS.

Paracellular tracer flux analysis

Cells were seeded on 6.5-mm-diameter Transwell permeable supports (pore size 0.4 µm; Corning), cultured in complete culture medium, and assayed for permeability to FITC-dextran (70 kD; Sigma-Aldrich). Next, FITC-dextran was added to the medium of the Transwell apical compartment at a concentration of 1 mg/ml. At different times of incubation, a 50-µl aliquot of the medium was collected from the basal compartment, and the paracellular tracer flux was measured as the amount of FITC-dextran in the medium using a fluorometer (Wallac Victor3 1420 multilabel counter; PerkinElmer).

Active Rho and Rac pull-down assay

To detect active Rho, we used the Active Rho Pull-Down and Detection kit (Thermo Fisher Scientific) in accordance with the manufacturer's instructions. To detect active Rac, we used the G-LISA Rac activation assay (Cytoskeleton, Inc.) in accordance with the manufacturer's instructions.

Treatments

ECs were starved overnight before any treatment. 10-µM LY294002 (Cell Signaling Technology) was added overnight at 37°C.

Constructs

A form of Akt that is constitutively active (myr-Akt) was a gift from C. Daly (Regeneron Pharmaceuticals Inc., Tarrytown, NY). Cytomegalovirus promoter–based, elongation factor-1 promoter–based eukaryotic expression vectors, and GST bacterial expression vectors were generated by recombinant PCR. His6-tagged α-catenin full-length was a gift from B. Weis and W.J. Nelson (Stanford University, Stanford, CA). MBP–14–3-3 was procured from GeneCopoeia. All constructs were verified by sequencing.

Protein purification

Recombinant full-length His-EPS8, His-Irsp53, and GST-EPS8 fragments were expressed and purified as previously described (Disanza et al., 2006, 2013; Hertzog et al., 2010). In brief, recombinant fragments were expressed as His- or GST-fusion proteins in the BL21 *Escherichia coli* strain (Agilent Technologies) and affinity purified using GS4B glutathione–Sepharose beads (GE Healthcare) or nickel–nitrilotriacetic acid agarose. Eluted proteins were dialyzed in 50-mM Tris-HCl, 150-mM NaCl, 1-mM DTT, and 20% glycerol. GST–VE-cadherin intracellular domain was expressed in BL21 Rosetta strain (Agilent Technologies) and affinity purified using GS4B glutathione–Sepharose beads. His–α-catenin was expressed in the BL21 *E. coli* strain (Agilent Technologies) and affinity purified using nickel–nitrilotriacetic acid (Ni-NTA) agarose according to standard procedures. Recombinant purified protein was eluted with 200-mM imidazole and dialyzed in 50-mM Tris, pH 7.8, 150-mM NaCl, 1-mM DTT, and 5% glycerol. MBP–14–3-3 was purified by standard procedures using amylose–Sepharose affinity purification.

In vitro binding assay

MBP–14–3-3–α-catenin ± EPS8. Recombinant purified proteins were incubated overnight at 4°C in Xb buffer (50-mM Tris-HCl, pH 7.4, 150-mM NaCl, 0.02% Triton X-100, 20-mM imidazole, 1-mM DTT, and protease inhibitor cocktail). Samples were then incubated for 1 h at 4°C with amylose–Sepharose beads and washed three times with Xb buffer. Amylose–Sepharose beads were resuspended in a 1:1 volume of 2× SDS-PAGE sample buffer, boiled for 5 min at 95°C, spun down for 1 min, and loaded on acrylamide gels.

EPS8 full-length/VE-cadherin cytoplasmic tail. Recombinant purified His-EPS8 and VE-cadherin–C-terminal fragment were incubated for 1 h at 4°C with Ni-NTA beads in Xa buffer (50-mM Tris, pH 8, 300-mM NaCl, 0.1% Triton X-100, 20-mM imidazole, 1-mM DTT, and protease inhibitor cocktail). Samples were washed three times in Xb buffer. Beads were resuspended in a 1:1 volume of 2× SDS-PAGE sample buffer, boiled for 5 min at 95°C, spun down for 1 min, and loaded on acrylamide gels.

EPS8 fragments/α-catenin full length. Recombinant purified GST-EPS8 fragments and His–α-catenin were incubated for 1 h at 4°C with Ni-NTA beads in Xb buffer. Samples were washed three times in Xb buffer. Beads were resuspended in a 1:1 volume of 2× SDS-PAGE sample buffer, boiled for 5 min at 95°C, spun down for 1 min, and loaded on acrylamide gels.

EPS8 fragments/VE-cadherin cytoplasmic tail. Equal amounts of cell lysates overexpressing VE-cadherin cDNA were incubated with GST-EPS8 fragments (GST as control) for 2 h at 4°C in the presence of GS4B glutathione–Sepharose beads. Samples were washed three times in lysis buffer. Beads were resuspended in a 1:1 volume of 2× SDS-PAGE sample buffer, boiled for 5 min at 95°C, spun down for 1 min, and loaded on acrylamide gels.

RNAi

To interfere with α-catenin, we used siRNA (ON-TARGETplus L-048960-01; SMARTpool duplex Ctnna1) from GE Healthcare and the corresponding nontargeting pool (ONTARGETplus). Transfection was performed with Lipofectamine 2000 (Invitrogen) in accordance with the manufacturer's instructions.

Online supplemental material

Fig. S1 describes EPS8 reconstitution in EPS8$^-$ ECs. Fig. S2 shows that YAP transcriptional activity is regulated by VE-cadherin. Fig. S3 shows that EPS8 expression does not influence the Hippo pathway and Rho and Rac activity in ECs. Fig. S4 shows that YAP binding to VE-cadherin negatively regulates its transcriptional activity. Fig. S5 shows the high-size permeability control in vivo. Online supplemental material is available at http://www.jcb.org/cgi/content/full/jcb.201501089/DC1.

Acknowledgments

We thank F. Orsenigo, F. Pisati, and L. Terreran for technical help.

This work was supported by grants from Associazione Italiana per la Ricerca sul Cancro (AIRC; 10168 to G. Scita and 14471 to E. Dejana), "Special Program Molecular Clinical Oncology 5x1000" (to AIRC-Gruppo Italiano Malattie Mieloproliferative), the European Research Council (projects EU-ERC 268870 to E. Dejana and EU-ERC 268836 to G. Scita), the European Community (ITN VESSEL 317250, BtBRAIN to E. Dejana), the Telethon Foundation (GGP14149 to E. Dejana), the Italian Ministry of Education, University and Research (MIUR-PRIN-2009X23L78), the Italian Ministry of Health, the Association for International Cancer Research (09-0582 to G. Scita), the CAR IPLO Foundation (2010-0737 to G. Scita, 2011-0596 to A. Disanza, and 2012-0678 to E. Dejana), and the German Research Foundation (SFB829 to C. Niessen).

The authors declare no competing financial interests.

Submitted: 21 January 2015
Accepted: 10 November 2015

References

Aragona, M., T. Panciera, A. Manfrin, S. Giulitti, F. Michielin, N. Elvassore, S. Dupont, and S. Piccolo. 2013. A mechanical checkpoint controls multicellular growth through YAP/TAZ regulation by actin-processing factors. *Cell.* 154:1047–1059. http://dx.doi.org/10.1016/j.cell.2013.07.042

Auciello, G., D.L. Cunningham, T. Tatar, J.K. Heath, and J.Z. Rappoport. 2013. Regulation of fibroblast growth factor receptor signalling and trafficking by Src and Eps8. *J. Cell Sci.* 126:613–624. http://dx.doi.org/10.1242/jcs.116228

Balconi, G., R. Spagnuolo, and E. Dejana. 2000. Development of endothelial cell lines from embryonic stem cells: A tool for studying genetically manipulated endothelial cells in vitro. *Arterioscler. Thromb. Vasc. Biol.* 20:1443–1451. http://dx.doi.org/10.1161/01.ATV.20.6.1443

Barrios-Rodiles, M., K.R. Brown, B. Ozdamar, R. Bose, Z. Liu, R.S. Donovan, F. Shinjo, Y. Liu, J. Dembowy, I.W. Taylor, et al. 2005. High-throughput mapping of a dynamic signaling network in mammalian cells. *Science.* 307:1621–1625. http://dx.doi.org/10.1126/science.1105776

Basu, S., N.F. Totty, M.S. Irwin, M. Sudol, and J. Downward. 2003. Akt phosphorylates the Yes-associated protein, YAP, to induce interaction with 14-3-3 and attenuation of p73-mediated apoptosis. *Mol. Cell.* 11:11–23. http://dx.doi.org/10.1016/S1097-2765(02)00776-1

Brown, D.J., E.M. Rzucidlo, B.L. Merenick, R.J. Wagner, K.A. Martin, and R.J. Powell. 2005. Endothelial cell activation of the smooth muscle cell phosphoinositide 3-kinase/Akt pathway promotes differentiation. *J. Vasc. Surg.* 41:509–516. http://dx.doi.org/10.1016/j.jvs.2004.12.024

Carmeliet, P., M.G. Lampugnani, L. Moons, F. Breviario, V. Compernolle, F. Bono, G. Balconi, R. Spagnuolo, B. Oosthuyse, M. Dewerchin, et al. 1999. Targeted deficiency or cytosolic truncation of the VE-cadherin gene in mice impairs VEGF-mediated endothelial survival and angiogenesis. *Cell.* 98:147–157. http://dx.doi.org/10.1016/S0092-8674(00)81010-7

Caveda, L., I. Martin-Padura, P. Navarro, F. Breviario, M. Corada, D. Gulino, M.G. Lampugnani, and E. Dejana. 1996. Inhibition of cultured cell growth by vascular endothelial cadherin (cadherin-5/VE-cadherin). *J. Clin. Invest.* 98:886–893. http://dx.doi.org/10.1172/JCI118870

Choi, H.J., H. Zhang, H. Park, K.S. Choi, H.W. Lee, V. Agrawal, Y.M. Kim, and Y.G. Kwon. 2015. Yes-associated protein regulates endothelial cell contact-mediated expression of angiopoietin-2. *Nat. Commun.* 6:6943. http://dx.doi.org/10.1038/ncomms7943

Corada, M., L. Zanetta, F. Orsenigo, F. Breviario, M.G. Lampugnani, S. Bernasconi, F. Liao, D.J. Hicklin, P. Bohlen, and E. Dejana. 2002. A monoclonal antibody to vascular endothelial-cadherin inhibits tumor angiogenesis without side effects on endothelial permeability. *Blood.* 100:905–911. http://dx.doi.org/10.1182/blood.V100.3.905

Croce, A., G. Cassata, A. Disanza, M.C. Gagliani, C. Tacchetti, M.G. Malabarba, M.F. Carlier, G. Scita, R. Baumeister, and P.P. Di Fiore. 2004. A novel actin barbed-end-capping activity in EPS-8 regulates apical morphogenesis in intestinal cells of *Caenorhabditis elegans*. *Nat. Cell Biol.* 6:1173–1179. http://dx.doi.org/10.1038/ncb1198

Dejana, E., and C. Giampietro. 2012. Vascular endothelial-cadherin and vascular stability. *Curr. Opin. Hematol.* 19:218–223. http://dx.doi.org/10.1097/MOH.0b013e3283523e1c

Dejana, E., and D. Vestweber. 2013. The role of VE-cadherin in vascular morphogenesis and permeability control. *Prog. Mol. Biol. Transl. Sci.* 116:119–144. http://dx.doi.org/10.1016/B978-0-12-394311-8.00006-6

Dejana, E., E. Tournier-Lasserve, and B.M. Weinstein. 2009. The control of vascular integrity by endothelial cell junctions: Molecular basis and pathological implications. *Dev. Cell.* 16:209–221. http://dx.doi.org/10.1016/j.devcel.2009.01.004

Di Fiore, P.P., and G. Scita. 2002. Eps8 in the midst of GTPases. *Int. J. Biochem. Cell Biol.* 34:1178–1183. http://dx.doi.org/10.1016/S1357-2725(02)00064-X

Disanza, A., M.F. Carlier, T.E. Stradal, D. Didry, E. Frittoli, S. Confalonieri, A. Croce, J. Wehland, P.P. Di Fiore, and G. Scita. 2004. Eps8 controls actin-based motility by capping the barbed ends of actin filaments. *Nat. Cell Biol.* 6:1180–1188. http://dx.doi.org/10.1038/ncb1199

Disanza, A., S. Mantoani, M. Hertzog, S. Gerboth, E. Frittoli, A. Steffen, K. Berhoerster, H.J. Kreienkamp, F. Milanesi, P.P. Di Fiore, et al. 2006. Regulation of cell shape by Cdc42 is mediated by the synergic actin-bundling activity of the Eps8-IRSp53 complex. *Nat. Cell Biol.* 8:1337–1347. http://dx.doi.org/10.1038/ncb1502

Disanza, A., S. Bisi, M. Winterhoff, F. Milanesi, D.S. Ushakov, D. Kast, P. Marighetti, G. Romet-Lemonne, H.M. Müller, W. Nickel, et al. 2013. CDC42 switches IRSp53 from inhibition of actin growth to elongation by clustering of VASP. *EMBO J.* 32:2735–2750. http://dx.doi.org/10.1038/emboj.2013.208

Dong, Q.G., S. Bernasconi, S. Lostaglio, R.W. De Calmanovici, I. Martin-Padura, F. Breviario, C. Garlanda, S. Ramponi, A. Mantovani, and A. Vecchi. 1997. A general strategy for isolation of endothelial cells from murine tissues. Characterization of two endothelial cell lines from the murine lung and subcutaneous sponge implants. *Arterioscler. Thromb. Vasc. Biol.* 17:1599–1604. http://dx.doi.org/10.1161/01.ATV.17.8.1599

Dupont, S., L. Morsut, M. Aragona, E. Enzo, S. Giulitti, M. Cordenonsi, F. Zanconato, J. Le Digabel, M. Forcato, S. Bicciato, et al. 2011. Role of YAP/TAZ in mechanotransduction. *Nature.* 474:179–183. http://dx.doi.org/10.1038/nature10137

Frittoli, E., G. Matteoli, A. Palamidessi, E. Mazzini, L. Maddaluno, A. Disanza, C. Yang, T. Svitkina, M. Rescigno, and G. Scita. 2011. The signaling adaptor Eps8 is an essential actin capping protein for dendritic cell migration. *Immunity.* 35:388–399. http://dx.doi.org/10.1016/j.immuni.2011.07.007

Gavard, J., and J.S. Gutkind. 2006. VEGF controls endothelial-cell permeability by promoting the β-arrestin-dependent endocytosis of VE-cadherin. *Nat. Cell Biol.* 8:1223–1234. http://dx.doi.org/10.1038/ncb1486

Giampietro, C., A. Taddei, M. Corada, G.M. Sarra-Ferraris, M. Alcalay, U. Cavallaro, F. Orsenigo, M.G. Lampugnani, and E. Dejana. 2012. Overlapping and divergent signaling pathways of N-cadherin and VE-cadherin in endothelial cells. *Blood.* 119:2159–2170. http://dx.doi.org/10.1182/blood-2011-09-381012

Giannotta, M., M. Trani, and E. Dejana. 2013. VE-cadherin and endothelial adherens junctions: Active guardians of vascular integrity. *Dev. Cell.* 26:441–454. http://dx.doi.org/10.1016/j.devcel.2013.08.020

Goddard, L.M., and M.L. Iruela-Arispe. 2013. Cellular and molecular regulation of vascular permeability. *Thromb. Haemost.* 109:407–415. http://dx.doi.org/10.1160/TH12-09-0678

Hertzog, M., F. Milanesi, L. Hazelwood, A. Disanza, H. Liu, E. Perlade, M.G. Malabarba, S. Pasqualato, A. Maiolica, S. Confalonieri, et al. 2010. Molecular basis for the dual function of Eps8 on actin dynamics: Bundling and capping. *PLoS Biol.* 8:e1000387. http://dx.doi.org/10.1371/journal.pbio.1000387

Kim, N.G., E. Koh, X. Chen, and B.M. Gumbiner. 2011. E-cadherin mediates contact inhibition of proliferation through Hippo signaling-pathway components. *Proc. Natl. Acad. Sci. USA.* 108:11930–11935. http://dx.doi.org/10.1073/pnas.1103345108

Kluger, M.S., P.R. Clark, G. Tellides, V. Gerke, and J.S. Pober. 2013. Claudin-5 controls intercellular barriers of human dermal microvascular but not human umbilical vein endothelial cells. *Arterioscler. Thromb. Vasc. Biol.* 33:489–500. http://dx.doi.org/10.1161/ATVBAHA.112.300893

Lampugnani, M.G., M. Corada, P. Andriopoulou, S. Esser, W. Risau, and E. Dejana. 1997. Cell confluence regulates tyrosine phosphorylation of adherens junction components in endothelial cells. *J. Cell Sci.* 110:2065–2077.

Lanzetti, L., V. Rybin, M.G. Malabarba, S. Christoforidis, G. Scita, M. Zerial, and P.P. Di Fiore. 2000. The Eps8 protein coordinates EGF receptor signalling through Rac and trafficking through Rab5. *Nature.* 408:374–377. http://dx.doi.org/10.1038/35042605

Levéen, P., M. Pekny, S. Gebre-Medhin, B. Swolin, E. Larsson, and C. Betsholtz. 1994. Mice deficient for PDGF B show renal, cardiovascular, and

hematological abnormalities. *Genes Dev.* 8:1875–1887. http://dx.doi.org/10.1101/gad.8.16.1875

Manor, U., A. Disanza, M. Grati, L. Andrade, H. Lin, P.P. Di Fiore, G. Scita, and B. Kachar. 2011. Regulation of stereocilia length by myosin XVa and whirlin depends on the actin-regulatory protein Eps8. *Curr. Biol.* 21:167–172. http://dx.doi.org/10.1016/j.cub.2010.12.046

McCrea, P.D., D. Gu, and M.S. Balda. 2009. Junctional music that the nucleus hears: Cell-cell contact signaling and the modulation of gene activity. *Cold Spring Harb. Perspect. Biol.* 1:a002923. http://dx.doi.org/10.1101/cshperspect.a002923

Menna, E., A. Disanza, C. Cagnoli, U. Schenk, G. Gelsomino, E. Frittoli, M. Hertzog, N. Offenhauser, C. Sawallisch, H.J. Kreienkamp, et al. 2009. Eps8 regulates axonal filopodia in hippocampal neurons in response to brain-derived neurotrophic factor (BDNF). *PLoS Biol.* 7:e1000138. http://dx.doi.org/10.1371/journal.pbio.1000138

Miller, B.W., G. Lau, C. Grouios, E. Mollica, M. Barrios-Rodiles, Y. Liu, A. Datti, Q. Morris, J.L. Wrana, and L. Attisano. 2009. Application of an integrated physical and functional screening approach to identify inhibitors of the Wnt pathway. *Mol. Syst. Biol.* 5:315. http://dx.doi.org/10.1038/msb.2009.72

Morgan, J.T., C.J. Murphy, and P. Russell. 2013. What do mechanotransduction, Hippo, Wnt, and TGFβ have in common? YAP and TAZ as key orchestrating molecules in ocular health and disease. *Exp. Eye Res.* 115:1–12. http://dx.doi.org/10.1016/j.exer.2013.06.012

Morin-Kensicki, E.M., B.N. Boone, M. Howell, J.R. Stonebraker, J. Teed, J.G. Alb, T.R. Magnuson, W. O'Neal, and S.L. Milgram. 2006. Defects in yolk sac vasculogenesis, chorioallantoic fusion, and embryonic axis elongation in mice with targeted disruption of Yap65. *Mol. Cell. Biol.* 26:77–87. http://dx.doi.org/10.1128/MCB.26.1.77-87.2006

Muslin, A.J., and H. Xing. 2000. 14-3-3 proteins: Regulation of subcellular localization by molecular interference. *Cell. Signal.* 12:703–709. http://dx.doi.org/10.1016/S0898-6568(00)00131-5

Navarro, P., L. Caveda, F. Breviario, I. Mândoteanu, M.G. Lampugnani, and E. Dejana. 1995. Catenin-dependent and -independent functions of vascular endothelial cadherin. *J. Biol. Chem.* 270:30965–30972. http://dx.doi.org/10.1074/jbc.270.52.30965

Orsenigo, F., C. Giampietro, A. Ferrari, M. Corada, A. Galaup, S. Sigismund, G. Ristagno, L. Maddaluno, G.Y. Koh, D. Franco, et al. 2012. Phosphorylation of VE-cadherin is modulated by haemodynamic forces and contributes to the regulation of vascular permeability in vivo. *Nat. Commun.* 3:1208. http://dx.doi.org/10.1038/ncomms2199

Pannekoek, W.J., J.J. van Dijk, O.Y. Chan, S. Huveneers, J.R. Linnemann, E. Spanjaard, P.M. Brouwer, A.J. van der Meer, F.J. Zwartkruis, H. Rehmann, et al. 2011. Epac1 and PDZ-GEF cooperate in Rap1 mediated endothelial junction control. *Cell. Signal.* 23:2056–2064. http://dx.doi.org/10.1016/j.cellsig.2011.07.022

Ribatti, D., B. Nico, A. Vacca, L. Roncali, and F. Dammacco. 2002. Endothelial cell heterogeneity and organ specificity. *J. Hematother. Stem Cell Res.* 11:81–90. http://dx.doi.org/10.1089/152581602753448559

Schlegelmilch, K., M. Mohseni, O. Kirak, J. Pruszak, J.R. Rodriguez, D. Zhou, B.T. Kreger, V. Vasioukhin, J. Avruch, T.R. Brummelkamp, and F.D. Camargo. 2011. Yap1 acts downstream of α-catenin to control epidermal proliferation. *Cell.* 144:782–795. http://dx.doi.org/10.1016/j.cell.2011.02.031

Scita, G., J. Nordstrom, R. Carbone, P. Tenca, G. Giardina, S. Gutkind, M. Bjarnegård, C. Betsholtz, and P.P. Di Fiore. 1999. EPS8 and E3B1 transduce signals from Ras to Rac. *Nature.* 401:290–293. http://dx.doi.org/10.1038/45822

Silvis, M.R., B.T. Kreger, W.H. Lien, O. Klezovitch, G.M. Rudakova, F.D. Camargo, D.M. Lantz, J.T. Seykora, and V. Vasioukhin. 2011. α-catenin is a tumor suppressor that controls cell accumulation by regulating the localization and activity of the transcriptional coactivator Yap1. *Sci. Signal.* 4:ra33.

Spagnuolo, R., M. Corada, F. Orsenigo, L. Zanetta, U. Deuschle, P. Sandy, C. Schneider, C.J. Drake, F. Breviario, and E. Dejana. 2004. Gas1 is induced by VE-cadherin and vascular endothelial growth factor and inhibits endothelial cell apoptosis. *Blood.* 103:3005–3012. http://dx.doi.org/10.1182/blood-2003-07-2459

Taddei, A., C. Giampietro, A. Conti, F. Orsenigo, F. Breviario, V. Pirazzoli, M. Potente, C. Daly, S. Dimmeler, and E. Dejana. 2008. Endothelial adherens junctions control tight junctions by VE-cadherin-mediated upregulation of claudin-5. *Nat. Cell Biol.* 10:923–934. http://dx.doi.org/10.1038/ncb1752

Taylor, M.J., E.R. Tiangga, R.N. Mhuircheartaigh, and P.J. Cowen. 2012. Lack of effect of ketamine on cortical glutamate and glutamine in healthy volunteers: A proton magnetic resonance spectroscopy study. *J. Psychopharmacol. (Oxford).* 26:733–737. http://dx.doi.org/10.1177/0269881111405359

Tocchetti, A., C.B. Soppo, F. Zani, F. Bianchi, M.C. Gagliani, B. Pozzi, J. Rozman, R. Elvert, N. Ehrhardt, B. Rathkolb, et al. 2010. Loss of the actin remodeler Eps8 causes intestinal defects and improved metabolic status in mice. *PLoS One.* 5:e9468. http://dx.doi.org/10.1371/journal.pone.0009468

Vandenbroucke, E., D. Mehta, R. Minshall, and A.B. Malik. 2008. Regulation of endothelial junctional permeability. *Ann. N.Y. Acad. Sci.* 1123:134–145. http://dx.doi.org/10.1196/annals.1420.016

Varelas, X. 2014. The Hippo pathway effectors TAZ and YAP in development, homeostasis and disease. *Development.* 141:1614–1626. http://dx.doi.org/10.1242/dev.102376

Vestweber, D., M. Winderlich, G. Cagna, and A.F. Nottebaum. 2009. Cell adhesion dynamics at endothelial junctions: VE-cadherin as a major player. *Trends Cell Biol.* 19:8–15. http://dx.doi.org/10.1016/j.tcb.2008.10.001

Vestweber, D., A. Broermann, and D. Schulte. 2010. Control of endothelial barrier function by regulating vascular endothelial-cadherin. *Curr. Opin. Hematol.* 17:230–236. http://dx.doi.org/10.1097/MOH.0b013e328338664b

Zhao, B., X. Wei, W. Li, R.S. Udan, Q. Yang, J. Kim, J. Xie, T. Ikenoue, J. Yu, L. Li, et al. 2007. Inactivation of YAP oncoprotein by the Hippo pathway is involved in cell contact inhibition and tissue growth control. *Genes Dev.* 21:2747–2761. http://dx.doi.org/10.1101/gad.1602907

Zhao, B., K. Tumaneng, and K.L. Guan. 2011. The Hippo pathway in organ size control, tissue regeneration and stem cell self-renewal. *Nat. Cell Biol.* 13:877–883. http://dx.doi.org/10.1038/ncb2303

REFERENCES

Adler, J.J., Johnson, D.E., Heller, B.L., Bringman, L.R., Ranahan, W.P., Conwell, M.D., Sun, Y., Hudmon, A., and Wells, C.D. (2013). Serum deprivation inhibits the transcriptional co-activator YAP and cell growth via phosphorylation of the 130-kDa isoform of Angiomotin by the LATS1/2 protein kinases. Proc Natl Acad Sci U S A *110*, 17368-17373.

Alarcon, C., Zaromytidou, A.I., Xi, Q., Gao, S., Yu, J., Fujisawa, S., Barlas, A., Miller, A.N., Manova-Todorova, K., Macias, M.J*., et al.* (2009). Nuclear CDKs drive Smad transcriptional activation and turnover in BMP and TGF-beta pathways. Cell *139*, 757-769.

Anderberg, C., Cunha, S.I., Zhai, Z., Cortez, E., Pardali, E., Johnson, J.R., Franco, M., Paez-Ribes, M., Cordiner, R., Fuxe, J*., et al.* (2013). Deficiency for endoglin in tumor vasculature weakens the endothelial barrier to metastatic dissemination. J Exp Med *210*, 563-579.

Aragon, E., Goerner, N., Zaromytidou, A.I., Xi, Q., Escobedo, A., Massague, J., and Macias, M.J. (2011). A Smad action turnover switch operated by WW domain readers of a phosphoserine code. Genes Dev *25*, 1275-1288.

Aragona, M., Panciera, T., Manfrin, A., Giulitti, S., Michielin, F., Elvassore, N., Dupont, S., and Piccolo, S. (2013). A mechanical checkpoint controls multicellular growth through YAP/TAZ regulation by actin-processing factors. Cell *154*, 1047-1059.

Aspalter, I.M., Gordon, E., Dubrac, A., Ragab, A., Narloch, J., Vizan, P., Geudens, I., Collins, R.T., Franco, C.A., Abrahams, C.L*., et al.* (2015). Alk1 and Alk5 inhibition by Nrp1 controls vascular sprouting downstream of Notch. Nat Commun *6*, 7264.

Atkins, G.B., Jain, M.K., and Hamik, A. (2011). Endothelial differentiation: molecular mechanisms of specification and heterogeneity. Arterioscler Thromb Vasc Biol *31*, 1476-1484.

Azhar, M., Runyan, R.B., Gard, C., Sanford, L.P., Miller, M.L., Andringa, A., Pawlowski, S., Rajan, S., and Doetschman, T. (2009). Ligand-specific function of transforming growth factor beta in epithelial-mesenchymal transition in heart development. Dev Dyn *238*, 431-442.

Azzolin, L., Panciera, T., Soligo, S., Enzo, E., Bicciato, S., Dupont, S., Bresolin, S., Frasson, C., Basso, G., Guzzardo, V*., et al.* (2014). YAP/TAZ incorporation in the beta-catenin destruction complex orchestrates the Wnt response. Cell *158*, 157-170.

Basu, S., Totty, N.F., Irwin, M.S., Sudol, M., and Downward, J. (2003). Akt phosphorylates the Yes-associated protein, YAP, to induce interaction with 14-3-3 and attenuation of p73-mediated apoptosis. Mol Cell *11*, 11-23.

Bazzoni, G., and Dejana, E. (2001). Pores in the sieve and channels in the wall: control of paracellular permeability by junctional proteins in endothelial cells. Microcirculation *8*, 143-152.

Beyer, T.A., Weiss, A., Khomchuk, Y., Huang, K., Ogunjimi, A.A., Varelas, X., and Wrana, J.L. (2013). Switch enhancers interpret TGF-beta and Hippo signaling to control cell fate in human embryonic stem cells. Cell Rep *5*, 1611-1624.

Bohnsack, B.L., Lai, L., Dolle, P., and Hirschi, K.K. (2004). Signaling hierarchy downstream of retinoic acid that independently regulates vascular remodeling and endothelial cell proliferation. Genes Dev *18*, 1345-1358.

Boyer, A.S., Ayerinskas, II, Vincent, E.B., McKinney, L.A., Weeks, D.L., and Runyan, R.B. (1999). TGFbeta2 and TGFbeta3 have separate and sequential

activities during epithelial-mesenchymal cell transformation in the embryonic heart. Dev Biol *208*, 530-545.

Breier, G., Breviario, F., Caveda, L., Berthier, R., Schnurch, H., Gotsch, U., Vestweber, D., Risau, W., and Dejana, E. (1996). Molecular cloning and expression of murine vascular endothelial-cadherin in early stage development of cardiovascular system. Blood *87*, 630-641.

Cai, J., Zhang, N., Zheng, Y., de Wilde, R.F., Maitra, A., and Pan, D. (2010). The Hippo signaling pathway restricts the oncogenic potential of an intestinal regeneration program. Genes Dev *24*, 2383-2388.

Camargo, F.D., Gokhale, S., Johnnidis, J.B., Fu, D., Bell, G.W., Jaenisch, R., and Brummelkamp, T.R. (2007). YAP1 increases organ size and expands undifferentiated progenitor cells. Curr Biol *17*, 2054-2060.

Camenisch, T.D., Molin, D.G., Person, A., Runyan, R.B., Gittenberger-de Groot, A.C., McDonald, J.A., and Klewer, S.E. (2002). Temporal and distinct TGFbeta ligand requirements during mouse and avian endocardial cushion morphogenesis. Dev Biol *248*, 170-181.

Cao, X., Pfaff, S.L., and Gage, F.H. (2008). YAP regulates neural progenitor cell number via the TEA domain transcription factor. Genes Dev *22*, 3320-3334.

Carmeliet, P., Ferreira, V., Breier, G., Pollefeyt, S., Kieckens, L., Gertsenstein, M., Fahrig, M., Vandenhoeck, A., Harpal, K., Eberhardt, C.*, et al.* (1996). Abnormal blood vessel development and lethality in embryos lacking a single VEGF allele. Nature *380*, 435-439.

Carmeliet, P., Lampugnani, M.G., Moons, L., Breviario, F., Compernolle, V., Bono, F., Balconi, G., Spagnuolo, R., Oosthuyse, B., Dewerchin, M.*, et al.* (1999). Targeted deficiency or cytosolic truncation of the VE-cadherin gene in mice impairs VEGF-mediated endothelial survival and angiogenesis. Cell *98*, 147-157.

Chan, S.W., Lim, C.J., Chong, Y.F., Pobbati, A.V., Huang, C., and Hong, W. (2011). Hippo pathway-independent restriction of TAZ and YAP by angiomotin. J Biol Chem *286*, 7018-7026.

Choi, H.J., Zhang, H., Park, H., Choi, K.S., Lee, H.W., Agrawal, V., Kim, Y.M., and Kwon, Y.G. (2015). Yes-associated protein regulates endothelial cell contact-mediated expression of angiopoietin-2. Nat Commun *6*, 6943.

Choi, K. (2002). The hemangioblast: a common progenitor of hematopoietic and endothelial cells. J Hematother Stem Cell Res *11*, 91-101.

Colak, S., and Ten Dijke, P. (2017). Targeting TGF-beta Signaling in Cancer. Trends Cancer *3*, 56-71.

Corada, M., Nyqvist, D., Orsenigo, F., Caprini, A., Giampietro, C., Taketo, M.M., Iruela-Arispe, M.L., Adams, R.H., and Dejana, E. (2010). The Wnt/beta-catenin pathway modulates vascular remodeling and specification by upregulating Dll4/Notch signaling. Dev Cell *18*, 938-949.

Corada, M., Orsenigo, F., Morini, M.F., Pitulescu, M.E., Bhat, G., Nyqvist, D., Breviario, F., Conti, V., Briot, A., Iruela-Arispe, M.L.*, et al.* (2013). Sox17 is indispensable for acquisition and maintenance of arterial identity. Nat Commun *4*, 2609.

Cuttano, R., Rudini, N., Bravi, L., Corada, M., Giampietro, C., Papa, E., Morini, M.F., Maddaluno, L., Baeyens, N., Adams, R.H.*, et al.* (2016). KLF4 is a key determinant in the development and progression of cerebral cavernous malformations. EMBO Mol Med *8*, 6-24.

Dejana, E. (2004). Endothelial cell-cell junctions: happy together. Nat Rev Mol Cell Biol *5*, 261-270.

Dejana, E., Tournier-Lasserve, E., and Weinstein, B.M. (2009). The control of vascular integrity by endothelial cell junctions: molecular basis and pathological implications. Dev Cell *16*, 209-221.

Dennler, S., Itoh, S., Vivien, D., ten Dijke, P., Huet, S., and Gauthier, J.M. (1998). Direct binding of Smad3 and Smad4 to critical TGF beta-inducible elements in the promoter of human plasminogen activator inhibitor-type 1 gene. EMBO J *17*, 3091-3100.

Dong, J., Feldmann, G., Huang, J., Wu, S., Zhang, N., Comerford, S.A., Gayyed, M.F., Anders, R.A., Maitra, A., and Pan, D. (2007). Elucidation of a universal size-control mechanism in Drosophila and mammals. Cell *130*, 1120-1133.

Dong, Q.G., Bernasconi, S., Lostaglio, S., De Calmanovici, R.W., Martin-Padura, I., Breviario, F., Garlanda, C., Ramponi, S., Mantovani, A., and Vecchi, A. (1997). A general strategy for isolation of endothelial cells from murine tissues. Characterization of two endothelial cell lines from the murine lung and subcutaneous sponge implants. Arterioscler Thromb Vasc Biol *17*, 1599-1604.

Dupont, S., Morsut, L., Aragona, M., Enzo, E., Giulitti, S., Cordenonsi, M., Zanconato, F., Le Digabel, J., Forcato, M., Bicciato, S.*, et al.* (2011). Role of YAP/TAZ in mechanotransduction. Nature *474*, 179-183.

Edgar, B.A. (2006). From cell structure to transcription: Hippo forges a new path. Cell *124*, 267-273.

Engebretsen, K.V., Skardal, K., Bjornstad, S., Marstein, H.S., Skrbic, B., Sjaastad, I., Christensen, G., Bjornstad, J.L., and Tonnessen, T. (2014). Attenuated development of cardiac fibrosis in left ventricular pressure overload by SM16, an orally active inhibitor of ALK5. J Mol Cell Cardiol *76*, 148-157.

Estaras, C., Benner, C., and Jones, K.A. (2015). SMADs and YAP compete to control elongation of beta-catenin:LEF-1-recruited RNAPII during hESC differentiation. Mol Cell *58*, 780-793.

Fernandez, L.A., Northcott, P.A., Dalton, J., Fraga, C., Ellison, D., Angers, S., Taylor, M.D., and Kenney, A.M. (2009). YAP1 is amplified and up-regulated in hedgehog-associated medulloblastomas and mediates Sonic hedgehog-driven neural precursor proliferation. Genes Dev *23*, 2729-2741.

Ferrara, N., Carver-Moore, K., Chen, H., Dowd, M., Lu, L., O'Shea, K.S., Powell-Braxton, L., Hillan, K.J., and Moore, M.W. (1996). Heterozygous embryonic lethality induced by targeted inactivation of the VEGF gene. Nature *380*, 439-442.

Ferrigno, O., Lallemand, F., Verrecchia, F., L'Hoste, S., Camonis, J., Atfi, A., and Mauviel, A. (2002). Yes-associated protein (YAP65) interacts with Smad7 and potentiates its inhibitory activity against TGF-beta/Smad signaling. Oncogene *21*, 4879-4884.

Francois, M., Caprini, A., Hosking, B., Orsenigo, F., Wilhelm, D., Browne, C., Paavonen, K., Karnezis, T., Shayan, R., Downes, M.*, et al.* (2008). Sox18 induces development of the lymphatic vasculature in mice. Nature *456*, 643-647.

Fujii, M., Toyoda, T., Nakanishi, H., Yatabe, Y., Sato, A., Matsudaira, Y., Ito, H., Murakami, H., Kondo, Y., Kondo, E.*, et al.* (2012). TGF-beta synergizes with defects in the Hippo pathway to stimulate human malignant mesothelioma growth. J Exp Med *209*, 479-494.

Gaffney, C.J., Oka, T., Mazack, V., Hilman, D., Gat, U., Muramatsu, T., Inazawa, J., Golden, A., Carey, D.J., Farooq, A.*, et al.* (2012). Identification, basic characterization and evolutionary analysis of differentially spliced mRNA isoforms of human YAP1 gene. Gene *509*, 215-222.

Gao, S., Alarcon, C., Sapkota, G., Rahman, S., Chen, P.Y., Goerner, N., Macias, M.J., Erdjument-Bromage, H., Tempst, P., and Massague, J. (2009). Ubiquitin ligase Nedd4L targets activated Smad2/3 to limit TGF-beta signaling. Mol Cell *36*, 457-468.

Gasparics, A., Rosivall, L., Krizbai, I.A., and Sebe, A. (2016). When the endothelium scores an own goal: endothelial cells actively augment metastatic

extravasation through endothelial-mesenchymal transition. Am J Physiol Heart Circ Physiol *310*, H1055-1063.

Giampietro, C., Disanza, A., Bravi, L., Barrios-Rodiles, M., Corada, M., Frittoli, E., Savorani, C., Lampugnani, M.G., Boggetti, B., Niessen, C.*, et al.* (2015). The actin-binding protein EPS8 binds VE-cadherin and modulates YAP localization and signaling. J Cell Biol *211*, 1177-1192.

Giampietro, C., Taddei, A., Corada, M., Sarra-Ferraris, G.M., Alcalay, M., Cavallaro, U., Orsenigo, F., Lampugnani, M.G., and Dejana, E. (2012). Overlapping and divergent signaling pathways of N-cadherin and VE-cadherin in endothelial cells. Blood *119*, 2159-2170.

Goldie, L.C., Nix, M.K., and Hirschi, K.K. (2008). Embryonic vasculogenesis and hematopoietic specification. Organogenesis *4*, 257-263.

Gong, H., Lyu, X., Wang, Q., Hu, M., and Zhang, X. (2017). Endothelial to mesenchymal transition in the cardiovascular system. Life Sci *184*, 95-102.

Goumans, M.J., Lebrin, F., and Valdimarsdottir, G. (2003a). Controlling the angiogenic switch: a balance between two distinct TGF-b receptor signaling pathways. Trends Cardiovasc Med *13*, 301-307.

Goumans, M.J., and Ten Dijke, P. (2017). TGF-beta Signaling in Control of Cardiovascular Function. Cold Spring Harb Perspect Biol.

Goumans, M.J., Valdimarsdottir, G., Itoh, S., Lebrin, F., Larsson, J., Mummery, C., Karlsson, S., and ten Dijke, P. (2003b). Activin receptor-like kinase (ALK)1 is an antagonistic mediator of lateral TGFbeta/ALK5 signaling. Mol Cell *12*, 817-828.

Goumans, M.J., Valdimarsdottir, G., Itoh, S., Rosendahl, A., Sideras, P., and ten Dijke, P. (2002). Balancing the activation state of the endothelium via two distinct TGF-beta type I receptors. EMBO J *21*, 1743-1753.

Grannas, K., Arngarden, L., Lonn, P., Mazurkiewicz, M., Blokzijl, A., Zieba, A., and Soderberg, O. (2015). Crosstalk between Hippo and TGFbeta: Subcellular Localization of YAP/TAZ/Smad Complexes. J Mol Biol *427*, 3407-3415.

Gu, C., Rodriguez, E.R., Reimert, D.V., Shu, T., Fritzsch, B., Richards, L.J., Kolodkin, A.L., and Ginty, D.D. (2003). Neuropilin-1 conveys semaphorin and VEGF signaling during neural and cardiovascular development. Dev Cell *5*, 45-57.

Halder, G., Dupont, S., and Piccolo, S. (2012). Transduction of mechanical and cytoskeletal cues by YAP and TAZ. Nat Rev Mol Cell Biol *13*, 591-600.

Hannon, G.J., and Beach, D. (1994). p15INK4B is a potential effector of TGF-beta-induced cell cycle arrest. Nature *371*, 257-261.

Hao, Y., Chun, A., Cheung, K., Rashidi, B., and Yang, X. (2008). Tumor suppressor LATS1 is a negative regulator of oncogene YAP. J Biol Chem *283*, 5496-5509.

Harvey, K.F., Pfleger, C.M., and Hariharan, I.K. (2003). The Drosophila Mst ortholog, hippo, restricts growth and cell proliferation and promotes apoptosis. Cell *114*, 457-467.

Hashimoto, N., Phan, S.H., Imaizumi, K., Matsuo, M., Nakashima, H., Kawabe, T., Shimokata, K., and Hasegawa, Y. (2010). Endothelial-mesenchymal transition in bleomycin-induced pulmonary fibrosis. Am J Respir Cell Mol Biol *43*, 161-172.

Heallen, T., Zhang, M., Wang, J., Bonilla-Claudio, M., Klysik, E., Johnson, R.L., and Martin, J.F. (2011). Hippo pathway inhibits Wnt signaling to restrain cardiomyocyte proliferation and heart size. Science *332*, 458-461.

Hellstrom, M., Phng, L.K., Hofmann, J.J., Wallgard, E., Coultas, L., Lindblom, P., Alva, J., Nilsson, A.K., Karlsson, L., Gaiano, N.*, et al.* (2007). Dll4 signalling through Notch1 regulates formation of tip cells during angiogenesis. Nature *445*, 776-780.

Hiemer, S.E., Szymaniak, A.D., and Varelas, X. (2014). The transcriptional regulators TAZ and YAP direct transforming growth factor beta-induced tumorigenic phenotypes in breast cancer cells. J Biol Chem *289*, 13461-13474.

Hill, C.S. (2009). Nucleocytoplasmic shuttling of Smad proteins. Cell Res *19*, 36-46.

Hill, C.S. (2016). Transcriptional Control by the SMADs. Cold Spring Harb Perspect Biol *8*.

Huang, J., Wu, S., Barrera, J., Matthews, K., and Pan, D. (2005). The Hippo signaling pathway coordinately regulates cell proliferation and apoptosis by inactivating Yorkie, the Drosophila Homolog of YAP. Cell *122*, 421-434.

Inazaki, K., Kanamaru, Y., Kojima, Y., Sueyoshi, N., Okumura, K., Kaneko, K., Yamashiro, Y., Ogawa, H., and Nakao, A. (2004). Smad3 deficiency attenuates renal fibrosis, inflammation,and apoptosis after unilateral ureteral obstruction. Kidney Int *66*, 597-604.

Jakobsson, L., Franco, C.A., Bentley, K., Collins, R.T., Ponsioen, B., Aspalter, I.M., Rosewell, I., Busse, M., Thurston, G., Medvinsky, A.*, et al.* (2010). Endothelial cells dynamically compete for the tip cell position during angiogenic sprouting. Nat Cell Biol *12*, 943-953.

Jakobsson, L., and van Meeteren, L.A. (2013). Transforming growth factor beta family members in regulation of vascular function: in the light of vascular conditional knockouts. Exp Cell Res *319*, 1264-1270.

Jia, J., Zhang, W., Wang, B., Trinko, R., and Jiang, J. (2003). The Drosophila Ste20 family kinase dMST functions as a tumor suppressor by restricting cell proliferation and promoting apoptosis. Genes Dev *17*, 2514-2519.

Kalluri, R., and Weinberg, R.A. (2009). The basics of epithelial-mesenchymal transition. J Clin Invest *119*, 1420-1428.

Kapur, N.K., Wilson, S., Yunis, A.A., Qiao, X., Mackey, E., Paruchuri, V., Baker, C., Aronovitz, M.J., Karumanchi, S.A., Letarte, M.*, et al.* (2012). Reduced endoglin activity limits cardiac fibrosis and improves survival in heart failure. Circulation *125*, 2728-2738.

Kawczyk-Krupka, A., Bugaj, A.M., Potempa, M., Wasilewska, K., Latos, W., and Sieron, A. (2015). Vascular-targeted photodynamic therapy in the treatment of neovascular age-related macular degeneration: Clinical perspectives. Photodiagnosis Photodyn Ther *12*, 161-175.

Kim, J., Kim, Y.H., Kim, J., Park, D.Y., Bae, H., Lee, D.H., Kim, K.H., Hong, S.P., Jang, S.P., Kubota, Y.*, et al.* (2017). YAP/TAZ regulates sprouting angiogenesis and vascular barrier maturation. J Clin Invest *127*, 3441-3461.

Kim, N.G., Koh, E., Chen, X., and Gumbiner, B.M. (2011). E-cadherin mediates contact inhibition of proliferation through Hippo signaling-pathway components. Proc Natl Acad Sci U S A *108*, 11930-11935.

Klein, P.S., and Melton, D.A. (1996). A molecular mechanism for the effect of lithium on development. Proc Natl Acad Sci U S A *93*, 8455-8459.

Komarova, Y., and Malik, A.B. (2010). Regulation of endothelial permeability via paracellular and transcellular transport pathways. Annu Rev Physiol *72*, 463-493.

Komuro, A., Nagai, M., Navin, N.E., and Sudol, M. (2003). WW domain-containing protein YAP associates with ErbB-4 and acts as a co-transcriptional activator for the carboxyl-terminal fragment of ErbB-4 that translocates to the nucleus. J Biol Chem *278*, 33334-33341.

Krizbai, I.A., Gasparics, A., Nagyoszi, P., Fazakas, C., Molnar, J., Wilhelm, I., Bencs, R., Rosivall, L., and Sebe, A. (2015). Endothelial-mesenchymal transition of brain endothelial cells: possible role during metastatic extravasation. PLoS One *10*, e0119655.

Lai, L., Bohnsack, B.L., Niederreither, K., and Hirschi, K.K. (2003). Retinoic acid regulates endothelial cell proliferation during vasculogenesis. Development *130*, 6465-6474.

Lai, Z.C., Wei, X., Shimizu, T., Ramos, E., Rohrbaugh, M., Nikolaidis, N., Ho, L.L., and Li, Y. (2005). Control of cell proliferation and apoptosis by mob as tumor suppressor, mats. Cell *120*, 675-685.

Lampugnani, M.G., Orsenigo, F., Gagliani, M.C., Tacchetti, C., and Dejana, E. (2006). Vascular endothelial cadherin controls VEGFR-2 internalization and signaling from intracellular compartments. J Cell Biol *174*, 593-604.

Lampugnani, M.G., Resnati, M., Raiteri, M., Pigott, R., Pisacane, A., Houen, G., Ruco, L.P., and Dejana, E. (1992). A novel endothelial-specific membrane protein is a marker of cell-cell contacts. J Cell Biol *118*, 1511-1522.

Larrivee, B., Prahst, C., Gordon, E., del Toro, R., Mathivet, T., Duarte, A., Simons, M., and Eichmann, A. (2012). ALK1 signaling inhibits angiogenesis by cooperating with the Notch pathway. Dev Cell *22*, 489-500.

Lawson, N.D., Vogel, A.M., and Weinstein, B.M. (2002). sonic hedgehog and vascular endothelial growth factor act upstream of the Notch pathway during arterial endothelial differentiation. Dev Cell *3*, 127-136.

le Noble, F., Moyon, D., Pardanaud, L., Yuan, L., Djonov, V., Matthijsen, R., Breant, C., Fleury, V., and Eichmann, A. (2004). Flow regulates arterial-venous differentiation in the chick embryo yolk sac. Development *131*, 361-375.

Lebrin, F., Goumans, M.J., Jonker, L., Carvalho, R.L., Valdimarsdottir, G., Thorikay, M., Mummery, C., Arthur, H.M., and ten Dijke, P. (2004). Endoglin promotes endothelial cell proliferation and TGF-beta/ALK1 signal transduction. EMBO J *23*, 4018-4028.

Letterio, J.J., Geiser, A.G., Kulkarni, A.B., Roche, N.S., Sporn, M.B., and Roberts, A.B. (1994). Maternal rescue of transforming growth factor-beta 1 null mice. Science *264*, 1936-1938.

Li, J., Qu, X., and Bertram, J.F. (2009). Endothelial-myofibroblast transition contributes to the early development of diabetic renal interstitial fibrosis in streptozotocin-induced diabetic mice. Am J Pathol *175*, 1380-1388.

Li, J., Qu, X., Yao, J., Caruana, G., Ricardo, S.D., Yamamoto, Y., Yamamoto, H., and Bertram, J.F. (2010). Blockade of endothelial-mesenchymal transition by a Smad3 inhibitor delays the early development of streptozotocin-induced diabetic nephropathy. Diabetes *59*, 2612-2624.

Li, Y., Zhou, H., Li, F., Chan, S.W., Lin, Z., Wei, Z., Yang, Z., Guo, F., Lim, C.J., Xing, W.*, et al.* (2015). Angiomotin binding-induced activation of Merlin/NF2 in the Hippo pathway. Cell Res *25*, 801-817.

Liang, K., Zhou, G., Zhang, Q., Li, J., and Zhang, C. (2014). Expression of hippo pathway in colorectal cancer. Saudi J Gastroenterol *20*, 188-194.

Liebner, S., Corada, M., Bangsow, T., Babbage, J., Taddei, A., Czupalla, C.J., Reis, M., Felici, A., Wolburg, H., Fruttiger, M.*, et al.* (2008). Wnt/beta-catenin signaling controls development of the blood-brain barrier. J Cell Biol *183*, 409-417.

Liu, W., Selever, J., Wang, D., Lu, M.F., Moses, K.A., Schwartz, R.J., and Martin, J.F. (2004). Bmp4 signaling is required for outflow-tract septation and branchial-arch artery remodeling. Proc Natl Acad Sci U S A *101*, 4489-4494.

Liu-Chittenden, Y., Huang, B., Shim, J.S., Chen, Q., Lee, S.J., Anders, R.A., Liu, J.O., and Pan, D. (2012). Genetic and pharmacological disruption of the TEAD-YAP complex suppresses the oncogenic activity of YAP. Genes Dev *26*, 1300-1305.

Lu, L., Li, Y., Kim, S.M., Bossuyt, W., Liu, P., Qiu, Q., Wang, Y., Halder, G., Finegold, M.J., Lee, J.S.*, et al.* (2010). Hippo signaling is a potent in vivo growth and tumor suppressor pathway in the mammalian liver. Proc Natl Acad Sci U S A *107*, 1437-1442.

Ma, L., Lu, M.F., Schwartz, R.J., and Martin, J.F. (2005). Bmp2 is essential for cardiac cushion epithelial-mesenchymal transition and myocardial patterning. Development *132*, 5601-5611.

Maddaluno, L., Rudini, N., Cuttano, R., Bravi, L., Giampietro, C., Corada, M., Ferrarini, L., Orsenigo, F., Papa, E., Boulday, G.*, et al.* (2013). EndMT contributes to the onset and progression of cerebral cavernous malformations. Nature *498*, 492-496.

Mana-Capelli, S., Paramasivam, M., Dutta, S., and McCollum, D. (2014). Angiomotins link F-actin architecture to Hippo pathway signaling. Mol Biol Cell *25*, 1676-1685.

Marcelo, K.L., Goldie, L.C., and Hirschi, K.K. (2013). Regulation of endothelial cell differentiation and specification. Circ Res *112*, 1272-1287.

Markwald, R.R., Fitzharris, T.P., and Smith, W.N. (1975). Sturctural analysis of endocardial cytodifferentiation. Dev Biol *42*, 160-180.

Massague, J. (2012). TGFbeta signalling in context. Nat Rev Mol Cell Biol *13*, 616-630.

Massague, J., Seoane, J., and Wotton, D. (2005). Smad transcription factors. Genes Dev *19*, 2783-2810.

McClatchey, A.I., and Giovannini, M. (2005). Membrane organization and tumorigenesis--the NF2 tumor suppressor, Merlin. Genes Dev *19*, 2265-2277.

Medici, D., Potenta, S., and Kalluri, R. (2011). Transforming growth factor-beta2 promotes Snail-mediated endothelial-mesenchymal transition through convergence of Smad-dependent and Smad-independent signalling. Biochem J *437*, 515-520.

Medici, D., Shore, E.M., Lounev, V.Y., Kaplan, F.S., Kalluri, R., and Olsen, B.R. (2010). Conversion of vascular endothelial cells into multipotent stem-like cells. Nat Med *16*, 1400-1406.

Millan, F.A., Denhez, F., Kondaiah, P., and Akhurst, R.J. (1991). Embryonic gene expression patterns of TGF beta 1, beta 2 and beta 3 suggest different developmental functions in vivo. Development *111*, 131-143.

Miller, E., Yang, J., DeRan, M., Wu, C., Su, A.I., Bonamy, G.M., Liu, J., Peters, E.C., and Wu, X. (2012). Identification of serum-derived sphingosine-1-phosphate as a small molecule regulator of YAP. Chem Biol *19*, 955-962.

Mo, J.S., Yu, F.X., Gong, R., Brown, J.H., and Guan, K.L. (2012). Regulation of the Hippo-YAP pathway by protease-activated receptors (PARs). Genes Dev *26*, 2138-2143.

Moonen, J.R., Krenning, G., Brinker, M.G., Koerts, J.A., van Luyn, M.J., and Harmsen, M.C. (2010). Endothelial progenitor cells give rise to pro-angiogenic smooth muscle-like progeny. Cardiovasc Res *86*, 506-515.

Morin-Kensicki, E.M., Boone, and Howell, M. (2006). Defects in yolk sac vasculogenesis, chorioallantoic fusion, and embryonic axis elongation in mice with targeted disruption of Yap65. Defects in yolk sac vasculogenesis, chorioallantoic fusion, and embryonic axis elongation in mice with targeted disruption of Yap65.

Moya, I.M., Umans, L., Maas, E., Pereira, P.N., Beets, K., Francis, A., Sents, W., Robertson, E.J., Mummery, C.L., Huylebroeck, D.*, et al.* (2012). Stalk cell phenotype depends on integration of Notch and Smad1/5 signaling cascades. Dev Cell *22*, 501-514.

Nagasawa-Masuda, A., and Terai, K. (2017). Yap/Taz transcriptional activity is essential for vascular regression via Ctgf expression and actin polymerization. PLoS One *12*, e0174633.

Nakae, J., Kitamura, T., Kitamura, Y., Biggs, W.H., 3rd, Arden, K.C., and Accili, D. (2003). The forkhead transcription factor Foxo1 regulates adipocyte differentiation. Dev Cell *4*, 119-129.

Nakajima, H., Yamamoto, K., Agarwala, S., Terai, K., Fukui, H., Fukuhara, S., Ando, K., Miyazaki, T., Yokota, Y., Schmelzer, E.*, et al.* (2017). Flow-Dependent Endothelial YAP Regulation Contributes to Vessel Maintenance. Dev Cell *40*, 523-536 e526.

Nallet-Staub, F., Yin, X., Gilbert, C., Marsaud, V., Ben Mimoun, S., Javelaud, D., Leof, E.B., and Mauviel, A. (2015). Cell density sensing alters TGF-beta signaling in a cell-type-specific manner, independent from Hippo pathway activation. Dev Cell *32*, 640-651.

Nishio, M., Sugimachi, K., Goto, H., Wang, J., Morikawa, T., Miyachi, Y., Takano, Y., Hikasa, H., Itoh, T., Suzuki, S.O.*, et al.* (2016). Dysregulated YAP1/TAZ and TGF-beta signaling mediate hepatocarcinogenesis in Mob1a/1b-deficient mice. Proc Natl Acad Sci U S A *113*, E71-80.

Nusse, R., and Clevers, H. (2017). Wnt/beta-Catenin Signaling, Disease, and Emerging Therapeutic Modalities. Cell *169*, 985-999.

Overholtzer, M., Zhang, J., Smolen, G.A., Muir, B., Li, W., Sgroi, D.C., Deng, C.X., Brugge, J.S., and Haber, D.A. (2006). Transforming properties of YAP, a candidate oncogene on the chromosome 11q22 amplicon. Proc Natl Acad Sci U S A *103*, 12405-12410.

Pantalacci, S., Tapon, N., and Leopold, P. (2003). The Salvador partner Hippo promotes apoptosis and cell-cycle exit in Drosophila. Nat Cell Biol *5*, 921-927.

Paramasivam, M., Sarkeshik, A., Yates, J.R., 3rd, Fernandes, M.J., and McCollum, D. (2011). Angiomotin family proteins are novel activators of the LATS2 kinase tumor suppressor. Mol Biol Cell *22*, 3725-3733.

Pei, T., Li, Y., Wang, J., Wang, H., Liang, Y., Shi, H., Sun, B., Yin, D., Sun, J., Song, R.*, et al.* (2015). YAP is a critical oncogene in human cholangiocarcinoma. Oncotarget *6*, 17206-17220.

Potente, M., and Makinen, T. (2017). Vascular heterogeneity and specialization in development and disease. Nat Rev Mol Cell Biol *18*, 477-494.

Reynisdottir, I., Polyak, K., Iavarone, A., and Massague, J. (1995). Kip/Cip and Ink4 Cdk inhibitors cooperate to induce cell cycle arrest in response to TGF-beta. Genes Dev *9*, 1831-1845.

Rivera-Feliciano, J., and Tabin, C.J. (2006). Bmp2 instructs cardiac progenitors to form the heart-valve-inducing field. Dev Biol *295*, 580-588.

Rouleau, G.A., Merel, P., Lutchman, M., Sanson, M., Zucman, J., Marineau, C., Hoang-Xuan, K., Demczuk, S., Desmaze, C., Plougastel, B.*, et al.* (1993). Alteration in a new gene encoding a putative membrane-organizing protein causes neuro-fibromatosis type 2. Nature *363*, 515-521.

Rudini, N., Felici, A., Giampietro, C., Lampugnani, M., Corada, M., Swirsding, K., Garre, M., Liebner, S., Letarte, M., ten Dijke, P.*, et al.* (2008). VE-cadherin is a critical endothelial regulator of TGF-beta signalling. EMBO J *27*, 993-1004.

Sato, M., Muragaki, Y., Saika, S., Roberts, A.B., and Ooshima, A. (2003). Targeted disruption of TGF-beta1/Smad3 signaling protects against renal tubulointerstitial fibrosis induced by unilateral ureteral obstruction. J Clin Invest *112*, 1486-1494.

Scharpfenecker, M., van Dinther, M., Liu, Z., van Bezooijen, R.L., Zhao, Q., Pukac, L., Lowik, C.W., and ten Dijke, P. (2007). BMP-9 signals via ALK1 and inhibits bFGF-induced endothelial cell proliferation and VEGF-stimulated angiogenesis. J Cell Sci *120*, 964-972.

Schlegelmilch, K., Mohseni, M., Kirak, O., and Pruszak, J. (2011). Yap1 acts downstream of α-catenin to control epidermal proliferation. Cell.

Sena, C.M., Pereira, A.M., and Seica, R. (2013). Endothelial dysfunction - a major mediator of diabetic vascular disease. Biochim Biophys Acta *1832*, 2216-2231.

Shao, D.D., Xue, W., Krall, E.B., Bhutkar, A., Piccioni, F., Wang, X., Schinzel, A.C., Sood, S., Rosenbluh, J., Kim, J.W.*, et al.* (2014). KRAS and YAP1 converge to regulate EMT and tumor survival. Cell *158*, 171-184.

Shore, E.M., Xu, M., Feldman, G.J., Fenstermacher, D.A., Cho, T.J., Choi, I.H., Connor, J.M., Delai, P., Glaser, D.L., LeMerrer, M.*, et al.* (2006). A recurrent mutation in the BMP type I receptor ACVR1 causes inherited and sporadic fibrodysplasia ossificans progressiva. Nat Genet *38*, 525-527.

Silvis, M.R., Kreger, B.T., Lien, W.H., Klezovitch, O., Rudakova, G.M., Camargo, F.D., Lantz, D.M., Seykora, J.T., and Vasioukhin, V. (2011). alpha-catenin is a tumor suppressor that controls cell accumulation by regulating the localization and activity of the transcriptional coactivator Yap1. Sci Signal *4*, ra33.

Snijders, A.M., Schmidt, B.L., Fridlyand, J., Dekker, N., Pinkel, D., Jordan, R.C., and Albertson, D.G. (2005). Rare amplicons implicate frequent deregulation of cell fate specification pathways in oral squamous cell carcinoma. Oncogene *24*, 4232-4242.

Sorrentino, G., Ruggeri, N., Specchia, V., Cordenonsi, M., Mano, M., Dupont, S., Manfrin, A., Ingallina, E., Sommaggio, R., Piazza, S.*, et al.* (2014). Metabolic control of YAP and TAZ by the mevalonate pathway. Nat Cell Biol *16*, 357-366.

Spagnuolo, R., Corada, M., Orsenigo, F., Zanetta, L., Deuschle, U., Sandy, P., Schneider, C., Drake, C.J., Breviario, F., and Dejana, E. (2004). Gas1 is induced by VE-cadherin and vascular endothelial growth factor and inhibits endothelial cell apoptosis. Blood *103*, 3005-3012.

Sridurongrit, S., Larsson, J., Schwartz, R., Ruiz-Lozano, P., and Kaartinen, V. (2008). Signaling via the Tgf-beta type I receptor Alk5 in heart development. Dev Biol *322*, 208-218.

Stein, C., Bardet, A.F., Roma, G., Bergling, S., Clay, I., Ruchti, A., Agarinis, C., Schmelzle, T., Bouwmeester, T., Schubeler, D.*, et al.* (2015). YAP1 Exerts Its Transcriptional Control via TEAD-Mediated Activation of Enhancers. PLoS Genet *11*, e1005465.

Striedinger, K., VandenBerg, S.R., Baia, G.S., McDermott, M.W., Gutmann, D.H., and Lal, A. (2008). The neurofibromatosis 2 tumor suppressor gene product, merlin, regulates human meningioma cell growth by signaling through YAP. Neoplasia *10*, 1204-1212.

Sudol, M. (1994). Yes-associated protein (YAP65) is a proline-rich phosphoprotein that binds to the SH3 domain of the Yes proto-oncogene product. Oncogene *9*, 2145-2152.

Sudol, M., Bork, P., Einbond, A., Kastury, K., Druck, T., Negrini, M., Huebner, K., and Lehman, D. (1995a). Characterization of the mammalian YAP (Yes-associated protein) gene and its role in defining a novel protein module, the WW domain. J Biol Chem *270*, 14733-14741.

Sudol, M., Chen, H.I., Bougeret, C., Einbond, A., and Bork, P. (1995b). Characterization of a novel protein-binding module--the WW domain. FEBS Lett *369*, 67-71.

Sugi, Y., Yamamura, H., Okagawa, H., and Markwald, R.R. (2004). Bone morphogenetic protein-2 can mediate myocardial regulation of atrioventricular cushion mesenchymal cell formation in mice. Dev Biol *269*, 505-518.

Sun, J.G., Chen, X.W., Zhang, L.P., Wang, J., and Diehn, M. (2016). Yap1 promotes the survival and self-renewal of breast tumor initiating cells via inhibiting Smad3 signaling. Oncotarget *7*, 9692-9706.

Szeto, S.G., Narimatsu, M., Lu, M., He, X., Sidiqi, A.M., Tolosa, M.F., Chan, L., De Freitas, K., Bialik, J.F., Majumder, S.*, et al.* (2016). YAP/TAZ Are Mechanoregulators of TGF-beta-Smad Signaling and Renal Fibrogenesis. J Am Soc Nephrol *27*, 3117-3128.

Taddei, A., Giampietro, C., Conti, A., Orsenigo, F., Breviario, F., Pirazzoli, V., Potente, M., Daly, C., Dimmeler, S., and Dejana, E. (2008). Endothelial adherens junctions control tight junctions by VE-cadherin-mediated upregulation of claudin-5. Nat Cell Biol *10*, 923-934.

Tapon, N., Harvey, K.F., Bell, D.W., Wahrer, D.C., Schiripo, T.A., Haber, D., and Hariharan, I.K. (2002). salvador Promotes both cell cycle exit and apoptosis in Drosophila and is mutated in human cancer cell lines. Cell *110*, 467-478.

Tian, Y., Kolb, R., Hong, J.H., Carroll, J., and Li, D. (2007). TAZ promotes PC2 degradation through a SCFβ-Trcp E3 ligase complex. … and cellular biology.

Trindade, A., Kumar, S.R., Scehnet, J.S., Lopes-da-Costa, L., Becker, J., Jiang, W., Liu, R., Gill, P.S., and Duarte, A. (2008). Overexpression of delta-like 4 induces arterialization and attenuates vessel formation in developing mouse embryos. Blood *112*, 1720-1729.

van Meeteren, L.A., and ten Dijke, P. (2012). Regulation of endothelial cell plasticity by TGF-beta. Cell Tissue Res *347*, 177-186.

Varelas, X. (2014). The Hippo pathway effectors TAZ and YAP in development, homeostasis and disease. Development *141*, 1614-1626.

Varelas, X., Samavarchi-Tehrani, P., Narimatsu, M., Weiss, A., Cockburn, K., Larsen, B.G., Rossant, J., and Wrana, J.L. (2010). The Crumbs complex couples cell density sensing to Hippo-dependent control of the TGF-beta-SMAD pathway. Dev Cell *19*, 831-844.

Vassilev, A., Kaneko, K.J., Shu, H., Zhao, Y., and DePamphilis, M.L. (2001). TEAD/TEF transcription factors utilize the activation domain of YAP65, a Src/Yes-associated protein localized in the cytoplasm. Genes Dev *15*, 1229-1241.

Velasco, S., Alvarez-Munoz, P., Pericacho, M., Dijke, P.T., Bernabeu, C., Lopez-Novoa, J.M., and Rodriguez-Barbero, A. (2008). L- and S-endoglin differentially modulate TGFbeta1 signaling mediated by ALK1 and ALK5 in L6E9 myoblasts. J Cell Sci *121*, 913-919.

Velden, J.L., Alcorn, J.F., Guala, A.S., Badura, E.C., and Janssen-Heininger, Y.M. (2011). c-Jun N-terminal kinase 1 promotes transforming growth factor-beta1-induced epithelial-to-mesenchymal transition via control of linker phosphorylation and transcriptional activity of Smad3. Am J Respir Cell Mol Biol *44*, 571-581.

von Gise, A., Lin, Z., Schlegelmilch, K., Honor, L.B., Pan, G.M., Buck, J.N., Ma, Q., Ishiwata, T., Zhou, B., Camargo, F.D.*, et al.* (2012). YAP1, the nuclear target of Hippo signaling, stimulates heart growth through cardiomyocyte proliferation but not hypertrophy. Proc Natl Acad Sci U S A *109*, 2394-2399.

Wada, K., Itoga, K., Okano, T., Yonemura, S., and Sasaki, H. (2011). Hippo pathway regulation by cell morphology and stress fibers. Development *138*, 3907-3914.

Wang, G., Matsuura, I., He, D., and Liu, F. (2009a). Transforming growth factor-{beta}-inducible phosphorylation of Smad3. J Biol Chem *284*, 9663-9673.

Wang, H.U., Chen, Z.F., and Anderson, D.J. (1998). Molecular distinction and angiogenic interaction between embryonic arteries and veins revealed by ephrin-B2 and its receptor Eph-B4. Cell *93*, 741-753.

Wang, K.C., Yeh, Y.T., Nguyen, P., Limqueco, E., Lopez, J., Thorossian, S., Guan, K.L., Li, Y.J., and Chien, S. (2016a). Flow-dependent YAP/TAZ activities regulate endothelial phenotypes and atherosclerosis. Proc Natl Acad Sci U S A *113*, 11525-11530.

Wang, M., Zhao, J., Zhang, L., Wei, F., Lian, Y., Wu, Y., Gong, Z., Zhang, S., Zhou, J., Cao, K.*, et al.* (2017). Role of tumor microenvironment in tumorigenesis. J Cancer *8*, 761-773.

Wang, N., Tytell, J.D., and Ingber, D.E. (2009b). Mechanotransduction at a distance: mechanically coupling the extracellular matrix with the nucleus. Nat Rev Mol Cell Biol *10*, 75-82.

Wang, S., Li, H., Wang, G., Zhang, T., Fu, B., Ma, M., Quan, Z., and Chen, G. (2016b). Yes-associated protein (YAP) expression is involved in epithelial-mesenchymal transition in hepatocellular carcinoma. Clin Transl Oncol *18*, 172-177.

Wang, Y., Dong, Q., Zhang, Q., Li, Z., Wang, E., and Qiu, X. (2010). Overexpression of yes-associated protein contributes to progression and poor prognosis of non-small-cell lung cancer. Cancer Sci *101*, 1279-1285.

Watabe, T., Nishihara, A., Mishima, K., Yamashita, J., Shimizu, K., Miyazawa, K., Nishikawa, S., and Miyazono, K. (2003). TGF-beta receptor kinase inhibitor enhances growth and integrity of embryonic stem cell-derived endothelial cells. J Cell Biol *163*, 1303-1311.

Weiss, A., and Attisano, L. (2013). The TGFbeta superfamily signaling pathway. Wiley Interdiscip Rev Dev Biol *2*, 47-63.

Welch-Reardon, K.M., Wu, N., and Hughes, C.C. (2015). A role for partial endothelial-mesenchymal transitions in angiogenesis? Arterioscler Thromb Vasc Biol *35*, 303-308.

Winnier, G., Blessing, M., Labosky, P.A., and Hogan, B.L. (1995). Bone morphogenetic protein-4 is required for mesoderm formation and patterning in the mouse. Genes Dev *9*, 2105-2116.

Wu, S., Huang, J., Dong, J., and Pan, D. (2003). hippo encodes a Ste-20 family protein kinase that restricts cell proliferation and promotes apoptosis in conjunction with salvador and warts. Cell *114*, 445-456.

Wu, S., Liu, Y., Zheng, Y., Dong, J., and Pan, D. (2008). The TEAD/TEF family protein Scalloped mediates transcriptional output of the Hippo growth-regulatory pathway. Dev Cell *14*, 388-398.

Xiao, H., Jiang, N., Zhou, B., Liu, Q., and Du, C. (2015). TAZ regulates cell proliferation and epithelial-mesenchymal transition of human hepatocellular carcinoma. Cancer Sci *106*, 151-159.

Xin, M., Kim, Y., Sutherland, L.B., Murakami, M., Qi, X., McAnally, J., Porrello, E.R., Mahmoud, A.I., Tan, W., Shelton, J.M.*, et al.* (2013). Hippo pathway effector Yap promotes cardiac regeneration. Proc Natl Acad Sci U S A *110*, 13839-13844.

Xin, M., Kim, Y., Sutherland, L.B., Qi, X., McAnally, J., Schwartz, R.J., Richardson, J.A., Bassel-Duby, R., and Olson, E.N. (2011). Regulation of insulin-like growth factor signaling by Yap governs cardiomyocyte proliferation and embryonic heart size. Sci Signal *4*, ra70.

Xu, T., Wang, W., Zhang, S., Stewart, R.A., and Yu, W. (1995). Identifying tumor suppressors in genetic mosaics: the Drosophila lats gene encodes a putative protein kinase. Development *121*, 1053-1063.

Yagi, R., Chen, L.F., Shigesada, K., Murakami, Y., and Ito, Y. (1999). A WW domain-containing yes-associated protein (YAP) is a novel transcriptional co-activator. EMBO J *18*, 2551-2562.

Yamagishi, T., Ando, K., and Nakamura, H. (2009). Roles of TGFbeta and BMP during valvulo-septal endocardial cushion formation. Anat Sci Int *84*, 77-87.

Ye, F., and Zhang, M. (2013). Structures and target recognition modes of PDZ domains: recurring themes and emerging pictures. Biochem J *455*, 1-14.

Yi, C., Shen, Z., Stemmer-Rachamimov, A., Dawany, N., Troutman, S., Showe, L.C., Liu, Q., Shimono, A., Sudol, M., Holmgren, L.*, et al.* (2013). The p130 isoform of angiomotin is required for Yap-mediated hepatic epithelial cell proliferation and tumorigenesis. Sci Signal *6*, ra77.

Yi, C., Troutman, S., Fera, D., Stemmer-Rachamimov, A., Avila, J.L., Christian, N., Persson, N.L., Shimono, A., Speicher, D.W., Marmorstein, R.*, et al.* (2011). A

tight junction-associated Merlin-angiomotin complex mediates Merlin's regulation of mitogenic signaling and tumor suppressive functions. Cancer Cell *19*, 527-540.

You, L.R., Lin, F.J., Lee, C.T., DeMayo, F.J., Tsai, M.J., and Tsai, S.Y. (2005). Suppression of Notch signalling by the COUP-TFII transcription factor regulates vein identity. Nature *435*, 98-104.

Yu, F.X., Zhao, B., Panupinthu, N., Jewell, J.L., Lian, I., Wang, L.H., Zhao, J., Yuan, H., Tumaneng, K., Li, H.*, et al.* (2012). Regulation of the Hippo-YAP pathway by G-protein-coupled receptor signaling. Cell *150*, 780-791.

Yuan, M., Tomlinson, V., Lara, R., Holliday, D., Chelala, C., Harada, T., Gangeswaran, R., Manson-Bishop, C., Smith, P., Danovi, S.A.*, et al.* (2008). Yes-associated protein (YAP) functions as a tumor suppressor in breast. Cell Death Differ *15*, 1752-1759.

Yuan, Y., Li, D., Li, H., Wang, L., Tian, G., and Dong, Y. (2016). YAP overexpression promotes the epithelial-mesenchymal transition and chemoresistance in pancreatic cancer cells. Mol Med Rep *13*, 237-242.

Zanconato, F., Forcato, M., Battilana, G., Azzolin, L., Quaranta, E., Bodega, B., Rosato, A., Bicciato, S., Cordenonsi, M., and Piccolo, S. (2015). Genome-wide association between YAP/TAZ/TEAD and AP-1 at enhancers drives oncogenic growth. Nat Cell Biol *17*, 1218-1227.

Zeisberg, E.M., Potenta, S., Xie, L., Zeisberg, M., and Kalluri, R. (2007a). Discovery of endothelial to mesenchymal transition as a source for carcinoma-associated fibroblasts. Cancer Res *67*, 10123-10128.

Zeisberg, E.M., Potenta, S.E., Sugimoto, H., Zeisberg, M., and Kalluri, R. (2008). Fibroblasts in kidney fibrosis emerge via endothelial-to-mesenchymal transition. J Am Soc Nephrol *19*, 2282-2287.

Zeisberg, E.M., Tarnavski, O., Zeisberg, M., Dorfman, A.L., McMullen, J.R., Gustafsson, E., Chandraker, A., Yuan, X., Pu, W.T., Roberts, A.B.*, et al.* (2007b). Endothelial-to-mesenchymal transition contributes to cardiac fibrosis. Nat Med *13*, 952-961.

Zender, L., Spector, M.S., Xue, W., Flemming, P., Cordon-Cardo, C., Silke, J., Fan, S.T., Luk, J.M., Wigler, M., Hannon, G.J.*, et al.* (2006). Identification and validation of oncogenes in liver cancer using an integrative oncogenomic approach. Cell *125*, 1253-1267.

Zhang, H., von Gise, A., Liu, Q., Hu, T., Tian, X., He, L., Pu, W., Huang, X., He, L., Cai, C.-L.*, et al.* (2014). Yap1 Is Required for Endothelial to Mesenchymal Transition of the Atrioventricular Cushion. Journal of Biological Chemistry *289*, 18681-18692.

Zhang, L., Ren, F., Zhang, Q., Chen, Y., Wang, B., and Jiang, J. (2008). The TEAD/TEF family of transcription factor Scalloped mediates Hippo signaling in organ size control. Dev Cell *14*, 377-387.

Zhang, N., Bai, H., David, K.K., Dong, J., Zheng, Y., Cai, J., Giovannini, M., Liu, P., Anders, R.A., and Pan, D. (2010). The Merlin/NF2 tumor suppressor functions through the YAP oncoprotein to regulate tissue homeostasis in mammals. Dev Cell *19*, 27-38.

Zhang, Y., Alexander, P.B., and Wang, X.-F. (2016). TGF-β Family Signaling in the Control of Cell Proliferation and Survival. Cold Spring Harbor Perspectives in Biology *9*.

Zhang, Z.W., Men, T., Feng, R.C., Li, Y.C., and Zhou, D. (2013). miR-375 inhibits proliferation of mouse pancreatic progenitor cells by targeting YAP1. Cellular Physiology and ….

Zhao, B., Kim, J., Ye, X., Lai, Z.C., and Guan, K.L. (2009). Both TEAD-binding and WW domains are required for the growth stimulation and oncogenic transformation activity of yes-associated protein. Cancer Res *69*, 1089-1098.

Zhao, B., Li, L., Lu, Q., Wang, L.H., Liu, C.Y., Lei, Q., and Guan, K.L. (2011). Angiomotin is a novel Hippo pathway component that inhibits YAP oncoprotein. Genes Dev *25*, 51-63.

Zhao, B., Li, L., Wang, L., Wang, C.Y., Yu, J., and Guan, K.L. (2012). Cell detachment activates the Hippo pathway via cytoskeleton reorganization to induce anoikis. Genes Dev *26*, 54-68.

Zhao, B., Wei, X., Li, W., Udan, R.S., Yang, Q., Kim, J., Xie, J., Ikenoue, T., Yu, J., Li, L.*, et al.* (2007). Inactivation of YAP oncoprotein by the Hippo pathway is involved in cell contact inhibition and tissue growth control. Genes Dev *21*, 2747-2761.

Zhao, B., Ye, X., Yu, J., Li, L., Li, W., Li, S., Yu, J., Lin, J.D., Wang, C.Y., Chinnaiyan, A.M.*, et al.* (2008). TEAD mediates YAP-dependent gene induction and growth control. Genes Dev *22*, 1962-1971.

Zhou, D., Conrad, C., Xia, F., Park, J.S., Payer, B., Yin, Y., Lauwers, G.Y., Thasler, W., Lee, J.T., Avruch, J.*, et al.* (2009). Mst1 and Mst2 maintain hepatocyte quiescence and suppress hepatocellular carcinoma development through inactivation of the Yap1 oncogene. Cancer Cell *16*, 425-438.

Zhou, G.X., Li, X.Y., Zhang, Q., Zhao, K., Zhang, C.P., Xue, C.H., Yang, K., and Tian, Z.B. (2013). Effects of the hippo signaling pathway in human gastric cancer. Asian Pac J Cancer Prev *14*, 5199-5205.

Zhu, H., Kavsak, P., Abdollah, S., Wrana, J.L., and Thomsen, G.H. (1999). A SMAD ubiquitin ligase targets the BMP pathway and affects embryonic pattern formation. Nature *400*, 687-693.

Acknowledgements

And here I am, writing probably the most important chapter of all.
Four years ago, when my PhD journey began, I would have never imagined where this path would actually bring me to. I knew I wanted to become a biomedical researcher, I wanted to master new molecular biology techniques and contribute with my effort to the overall scientific advancement. I ended up learning how to survive many stressful conditions, to deal with unexpected situations and to look at the world with more “grown-up” eyes. I discovered that a PhD is a true life-coaching companion, that often challenges your motivation, your results, yourself. But that teaches you how to survive and not give up, it forces you to believe in yourself unless you want to surrender, it forges you as a person before making you a scientist. Now, I can understand how important it has been for my personal and carrier-wise progress. And I am so grateful that I never gave up. For this reason, I need to thank one by one all the people that shared with me this rollercoaster journey, without whom today you would not be able to read about my project and OUR results.

My gratefulness goes to prof. Elisabetta Dejana, for giving me the opportunity to work in one of the top-notch and leading group in the world in the field of vascular biology, and for her constant critical support, which stimulated my curiosity in further developing my research project.

A special and big thank goes to Costanza, for guiding me thorough these four years, always believing in my capabilities and being my mentor in good and bad moments. Thanks for correcting me every time I needed that, because it pushed me to grow up and to constantly improve as a scientist and as a person. Now I can finally understand how important it was every single teaching step you did with me. Thanks for being there whenever I needed that and for allowing me to become more and more independent along the way.

I am grateful to my internal and external supervisors, prof. Stefano Campaner and prof. Johan de Rooij for their support and their invaluable suggestions.

Thanks also to my examining committee, prof. Kristian Pietras and prof. Giorgio Scita, for having carefully read my thesis and for all the suggestions they are going to give me.

Warm thanks go to Linda and Eleonora, it has been a pleasure to share with you all the frustrations of doing research on YAP and for becoming my friends.

Thanks to Roberta, for everything. For having taught me how to be a teacher, for having constantly challenged me with your simple questions, for having completely turned upside down our project on a Friday evening at 7 pm, and for having been a constant source of inspiration and of energy. Thanks for having been an impeccable master thesis student that helped me more than what supposed to.

Thanks to Monica Giannotta, for having carefully listened to my ideas and believed in them, and for taking good care of me when I was struggling.

I am grateful to all the past and present members of Dejana's group, for all the help they gave me in many different ways. To Matteo, for having pity of me and taught me how to quantify IF stainings. To Claudio, for being a friend. To Nikos, for making me smile every time he saw me sad. To Mariagrazia, Monica Corada, Fabrizio e Ferruccio for their constant and precious technical support. To Carlotta, for all the figures she modified for me, using her time for me instead of working on her project. To Marco, for his never-ending curiosity. To Noemi, Surya, Roberto, Ganesh, Luca, Benny and Azzurra for your help.

Thanks also to all the people in IFOM that became my friends, expecially to Camilla, Emanuele and Alba.

And thanks with all my heart to my family. Thanks mum, for the countless hours at the phone, trying to encourage me every time I was crying and for rejoicing with me for every single little achievement I made. Thanks dad, for hugging me everytime I needed to recharge myself. Thank you, because without you, I would not be here now, I would have given up long time ago, missing the chance to learn what a PhD teaches you. Thanks for having always believed in me, even when I myself stopped doing that. I will always remember how much you love me and helped me. Thanks to my sister and my brother, for having always always always pushed me to go on, and to my nephews and nieces for bringing infinite joy in my life.

Last but not least, thanks to my friends for sharing the good and bad of these years. A huge thank goes to Chiara, for always listening and supporting me like a sister. To Roberta, for her vocal messages/words of wisdom that energized me. To my rowing mates, for keeping me physically but also mentally healthy during these years. To Milo, Silvia, Giuliano, Hamzah, Edyta, Vibeke for being close to me although living far away. And thanks to Luca, thanks of you. Thanks for being next to me always, for making me smile and laugh when the experiments did not work out well enough, for accepting my very long working hours without complaining,

actually looking proudly at me for my job, thanks for taking care of me with love, for sharing everything of this last intense but rich year and for your sincere love.

Truly thanks to you all.

Ed eccomi qui a scrivere probabilmente il capitolo più importante di tutti.

Quattro anni fa, quando ho intrapreso questo percorso chiamato “dottorato di ricerca”, non avrei mai immaginato dove mi avrebbe portato in realtà. Io volevo diventare una ricercatrice biomedica, volevo acquisire delle tecniche nuove e contribuire con i miei sforzi all’avanzamento scientifico. In realtà, ho imparato come sopravvivere a molte condizioni stressanti, ad affrontare situazioni inaspettate e a guardare il mondo con occhi “più maturi”. Ho scoperto che un PhD è una vera e propria scuola di vita, che spesso mette a dura prova le tue motivazioni, i tuoi risultati e te stesso. Ma che ti insegna come sopravvivere e a non arrenderti, che ti forza a credere in te stesso se non vuoi arrenderti, che ti forgia come persona ancora prima che come scienziato. Adesso, posso capire quanto sia stato importante per la mia carriera e per la mia crescita personale. E ora sono così felice di non aver mai mollato. Per questo motivo, sento di dover ringraziare ad una ad una tutte le persone che hanno condiviso con me questo percorso altalenante, perché senza di loro oggi non potreste ora leggere del mio progetto e dei NOSTRI risultati.

Perciò ringrazio la prof.ssa Elisabetta Dejana per avermi offerto l’opportunità di lavorare in uno dei gruppi scientificamente e tecnicamente più preparati al mondo nel settore della biologia vascolare e per aver costantemente apportato critiche costruttive al mio progetto, stimolando in me la curiosità di approfondire sempre di più il mio lavoro.

Un ringraziamento speciale e doveroso va a Costanza, per avermi guidato lungo questi quattro anni, per aver sempre creduto nelle mie capacità e per essere stata la mia mentore sia nei bei momenti che in quelli brutti. Grazie per avermi corretto ogni volta che serviva, perché ciò mi ha permesso di crescere e di maturare sia come scienziata che come persona. Ora posso finalmente comprendere quanto siano stati importanti tutti i tuoi insegnamenti. Grazie per essermi stata vicina quando avevo bisogno e per avermi permesso di diventare via via sempre più una ricercatrice indipendente.

Grazie ai miei supervisor interni ed esterni, prof. Stefano Campaner e prof. Johan de Rooij per il loro supporto e gli importanti suggerimenti.

Grazie anche alla mia commissione esaminatrice, prof. Kristian Pietras e prof Giorgio Scita, per aver letto attentamente la mia tesi per tutti i suggerimenti che mi forniranno.

Grazie di cuore a Linda ed Eleonora, è stato bello poter condividere con voi le frustrazioni della ricerca su YAP e per essere diventate mie amiche.

Grazie a Roberta, per tutto. Per avermi insegnato ad essere un'insegnante, per avermi messo in difficoltà con le tue domande semplici, per aver rivoluzionato il nostro progetto alle sette del venerdì sera e per essere stata una fonte costante ed inesauribile di ispirazione e di forza. Grazie per essere stata una studentessa modello e per avermi aiutata anche oltre i tuoi compiti da studentessa di tesi.

Grazie a Monica Giannotta, per aver ascoltato le mie idee, per averci creduto fin da subito e per esserti presa cura di me quando ero in difficoltà.

Grazie a tutti i membri presenti e passati del gruppo Dejana per avermi aiutato in tanti modi diversi. A Matteo, per aver avuto pietà di me ed avermi insegnato a quantificare le IF. A Claudio, per essere stato un amico. A Nikos, per avermi portato il sorriso ogni volta che mi vedeva triste. A Mariagrazia, Monica Corada, Fabrizio e Ferruccio per il loro costante e prezioso supporto tecnico. A Carlotta, per tutte le illustrazioni che ha modificato per me, sottraendo tempo al suo progetto. A Marco, per le sue continue curiosità. A Noemi, a Surya, a Roberto, a Ganesh, a Luca, a Benny ed Azzurra, per il vostro aiuto.

Grazie anche a tutte quelle persone in IFOM che sono diventate mie amiche, specialmente Camilla, Emanuele ed Alba.

Grazie con tutto il mio cuore alla mia famiglia. Grazie a mia madre, per le interminabili ore al telefono, per avermi incoraggiata ogni volta che piangevo e per aver gioito insieme a me per ogni mio piccolo traguardo. Grazie a mio padre, per avermi abbracciata a sé ogni volta che avevo bisogno di ricaricarmi. Grazie perché, senza di voi, non sarei qui adesso e avrei mollato tanto tempo fa, non imparando ciò che un dottorato insegna, e grazie per aver sempre creduto in me anche quando non ci credevo più io stessa. Non mi scorderò mai quanto mi amate e quanto mi abbiate aiutata. Grazie a mia sorella e mio fratello, per avermi sempre sempre sempre spronata e grazie ai miei nipoti per aver portato gioia infinita nella mia vita.

Infine, grazie ai miei amici, per aver condiviso con me le gioie e i dolori di questi anni. Un grazie immenso va a Chiara, per avermi sempre ascoltata e supportata

come una sorella. A Roberta, per i suoi messaggi vocali/pillole di saggezza e di carica infinita. Al mio gruppo di canottaggio, per avermi permesso di mantenere una certa sanità mentale oltre che fisica in questi anni. A Milo, Silvia, Giuliano, Hamzah, Edyta e Vibeke, per essermi stati vicini, seppur lontani. E grazie a Luca, grazie di te. Grazie di essermi sempre stato accanto, di avermi fatto sorridere e ridere ogni volta che un esperimento non funzionava, di aver accettato le mie lunghe ore al lavoro senza mai lamentarti, anzi, guardandomi con occhi orgogliosi per ciò che faccio, di esserti preso cura di me con amore, di aver condiviso tutto con me in questo ultimo anno intenso e ricco, e grazie del tuo amore sincero.

Grazie davvero a tutti voi.